UNIVERSITY OF LIVERPOOL

The relationship between metastasis-inducing S100 proteins (MIPs) and matrix metalloproteinases (MMPs) in rat and human breast cancer

Thesis submitted in accordance with the requirements of the University of Liverpool for the degree of Doctor in Philosophy by

Morteta H. Al-Medhtiy

September 2018

DECLARATION

I, Morteta H. Al-Medhtiy, confirm that the work presented in this thesis is my own. Where information has been derived from other sources, I confirm this has been indicated in the thesis.

Morteta H. Al-Medhtiy

SUPERVISORS CERTIFICATION

We certify that the thesis entitled "**The relationship between metastasis-inducing S100 proteins (MIPs) and matrix metalloproteinases (MMPs) in rat and human breast cancer**" was prepared under our supervision at the Department of Biological Sciences\Molecular Histology, Institute of Integrative Biology, Faculty of Health and Life Sciences, University of Liverpool as partial fulfilment of the requirements of University of the Liverpool for the degree of Doctor in Philosophy.

Signature:
Name: Prof. Philip Rudland
Title: Director of Study (DoS)
Address: Institute of Integrative Biology, University of Liverpool, Bioscience Building, Crown Street, Liverpool, L69 7ZB, UK
Date:

Signature:
Name: Dr. Roger Barraclough
Title: Second Supervisor
Address: Institute of Integrative Biology, University of Liverpool, Bioscience Building, Crown Street, Liverpool, L69 7ZB
Date:

Acknowledgements

In the name of Allah, the Most Gracious and the Most Merciful. Alhamdulillah, all praises to Allah for the strengths and His blessing in completing this thesis. I would like to thank my supervisors Prof Philip Rudland, Dr Roger Barraclough, and Dr Mark Wilkinson for all their supervision, constant support and help throughout this project. I would also like to acknowledge the help of several people, all of whom are members of my laboratory group for all the advice and technical help they have given me, at the Institute of Integrative Biology, University of Liverpool. I would like to acknowledge Dr Thamir Ismail, Dr Christopher Clarke, Dr. Min Du, Dr. Dominic P Byrne and Dr. Richard Thomas Smith for their help and advice in tissue culture and laboratory techniques, Mrs Angela Platt-Higgins for her help and advice with immunohistochemistry and data analysis.

I gratefully acknowledge financial support from the University of Kufa, Ministry of Higher Education and Scientific Research-Iraq (MOHESR) and the Iraqi Cultural Attaché, London for making this research possible and enabling me to obtain this degree.

I wish to express my thanks and gratitude to my parents, the ones who can never ever be thanked enough, for the overwhelming love and care they bestowed upon me, and who have supported me financially as well as morally, and without whose proper guidance, it would have been impossible for me to complete my higher education.

My special, profound and affectionate thanks, love, affectionate gratitude and deep indebtedness are due to my wife, who has been struggling with me, hand in hand, to secure and shape a brighter future. Her understanding, support, commitment and looking after my children during my study, all stand behind my success. At the same time, I would like to express my love and thanks to 'the beats of my heart', my children, who are the source of inspiration to me, and it is their love and innocent smiles that have made the hardship of this task bearable. My deep love and thanks are due to my brothers, sisters and the entire family.

The relationship between metastasis-inducing S100 proteins (MIPs) and matrix metalloproteinases (MMPs) in rat and human breast cancer

Morteta H. Al-Medhtiy

Abstract

Breast cancer metastasis is the most common cause of death amongst females worldwide. The presence of metastasis-inducing proteins such as S100P or S100A4 in primary breast tumours has been reported to be associated with a reduction in patient survival times *in vivo* and these proteins enhanced cell migration and invasion *in vitro* as well. However, the pathway of S100P/A4 in inducing metastasis or cell migration/invasion is still controversial and not clear. To investigate the role of matrix metalloproteinases as mediators of S100P/A4-stimulated cell migration/invasion, human HeLa and rat mammary 37 (R37) and S100P/A4 overexpressing cell lines (R37-S100P/A4) were used to demonstrate levels and activities of matrix metalloproteinases (MMPs) using antibody arrays, zymography and Western blots. siRNAs to specific MMPs and direct addition of S100 proteins were used to measure effects on cell migration and invasion. Primary tumours from 183 breast cancer patients were immunohistochemically stained to investigate the association between MMPs and S100 proteins and their effect on patients' survival times using relative association and Cox's multivariate regression analysis. *In vitro*, R37-S100P/A4 cells significantly ($P \leq 0.035$) produced only MMP-2, -9 and -13. In addition, MMP-2 and MMP-13 showed significant (Student's t-test, $P \leq 0.031$) proteinase activity (active and pro forms) on specific substrates, but MMP-9 showed only the inactive proform. Knock-down of each MMP significantly reduced R37-S100P/A4 cell migration and invasion ($P \leq 0.037$). Extracellular additions of S100P/A4 to R37 cells caused significant increases in these same MMPs ($P \leq 0.026$) and in cell migration and invasion ($P \leq 0.025$). RAGE receptor levels were expressed significantly higher in invasive carcinoma R37-S100P/A4 cells compared to control R37 cells. When the RAGE receptor was inhibited, it caused a significant reduction in R37-S100P/A4 ($P \leq 0.037$) or S100P/A4-treated R37 wt cell ($P \leq 0.007$) invasion. *In vivo*, the presence of one of S100P, S100A4, MMP-2, MMP-9 and MMP-13 showed significant reduction in patients' survival times. There was a strong association between MMPs and S100P/S100A4 and both S100 proteins partially confounded the MMPs effect on patients' survival times and death-risk. Since manipulation of the levels of S100P/A4 and the three MMPs caused changes in cell migration/invasion, the three MMPs are probably some of the S100 downstream effectors, particularly for cell invasion. Moreover, there was more association of one S100 protein with a particular MMP in cultured cells and in human breast tumours, suggesting that different S100 proteins are likely to promote selective enhancement of individual MMPs. This conclusion may explain the observed synergistic effect (Wang et al., 2006) of the combination of S100P and S100A4 on early patient demise in breast cancer.

Table of Contents

List of Figures

List of Tables

Appendices

Abbreviations

AGEs	**Advanced glycation end products proteins**
APS	**Ammonium persulphate**
ATF4	**Activating transcription factor 4**
BCA	**Bicinchonic acid assay for protein normalization**
BSA	**Bovine serum albumen**
BxPC3	**Biopsy xenograft of Pancreatic Carcinoma cell line-3**
CaP	**Human prostate cancer**
cDNA	**Complementary deoxyribonucleic acid**
CK14	**Cytokeratin 14**
CK5/6	**Cytokeratin 5/6**
CL	**Cell lysate**
CM	**Conditioned media**
CO_2	**Carbon dioxide**
Cys^{73}	**Cysteine residue number 73**
dH_2O	**Distilled water**
DMEM	**Dulbecco's modified Eagle's Medium**
DMSO	**Dimethyl sulphoxide**
DPX	**Distyrene, a plasticizer and xylene**
ECM	**Extracellular matrix**
EMMPRIN	**Extracellular matrix metalloproteinases inducer**
ERBB-2	**Receptor tyrosine protein kinase-2**
ERK1/2	**Extracellular signal–regulated kinases 1 and 2**
ERα	**Estrogen receptor α**
FCS	**Fetal calf serum**
FISH	**Fluorescence in situ hybridization**
FSM	**Full supplemented media**
g/L	**Gram/litre**

GAPDH	**Glyceraldehyde-3-phosphate dehydrogenase**
HeLa A3	**Henrietta Lacks subclone A3**
HER2	**Human epidermal growth factor receptor 2**
HMGB-1	**High mobility group box-1**
IHC	**Immunohistochemistry**
IκBα	**Nuclear factor of kappa light polypeptide gene enhancer in B-cell inhibitor, alpha**
JNK	**C-Jun N-terminal kinase**
kDa	**kilo dalton**
MAPK/ERK	**Mitogen activated protein kinase / Extracellular signalling-regulated kinase**
MDA-MB-231	**M.D. Anderson - metastatic breast-231**
mg/mL	**Milligram/millilitre**
MIPs	**Metastasis-inducing proteins**
mM	**Millimolar**
MMP	**Matrix metalloproteinase**
mRNA	**Messenger ribonucleic acid**
MT-MMP	**Membrane-linked type of matrix metalloproteinase**
NEAA	**Non-essential amino acids**
NFκB	**Nuclear protein factor kappa-light-chain-enhancer of activated B cells**
ng/mL	**Nanogram/millilitre**
nM	**Nanomolar**
NMIIA	**Non-muscle myosin IIA**
NSAIDs	**Non-steroidal anti-inflammatory drugs**
PDAC	**Pancreatic ductal adenocarcinoma**
proMMP-13	**Proform of MMP-13**
Pyk-2	**Phosphorylation of protein tyrosine kinase-2**
RAGE	**Receptor for advanced glycation endproducts**
Rama 37	**Rat mammary 37**

RECK	**Reversion-inducing cysteine-rich protein with Kazal motifs**
RO	**Reverse osmosis purified water**
siRNA	**Small interfering RNA**
TBS-T	**Tris buffer saline – Tween 20**
TCA	**Trichloroacetic acid**
TEMED	**N, N, N', N'-tetramethylethylenediamine**
TGF-β	**Transforming growth factor-beta**
TIPMs	**Tissue inhibitors of metalloproteinases**
TRAMP	**Transgenic adenocarcinoma of the mouse prostate**
v/v	**Volume/volume**
w/v	**Weight/volume**
Zn^{2+}	**Zinc ion**
µg/mL	**Microgram/millilitre**
R37 wt	**Parental rat mammary 37 wild type cells**

Chapter 1

Introduction

1.1 Breast cancer

The most commonly diagnosed cancer, which causes death among women worldwide is breast cancer (Moravkova et al., 2016). The three most common cancers are breast, lung, and colorectum, which collectively represent one-half of all cases; breast cancer alone accounts for 30% of all new cancer diagnoses in women (Siegel et al., 2018). Metastasis is the greatest cause of breast cancer mortality in females. Breast cancer is a malignant tumour, which begins in the cells of breast tissues. This type of cancer is able to invade and spread beyond its original location (metastasise) and to populate other organs in the body, such as the liver, brain or bone (Cancer Facts & Figures, 2014). Unfortunately, metastasis can occur early in the development of cancer. Therefore, there is an urgent need to stop and/or reduce metastasis in breast cancer at an early stage, before it becomes life threatening.

1.1.1 Breast cancer subgroups

Previously, breast cancer has been divided into two main groups: 80-90% ductal carcinoma and 5-15% lobular carcinoma, both typically initiated from the terminal ductal lobular units (de Silva Rudland et al., 2011; Wellings et al., 1975). Recently, by using microarray gene expression profiling techniques, breast cancer has been divided into five subgroups; two luminal-like (A and B), one ERBB-2 type

(HER2-overexpressing), one normal breast tissue-like and one basal-like category (Sorlie et al., 2003). The luminal type subgroups present some similarities to the expression of mRNAs which exist in normal luminal epithelial cells and both are positive for estrogen receptor α (ERα) using immunohistochemistry (IHC). The ERBB-2 subtype produces large amounts of the c-erbB-2 receptor, this protein is identified by IHC and by amplification of its gene using FISH (fluorescence in situ hybridization). The normal breast tissue-like subtype expresses genes entirely typical of normal luminal epithelial cells and contains less ERα compared to the Luminal A and B subtypes. The basal-like subtype produces the stratified epithelial cytokeratins CK5/6 and CK14 which are usually found in basal epithelial and myoepithelial cells of the breast (Moll et al., 1982; Sorlie et al., 2003). The basal-like subtype lacks other markers, like smooth muscle actin/myosin which are usually observed in completely differentiated myoepithelial cells (Rudland et al., 1993). Researchers have found that the protein markers CK5/6 and CK14 of the basal-like subtype are associated with high grade breast cancer and poor patient prognosis (de Silva Rudland et al., 2011; Fan et al., 2006). But what actually kills patients is the process of metastasis.

1.2 Metastasis

Metastasis is a complicated process and is still the greatest challenge in the management of cancer (**Figure 1.1**). In fact, metastasis may occur after many years from first diagnosis, or before the first diagnosis of primary cancer. There are several hypotheses to explain the metastatic process, but none of these entirely explain the biological and clinical events (Nguyen, 2004). In general, a cancer cell is required to follow a sequential series of steps, before it establishes itself at a secondary cancer

site. Usually, but not always, these steps involve detachment from the primary tumour, invasion throughout the adjacent tissues, access to, survival in and exit from circulatory (blood and lymphatic) systems or even in the peritoneal space, and finally survival and growth in a secondary target (Al-Mehdi et al., 2000).

Patients with only a primary tumour have a better prognosis compared to those with an additional metastasis (Nguyen, 2004; Stetler-Stevenson et al., 1993). The initial steps of metastasis are believed to occur as an early event, often even before the diagnosis of the primary tumour (Schmidt-Kittler et al., 2003). Therefore, metastasis is the most important aspect in the clinical management of cancer after removal of the primary tumour. The next step in the description of metastatic cancer is to determine those proteins which control this process.

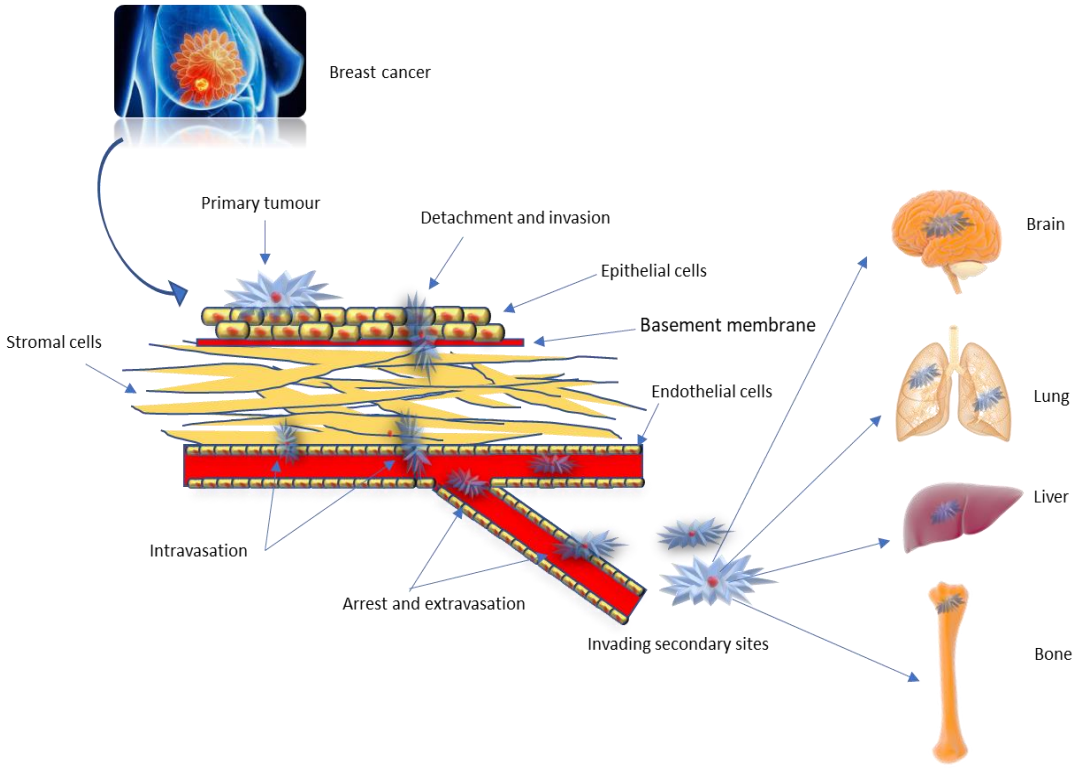

Figure 1.1: Illustration of the most common steps which metastatic breast cancer cells follow to migrate and localise in a distant organ. This figure was modified from Nguyen (2004).

1.2.1 Metastasis-inducing proteins (MIPs)

Metastasis-inducing proteins (MIPs) have been discovered in experimental rodents and these proteins can induce the metastatic process. These MIPs include S100A4 (Davies et al., 1993) , osteopontin (Oates et al., 1996), anterior gradient-2 (Liu et al., 2005) and S100P (Wang et al., 2006). The metastasis-inducing proteins (MIPs) also occur in normal tissue, but much more is known about them in relation to cancer (Fei *et al.*, 2017).

1.2.2 S100 protein family

The name S100 is derived from the ability of most members of this family to be soluble in 100% (w/v) ammonium sulphate at neutral pH (pH 7.0-7.5) (Deloulme et al., 2002; Moore, 1965). The first member of the S100 family of proteins was identified in bovine brain (Moore, 1965). This family has 25 members in humans (Moravkova et al., 2016), which consists of 16 S100A (S100A1-S100A16) as well as others, such as S100B, S100G, S100P and S100Z (Gross et al., 2014). They are characterized by being low-molecular-weight acidic polypeptides (9-13 kDa) (reviewed in Donato, 2003; Gross et al., 2014; Bresnick et al., 2015; Moravkova et al. 2016). The most common feature of all the S100 proteins is a pair of calcium-binding, helix-loop-helix domains which include EF hand, calcium-binding regions situated towards the protein termini; they are divided by a hinge region (Gross et al., 2014). S100 proteins have been reported to possess a wide spectrum of substantial intracellular and extracellular functions (Moravkova et al., 2016).

The presence of some of these S100 proteins, e.g., S100P and S100A4 in the primary breast tumour shows a strong correlation with early death of patients and, therefore, a poor prognosis in cancer patients (Rudland et al., 2000; Wang et al., 2006), in part, due to their ability to induce migration of cancer cells to a secondary location (Jenkinson et al., 2004; Wang et al., 2006). Increased expression of certain S100 proteins has been reported in several types of cancer, such as those of the breast, lung, bladder, kidney, thyroid, stomach, prostate and oral cancers (Salama et al., 2008). A recent study has suggested that expression of S100 proteins in cancerous tissues and serum of patients might be used as a diagnostic and prognostic marker and as a target for therapy (Moravkova et al., 2016). When introduced into

experimental syngeneic animal models, overexpression of S100A4 can enhance metastatic potential of a benign rat mammary (Davies et al., 1993) and bladder tumour (Levett et al., 2002) cell line. Moreover, overexpression of S100P can promote tumour growth in many other tumour models, such as those from the lung, prostate, colorectum, pancreas, as well as tumour cell proliferation in certain animal cells (Bresnick et al., 2015; Wang et al., 2006). In contrast, other members of the S100 family can cause tumours to be suppressed, for example S100A2 in malignant melanoma (Maelandsmo et al., 1997), in prostate (Maelandsmo et al., 1997), lung (Feng et al., 2001) and in breast cancer (Liu et al., 2000).

1.2.2.1 S100A4 protein

S100A4 (11 kDa protein with 101 amino acids) has been reported to be a biomarker for poor patient outcome in cancer prognosis, such as breast (Rudland et al., 2000) and colorectal cancer (Gongoll et al., 2002). The nuclear expression of S100A4 is also reported to be a prognostic marker for colorectal cancer (Boye and Maelandsmo, 2010). The association between patient survival times and expression of S100A4 has been reported in many types of cancers, including pancreatic cancer, non-small cell lung cancer, stomach cancer, ovarian carcinoma (reviewed by Boye and Maelandsmo, 2010). S100A4 can increase cell motility and invasion in cancer cell lines of the breast, colorectum, pancreas, lung and esophageal squamous epithelium (Jenkinson et al., 2004). *In vitro,* S100A4 expressed intracellularly can regulate cell motility in renal proximal tubular epithelial cells via epidermal growth factor (EGF) and TGF-β1 stimulation, which can lead to more elongated cells (mesenchymal, fibroblastic morphology) (Okada et al., 1997; Strutz et al., 1995). *In vivo* S100A4 can

induce invasion of epithelial cells into the mammary fat pad by branching morphogenesis via TGF-β-related pathways (Gross et al., 2014), possibly mediated by matrix metalloproteinase-3 (MMP-3) (Andersen et al., 2011). Overexpression of S100A4 in tumour cells *in vitro* led to significant changes in the cells' architecture, producing a more mesenchymal behaviour of the cells (Davies et al., 1993). This change occurred via reorganization of the cytoskeleton and motility-related protrusions, with significantly increased numbers of lamellipodial projections, some to focal adhesions on the leading edge of the cell (Li and Bresnick, 2006). These changes are caused predominantly by the binding of intracellular S100A4 to non-muscle myosin IIA. Addition of S100A4 to cultured cells could also enhance cell motility of the smooth muscle cells of human pulmonary arteries (Li and Bresnick, 2006). The enhancing activity of exogenously-added S100A4 may be due to the release and stimulation of MMP-13 (Vicente-Manzanares et al., 2007), perhaps via specific cell surface receptors such as annexin 2/plasmin (Semov et al., 2005) and/or RAGE (Lawrie et al., 2005).

1.2.2.2 S100P protein

S100P is another member of the S100 protein family and consists of 95-amino acids. Its overexpression has been associated with drug resistance, metastasis and poor clinical outcomes (Arumugam and Logsdon, 2011). It was originally purified from placenta, hence the P designation (Becker et al., 1992). S100P has a unique location on human chromosome 4q16, while most other members of the S100 protein family are juxtaposed together on human chromosome 1 (Schäfer et al., 1995). S100P has been reported to be associated with poor clinical outcomes in

several types of cancer, such as breast, colon, pancreas, prostate and lung cancer (reviewed in Arumugam & Logsdon, 2011).

S100P, in common with S100A4, enhances cellular motility in several various diseases, such as cancer (Du et al., 2012) and is increased in endometriosis (Hapangama et al., 2012). In pancreatic cancer, S100P is one of the most frequently overexpressed genes which might make it a useful histological marker (Schäfer et al., 1995). In breast cancer, activation of c-ERB-B2 enhances breast cancer cells to express S100P (Mackay et al., 2003). Overexpression of intracellular S100P in a human breast cancer cell line is able to enhance cellular motility (Zhou et al. 2012). *In vivo*, upregulating the level of intracellular S100P by overexpression from transgenes enhanced cell invasion and metastasis (Barry et al., 2013; Wang et al., 2006), while down regulation of expression of S100P leads to a reduction in both cell migration and formation of secondary lesions (Jiang et al., 2011). S100P protein is associated with a decrease in patients' survival times in human breast cancer, and when overexpressed, induces metastatic properties in otherwise benign rat mammary tumour cells (Wang et al., 2006). Like S100A4, S100P also can directly interact with non-muscle myosin IIA to cause an increase in cell motility (Du et al., 2012). Moreover, expression of S100P intracellularly in cancer cells has been linked to promoting destabilization of DNA methylation patterns by hypomethylation of specific genes (Sato et al., 2004).

Addition of extracellular S100P has been reported to activate intracellular signalling via binding to extracellular receptors of advance glycation end protein (RAGE), and in this way it might also increase tumour growth, drug resistance and metastasis in pancreatic and colon cancer cell lines (reviewed in Arumugam &

Logsdon 2011). A further study on MKN45, and Kato III (human carcinoma cell lines derived from the stomach) has shown that when S100P was overexpressed in isolated tumour samples, it can function both via intracellular and extracellular pathways (Namba et al.2009). This latter study also found that up-regulation of S100P could be caused by addition of non-steroidal, anti-inflammatory drugs (NSAIDs) like celecoxib. This up-regulation of S100P was suppressed by silencing the activating transcription factor 4 (ATF4). Silencing this factor resulted in a suppression of the cells' invasive ability, which may happen due to suppression of the S100P-RAGE interaction, cell growth and level of MMP-9 expression (Namba et al.2009). Thus, the S100 proteins are important in promoting the process metastasis and the next step is to investigate their main downstream targets, one of these is the family of proteases known as matrix metalloproteinases (MMPs) (Berge and Mælandsmo, 2011; Mishra et al., 2012; Saleem et al., 2006).

1.3 Matrix metalloproteinases (MMPs)

MMPs are family of zinc-dependent and calcium-containing endopeptidases, which are able to degrade most of the components of the extracellular matrix (ECM) such as elastin, collagen, fibronectin, laminin, gelatin and vitronectin (reviewed in Liotta et al., 1980). This family has 26 members, some of which can be produced by the cancer cells themselves; for example MMP-2 and MMP-9 are secreted by cervical and ovarian cancers, respectively (Roomi et al., 2010). Some MMPs are secreted by the cells immediately surrounding the tumour. For example, MMP-13 is expressed by stromal cells immediately adjacent to the tumour cells, as well as in the cancer cells themselves in breast cancer (Leeman et al., 2002). Therefore, the reactive stromal

cells round a beast tumour may participate in degradation of the extracellular matrix and basement membrane (Salamonsen, 1996). Thus, MMPs from both cancer cells and host stromal cells may play a significant role in remodelling and degradation of the extracellular matrix (ECM).

MMPs are classified according to their substrate specificity into matrilysins, stromelysins, gelatinases and collagenases **(Table 1.1)**. The MMPs in general have four prominent domains: the N-terminal pro-domain; the catalytic domain which is approximately spherical with a diameter of roughly 40 Å and is almost the same in all types of MMPs; the hinge region; and the C-terminal hemopexin-like domain. The last domain may be responsible for interaction with tissue inhibitors of metalloproteinases (TIMPs) and appears to be regulating the enzymic activity of most of the MMPs, except MMP-7 and MMP-26 (reviewed in Verma and Hansch, 2007). Additionally, the membrane type of MMPs (MT-MMPs) have transmembrane and cytoplasmic domains (Cathcart et al., 2015; Sela-Passwell et al., 2010; Skiles et al., 2000; Verma and Hansch, 2007) **(Figure 1.2).**

In pathological processes, MMPs have a crucial role in cancer cell invasion, migration and tumorigenesis (Liotta et al., 1980; Stetler-Stevenson, 2001, 1990). MMP-2 and MMP-9 are reported to play a critical role in invasion and metastasis in breast, cervical and ovarian cancers (Freije et al., 1994; Roomi et al., 2010). MMP-2 and MMP-9 are gelatinases (gelatinase A and gelatinase B, respectively) that cleave relatively-unwindable collagen fibrils of both collagen I and III, which themselves have been previously cleaved by other collagenases, e.g. MMP-1, 8 or 13. Moreover, gelatinases are able to cut other types of nonfibrillar collagens and extracellular

matrix elements such as collagen IV, small-diameter fibrillary collagen V, epithelial-anchoring collagen VII and elastin (Birkedal-Hansen, 1995).

Table 1.1. Subgroups of MMP family with their respective substrates [a].

Subgroup	MMP [b]	Name	Substrate
Collagenases	MMP1	Collagenase-1 (Interstitial collagenase)	Collagen I, II, III, VII, VIII, X, gelatin
	MMP8	Collagenase-2 (Neutrophil collagenase)	Collagen I, II, III, VII, VIII, X, aggrecan, gelatin
	MMP13	Collagenase-3	Collagen I, II, III, VII, VIII, X, gelatin, casein
Gelatinases	MMP2	Gelatinase A	Gelatin, collagen, I, II, III, IV, VII, X
	MMP9	Gelatinase B	Gelatin, collagen, IV, V
Stromelysins	MMP3	Stromelysin-1	Collagen II, IV, IX, X, XI, gelatin
	MMP10	Stromelysin-2	Collagen IV, laminin, fibronectin, elastin
	MMP11	Stromelysin-3	Collagen IV, aggrecan, laminin, fibronectin
Matrilysins	MMP7	Matrilysin-1	Fibronectin, laminin, collagen IV, gelatin
	MMP27	Matrilysin-2	Fibrinogen, fibronectin, gelatin
MT-MMP [c]	MMP14	MT1-MMP	Gelatin, fibronectin, laminin
	MMP15	MT2-MMP	Gelatin, fibronectin, laminin
	MMP16	MT3-MMP	Gelatin, fibronectin, laminin
	MMP17	MT4-MMP	Fibrinogen, fibrin
	MMP24	MT5-MMP	Gelatin, fibronectin, laminin
	MMP25	MT6-MMP	Gelatin
Others	MMP12	Macrophage Metalloelastase	Elastin, fibronectin, collagen IV
	MMP19		Aggrecan, elastin, fibrillin, collagen IV, gelatin
	MMP20	Enamelysin	Aggrecan
	MMP21	XMMP [d]	Aggrecan
	MMP23		Gelatin, casein, fibronectin
	MMP27	CMMP [e]	Unknown
	MMP28	Epilysin	Unknown

[a] Schmidt-Hansen et al. 2004; Snoek-van Beurden & von den Hoff, 2005.

[b] Matrix metalloproteinase.

[c] Membrane type of matrix metalloproteinase.

[d] *Xenopus laevis* matrix metalloproteinase is an additional insertion of approximately 30 amino acids between the pro-domain and the catalytic domain of MMP (Ahokas et al., 2002).

[e] Cloned matrix metalloproteinase from cultured primary chicken embryo fibroblasts (Yang and Kurkinen, 1998).

Another MMP often reported in human cancer is MMP-13. MMP-13 (54, 60 kDa) is a member of the collagenase subfamily. MMP-13 is reported to be secreted by reactive tumour stromal fibroblast-like cells, e.g., myofibroblasts (Crawford and Matrisian, 1996; Engelholm et al., 2001; Nielsen et al., 2001), as well as by the tumour cells themselves (Nielsen et al., 2001), e.g., invasive breast carcinoma cells (Balduyck et al., 2000). MMP-13 produces a single cleavage in a small section of unwound triple helix of fibrillar collagen I, II and III. This cleavage allows comprehensive denaturation of the native, tight, triple helix form of fibrillar collagens which, in turn, allows further digestion by the gelatinases into small soluble peptides (Armstrong and Jude, 2002; Stechmiller et al., 2010). How this digestion process occurs is described in the next section.

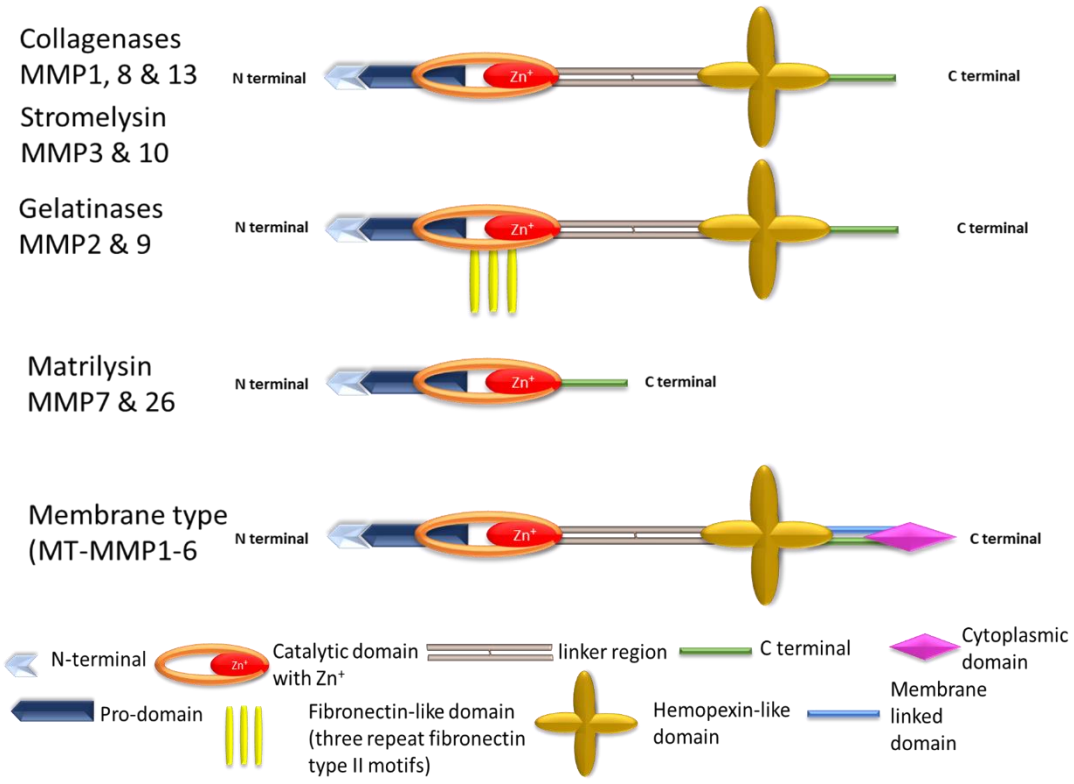

Figure 1.2. The structural form and domains of MMP members. Abbreviations: Matrix metalloprotein, MMP; Membrane type – matrix metalloprotein, MT-MMP.

1.3.1 Molecular activation of MMPs

Activation of MMPs is regulated at several levels, starting with gene transcription and the synthesis of proenzymes. Moreover, their activity is usually terminated by TIMPs which can inhibit the active MMPs and underpin substantial regulatory processes (Springman et al., 1990; Van Wart and Birkedal-Hansent, 1990). MMPs are first produced as an inactive zymogen, which requires activation. The propeptide domain possesses a cysteine residue (Cys), which acts as a stabilizer of the proMMP. The catalytic domain has a Zn^{2+} binding site which binds to the Cys forming the pro-form of MMP. Activation occurs when the bond between Cys - Zn^{2+} breaks, and this mechanism is called “the cysteine switch”. After the cysteine switch, a water molecule binds to the Zn^{2+} ion to replace the cysteine residue and converts the noncatalytic zinc to a catalytic zinc, leading to creation of an intermediate active form of enzyme. In addition, full activation occurs when the propeptide becomes removed by autolytic cleavage or by the action of other enzymes. Usually the molecular weight of the cleaved part is about 8-10 kDa , which results in an active enzyme with lower molecular weight compared to the proenzyme form(Park et al., 1991; P. A. M. Snoek-van Beurden and Von den Hoff, 2005).

1.3.2 Cellular activation and inhibition of MMPs

Activation steps can be accomplished by endopeptidases, catalysed by other MMPs and by several inorganic compounds. MMP-13 (collagenase-3) assumes a key position in the MMPs’ activation processes and results have been obtained from more than one human cell line (Leeman et al., 2002). MMP-13 is formed first as a zymogen and activation occurs by cleavage of the N-terminal propeptide by

autoproteolytic activity, as is the case for other MMPs and by other inductive factors such as circulating hormones. In normal physiological conditions, tissue inhibitors, TIMPs are capable of inhibition of MMP-13 in a 1:1 molar ratio, but this ratio can be changed in pathological conditions (Leeman et al., 2002). Stromelysin-1 (MMP-3) is able to activate proMMP-13 in a concentration-dependent manner (Knäuper et al., 1996). MMP-2 (gelatinase-A) and membrane-type metalloproteinase (MT1-MMP) are also able to activate proMMP-13 to a fully active form (Knauper et al., 1996). The activation process for proMMP-13 by MT1-MMP is enhanced by the presence of proMMP-2, thereby demonstrating a distinctive new activation cascade involving three members of the MMP family. During the activation process of proMMP-13 by MT1-MMP, the latter also generates active MMP-2 which, in turn, contributes to forming active MMP-13 (Knauper et al., 1996).

Fibroblasts express MT1-MMP when stimulated by concanavalin-A. Fibroblast-derived plasma membranes are able to activate an intermediate form of MMP-13 to full activation in the presence of proMMP-2 (Knauper et al., 1996; Matthew F. Leeman et al., 2002). Plasmin activates MMP-13 by cleaving the N-terminal propeptide domain. In addition, autoproteolysis occurs; this leads to release of the rest of the propeptide domain at the N-terminus and results in active MMP-13 (Knauper et al., 1996). Active MMP-9 (gelatinase-B) is generated when MMP-2 and MMP-13 are activated (Knauper et al., 1997). In a human chondrosarcoma cell line SW1353, MMP-1 (collagenase-1) and MMP-13 (collagenase-3) were shown to have separate independent mechanisms for activation. Activation of MMP-1 is independent of the activation pathways of MMP-2, MMP-9 and MMP-13 (Cowell et al., 1998). Finally, hormones such as parathyroid hormone can influence the ratio of

MMP-13 degradation and activation (Leeman et al., 2002; Orgaz et al., 2014), presumably indirectly by influencing gene transcription and thereby protein degradation.

1.4 Breast cancer metastasis and the relationship between matrix metalloproteinases and metastasis-inducing proteins S100P and S100A4

There are several barriers that cells must pass through to reach the secondary tumour site during the metastatic process. One of the major barriers is a continuous collagen-containing structural barrier produced around and in response to the tumour; this barrier also exists naturally in several organs of the body. Thus, invasion and spread of tumour cells within the primary tissue need degradation of the extracellular matrix (ECM) and other insoluble proteinaceous molecules by a sufficient number of degradative enzymes (Barsky et al., 1983; Kim et al., 2012). Moreover, intravasation and extravasation processes require the breakdown of the ECM and basement membrane barriers which underlie endothelial cells, before the cancer cells can enter or leave the circulatory systems, respectively, prior to their deposition at secondary sites. In addition, tumour-associated host cells, particularly the surrounding stromal tissue and tumour- infiltrating immune cells, may also play crucial roles in producing some of these degradative enzymes (Barsky et al., 1983; Chambers and Matrisian, 1997). There have been many studies in the past that have shown that malignant tumour cells can produce enhanced proteolytic activity which is efficient in degrading collagen *in vitro* (e.g. Salo et al., 1982). The development of biochemical and molecular biological techniques have helped to identify individual

proteases in the tumour and many may play crucial roles in these digestive activities (Salo et al., 1982). The major classes of proteases which have been associated with malignant tumours are serine, aspartic, cysteine, threonine and metalloproteinases (Brünner et al., 1994).

Perhaps the most important proteases in cancers are the MMPs, since they are able to degrade the ECM and basement membrane, the principle components through which the cancer cells have to pass. Type IV collagen is the main structural protein in basement membranes (Kalluri, 2003; Tanjore and Kalluri, 2006). MMP-2 (Gelatinase A) or MMP-9 (gelatinase B) is responsible for degradation of type IV collagen; they possess molecular weights of 66 - 72 kDa and 82 - 92 kDa, respectively. The most common three subgroups of MMPs found in cancers can be identified by their substrate preferences: the collagenases (e.g. MMP-13, 54 - 60 kDa), the stromelysins (MMP-1, 10 & 11), and gelatinases (e.g. MMP-2 and MMP-9). The collagenases digest fibrillar collagens, stromelysins degrade proteoglycans/glycoproteins, and gelatinases digest nonfibrillar collagens (gelatin) (**Table 1.1**) (reviewed in Chambers and Matrisian, 1997; Stechmiller, Cowan and Schultz, 2010) Thus, one promising target for the treatment of cancer are the matrix metalloproteinases or MMPs. There is also a strong association of specific MMPs e.g., MMP-2, MMP-9, MMP-13, MMP-1 and MMP-7 with malignant tumour pathologies (Verma and Hansch, 2007). Therefore, there is an urgent need to examine the production of active MMPs and their relationship with other major players that can induce metastasis, particularly the most widespread proteins in metastatic cancers, the S100 proteins, S100A4 and S100P.

The direct relationship between S100 proteins and the MMPs has been established in two different ways. Firstly, by overexpressing the S100 proteins intracellularly in tissue cultured cells and secondly by directly adding exogenously the S100 proteins to noncancerous cells (Bresnick et al., 2015). Thus, when S100A4 is overexpressed in a transgenic adenocarcinoma of the mouse prostate (TRAMP) model, its overexpression is associated with metastasis (Saleem et al., 2006) and with the level of gene expression and proteolytic activity of MMP-9 and its tissue inhibitor TIMP-1. There is also a positive correlation between overexpression of S100A4 and of MMP-13 in a breast cancer cell line MDA-MB-231 *in vitro* and *in vivo* (Wang et al., 2012). Thus, upregulation of S100A4 can cause an increase in MMP-13 and this increase led to increased cell migration and angiogenesis in the MDA-MB-231 breast cancer cell line. However, although downregulation of S100A4 by siRNA treatment lead to the anticipated downregulation of MMP-13, it produced cells with little significant effects on cell migration and angiogenesis (Wang et al., 2012), suggesting involvement of other factors. These studies suggest that the invasion process may be regulated, in part, by intracellular S100A4, in turn regulating MMP-13 levels, at least in model breast cancer systems. Furthermore, genetic studies in a *Drosophila* model have shown that overexpression of mutant Ras ^{Val12} and S100A4 increased the activation of the stress kinase JNK and the level of *Drosophila* MMP-1; all these components in that order were required to enhance greatly invasion and metastasis (Ismail et al., 2017).

When S100A4 was added extracellularly to the human pancreatic cancer cell line BxPC3, it stimulated the IκB signalling pathway and MMP-9 secretion, which in turn lead to stimulation of cell proliferation and invasion and mAbs against S100A4

block these activities (Dakhel et al., 2014). Moreover, when Zhang et al. (2011) added S100A4 extracellularly to endothelial cells, it stimulated angiogenesis by the paracrine production of MMP-13, and thereby facilitated cell invasion into the surrounding tissue (Ambartsumian et al. 2001; Schmidt-Hansen et al. 2004; Sack & Stein 2009; Donato et al. 2013).

It appears that S100 proteins may function both intracellularly and extracellularly in the same system. Thus, when intracellular S100P was induced from a transfected transgene in Rama 37-T25 or HeLa-A3 cells, substantial changes occurred in cytoskeletal organisation *in vitro* in both rat mammary or in human cervical cancer HeLa cells. These changes, in turn, created a disturbance in the formation and stability of cellular focal adhesions (FA). The combination of the changes in the cytoskeleton and FA was responsible, in part, for the observed increase in cell migration (Du et al., 2012). However, when 100 nM S100P was added externally to uninduced Rama 37-T25 or HeLa-A3 cells, it failed to produce a significant increase in cell migration, but instead caused a very significant increase in cell invasion through a collagen I artificial matrix (Du et al., 2012). This result suggested that extracellularly-added S100P stimulated an unknown product which could partially digest the artificial collagen I matrix in the Boyden chambers, most likely a protease like the MMPs. Thus, intracellular and extracellular S100A4 or S100P from both tumour and host stromal sources, respectively, can mediate breast cancer progression and metastasis in a model system. The types of stromal cells which contribute to S100-mediated cancer dissemination are not well described. But both reactive myofibroblasts and endothelial cells produce S100A4 and additionally

endothelial cells secrete MMPs (Bresnick et al., 2015), so any one or both these cell types could make such a contribution *in vivo*.

Zhang et al., (2011) found overexpression of S100A4 mRNA and increased levels of MMP-9 proteolytic activity in specimens from 16 osteosarcoma patients who had lymph node or distant metastases. Moreover, in specimens of human breast cancer, the levels of MMP-2, MMP-9 or MMP-13 alone correlated with patient demise from metastatic disease and these MMPs were produced in the same cells as those expressing S100A4 (Ismail et al., 2017). The most frequent reports of links between S100 proteins and MMPs concern MMP-13 (Uría et al., 1997; Wang et al., 2012), followed by MMP-9 and MMP-2 (Dakhel et al. 2014; Freije et al. 1994; Roomi et al. 2010). Finally, studies by Yammani et al. (2006) have shown that S100A4 can bind to a receptor called RAGE and its binding can stimulate the expression of MMP-13 by a signalling cascade in human articular chondrocytes. The RAGE receptor would appear to be one of the main initial targets for surface-acting S100 proteins (Leclerc et al., 2009).

1.5 Receptor for advanced glycation end products (RAGE) and S100 proteins/MMPs

1.5.1 RAGE receptor

The receptor for advanced glycation end products (RAGE) is a receptor capable of binding to advanced glycation end product proteins (AGEs). RAGE occurs at the cell surface and is defined as a single transmembrane multi-ligand receptor of the immunoglobulin gene superfamily (reviewed by Chuah et al. 2013). This receptor is capable of binding to diverse ligands, these ligands lack sequence similarities due

to RAGE's ability to recognize three-dimensional structures instead of specific amino acid sequences (reviewed by Chuah et al. 2013). The RAGE receptor consists of an intracellular tail domain, transmembrane domain, two C-type domains (C1 & C2 type) and an N-terminal V-type domain. The V-type domain is the active site responsible for interaction with potential extracellular ligands (Bopp et al., 2008; Chuah et al., 2013; Schmidt et al., 2001).

RAGE receptor was discovered in 1992 and since that time it has been reported to be involved in a broad spectrum of human diseases such as diabetes, chronic inflammation, Alzheimer's disease (Leclerc et al., 2009), cardiovascular diseases, osteoarthritis and most importantly cancer (Xie et al., 2013), particularly breast cancer (Radia et al., 2013). In breast cancer, the role of RAGE in tumour development and cell proliferation is still unknown, but its expression levels are associated with the degree of severity of the disease (Radia et al., 2013). This receptor has been reported to be highly expressed throughout normal development, predominately in the brain, but its expression level falls in aged and mature tissues. Thus, low levels of RAGE have been found in neurons, uterus smooth muscle, kidney glomerulus mesangial cells, mononuclear phagocytes, hepatocytes and cardiac myocytes, while in lung and skeletal muscle tissues with appreciable turnover rates, it is found in high levels but its role unlike that in metastasis is unknown (Brett et al., 1993).

1.5.2 RAGE-S100 protein interactions and MMPs

As stated above RAGE can be stimulated by many ligands such as advanced glycation end products (AGE) (Schmidt et al., 1992), β-amyloid peptide (Deane et al., 2003), amphoterin (HMGB1) (Hori et al., 1995), and members of the S100 protein family (Hofmann et al., 1999; Schmidt et al., 2000). The specific S100 proteins that can interact with the RAGE receptor include the following: S100B, S100A1, S100A2, S100A4, S100A5, S100A6, S100A7, S100A8, S100A9, S100A11, S100A12, S100A13 and S100P (Leclerc et al., 2009). How S100 proteins are secreted extracellularly is still controversial, due to their lack of a signal peptide for secretion via the traditional Golgi apparatus-mediated pathway. Also, the reasons for their occurrence extracellularly is still controversial, particularly whether they are secreted somehow from living cells or are released from dying lysed cells (Bresnick et al., 2015). Nevertheless, studies by Perrone et al. (2008) showed that secretion of S100B could occur in secretory vesicles and this process required phosphorylation of caveolin-1 and depended on endocytosis of the RAGE receptor. Recent studies by Leclerc & Vetter (2015) suggested that RAGE receptor and S100 protein ligands have crucial roles to play in the progression of pancreatic ductal adenocarcinoma (PDAC), and this study indicated that the potential RAGE ligands, S100P and S100A6, were highly expressed in pancreatic-tumour compared to their control samples. An investigation by Arumugam & Logsdon (2011) revealed that, when extracellular S100P bound to the RAGE receptor and stimulated cellular signalling, it could also stimulate drug resistance, tumour growth and metastasis in pancreatic cancer cells. Moreover, when S100P was added extracellularly to SW480 human colon cancer cell lines, it enhanced cell growth, migration, and both Erk1/2 phosphorylation and NFκB activation

(Fuentes et al., 2007). Moreover, when S100P was added to SW480 cells, they showed an increased expression of RAGE protein, which may indicate that the RAGE-S100P complex was the key to simulating activation of NFκB and phosphorylation of Erk1/2 (Fuentes et al., 2007). Conversely when the S100P-RAGE interaction is inhibited, this led to significantly decreased NFκB activation, cell growth and invasion in pancreatic cancer cells (BxPC-3) (Arumugam et al., 2006). However, experimental evidence to support individual pathways has not been reported. Moreover, the S100P-RAGE reaction could control oncogenic miR-21 levels in SW480 human colon cancer cell lines. Thus, when S100P was added extracellularly to SW480 wild type cells, this led to upregulation of miR-21. In contrast, silencing S100P in overexpressing SW480-S100P cells reduced level of miR-21. Finally when the RAGE receptor was blocked with anti-RAGE antibody, this caused a decrease in the inductive effect of S100P on miR-21 (Mercado-Pimentel et al., 2015). The oncogene miR-21 also reduced the level of the reversion-inducing cysteine-rich protein with Kazal motifs (RECK) in U87MG glioma cells (Chen and Tseng, 2012; Gabriely et al., 2008). RECK is a gene responsible for inhibiting tumour and metastatic activity and can inhibit many matrix metalloproteinase such as MMP-2 and MMP-9 which are usually upregulated in tumour formation, angiogenesis and metastasis (reveiwed in Noda & Takahashi 2007). In summary, exogenous S100P added to human colonic cancer cell lines could supress RECK protein levels due to upregulation of miR-21 (Mercado-Pimentel et al., 2015) and RECK's involvement could also be one reason why several MMPs were upregulated in different cancers.

In common with S100P, the S100A4-RAGE receptor interaction has been implicated in progression of many cancer, such as in human colorectal cancer (CRC)

(Dahlmann et al., 2014). This report showed that interaction of extracellular S100A4 with the RAGE receptor in cultured cells enhanced their motility and metastatic potential. Moreover, the S100A4-RAGE receptor interaction may have a role to play in promoting metastatic activity in human melanoma cells (A375) (Herwig et al., 2016). This study showed that when extracellular S100A4 was added to the A375 human melanoma cells stably transfected with the vector for RAGE cDNA (A375-hRAGE), the resultant cells showed enhanced cell motility, adhesion, migration and invasion. Extracellular S100A4 promoted cell migration in human umbilical vein endothelial cells (HUVEC) by interacting with RAGE. The S100A4-RAGE interaction led to signalling through activation of ERK1/2 and thence NFκB pathways, and activation of MMP-9 to enhance the migratory response in HUVECs (Hernández et al., 2013). Moreover, the stably transfected human melanoma cell line overexpressing S100A4 (A375-hS100A4), was shown to secrete S100A4 extracellularly by an endoplasmic reticulum-Golgi apparatus- dependent pathway. The use of this secretion pathway by S100A4 was proven by using different types of inhibitors. Thus, Bafilomycin A1 was used to block a vacuolar H^+ - ATPase, which defined the type of vehicle-carrying protein; Brefeldin A was used as a blocker of the conventional ER-Golgi secretion pathway; Cytochalasin B was used to block the actin filament-dependent pathway; and Nocodazole was used to depolymerize microtubules and inhibit the tubulin-dependent route. Another study in a melanoma cell line showed that S100A4 and S100A9 could be released extracellularly from the surrounding stromal cells and by signalling through the RAGE receptor and the extracellular MMP inducer EMMPRIN, respectively, they caused a stimulation of NFκB. NFκB, in turn, enhanced indirectly

cell expression of cytokines and MMPs which, once again in turn, boosted cell invasion and metastasis (Bresnick et al., 2015).

In summary, S100P and S100A4 have been reported to be involved in metastasis in a variety of cancers. Also, the RAGE receptor has been correlated with the activation of MMPs, such as MMP-2 or 9 in human diabetic plaques; MMP-3, 9 & 13 in an arthritic mouse model for rheumatoid arthritis, and MMP-9 in human pancreatic cancer cells (Cipollone et al., 2003; Hofmann et al., 2002; Takada et al. 2004). The active linkage is unclear.

1.6 Hypothesis

"S100 metastasis-inducing proteins induce migration and/or invasion by stimulating the production of a subset of MMPs".

1.7 Aims

To investigate what role the matrix metalloproteinases (MMPs) have in the S100A4/S100P stimulation of cell migration and invasion in breast cancer.

This aim will be accomplished in four experimental chapters with individual aims as follows:

1- To identify the MMPs stimulated by S100P and S100A4 in suitably-transfected, overexpressing rat mammary cell lines.

2- To examine the effect of siRNAs to specific MMPs on the cells' migration and invasion of S100P/A4 overexpressing cell lines.

3- To examine the effect of exogenously-added S100P/S100A4 on specific MMPs and migration/invasion of parental rat mammary cell lines.

4- To examine the relationship between specific MMPs and S100P/S100A4 in primary tumours and with survival times of breast cancer patients.

Chapter 2

Materials and Methods

2.1 Reagents and equipment

All chemicals and equipment used throughout the current study were obtained from our laboratory communal stocks or purchased from Sigma-Aldrich Co. (St. Louis, MO, UK), R&D system (Minneapolis, MN, USA), Gibco (Thermo Fisher Scientific, Waltham, MA, UK), Cell Signalling Technology, Inc., (Davrrers, MA, UK), Fisher Scientific UK Ltd. (Loughborough, UK), Bio-Rad Laboratories Inc. (Hercules, CA, USA) or Santa Cruz Biotechnology (Santa Cruz, CA, USA), unless otherwise stated. All cell culture equipment such as plastic ware was purchased from Corning Inc. (Corning, NY, UK), unless otherwise stated. Most buffers were prepared manually using ultra-pure distilled water, unless otherwise recorded.

2.2 Cell culture

The culture medium used in this project was purchased from Gibco, unless otherwise indicated. Cells were seeded in Dulbecco's Modified Eagle's Medium (DMEM), which in all cases contained 4.5 g/L D-glucose, non-essential amino acids (NEAA), 3.7 g/L sodium bicarbonate and phenol red. DMEM was further supplemented with 4 mM L-glutamine, 100 units/mL penicillin and 100 µg/mL streptomycin and 5% or 10% (v/v) foetal calf serum (FCS) from Sigma. This solution will hereafter be referred to as full supplemented media (**FSM**). Monolayer cells were

kept at 37°C in an incubator of humidified air with 10 % (v/v) CO_2. All steps for tissue culture were performed in a laminar flow tissue culture hood using sterile materials.

2.2.1 Cell lines

Rat mammary (Rama) 37, a non-metastatic benign rat mammary tumour-derived cell line (this cell line will hereafter be referred to as Rama 37 wild type (R37wt)) (Dunnington et al., 1983), and HeLa cells - epithelial, human cancer cells firstly obtained from cervical cancer from "Henrietta Lacks" (Scherer, 1953).

Rama 37 cell line was cultured in FSM with 5% (v/v) FCS, 10 ng/mL insulin and 10 ng/mL hydrocortisone (Clarke et al., 2017). HeLa cell line was cultured in FSM with 10 % (v/v) FCS (Du et al., 2012). All cell lines were incubated in the same conditions (Section **2.2**).

2.2.2 Transfected cell lines

The Rama 37 cells had been transfected previously with Piggy Bac-S100P and Piggy Bac vector alone (empty vector) as a control (R37-S100P, R37-EV), respectively (Clarke et al., 2017). The benign rat mammary cell line (Rama 37) had also been previously independently co-transfected with the human cDNA for S100A4 with pSV2neo (S5-R37) and PSV2neo (neo 1 – R37) vector alone (empty vector) as a control (R37-S100A4, R37 EV), respectively. These cell lines had been well characterised in previous publications (Clarke et al., 2017; Lloyd et al., 1998).

HeLa cells were transfected to give overexpression of S100P using a tetracycline inducible system. This system consists of two plasmids. The first one is pBTE plasmid which expresses the regulatory element rtTA2(S)-M2, that is

responsible for doxycycline switching, and the second is pTRE-ins, which is responsible for expression of the S100P protein (Lamartina et al., 2003). The inducible clone derived from HeLa is called HeLa-A3. One µg/ml of doxycycline was sufficient to induce HeLa-A3 cell line to produce S100P protein (Du et al., 2012). This antibiotic was prepared by dissolving 5 mg/mL doxycycline (Clontech Laboratories Inc., Mountain View, CA, USA) in distilled H_2O (d H_2O) as a stock solution. HeLa-A3 cells were seeded in 10 cm diameter Petri culture dishes for 24 h with 2 µL of doxycycline stock to give a final concentration of 1 µg/mL. When-long term inductions were required, the medium of the HeLa-A3 cells was changed to doxycycline containing-FSM every 48 h.

All stably-transfected cell lines (R37-S100P, R37-S100A4 and their vector alone controls) were cultured in FSM (Section **2.2**) with the addition of 1 mg/mL Geneticin 418 disulphate (G418) as a selection agent (Davies et al., 1993; Ke et al., 1998). These cell lines were used to investigate the presence and relationship between overexpression of S100P and S100A4 proteins and matrix metalloproteinases in their invasive ability. These cell lines have been successfully established as model systems for investigation of their metastatic phenotype (Rama 37-S100P ; Clarke et al., 2017) and Rama37-S100A4 ; Lloyd et al., 1998) in rat breast cancer, and HeLa in ovarian cancer (Du et al., 2012).

2.2.3 Thawing and sub-culturing cells

Cells were quickly thawed in a 37°C water bath for about a minute and then quickly seeded in 10 mL FSM of Rama 37 medium in 10 cm diameter Petri culture dishes. FSM was changed to new medium every 24 h.

Usually, cells were passaged after 2-3 days, when they became about 70-80 % confluenct. Monolayer cuboidal Rama 37 cells were washed twice with phosphate-buffered saline (PBS), then incubated for 10 minutes at 37°C with 1 mL Versene (0.02% w/v EDTA: ethylenediamine tetraacetic acid in PBS). Versene was aspirated and replaced with 1 mL Trypsin (0.05 % w/v with Versene) at 37°C for 3 minutes or at least when almost all the cells had detached. After that, cells were collected in FSM and replated in FSM at a ratio of 1:5 to 1:10, as needed.

Thawing and passaging for HeLa cells followed the same steps as for Rama 37 cells except for trypsinisation, they were incubated for 10 minutes at 37°C with Versene.

2.2.4 Freezing cells

Rama 37 or HeLa cells were collected when 80-90 % confluent as reported above. Cells from each 10 cm diameter Petri culture dish were centrifuged for 5 minutes at (1000 x *g*) at room temperature, and then the cell pellet was resuspended in 2 mL freezing medium (80 % (v/v) FSM, 7.5 % (v/v) DMSO and 4 % (v/v) FCS). Each 1 mL cell suspension was collected in a cryovial tube (Star Lab), and then all cryovials tubes were quickly packaged into a Cryo freezing container (Nalgene) for 24 h, at -80°C (to maintain a cooling rate of about -1°C per minute). After 24 h, cryovials tubes were moved to -135°C for long-term freezing and storage.

2.3 Cell lysate

2.3.1 Cell lysate (CL) for SDS-PAGE

Cells were lysed in 10 cm diameter Petri dishes on ice at 4°C by adding 90 µL RIPA Buffer [50 mM Tris-HCl, pH 8, 2 mM EDTA, 150 mM NaCl, 1% (v/v) Tergitol® (NP-40, nonyl phenoxypolyethoxylethanol-40), 0.5% (w/v) sodium deoxycholate, 0.1 % (w/v) SDS] and 10 µL protease inhibitor [10 µg/mL aprotinin (Sigma-Aldrich, A 1153), 2 µg/mL leupeptin (Sigma-Aldrich, L 9783), and 4 mM benzamidine (Sigma-Aldrich, B 6506)]. The contents were mixed well with a scraper, and the mixture collected and transferred to an Eppendorf tube. Eppendorf tubes were placed on end-over-end mixer for 1 h at 4°C. Samples were vortexed for 2-3 minutes and then centrifuged (Eppendorf 5415R refrigerated centrifuge) at 16000 x g for 20 min at 4°C. The supernatant was then transferred into a new tube and frozen at -80 °C for further use. RIPA buffer was made in dH_2O and then kept for up to 2 weeks at 4°C. Protease inhibitor reagents were individually prepared in dH_2O, aliquoted and kept at -20 °C. Protease inhibitors were added to RIPA buffer immediately before use. This protocol was adapted to fit in with the work plan (Köhrmann et al., 2009; Toth et al., 2012a; Toth and Fridman, 2001).

2.3.2 Cell lysate for Zymography assay

Cells in 10 cm diameter Petri dishes were lysed on ice by adding 90 µL Lysis Buffer [25 mM Tris-HCl, pH 7.5; 100 mM NaCl plus 1% (v/v) Nonidet P-40 (NP-40)] and just before lysis, a cocktail of protease inhibitor (Section **2.3.1**) was added; the contents were mixed well with a scraper, and the mixture collected and transferred to an Eppendorf tube. Eppendorf tubes were placed on end-over-end mixer for 1 h

at 4°C. Samples were vortexed for 2-3 minutes and then centrifuged at 16000 x *g* for 20 min at 4°C (Toth et al., 2012a; Toth and Fridman, 2001). The supernatant was then transferred into a new Eppendorf tube and frozen at -80 °C until further analysis. Lysis buffer was made up in dH_2O and then kept for 2 weeks at 4°C.

2.4 Conditioned medium (CM)

The CM contains Opti-MEM® I Reduced Serum Medium which is a modification of Eagle's Minimum Essential Media (Gibco) containing 10 ng/mL hydrocortisone, 100 units/ml penicillin, 100 µg/mL streptomycin, 4% (w/v) amino acids (Gibco), 25 mM D-glucose, 3.7 g/mL sodium bicarbonate (Gibco), and 1.8 mM calcium dichloride (Clarke et al., 2015). The Opti-MEM medium with all these supplements and after incubation with cultured cells will hereafter be referred to as 'conditioned media' (CM).

One million cells of Rama 37 or HeLa cell lines were counted using a Z1 Coulter® particle counter (Beckman Coulter., Brea, CA, USA), and then routinely cultured in FSM in 10 cm Petri culture dishes for two days (Section **2.2** and **2.2.1**). After this time, cells were approximately 70-80 % confluent. Cell monolayers were gently washed 3 times with Opti-MEM, and then incubated for 24 h in 7 ml CM. Next day, CM was collected and centrifuged for 5 min at 1000 X *g* at 4°C. Supernatants were concentrated to 0.25 mL using a centrifugal filter concentrator with 10 kDa cut-off (UFC901024, Merck Millipore Ltd., Co. Cork, Ireland) at 4000 X *g* at 4°C for 20 min. The concentration process was checked every 5 min.

2.5 Quantification of CL and CM protein concentrations

The concentrations of proteins in cell lysates were determined using the bicinchoninic acid assay kit (Pierce™ BCA. Protein Assay Kit, Thermo Fisher Scientific Inc., Waltham, MA USA). A standard curve for bovine serum albumin (BSA) was created using BSA dilutions in cell Lysis Buffer (0 - 2000 µg/mL) according to manufacturer's instructions**.** All samples were diluted 1:5 using Cell Lysis Buffer. Triplicate 10 µL of BSA or sample lysates were pipetted into a 96-well plate (Thermo Fisher Scientific, Waltham, MA, USA). BCA reagents (50A:1B) were used and 200 µL from the mixture were added to each well of a 96-well plate. The 96-well plate was covered, rocked using a plate shaker**,** and then incubated at 37°C for 30 min. After the incubation time, the absorbance of each well was measured using a Spectramax plus384 (Molecular Devices, Ismaning, Germany) plate reader at 562 nm. The linear standard curve of mean absorbance (three values) of BSA was used to measure the concentration of protein in the samples.

The CM samples were concentrated (Section **2.4**) and standardised before loading firstly, by seeding the same number of cells at the start of the experiment. Secondly, by estimating the total volume of the CM based on the BCA results of the cell lysate. This amount of total protein in CL was used to adjust the volume of CM in µL applied to the gel, so as to standardise CM input with respect to total CL protein.

2.6 Trichloroacetic acid (TCA) preparation steps

One million cells from R37-S100P, R37-S100A4 and their empty vector control cell lines were seeded at a density of 70-80 % in 10 cm diameter dishes with FSM then changed to CM as described in CM. The method was performed according to

Nandakumar et al. (2003) with slight modifications. The 7 mL CM from 2 plates were collected and proteins concentrated using TCA precipitation. TCA precipitation involved the following steps: 0.1% (w/v) (final concentration) N-lauroylsarcosine (N-LS) and 7.5% (w/v) (final concentration) TCA were added to CM samples. Samples were mixed and kept at -20 °C for 2 hours. Samples were thawed at room temperature and each 1.5 mL fractions were sequentially centrifuged in an Eppendorf 5415R refrigerated centrifuge at 10000 X g for 10 min at 4 °C. The centrifugation process was repeated using the same Eppendorf tube for the whole sample volume.

The remaining pellet containing the precipitated proteins was washed in 1 mL of –20 °C, ice-cold acetone two times, then centrifuged at 10000 x g for 10 min at 4 °C. Acetone was removed and the excess acetone allowed to evaporate for 5-10 min inside a fume hood. Ten µl of 200 mM NaOH on ice was added to the pellet for 5 min to help protein solubilisation (Nandakumar et al., 2003). Ninety µL of 1.1 X Solubilisation Buffer (50 mM Tris-HCl, pH 8.0 and 2% (w/v) SDS) was added to the samples, and the contents were mixed and sonicated for 10 min in a water bath at room temperature twice. Samples were heated to 95 °C in a heating block for 5 min and then incubated for 10 min in a sonicating water bath at room temperature. Finally, samples were centrifuged at 13000 rpm for 1 min to pellet any insoluble proteins, then the supernatant was frozen at -80 °C prior to its use for Western blotting.

2.7 SDS-PAGE technique (Western blot)

2.7.1 Sample preparation

Cell lines were cultured routinely in FSM (Section **2.2** and **2.2.1**). CL was prepared (as mentioned in Cell lysate (CL) for SDS-PAGE) and cell extract protein concentrations were quantified by BCA (Section **2.5**). CM for detection of MMPs were prepared, collected, concentrated (Section **2.4**) and normalized (Section **2.5**). CM for detection of external S100P/S100A4 was concentrated using TCA (Section **2.6**) and samples normalised following the same procedure as that in Section **2.5**.

2.7.2 Reagents for SDS-PAGE Western blot

Sample Loading Buffer (SLB) (3 X) consisted of 187.5 mM Tris-HCl, pH 6.8, 6 % (v/v) SDS, 30 % (v/v) glycerol, 300 mM DTT and 0.625 % (v/v) bromophenol blue. **Running Buffer (RB)** consisted of 50 mM Tris, pH 8.3, 192 mM glycine and 0.1 % (w/v) SDS. **Transfer Buffer (TB)** was 120 mM Tris, 192 mM glycine and 20 % (v/v) methanol. **Tris buffered saline-Tween 20** (**TBS-T)** was 20 mM Tris-HCl, pH 7.5, 150 mM NaCl and 0.1 % (v/v) Tween 20. **Blocking buffer** was 5 % (w/v) fat-free skimmed-milk (Marvel) or BSA in TBS-T.

2.7.3 Gel preparations for SDS-PAGE

Resolving gel buffer contained 750 mM Tris-HCl, pH 8.9, 0.1 % (v/v) SDS, 8 %, 10 % or 15 % acrylamide (30 % acrylamide:bis-acrylamide 37.5:1), 0.06 % (w/v) ammonium persulfate (APS), 0.015 % (v/v) TEMED. The Resolving Solution was poured into 1 mm-thick, 7.5 cm-wide and 10 cm-high glass plates for polymerisation

in a vertical casting apparatus (BioRad). Two hundred µL butanol to stretch the gel surface and avoid drying out the gel was overlaid above the Resolving Solution and then the solution was left to polymerise for 1 h at room temperature. When the Resolving Solution had set, the butanol was removed, and the surface of the resultant gel was gently washed 3 times with dH_2O. **The Stacking Gel Buffer** consisted of 250 mM Tris-HCl, pH 6.8, 0.1 % (v/v) SDS, 4 % acrylamide (30 % acrylamide:bis-acrylamide 37.5:1), 0.06 % (w/v) ammonium persulfate (APS), 0.015 % (v/v) TEMED. This Solution was poured over the set resolving gel. A 10 or 15 well comb was inserted directly into the stacking gel and the gel was left to polymerise for 30-60 minutes at room temperature.

2.7.4 Method

Gel surfaces were gently rinsed for up to 3 times with 1 X RB to remove the unpolymerized acrylamide and were then placed in vertical gel electrophoresis tanks (BioRad) and submerged in 1 X RB. For the cell lysate (CL) samples, 10 µg of cell lysate protein were mixed with 3 X SLB (volume made up with RIPA buffer to 15 or 21 µL). Samples were mixed by vortexing for 2-3 minutes, heated to 95°C for 5 min in a heating block and then briefly centrifuged in a bench top centrifuge before the supernatants were loaded onto the gel wells. Gels were run at 200 V for 60-75 min at room temperature, until the bromophenol blue dye reached the bottom of the gel.

The CM samples were all normalized based on the BCA assay of the cell lysate proteins (Section **2.5**). Sample volumes were made up to 21 µL with 1 X SLB before being loaded into the gel well. All the remaining steps for SDS-PAGE are the same as those for the CL samples described above. Precision Plus Protein™ Dual Color

Standards protein ladder (BioRad, cat. no. 161-0374) consisting of 10 different proteins of molecular weight (250, 150, 100, 75, 50, 37, 25, 20, 15 and 10 kDa) was loaded onto the gel, followed by samples using gel loading tips.

For Western blotting and transfer, all electrophoresed gels were gently detached from their casting-plates into a tray of cold, fresh transfer buffer for 15 minutes. Immobilon-P PVDF membranes (Millipore) were activated by immersing them in 100 % methanol for 1 min and then in TB in a tray. A sandwich cassette was set up as follows: a bottom layer of sponge, 3 layers of filter papers, the gel, the PVDF membrane, 2 layers of filter papers and then another layer of sponge. This sandwich was evacuated to remove air bubbles, fitted into a plastic cassette cover and then placed vertically in a transfer apparatus (BioRad). This apparatus was submerged with TB in a transfer tank. The tank was covered with ice and electroblotting was undertaken in a cold room at 100 V for 2 h.

To check the transfer efficiency, a membrane was immersed in an ATX Ponceau S stain (Sigma-Aldrich) for 2-3 min, washed with TBS-T to remove the stain, and then the next steps of the Western blot process could be continued.

Membranes were removed from the transfer cassette and rinsed with reverse osmosis (RO) water. Membranes were blocked with Blocking Buffer (BB) for 1 h at room temperature on rolling mixer to remove nonspecific absorption sites. After the blocking step, membranes were incubated with primary antibody (**Table 2.1.**) in BB overnight in the cold room on a roller mixer. Next day, membranes were washed 3 times with TBS-T for 10 min each, and then incubated with secondary antibody (**Table 2.1.**) for 2 h at room temperature. The membranes were then washed as before and blotted dry with blue roll tissue. The bands of immunoreactivity on the membranes

were then visualised using 1 mL of Amersham ECL™ substrate (GE Life Sciences, Buckinghamshire, UK) for 2 min following the manufacturer's instructions. ECL reagents were removed with blue roll tissue and membranes placed immediately in an X-ray film cassette and exposed to RX X-ray film (Kodak). Exposure times varied from 30 sec. to 15 min. If the bands were hardly detectable using ECL substrate, membranes were washed for 5 min with TBS-T and then ECL select™ substrate (GE Life Sciences) was used and the membranes re-exposed to X-ray film for 30 sec. to 7 min.

Table 2.1. Antibodies used for Western blotting.

Antibody Primary antibodies	Host species	Code	Dilution (blocking buffer)
S100P Polyclonal	Goat	R&D System AF2957	12:6000 (BSA)
S100A4 Polyclonal	Goat	Santa Cruz sc-19949	12:6000 (BSA)
MMP-2 Polyclonal	Rabbit	Abcam ab37150	2:6000 (milk)
MMP-9 Monoclonal	Rabbit	Abcam ab76003	1.5:6000 (milk)
MMP-13 Monoclonal	Mouse	Thermo MA5-14238	4:6000 (milk)
GAPDH Monoclonal	Mouse	Sigma G8795	0.5:20000 (milk)
RAGE Polyclonal	Rabbit	Abcam ab3611	2.5:6000 (milk)
Secondary antibodies			
HRP- conjugated, anti-goat IgG	Rabbit	Dako P0160	1:6000 (BSA)
HRP-Linked, anti-mouse IgG	Horse	Cell signalling 7076s	1:6000 (Milk)
HRP-Linked, anti-rabbit IgG	Horse	Cell signalling 7074s	1:6000 (Milk)

2.7.5 Densitometry

Protein signals on X-ray film blots were scanned using a flatbed scanner (MP C3004ex Ricoh, Tokyo, Japan). Density of protein bands was measured using ImageStudio Lite software version 5.2 (LI-COR Biosciences, Java).

2.8 Purified S100P and S100A4 proteins

Recombinant (r) S100P and S100A4 proteins were obtained from Dr. T. M. Ismail, University of Liverpool. The wild type S100P or S100A4 was produced in *E. coli* BL21 (DE3) cells (Thermo Fisher) using bacterial expression vector PET15b (Cat. No. 69661-3, Novagen, London, UK) (Ismail et al., 2010, 2008). The His-tagged recombinant proteins were purified on HisTrap columns (GE Healthcare, Buckinghamshire, UK). The His-Tag was removed by reacting with thrombin-agarose resin (Sigma). The cleaved native proteins were passed through HisTrap columns again to remove the his tag, and then protein in the run through was purified on Superdex 75 gel filteration columns (GE Healthcare). The preparations of rS100P and S100A4 gave single bands on 15 % (w/v) SDS-PAGE gels of apparent molecular weights of 7.5 kDa and 8.6 kDa, respectively, (Section **3.2.1**), in agreement with previous reports (Clarke et al., 2017; Ismail et al., 2010, 2008).

2.9 Activation of recombinant MMP-2, 9 and 13 *in vitro*

Recombinant rat MMP-2 (rrMMP-2) (R&D Systems, cat. no. 924-MP), recombinant human MMP-9 (rhMMP-9) (R&D Systems, cat. no. 911-MP) and recombinant human MMP-13 (rhMMP-13) (R&D System, cat no. 511-MM) were purchased as the proforms.

2.9.1 Working buffers and reagents

TCNB buffer (50 mM Tris, 10 mM CaCl2, 150 mM NaCl, 0.05% (w/v) Brij35, pH 7.5) was prepared manually. *P*-aminophenylmercuric acetate (APMA) (Sigma, A-9563) was prepared by dissolving APMA in DMSO to yield a 100 mM stock solution.

2.9.2 Methods

Following the manufacturer's instructions, rrMMP-2 was activated by diluting rrMMP-2 stock to 40 µg/mL with 1 mM *p*-aminophenylmercuric acetate (APMA) in TCNB, and then the mixture was incubated for 2 h at 37 °C. Five ng of rrMMP-2 treated with APMA (active form of rrMMP-2) and 5 ng of rMMP-2 untreated (proform of rrMMP-2) were loaded on 10 % (w/v) SDS-PAGE gels and both forms showed bands at 68 kDa and 62 kDa (Song et al., 2013), respectively, using Western blotting (**Figure 2.1**). Recombinant human MMP-9 (rhMMP-9) (R&D Systems, cat. no. 911-MP) and recombinant human MMP-13 (rhMMP-13) (R&D System, 511-MM) were diluted to 100 µg/mL in TCNB. RhMMP-9 and rhMMP-13 were activated by adding APMA to a final concentration of 1 mM. The activation mixture of rhMMP-9 was incubated at 37 °C for 24 h, but only 2 h for rhMMP-13. Using Western blotting, proform and active form of rhMMP-9 were detected at 92 kDa and 67 kDa (Shin et al., 2016), respectively (**Figure 2.2.)** and proform and active form of rhMMP-13 were detected at 60 kDa and 50 kDa (Ozeki et al., 2014), respectively (**Figure 2.3)**. The molecular weights were usually accurate to within about 5% of the stated value.

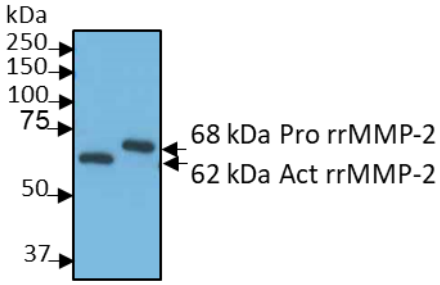

Figure 2.1. Proform (Pro) and active form (Act) of recombinant rat (rr) MMP-2.
Five ng of both forms of rrMMP-2 were loaded onto a 10 % (w/v) SDS-PAGE gel (as described under Activation process) and the resultant bands were detected using Western blotting techniques. Exposure time for the X-rays was 20 sec. Molecular weights were estimated from mobility on the gel compared to known standards (Bio-Rad, cat. no. 161-0374). The pro MMP-2 at 68 kDa and act MMP-2 at 62 kDa have been reported previously (Munesue et al., 2007), consistent with the loss of a 4 kDa propertied.

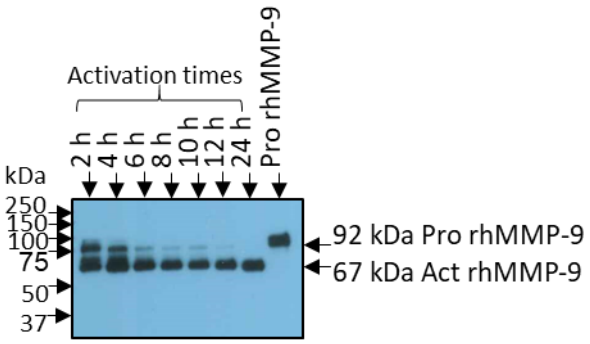

Figure 2.2. Proform (Pro) and active form (Act) of recombinant human MMP-9 (rhMMP-9).
One ng from each incubation time of 2, 4, 6, 8, 10, 12, 24 h or pro rhMMP-9 were loaded on a 10 % SDS-PAGE gel and bands were detected using Western blotting as described in **Figure 2.1**. Exposure time for X-ray was 1 min. Molecular weights were estimated as in **Figure 2.1.** showing original proMMP-9 at 92 kDa and 2 cleaved products at 87 kDa and subsequently at 67 kDa. The first peptide released from the N-terminus is 20 aa and the remaining protein would be 89 kDa. The chemical cleavage for the 20 pro-peptide occurs between Ala-Pro residues (Ogata et al., 1992; Okada et al., 1992). On further analysis, there is only one other Ala-Pro sequence in the proMMP-9 at 463/464 residues. Cleavage at this site would produce a second fragment at 65 kDa. Literature reported that for proMMP-9 at 92 kDa (Takino et al., 2003), the cleavage process resulted in either MMP-9 with molecular weight at 82 kDa (Ogata et al., 1992) or alternatively at 67 kDa (Okada et al., 1992). These calculations and literature reports are consistent with my results for the generation of 2 smaller fragment of proMMP-9 and these presumably represent the active forms.

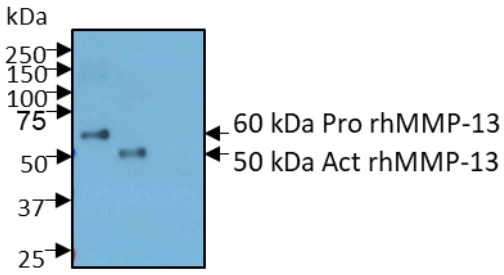

Figure 2.3. Proform (Pro) and active forms (Act) of recombinant human MMP-13 (rhMMP-13).
Three ng from both forms of rhMMP-13 were loaded on a 10 % (w/v) SDS-PAGE gel and bands were detected using Western blotting (**Section 2.7**). Exposure time for the X-ray film was 10 min. Molecular weights were estimated as in **Figure 2.1**. The proMMP-13 at 60 kDa and actMMP-13 at 52 kDa have been reported previously (Ravanti et al., 1999).

2.10 Relation between amount of protein loaded and band intensity

The whole CL of Rama 37 empty vector was normalised to constant protein concentration in BCA. Different amounts of proteins (5, 10, 15, 20 and 25 µg) were loaded on a 10 % (w/v) SDS-PAGE gel. Western blotting techniques were used to measure glyceraldehyde 3-phosphate dehydrogenase (GAPDH) protein's band intensity using ImageStudio Lite software Ver 5.2 (LI-COR Biosciences), to confirm the relationship between the amount of protein loaded on a gel and band intensity (Bell, 2016) (**Figure 2.4** and **Figure 2.5).**

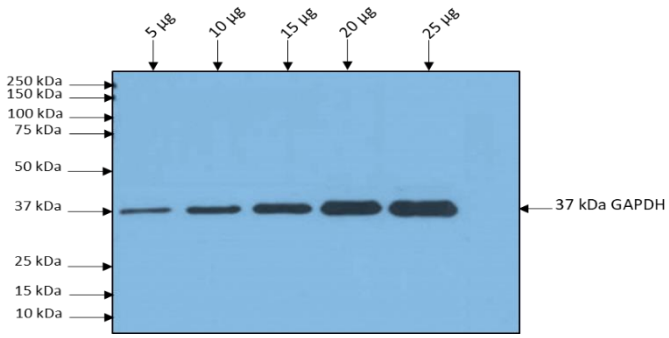

Figure 2.4. Western blot for different amounts of GAPDH loaded on a gel.

Different amounts of protein (5,10, 15, 20 and 25 µg) were applied to a 10% (w/v) polyacrylamide gel, the gel samples electrophoresed, and the resultant blot exposed to X-ray film. The GAPDH was used as a target protein to show the relationship between the amount of loaded protein on a gel using Western blotting and band intensities when measured via ImageStudio Lite software Ver 5.2 (LI-COR Biosciences).

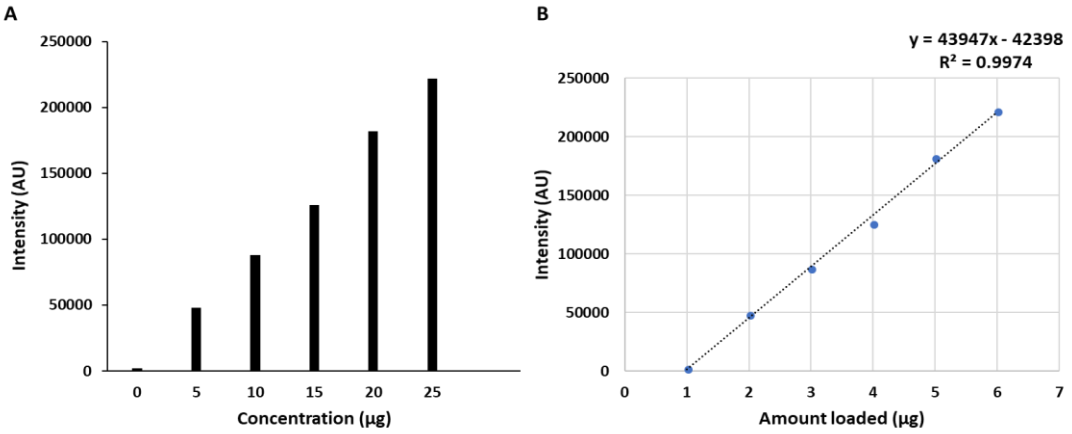

Figure 2.5. Histogram of amount of GAPDH protein loaded against its band intensity on a Western blot.

(**A**) The GAPDH X-ray film from (**Figure 2.4**) was scanned, subject to densitometry and the area under the same band in each track was plotted against the amount of GAPDH protein loaded per well in µg. (**B)** Linear relationship between the amount of protein loaded and intensity of the scanned bands in *(AU) Arbitrary Unit. Arbitrary Unit: is relative unit of intensity.

2.11 Simultaneous screening for different MMPs

Whole CL or CM of R37-S100P, R37-S100A4, HeLa-A3 or their control samples from vector alone transfected cells were screened simultaneously for detecting different MMPs using a semi-quantitative human MMP antibody array (ab134004, Abcam, Cambridge, UK). This kit has membranes pre-coated with polyclonal primary antibodies to 7 different MMPs (MMP-1, 2, 3, 8, 9, 10 and 13) and 3 different TIMPs (TIMP-1, 2 and 4) as dual spots for each target (**Table 2.2.**).

The membrane in Table 2.2 can detect 7 different MMPs and 3 different TIMPs using kit supplied by Abcam following the manufacturer's instruction (Baig et al., 2016). All steps were conducted at room temperature except membranes were incubated with samples at 4°C. The membranes were placed in a tray and incubated with 2 mL 1X Blocking Buffer for 30 min. After this time, Blocking Buffer was removed by aspiration and replaced with 1 mL of concentrated CM or 200 µg/mL CL proteins (volume made up to 1 mL with 1X Blocking Buffer) from any selected cell lines. The membranes with solutions were placed on a plate shaker overnight at 4°C. Membranes were then washed 3 times with fresh 1 X washing buffer type I (WBT I) for 30, 5 and 5 min, respectively and then 2 times with fresh 1 X WBT II, 5 min.

Table 2.2. Human MMP antibody array membrane [a].

	A	B	C	D	E	F	G	H
1	Pos	Pos	Neg	Neg	MMP-1	MMP-2	MMP-3	MMP-8
2	Pos	Pos	Neg	Neg	MMP-1	MMP-2	MMP-3	MMP-8
3	MMP-9	MMP-10	MMP-13	TIMP-1	TIMP-2	TIMP-4	Neg	Pos
4	MMP-9	MMP-10	MMP-13	TIMP-1	TIMP-2	TIMP-4	Neg	Pos

[a] This array aims to detect 7 MMPs and 3 TIMPs simultaneously in 32 different wells labelled (A to H x 1 to 4). This shows the arrangement of targets on the arrays.

After the washing steps, membranes were incubated with 1 mL of 1 X biotin-conjugated anti-MMPs for 2 h at room temperature. Membranes were then washed 3X with WBT I for 5 min and then 2X with WBT II. Two mL of HRP-conjugated streptavidin (1/1000 of 1X Blocking Buffer) were added to each membrane for 2 h at room temperature. Washing steps were repeated as above.

MMPs spots on the array were visualised using chemiluminescence. Equal volumes (1:1) of Reagent C and Reagent D (Abcam kit) were mixed well and 0.5 mL of this reagent mixture was used to coat the membrane for 2 min. Finally, all membranes were quickly placed in X-ray film cassettes and immediately exposed to Super RX X-ray film (Kodak) for 30 to 60 sec in a dark room to detect the chemiluminescent signals from the MMPs' spots. Positive control spots were used to compare different membranes from different experiments.

2.11.1 Densitometry

Developed X-ray films from human MMP antibody array were scanned using a flatbed scanner (Ricoh). The intensity of protein spots was analysed by densitometer and spot recognition analysis software (imageStudio Lite, Ver 5.2 (LI-COR Biosciences)).

2.12 Zymography technique

2.12.1 Sample preparation

R37-S100P and R37-S100A4 and their control cell lines were cultured routinely in FSM (Section **2.2** and **2.2.1**). CM was prepared, collected and concentrated (Section **2.4**). The processing was performed as described by Toth and Fridman (2001) and Toth et al. (2012) with some alterations to improve its efficiency under our conditions.

2.12.2 Reagents for Zymography technique

Four times **(4x) Sample Loading Buffer (SLB)** (250 mM Tris-HCl, pH 6.8, 40% (v/v) glycerol, 8% (w/v) SDS; and 0.01% (w/v) bromophenol blue) was used to mix with the samples. **Gelatin** (gelatin from porcine skin G1890, Sigma-Aldrich) or **casein** (casein from bovine milk C5890, Sigma-Aldrich) **0.25 % (w/v)** was prepared by dissolving the gelatin or casein in 10 mL dH_2O and then the mixture was heated with stirring at 60°C for 30 min. The mixture was left to cool down at room temperature and was always freshly prepared. **Running Buffer (1x) (RB)** was prepared by mixing 25 mM Tris base, pH 8.3, 192 mM glycine, 5 mL 20 % (v/v) SDS (added freshly) and the volume was made up to 1 L with dH_2O. **Renaturing Buffer (1x) (RNB)** was made

by mixing 2.5 % (v/v) Triton X-100 (Sigma-Aldrich) in dH_2O, stored at 4°C. **Developing Buffer (1x) (DB)** was prepared by mixing 50 mM Tris-HCl, pH 7.8, 200 mM NaCl, 5 mM $CaCl_2$ and 0.02 % (v/v) Brij 35, stored at 4°C. **Staining Solution (SS)** was made by adding 0.5 % (w/v) Coomassie blue R-250, 5 % (v/v) methanol and 10 % (v/v) acetic acid in dH_2O. **Destaining Solution (DS)** was prepared by mixing 10% (v/v) methanol, 5% (v/v) acetic acid in dH_2O.

2.12.3 Gelatin or casein - acrylamide gel preparations

Gelatin or casein – 10 % separating gel was prepared by mixing [10 mL 1.88 M Tris-HCl, pH 8.8, 17.8 ml of dH_2O, 5 ml of 0.25% (w/v) gelatin or casein, 16.6 ml of 30% (v/v) acrylamide-*bis*-acrylamide (37.5:1), 0.25 ml of 20% (w/v) SDS, 150 µl of 10% (w/v) APS, and 30 µl of TEMED] for preparation of eight gels. This mixture was poured into the 1 mm gap between glass plates in a vertical gel-casting apparatus (BioRad). Two hundred µL butanol was overlaid on the surface of the mixture to avoid drying out of the gel. The Separating solution was then left to polymerise for 1 h at room temperature. The butanol was removed after the separating gel had polymerised and the surface of the gel was gently washed 3 times with dH_2O. **Stacking gel (4%)** was made by mixing [11 mL of dH_2O, 2 mL of 30 % (v/v) acrylamide-*bis*-acrylamide (37.5:1), 2 mL of 1.25 M Tris-HCl, pH 6.8, 0.1 mL of 20 % (w/v) SDS, and 75 µL of 10 % (w/v) APS] sufficient for 8 gels. The stacking mixture was poured on top of the separating gel, a 1 mm comb (BioRad) (10 or 15 wells – comb as required) was gently immersed (to prevent any air bubbles) in the Stacking Gel mixture and then the mixture was left to polymerise for 30-60 min at room temperature. All gels were kept at 4°C for up to 2 weeks prior to use.

2.12.4 Methods

Gelatin or casein-containing acrylamide gels were gently washed up to 3 times with 1 x RB to remove any unpolymerized acrylamide. Gels were placed in a vertical gel electrophoresis tank (BioRad) and submerged in 1 x RB.

R37-S100P, R37-S100A4 and their control samples under reducing conditions were made up to the same volume with 1 x SLB and then mixed with 4 x SLB in a 3:1 ratio. Samples were mixed by vortexing for 2 min, briefly centrifuged and then the supernatant was micropipetted into the gel wells. Gels were run at constant voltage (125 V with 30-40 mA stable current) for 100 min at room temperature. The gel was then incubated two times for 15 min each at room temperature with gentle agitation in RNB to remove the SDS and allow the enzymes to refold. To reactivate the proteases, the gel was incubated in 1 x DB for 30 min at room temperature, and then with fresh DB for 48 h at 37C°. To detect the digested area in the casein or gelatine gel, the DB was decanted, and the gel was incubated in SS for at least 1 hour. Finally, the gel was destained with DS until areas of gelatinolytic or caseinolytic activity appeared as clear, sharp bands in a dark blue background of stained gelatine/casein.

The method to detect the MMP-13 activity using casein as a substrate rather than gelatin was the same as that for gelatinolytic activity, but with simple modifications. The renaturing step was achieved this time by washing the casein gel two times with 2.5% (v/v) Triton X-100, 50 mM Tris, pH 7.5 at room temperature for 20 min each to remove SDS, and then two more times with 50 mM Tris, pH 7.5 plus 5 mM $CaCl_2$. The rest of the experimental steps were the same as those in the gelatinolytic activity procedure.

2.12.5 Densitometry

Gelatine or casein gels were scanned linearly using an Image-Scanner III gel scanner (GE Life Sciences). Intensities of protein bands on gelatin or casein gels were measured using Image J software (Hu and Beeton, 2010).

2.13 Migration assay

Boyden Chambers consisting of 6.5 mm diameter polycarbonate membrane inserts with 8 µm diameter pores (Corning Costar, Acton, USA) were used, as described previously (Du et al., 2012), with some alterations to improve efficiently in our conditions. Warm DMEM (serum-free medium) was used to hydrate the chamber membranes by adding 250 µL to the interior space and 500 µL to the exterior space of the chambers (to the bottom of plate's wells), and then the chambers were incubated for at least 2 h in a humidified tissue culture incubator at 37˚C, 10 % (v/v) CO_2 atmosphere. One day prior to the experiment, cell lines were cultured routinely in FSM (Section **2.2** and **2.2.1**) in order to achieve 80-90 % confluence on the day of the experiment. After the hydration step, DMEM was aspirated from both sides of the chambers, 500 µL of FSM with 5 % (v/v) FCS was pipetted into the bottom of each well, and 250 µL of FSM with 1 % (v/v) FCS containing 7.5 X 10^3 cells were pipetted inside the top chamber in triplicate wells. All chambers were incubated for 24 h or 48 h in a humidified tissue culture incubator at 37˚C, 10 % (v/v) CO_2 atmosphere. After this time, the non-migrating cells on the top surface of the membranes were removed by a gentle wipe using cotton buds. The migrating cells on the lower surface of the membranes were fixed and stained by using a REAstain Quick Diff kit (Reagena., Siilinjärvi, Finland). Migration experiments were recorded from 3 wells repeated 3

times with different batches of cells (n=3) or recorded from 3 wells repeated 2 times with different batches of cells (n=2).

All migrating cells were counted manually using a light microscope with 4 x or 10 x objective. The procedure for cell counting was to use a zigzag pattern to avoid double counting of a cell (**Figure 2.6**).

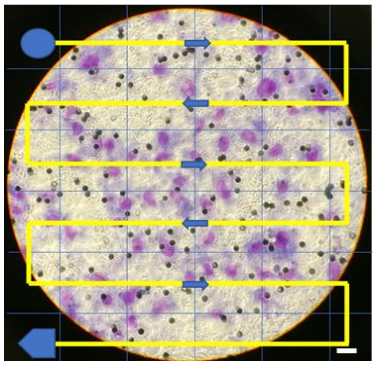

Figure 2.6. Zigzag pattern followed to count migrating or invading cells on bottom surface of transwell membranes. Bar = 20 µm.

2.14 Invasion assay

The BD BioCoat Matrigel Invasion chambers with 8µm diameter pores (BD Biosciences, Two Oak Park, Bedford, MA) were used in this experiment (Clarke et al. 2017). These chambers were shipped and stored at -20°C before use. The experimental protocol was the same as described in the Migration assay above, excepted the incubation time for rehydration was at least 6 h, and the number of cells seeded on the Matrigel invasion membrane was 15 X 10^3 cells / 500 µL of FSM with 1 % (v/v) FCS.

2.15 MMP small interfering (si) RNA transfection

2.15.1 Rat MMP-2 siRNA

A pool of 3 target-specific 19-25 nucleotide siRNAs (sc-108049, Santa Cruz Biotechnology, Santa Cruz, CA, USA) was purchased to knock-down gene expression of MMP-2 in the rat cell system. The manufacturer's instructions were followed, but with modifications (Lin et al., 2014) and some alterations in protocols were required to make the assay work efficiently. Lyophilized duplex MMP-2 siRNA was briefly centrifuged and the pellet was resuspended in 330 µL of the RNAse-free H_2O (D 2916, Santa Cruz) to give stock of 10 µM in buffer (0.01 mM Tris-HCl, pH 8.0, 20 mM NaCl, 1 mM EDTA). The stock was aliquoted and kept frozen at -20 °C.

2.15.2 Rat MMP-9 siRNA and Rat MMP-13 siRNA

MMP-9 and MMP-13 siRNA were purchased as an ON-TARGET plus Rat MMP-9 (81687) siRNA-SMART pool (L-093919) and ON-TARGET plus Rat MMP-13 (171052) siRNA-SMART pool (L-100431) (Dharmacon RNA Technologies, Buckinghamshire, UK) to knock-down gene expression of MMP-9 and MMP-13, respectively, in the rat cell system. The protocol was the same as that for Rat MMP-2 siRNA, except that for the 10 µM stock, 5 nmol of MMP-9 siRNA or MMP-13 siRNA were mixed with 500 µL of 1 X siRNA buffer (60 mM KCl, 6 mM HEPES, pH 7.5 and 0.2 mM $MgCl_2$) (B-002000-UB-100, Dharmacon RNA Technologies). The stock was aliquoted and kept frozen at -20 °C.

2.15.3 siRNA transfection for all MMPs (2, 9 and 13) at the same time

In this case, the same amount from each stock of siRNA for MMP-2 for MMP-9 and for MMP-13 were mixed together to examine the silencing of 3 MMPs in 1 transfection experiment on expression of these proteins and on the biological activity of the transfected cells.

2.15.4 Control siRNA-A for knock-down experiment

Control siRNA-A was purchased as a non-targeting 20-25 nucleotide siRNA (sc-37007, Santa Cruz Biotechnology, Santa Cruz, CA, USA) and was designed to be a negative control. The lyophilized control siRNA was resuspended in 66 µL of the RNAse-free H_2O and mixed with Buffer [0.01 mM Tris-HCl, pH 8.0, 20 mM NaCl, 1 mM EDTA] to give 10 µM stock. The stock was aliquoted and kept at -20 °C.

2.15.5 Working reagents and solutions

Different doses (2, 4 and 7 pmol or µL from 10 µM stock) of each siRNA for individually knocking-down MMPs were tested. Seven pmol dose was found to be the optimal, in agreement with the manufacturer's instructions (data not shown).

Solution (A), 70 pmol or 7 µL of MMP-2 or MMP-9 or MMP-13 siRNA stock were mixed with 100 µL Opti-MEM Reduced Serum Medium (Gibco), freshly prepared. **Solution (B),** 5 µL of transfection reagent (sc-29528, Santa Cruz) was mixed with 100 µL Opti-MEM Reduced Serum Medium, freshly prepared. In the case of knock-down of all 3 MMPs, which means silencing MMP-2, MMP-9 and MMP-13 at the same time; **Solution (A),** 3.5 µL from each MMP's siRNA were mixed together and

then added to 100 µL Opti-MEM Reduced Serum Medium. **Solution (B),** as described above.

2.15.6 Method

Stably transfected cell lines (R37-S100P and R37-S100A4) were seeded at 4 x 10^5 cells/well in 6 well tissue culture plates in antibiotic free-FSM and incubated at 37°C in 10 % (v/v) CO_2 for 24 h in order to achieve 80-90 % confluence. Next day, solution A and solution B were mixed together cautiously and incubated for 30 min at room temperature inside a laminar flow tissue culture hood. During this time, cells were washed once with 2 ml of Opti-MEM Reduced Serum Medium, the volume of the mixture of solution A+B was made up to 1 mL with Opti-MEM Reduced Serum Medium and then 1mL of the mixture was added to the washed cells. Cells were incubated at 37 °C for 6 to 8 h, based on observations of cell detachment/death due to the toxic effect of the transfection reagent and serum starvation. After the end of the incubation period, cells were supplied with 1 mL FSM containing 2 x FCS and 2 x antibiotic and then re-incubated for a total of 24 h. After the first 24 h incubation, cell medium was aspirated and replaced with fresh FSM for another 24h, the latter was changed every 24 h. For Western blotting of samples, cells required a 72 h incubation period. After these periods of cell culture, the cells and medium were collected (Section **2.3.1** and **2.4**). For migration and invasion assays, the cells were incubated for just 24 h in fresh FSM after the time of transfection, and then cells were routinely trypsinised, counted and seeded in the required numbers into Boyden chambers as dscribed in Sections **2.13** and **2.14**.

2.16 Effect of extracellular addition of S100 proteins on MMPs

2.16.1 Effect of different doses of S100P on levels of MMP-9

Rama 37 wild type (R37 wt) cell line was seeded in FSM at 4 x 10^5 cells/well in 6 well tissue culture plates and incubated at 37°C in an atmosphere of 10 % (v/v) CO_2 for 24 h in order to achieve 70-80 % confluence. The next day, cells were washed 3 x with Opti-MEM and 2 ml of CM was added to each well with different concentrations of purified S100P protein as follows: 0, 0.001, 0.01, 0.1, 1 and 5 µM. Each concentration was added in duplicate wells. After a 24 h incubation period, the cell lysate (CL) and conditioned medium (CM) were collected and normalized to process for Western blotting (Section **2.3.1** and **2.4**).

2.16.2 Effect of 1 µM S100P or S100A4 on levels of MMP-2, 9 and 13

One million cells of R37 wt in FSM were routinely seeded in two 10 cm dishes (Section **2.4**). One µM of S100P or S100A4 was added to CM of each plate. The CL and CM were collected after a 24 h incubation period and then normalized as described above in Section **2.5** to process samples for Western blotting.

2.17 Detection of RAGE receptor in cell lines

R37-S100P, R37-S100A4 and R37 wt in FSM were seeded in 10 cm diameter dishes. Cell lysates were collected and quantified as described in Section **2.3.1** and **2.5**. Samples were processed to examine the presence of Receptor for Advanced Glycation End Product (RAGE) in cell extracts using Western blotting. The identifiable RAGE band at ~45 kDa was confirmed by mixing 2.5 µL of anti-RAGE antibody (ab3611,

Abcam) with 5 µL of Rat RAGE-blocking peptide (ab41778) in 6 mL Blocking Buffer (BB) for half an hour at room temperature on a rolling mixer, and then the blot was incubated with the mixture (6 mL BB + RAGE antibody + RAGE blocking peptide) overnight at 4 °C on a rolling mixer (**Figure 2.7**), under these conditions the band at 45 kDa was eliminated. The band at 39 kDa remained after blocking and hence was considered unrelated to RAGE protein.

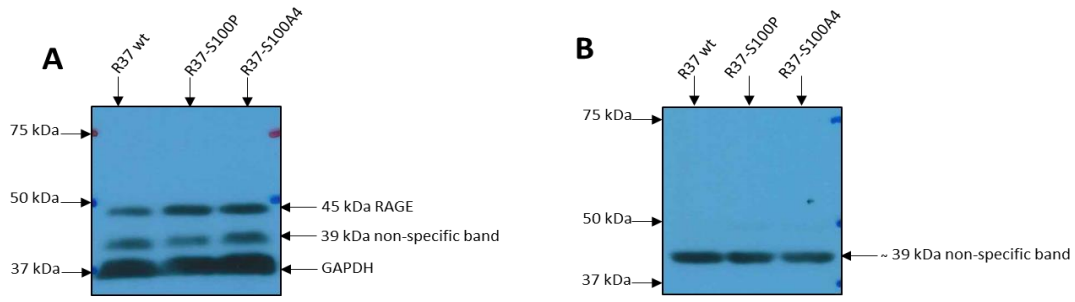

Figure 2.7. Western blot for RAGE receptor in cell lysates of R37 wt, R37-S100P and R37-S100A4.
(**A**) Blot was incubated with 2.5 µL / 6 mL anti-RAGE antibody in blocking buffer overnight. (**B**) Blot was incubated with 2.5 µL anti-RAGE antibody + 5 µL Rat RAGE blocking peptide in 6 mL blocking buffer overnight.

2.17.1 Effect of inhibiting RAGE receptor on cell biological activities promoted by intracellular/extracellular S100P or S100A4

R37 wt, R37-S100P and R37-S100A4 cell lines were cultured routinely in FSM (Section 2.2). Cromolyn sodium salt (C0399, Sigma-Aldrich) (Arumugam et al., 2006) and anti-RAGE antibody (ab3611, Abcam) (Dahlmann et al., 2014) were used to inhibit the RAGE receptor. Cromolyn is an antiallergic drug which can bind to S100 proteins and inhibit their binding to RAGE receptor (Arumugam et al., 2006; Okada et

al., 2002; Oyama et al., 1997). These experiments were repeated twice under the same conditions.

2.17.2 R37 wt with 1 µM S100P or S100A4 added extracellularly for migration and invasion experiments

R37 wt cells were seeded in each Boyden or Matrigel chambers for migration or invasion assays, respectively (Section **2.13** and **2.14**). For the Boyden or Matrigel chambers the 24 well plate was divided into 3 groups with 3 chambers for each group. **Group 1**: R37 wt cells were seeded alone as a negative control. **Group 2**: R37 wt with final concentration of 1 µM S100P on both sides of the membrane. **Groupe 3**: R37 wt with final concentration of 1 µM S100A4 on both sides of the membrane. Boyden chamber migration assay were carried out as described in Section 2.13. Matrigel chamber invasion assays were carried out as described in Section 2.14.

2.17.3 R37 wt with RAGE inhibitors for invasion experiment

R37 wt cells were seeded in the same way as described above (Section **2.14**). The 24 well plate was divided into 3 groups as follows: **Group 1**: R37 wt cells were seeded alone as a negative control. **Group 2**: R37 wt with 1/200 µL anti-RAGE antibody above and below the Matrigel membrane. **Groupe 3**: R37wt with 100 µM Cromolyn above and below the Matrigel membrane. Matrigel chamber invasion assays were carried out as described in Section 2.14.

2.17.4 R37 wt with 1 µM S100P or S100A4 added extracellularly with RAGE inhibitors for invasion experiment

R37 wt cells were seeded in the same way as described above (Section **2.14**). The 24 well plate was divided as follows: **Group 1**: R37 wt with final concentration of 1 µM S100P or S100A4 on both sides of the Matrigel membrane. **Group 2**: R37 wt with final concentration of 1 µM S100P or S100A4 and 1/200 µL anti-RAGE antibody on both sides of the Matrigel membrane. **Groupe 3**: R37 wt with 1 µM S100P or S100A4 and 100 µM Cromolyn on both sides of the Matrigel chamber. Matrigel chamber invasion assays were carried out as described in Section 2.14.

2.17.5 R37-S100P or R37-S100A4 with RAGE inhibitors for invasion assay

Stably transfected R37-S100P or R37-S100A4 were seeded in the same way as described above Section **2.14**. The 24 well plate was divided into 3 groups as follows: **Group 1**: R37-S100P or R37-S100A4 cells were seeded alone as a negative control. **Group 2**: R37-S100P or R37-S100A4 with 100 µM Cromolyn on both sides of the Matrigel membrane. **Groupe 3**: R37-S100P or R37-S100A4 with 1/200 µL anti-RAGE antibody on both sides of the Matrigel membrane. Matrigel chamber invasion assays were carried out as described in Section 2.14.

2.18 Human patient material and information

Specimens from 183 breast cancer specimens were collected between 1976 to 1982 from patients in the Merseyside Region of the North West of England. All had been treated by simple mastectomy and none had identifiable metastases at the time of presentation. None had any further hormone or chemotherapy. Information

regarding patient follow up, tumour pathology and ethical approval was obtained as described previously (de Silva Rudland et al., 2006). Specimens were originally fixed in buffered formalin, embedded in paraffin wax and stored at room temperature until further use, as described previously (de Silva Rudland et al., 2011).

2.18.1 Immunohistochemistry

Four to seven (4-7) µm sections from the stored paraffin blocks were cut and placed on 3-aminopropyltriethoxysilane (APES)-coated slides. Sections were dewaxed in xylene and rehydrated through graded ethanol to water mixtures (Warburton et al., 1982). Endogenous peroxidase activity was blocked by incubating them in 100 % methanol containing 0.05 % (v/v) H_2O_2 for 20 min at room temperature (Streefkerk, 1972). Sections were then incubated overnight at 4˚C in a humidity chamber with mouse monoclonal anti-MMP-2 (#MAB 13431, Millipore, Hertfordshire, UK), rabbit monoclonal anti-MMP-9 (#137867, Abcam, Cambridge, UK) or mouse monoclonal anti-MMP-13 (#MA5-14238, Thermo Fisher Scientific, MA, USA), at dilutions of 1:40 (MMP-2), 1:100 (MMP-9) and 1:60 (MMP-13) in 1 % (w/v) BSA/PBS. Indirect immunohistochemical staining was then carried out using a commercially available enhanced Horse Radish Peroxidase (HRP) labelled polymer system, the DAKO EnVision + System peroxidase (Dako Ltd, Ely, UK) (Sabattini et al., 1998), prepared according to the manufacturer's instructions. The labelled polymers, which bound to the sections were finally visualised by incubation with 0.05% (v/v) H2O2 and 3,3'-diaminobenzidine (DAB) to produce a brown precipitate. The sections were washed in running tap water and then the nuclei were counterstained with Mayer's haemalum. Sections were dehydrated in graded ethanol to water mixtures

and cleared in xylene. Coverslips were mounted on the slides in a mixture of Distyrene, a plasticizer, and xylene (DPX) (Merck, Poole, UK). Positive and negative controls using 1 % (w/v) BSA/PBS to replace the primary antibodies were used with each batch of about 20 stained sections. In most cases when positively stained, cytoplasm was the target. Controls using antibodies previously incubated with immunizing peptides to the proteins gave no specific stains. The purchased antibodies yielded a single band on Western blotting of the correct molecular weight according to the manufacturer's data sheets.

2.18.2 Scoring of samples and data analysis

Sections were scored by two observers independently (Prof. Philip Rudland and Mrs. Angela Platt-Higgins) using a light microscope and a 20 x objective (Leitz Laborlux 12). The percentage of tumour cells stained was estimated from counting 10 fields of 100-200 cells each across the whole section. The stained sections were subdivided into 5 categories as described in **Table 2.3.** and any differences between the two observers were resolved by subsequent discussion.

Table 2.3. Categories of immunohistochemical staining for breast cancer samples.

Percentage of breast cancer cells stained (%)[a]	Type	Group
<1	Negative	-
1-5	Borderline	+/-
5-25	Intermediate	+
25-50	Moderate	++
>50	Strong	+++

[a] Only staining of the cancer cells was recorded, that due to host stroma/blood vessels etc was not included.

Data analysis was performed by Mr Morteta AL-Medhtiy. First of all, the cumulative proportion of patients surviving for the different staining groups was plotted against time in the form of Kaplan Meirer plots, to identify the two most significantly different categorical staining groupings for each of the three MMPs. Usually the cut-off between two categorical staining groups was at either the 1% or 5% level of stained cancer cells (de Silva Rudland et al., 2011). For MMPs the cut-off was 5%. The significance of the difference and the relative risk between staining groups was computed by Wilcoxon-Gehan statistics and Cox's univariate analysis, respectively, as described previously (de Silva Rudland et al., 2011). Kaplan Meier plots and statistical analyses were performed for the two categorical groups for each MMP. Further analysis was undertaken with data already collected for staining for S100P and S100A4 (Rudland et al., 2000; Wang et al., 2006).

The significance of the association of paired stainings was computed from 2x2 tables using Fisher's Exact test (two sided) with the Bonferroni correction for multiple tests to reduce chance associations (de Silva Rudland et al., 2011; Rudland et al., 2000). Computations were undertaken for staining for MMP-2, -9, -13, S100P and S100A4. Logistic regression was carried out on staining for combinations of MMPs and S100 proteins. Cox's multivariate analyses to show significance of association with patient survival on staining sets containing combinations of these groups were also carried out to show significance of association with patient survival. All statistical analyses were performed using the IBM statistical package for the social sciences (SPSS) version 24.

Chapter 3

Levels of matrix-metalloproteinases in S100P and S100A4 overexpressing transfected rat mammary cells

3.1 Introduction

Overexpression of S100P /S100A4 has been correlated with increased metastatic activity and with promoting expression of MMPs in many cases of cancer (Berge and Mælandsmo, 2011; Bresnick et al., 2015; Mishra et al., 2012; Saleem et al., 2006). MMPs act as molecular scissors to cut and digest components of the ECM, e.g., collagen I, gelatine, and elastin fibers, and this destruction leads to remodelling of the ECM which aids the route along which dissemination of tumour cells occurs (Singletary & Connolly 2006; Rizwan et al. 2015).

Amongst many means to examine cellular activities, estimation of the levels of specific proteins is considered to be one of the most fruitful (Jones, 2014). Usually, cell functions are directly accomplished by proteins, and only indirectly via DNA or RNA. Moreover, experimental analyses have shown that a dissimilarity between mRNA levels and their corresponding proteins can exist under certain conditions (Mahmood and Yang, 2012). Therefore, an analysis of proteins is crucial to an understanding of intracellular and extracellular pathways. In this chapter Western blotting is used to detect specific proteins from entire protein mixtures using specific primary and secondary antibodies (Mahmood and Yang, 2012).

For the MMP proteinases the development of sensitive methods for their detection and activity are vital to determine their role in tissue degradation (Fernández-Resa et al., 1995). One of the most popular and reliable techniques is zymography for quantitative measurement of MMPs' activities (Lombard et al., 2005). In the past, ELISA has often been used to estimate levels of specific proteins in serum or urine samples (Avrameas and Ternynck, 1998) and immunohistochemistry for biopsy specimens (Hornick, 2014). These two methods are time-consuming, expensive and do not help to identify the molecular weight of the active enzymes. In contrast, zymography provides a cheaper and quicker screening method with the added advantage of visualising the MMP's molecular weight. To detect MMP-2, MMP-9 and MMP-13's activities in biological samples, zymography is used with gelatin or casein as substrate; it is a very sensitive assay for these enzymes (Hu and Beeton, 2010; Schmidt-Hansen et al., 2004; P. Snoek-van Beurden and Von den Hoff, 2005; Toth and Fridman, 2001; Yu and Woessner, 2001). This assay visualises their enzymatic activity in biological samples using sodium dodecyl sulphate (SDS) polyacrylamide gels impregnated with gelatin (Toth et al., 2012b) or casein (Schmidt-Hansen et al., 2004). The latter substrate is used for MMP-13, which only introduces a single cuts (¼ and ¾ fragments) in its target, collagen I, but cuts casein in many places leading to a more complete digestion (Snoek-van Beurden and von den Hoff, 2005; van Doren, 2015; Zitka et al., 2010). The biological samples are electrophoresed under nonreducing conditions, which maintains their proteolytic activity. Triton X-100 is then used to remove the SDS from the gel (renaturing buffer), a procedure which allows the enzymes to refold again. Calcium-containing buffer is then used to activate the enzymes, which can now degrade the gelatin, leaving a protein-cleared

zone, which can be observed as a unstained band after incubating the gel with Coomassie Blue R-250 stain (Toth and Fridman, 2001).

3.1.1 Chapter aims

To identify the MMPs stimulated by overexpression of S100P and S100A4 in stably-transfected rat mammary cell lines.

3.2 Results

3.2.1 Expression of S100P/A4 proteins in stably transfected rat mammary (R37) S100P/A4 cell lines

The R37-S100P / A4 cell lines were analysed for the presence of S100P/A4 proteins compared to the R37 empty vector-containing cell line. Thus, 20 µg of protein from each cell line estimated by the BCA method were run on SDS polyacrylamide gels. There was a (mean±SE) 21.9±0.9-fold increase in S100P (**Figure 3.1.A1**) and 127±30-fold increase in S100A4 in cell lysates (**Figure 3.1.C1**), and a 34.3±3.0-fold increase in S100P (**Figure 3.1.B1**) and a 75.94±12.89-fold increase in S100A4 (**Figure 3.1.D1**) in conditioned media. The amount of protein produced per 20 µg of total protein was estimated to be 16.6±3.8 ng and 18.1±0.5 ng for S100P and S100A4, respectively, in cell lysate, and 8.6±2.3 ng and 8.0±0.4 ng in 10 µL of loaded volume for S100P and S100A4, respectively, in conditioned media. Thus, approximately **14.4 %** of the total S100P and **13.1 %** of the total S100A4 was found in the conditioned medium. The molecular weights of S100P and S100A4 by comparison with standard recombinant proteins were estimated to be (mean±SE) 7.4 kDa ±0.24 and 8.5 kDa ±0.32, respectively (**Figure 3.1**).

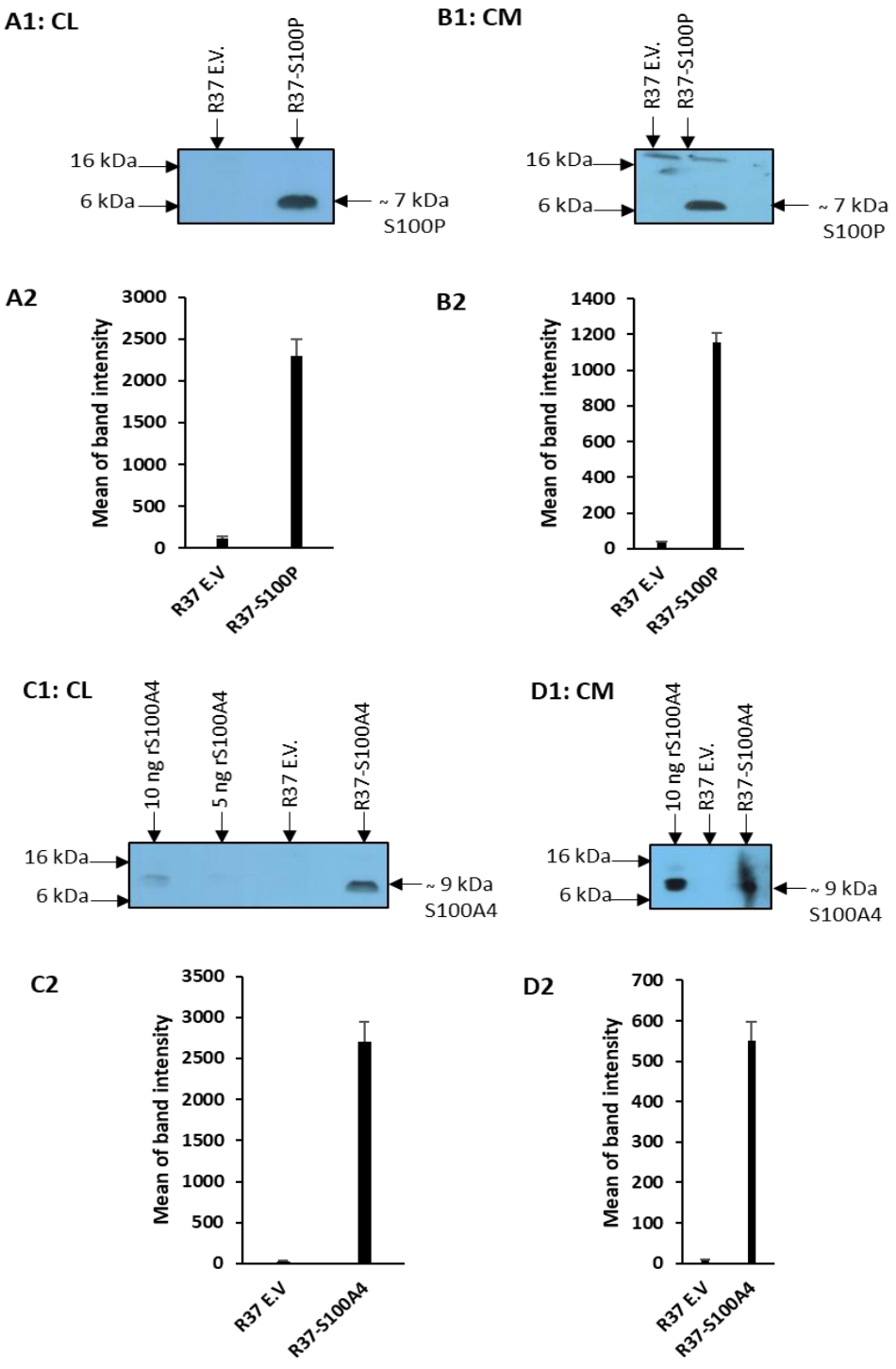

Figure 3.1. Overexpression of S100P and S100A4 proteins in transfected rat mammary cell lines.

Representative Western blots for (**A1** & **C1**) 20 µg protein cell lysate (CL) or (**B1** & **D1**) 10 µL of conditioned media (CM) were run on 15% (w/v) SDS-PAGE from the following. (**A1: CL**) Cell lysate (CL) from stably transfected Rama 37 with empty vector (R37 E.V.) or Rama 37 with S100P (R37-S100P) cell lines. (**A2**) Mean band intensity of S100P in (CL) of R37 E.V. (mean±SE: 114±20.5) or in R37-S100P (mean±SE: 2300±197.3) cell lines showed a 21.9±0.86-fold

increase. The amount of intracellular S100P protein was estimated to be (mean±SE) **16.59±3.77** ng in 20 µg of loaded protein by comparison with similar gels run with recombinant S100P (rS100P). (**B1: CM**) Conditioned media (CM) from R37 E.V. or R37-S100P cell lines. The level of protein in the CM was adjusted and normalized based on cell lysate BCA readings. (**B2**) Mean band intensity of S100P in CM of R37 E.V. (mean±SE: 34.46±4.45) over that from R37-S100P (mean±SE: 1156.66±49.10) cell lines showed a 34.32±2.99-fold increase. The amount of extracellular S100P protein was estimated to be **8.58±2.32** ng in 10 µL of loaded volume by comparison with similar gels run with rS100P. (**C1: CL**) Cell lysates (CL) from R37 E.V. or in R37-S100A4 cell lines were run on similar SDS-PAGE gels. In controls, recombinant 5 or 10 ng purified S100A4 (rS100A4) were also run in parallel. (**C2**) Mean band intensity of S100A4 in CL of R37 E.V. (mean±SE: 24.30±6.90) or in R37-S100A4 (mean±SE: 2706.67±243.40) cell lines showed a 127.95±29.77-fold increase. The amount of intracellular S100A4 protein was estimated to be **18.11±0.51** ng in 20 µg of loaded protein. (**D1: CM**) Conditioned media (CM) from R37 E.V. or R37-S100A4 cell lines. The level of protein in the CM was normalized based on cell lysate BCA readings. In controls, recombinant 10 ng purified S100A4 (rS100A4) was run alongside. (**D2**) Mean band intensity of S100A4 in CM of R37 E.V. (mean±SE: 7.53±0.90) over that from R37-S100A4 (mean±SE: 550.33±46.17) cell lines showed a 75.94±12.89-fold increase. The amount of extracellular S100A4 protein was estimated to be **8.03±0.41** ng in 10 µL of loaded volume. All in all, the percentage of S100P and S100A4 detected extracellularly were 14.4 % and 13.1 % respectively. **Appendix 1** shows the full length gel for overexpression of S100P and S100A4 in CL to confirm only one band being present.

3.2.2 Multi-screening for MMPs in conditioned media of overexpressing S100P/S100A4 cell lines

Conditioned media (CM) from the S100P-inducible human cervical carcinoma cell line HeLa-A3, the stably transfected rat mammary R37-S100P, R37-S100A4 and their empty vector control cell lines were used to investigate whether these cell lines produced MMPs, and if so which MMPs, using a general human MMP antibody array. This multiplex approach offered fundamental advantages for screening a defined set of proteinases in the CM at the same time and the human MMP antibody array used was capable of detecting the following: MMP-1, MMP-2, MMP-3, MMP-8, MMP-9, MMP-10, MMP-13, TIMP-1, TIMP-2 and TIMP-4. By visual inspection, the S100P-

induced HeLa-A3, R37-S100P and R37-S100A4 cell lines showed on increased presence in their CM of MMP-2, MMP-9 and MMP-13 compared to the control cell lines (**Figure 3.2**). The levels of MMP-2 (mean fold increase±SE: 1.09±0.23, n=3, Student's t-test, *P*=0.76) in S100P-induced HeLa-A3, (1.07±0.07, n=3, Student's t-test, *P*=0.48) in R37-S100P, and in R37-S100A4 cells (1.12±0.04, n=3, Student's t-test, *P*=0.33) were all nonsignificant increases compared to control cell lines. Also, the levels of MMP-9 (mean fold increase±SE: 1.2±0.2, n=3, Student's t-test, *P*=0.39) in S100P-induced HeLa-A3, (1.11±0.04, n=3, Student's t-test, *P*=0.24) in R37-S100P, and in R37-S100A4 cells (1.04±0.02, n=3, Student's t-test, *P*=0.81) were increased, but again were not significantly compared to controls. The level of MMP-13 was also increased, but not significantly (mean fold increase±SE: 1.50±0.15, n=3, Student's t-test, *P*=0.08) in S100P-induced HeLa-A3 cells, but was significantly increased in R37-S100P (mean fold increase±SE: 2.40±0.02, n=3, Student's t-test, *P*=0.002) and in R37-S100A4 (mean±SE: 3.6±0.3, n=3, Student's t-test, *P*<0.001) cells compared to controls. The remaining MMPs: MMP-1, MMP-3 and MMP-8 showed no significant increase in CM from both model systems, except that MMP-10 was increased significantly only in CM from R37-S100P and R37-S100A4 cells, but not in S100P-induced HeLa-A3 cells (**Appendix 2**). To undertake a more specific investigation based on function of the MMPs, zymography was undertaken in the cell culture models. These experiments were confined to rat cells, since the induced doxycycline in HeLa cells can at higher concentrations inhibit MMPs (Stechmiller et al., 2010) and more MMPs were significantly increased in the rat cells than in HeLa cells. The array produced only qualitative results and hence Zymography and Western blots were subsequently used to produce quantitative data in only rat cells.

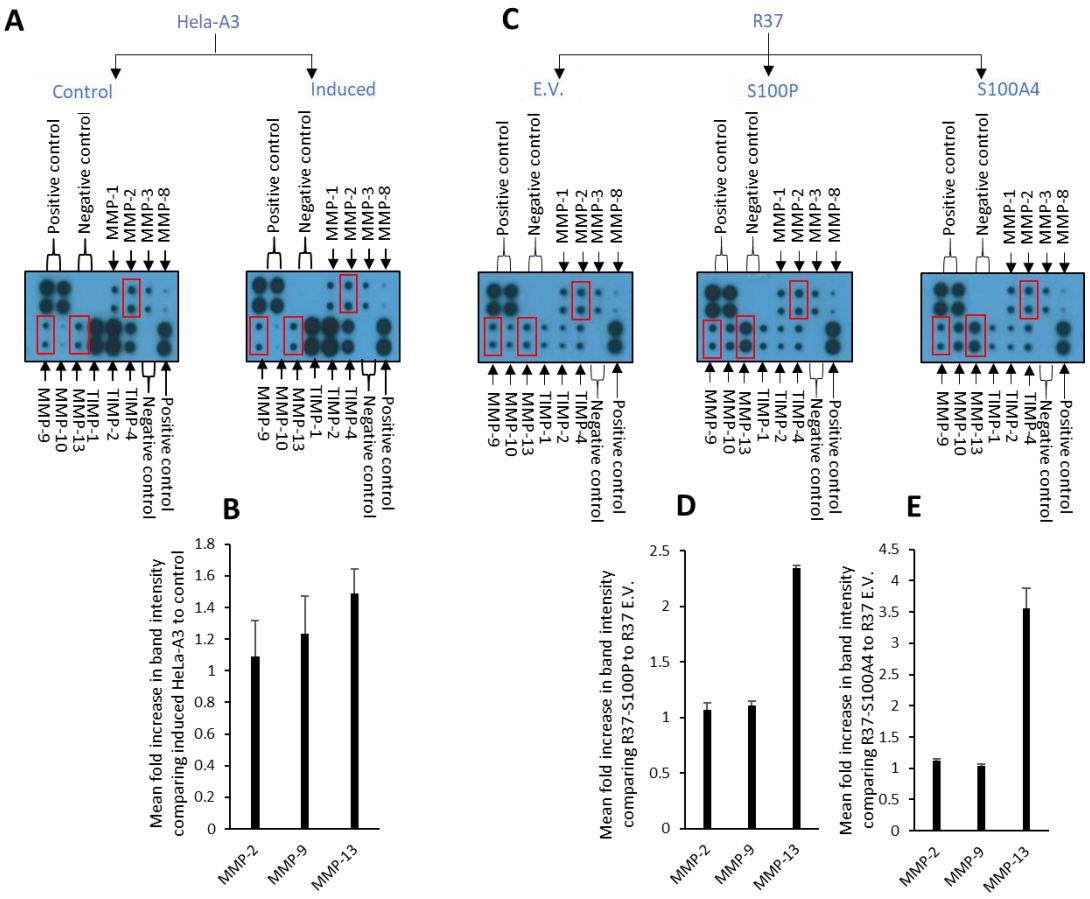

Figure 3.2. Multi-screening MMP array in S100P-induced HeLa-A3, stably transfected rat mammary Rama 37-S100P and Rama-S100A4 cell lines.

(**A**) Human MMP antibody array membranes represent levels of 7 MMPs and 3 TIMPs in CM from noninduced S100P HeLa-A3 or induced S100P HeLa-A3 cells. Membranes were probed with CM from S100P-noninduced HeLa-A3 (control) and S100P-induced HeLa-A3 cells (induced). (**B**) Histogram of 3 experiments from **A** showed the mean fold increase in band intensity for MMP-2, 9 and 13 in S100P-induced HeLa-A3 compared to their noninduced control. (**C**) Human MMP antibody array membranes represent levels of 7 MMPs and 3 TIMPs in CM from R37 empty vector (E.V), R37-S100P (S100P) and R37-S100A4 (S100A4) cells. Membranes were probed with CM from Rama 37 empty vector (E.V.), Rama 37-S100P (S100P) and Rama 37-S100A4 (S100A4) cells. (**D & E**) Histograms of 3 experiments from **C** showed mean fold increase in band intensities for MMP-2 and 9 were increased, but not significantly (Student's t-test, P>0.05), whilst that for MMP-13 was increased significantly in Rama 37-S100P and Rama 37-S100A4 cell lines (P=0.002 and P<0.001, respectively). Abbreviations: Matrix metalloproteinase (MMP). Tissue inhibitor of metalloproteinase (TIMP). Data for the remaining MMPs is shown in **Appendix 2**.

3.2.3 Functional activity assay for MMPs using zymography

The zymography technique was used as a second method to help confirm the functional activity of MMPs in conditioned media (CM) from R37 empty vector control, R37-S100P and R37-S100A4 cell lines. The CM was concentrated and normalized for total cell lysate protein determined by BCA (Section **2.4** and **2.5**). The volumes of CM corresponding to the proportion of cell lysate proteins were loaded onto the zymography gels. SDS gels containing gelatine were used for MMP-2 and MMP-9 investigations (gelatine-zymography) (Section **2.12.3**) and all the various forms of the proteases, both inactive and active, were chemically activated after the gel had been run (Section **2.12.3**). Using gelatine-zymography the CM samples showed distinct bands of cleared area which corresponded in size to both forms of recombinant human MMP-2 (rhMMP-2), the proform rhMMP-2 (68kDa) and active form rhMMP-2 (62 kDa)(da Silva et al., 2014; Shimokawa Ki et al., 2002) (**Figure 3.3.A1**), or one form of recombinant human MMP-9 (rhMMP-9), the proform rhMMP-9 (92 kDa) (Nair et al., 2006) (**Figure 3.3.B1**). Moreover, by visual inspection there were no cleared bands corresponding to the molecular weights of other members of the MMP family which may show gelatinolytic activity, including MMP-10. From the literature proteolytic activity of MMP-10 (stromelysin-2) has been tested also using gelatine-zymography (Wu et al., 2012). The latter study showed that MMP-10 has gelatinolytic activity for two forms, proform at 58 kDa and active form at 44 kDa in CM from gastric cancer cell lines. In our gelatine-zymography study, no band corresponding to MMP-10 was seen, thus it has been omitted from further investigations.

The gelatinolytic activity of MMP-2 in CM from the R37-S100P cell line showed the following results: proform MMP-2 was significantly decreased by 3-fold (mean±SE with respect to empty vector cells set at 1: 3.0±0.4, n =7, Student's t-test, *P*<0.0001). Active form MMP-2 showed a significant increase by about 2-fold (1.9±0.2, n =7, *P*=0.008) over empty vector controls. Moreover, gelatinolytic activity of MMP-2 in CM from the R37-S100A4 cell line showed the following results: proform MMP-2 was significantly decreased by 2.5-fold (mean±SE with respect to empty vector cells set at 1: 2.5±0.1, n=7, Student's t-test, *P*<0.0001). In contrast, active form MMP-2 was significantly increased by 2.4-fold (2.4±0.2, n=7, *P*<0.0001) over empty vector controls (**Figure 3.3.A2**).

Gelatinolytic activity of MMP-9 showed only proform MMP-9 in CM samples from both R37-S100P and R37-S100A4 cell lines. The proform MMP-9 was significantly increased by 1.9-fold (mean±SE with respect to empty vector cells set at 1: 1.94±0.16, n=7, Student's t-test, *P*<0.0001) in CM from R37-S100P, and by 2.3-fold (2.31±0.17, n=7, *P*<0.0001) in CM from R37-S100A4 cell lines over that in empty vector cells (**Figure 3.3.B2**).

Casein-zymography was used to identify the proteolytic activity of MMP-13, since its single cut in its target collagen I is not readily detectable by collagen-zymography (Chung et al., 2004; Van Doren, 2015). Caseinolytic activity of MMP-13 on casein gels showed distinct clear bands for proform MMP-13 (60 kDa) and active form MMP-13 (52 kDa) (**Figure 3.3.C1**). The CM from R37-S100P and R37-S100A4 cell lines showed significant decreases in proform MMP-13 of 2-fold (mean±SE with respect to empty vector cells set at 1: 1.96±0.05, n=3, Student's t-test, *P*=0.031) and 1.4-fold (1.4±0.02, n=3, *P*=0.001), respectively over empty vector cells. The active

form MMP-13 was significantly increased by 5.3-fold (5.26±0.25, n=3, *P*=0.001) in CM from R37-S100P and by 2.2-fold (2.16±0.06, n=3, *P*<0.0001) in CM from R37-S100A4 (**Figure 3.3.C2**) over empty vector cells. The MMPs identified by zymography were next investigated using the SDS-PAGE Western blotting technique.

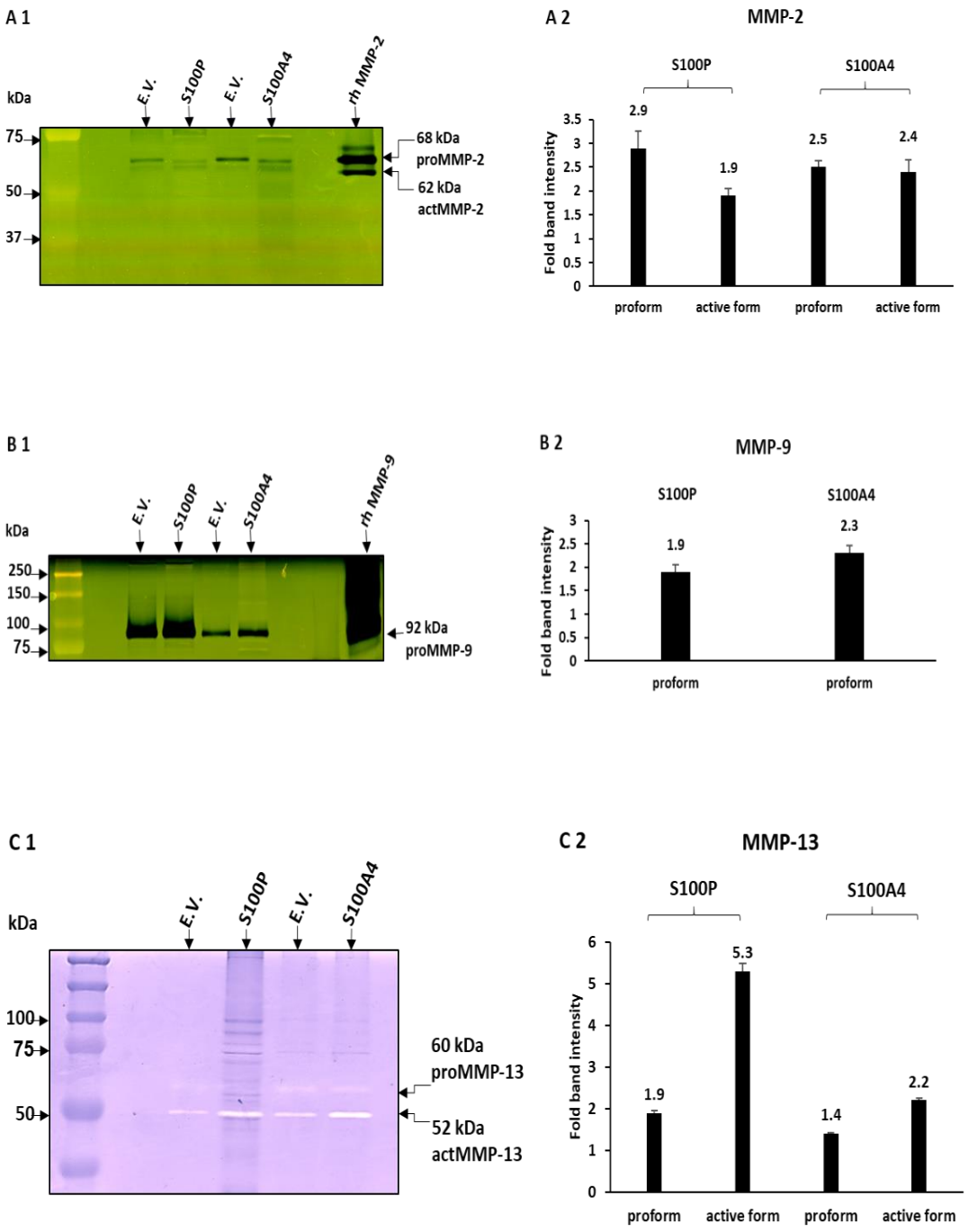

Figure 3.3. Gelatin- and casein-zymography for MMP's activity in conditioned media of rat mammary cell lines.

(**A1**) A representative gelatine gel showed proform (pro) MMP-2 (68 kDa) and active (act) form MMP-2 (62 kDa) in the CM of Rama 37 empty vector (E.V.), Rama 37-S100P (S100P) and Rama 37-S100A4 (S100A4) cells, which corresponded in size to both forms of a recombinant human MMP-2 (rhMMP-2). The bands appeared as a clear zone in the gelatine gel. The scanner setting was changed to show a negative film image to display the best possible contrast of the bands. (**A2**) Histogram of 7 experiments from **A1** showed the proform MMP-

2 in the CM of Rama 37-S100P was significantly decreased by 3.0±0.4-fold (Student t-test, *P*<0.0001), but active form MMP-2 was significantly increased by 1.9±0.2-fold (*P*=0.008) compared to E.V. control cells. Proform MMP-2 in the CM of Rama 37-S100A4 was significantly decreased by 2.5±0.14-fold (*P*<0.0001), but active form MMP-2 was significantly increased by 2.3±0.2-fold (*P*<0.0001). (**B1**) A representative gelatine gel showed only proform (pro) MMP-9 (92 kDa) in the CM from Rama 37 empty vector (E.V.), Rama 37-S100P (S100P) and Rama 37-S100A4 (S100A4) cells, which corresponded in size to a recombinant human MMP-9 (rhMMP-9). As above the scanner setting was changed to show a negative film image to display the best possible contrast of the bands. The rhMMP-9 was overloaded and hence produced an artificial tail in the gel. (**B2**) Histogram of 7 experiments from **B1** showed proform MMP-9 in the CM from Rama 37-S100P and Rama 37-S100A4 was significantly increased by 1.9±0.2-fold (*P*<0.0001) and by 2.3±0.2-fold (*P*<0.0001), respectively, over that in empty vector cells. (**C1**) A representative casein gel showed proform (pro) MMP-13 (60 kDa) and active (act) form MMP-13 (52 kDa) in the CM of Rama 37 empty vector (E.V.), Rama 37-S100P (S100P) and Rama 37-S100A4 (S100A4) cells. The bands appeared as a clear zone in the gelatin gel when recorded as a positive image. (**C2**) Histogram of 3 experiments from **C1** showed proform MMP-13 in the CM of Rama 37-S100P was significantly decreased by 1.96±0.05-fold (*P*=0.031), but active form MMP-13 was significantly increased by 5.3±0.2-fold (*P*=0.001). Proform MMP-13 in the CM of Rama 37-S100A4 was significantly decreased by 1.4±0.02-fold (*P*=0.001), but active form MMP-13 was significantly increased by 2.2±0.06-fold (*P*<0.0001). E.V. was different for empty vector control for R37-S100P and for R37-S100A4 cells (**Section 2.2.2**).

3.2.4 Western blot analysis to confirm identities of MMPs

A specific antibody for each of these MMPs was used in Western blotting as a third method to confirm the identities of MMP-2, -9 and -13 and to measure more accurately the levels of expressed protein. Cell lysate (CL) and conditioned media (CM) from the R37 empty vector, R37-S100P and R37-S100A4 cell lines were collected and normalized (Section **2.5**). The definitions used of precursor form, proform and active form of MMPs detected in this study using Western blotting are as follows. Precursor form is the intracellular form of MMP which is detected inside the cell in the cell lysate (CL). Proform and active form are the extracellular forms of MMP which are detected outside the cell in conditioned medium (CM) (Suzuki et al., 1995).

3.2.4.1 MMP-2

When Western blotting was used, the measured apparent molecular weight of the MMP-2 precursor in the CL and the MMP-2 proform and active forms in the CM were 72, 68 and 62 kDa, respectively, consistent with molecular weights reported previously (da Silva et al., 2014; Roomi et al., 2010; Takino et al., 1995). The levels of MMP-2 were changed significantly in both the CL and CM from R37-S100P and R37-S100A4 compared to R37 empty vector control cell lines. When Western blot was used on CL, the ratio of band intensity for the precursor MMP-2 at 72 kDa (precursor MMP-2/GAPDH ratio) was significantly increased by 1.6-fold (fold mean±SE: 1.57±0.068, n=3, Student's t-test, *P*=0.004) in the CL from R37-S100P and about 1.8-fold (1.81±0.079, n=3, *P*=0.004) in CL from R37-S100A4 compared to R37 empty vector control cell lines (**Figure 3.4.A1 & A2**). Moreover, both proform and active forms of MMP-2 in the CM from these cell lines were detected using Western blotting. The proform MMP-2 at 68 kDa was significantly decreased over empty vector by 3.8-fold (mean±SE with respect to empty vector cells set at 1: 3.8±0.07, n=7, *P*<0.0001) in the CM from R37-S100P and 1.2-fold (1.2±0.02, n=7, *P*<0.0001 with respect to empty vector cells set at 1) in the CM from R37-S100A4**.** In contrast**,** the **active MMP-2 at 62 kDa** was significantly increased by about 1.8-fold (1.83±0.03, n=7, *P*<0.0001) in the CM from R37-S100P and about 2.5-fold (2.47±0.06, n=7, *P*<0.0001) in the CM from R37-S100A4 over that in empty vector cells (**Figure 3.4.B1 & B2**).

3.2.4.2 MMP-9

The CL and CM from these cell lines showed only one form of MMP-9, a precursor/proform at 92 kDa, consistent with that reported previously (Orgaz et al., 2014) and no active MMP-9 reported molecular weight of 82 kDa (Zeng et al., 1999) was observed. The former finding confirmed the results for extracellular MMP-9 using gelatin-zymography (**Figure 3.3.B1**). The levels of MMP-9 were changed significantly in the CL and CM from R37-S100P and R37-S100A4 compared to R37 empty vector control cell lines when Western blot was used. Thus, the ratio of band intensity for the **precursor MMP-9 at 92 kDa** (precursor MMP-9/GAPDH ratio) was significantly increased in CL from R37-S100P and R37-S100A4 by 1.7-fold (fold mean±SE: 1.71±0.03, n=3, Student's t-test, *P*=0.035), and 2.5-fold (2.52±0.14, n=3, *P*=0.001), respectively, compared to empty vector control cell lines (**Figure 3.5. A1 & A2**). Moreover, the level of **proform MMP-9 at 92 kDa** was significantly increased by 1.6-fold (1.62±0.05, n=7, *P*<0.0001) in the CM from R37-S100P and 2.7-fold (2.7±0.2, n=7, *P*<0.0001) in the CM from R37-S100A4 compared to R37 empty vector control cell lines (**Figure 3.5. B1 & B2**).

3.2.4.3 MMP-13

When Western blotting was used for MMP-13, the measured apparent molecular weight of the MMP-13 precursor in the CL and the MMP-13 proform and active forms in the CM were 50, 60 and 52 kDa, respectively, consistent with those reported previously (Peeters-Joris et al., 1998; Schröpfer et al., 2010)**.** The levels of MMP-13 were changed significantly in the CL and CM from R37-S100P and R37-S100A4 compared to R37 empty vector control cell lines. When Western blot was

used on CL, the ratio of band intensity for the **precursor MMP-13 at 50 kDa** (precursor MMP-13/GAPDH ratio) was significantly increased by 3.6-fold (fold mean±SE: 3.64±0.14, n=3, Student's t-test, *P*=0.001) in the CL from R37-S100P and 2.9-fold (2.92±0.21, n=3, *P*=0.005) in the CL from R37-S100A4 compared to R37 empty vector control cell lines (**Figure 3.6. A1 & A2**). Moreover, the CM from R37-S100P, R37-S100A4 and R37 empty vector control cell lines all showed expression of 2 forms of MMP-13, the **proform at 60 kDa** and **active form at 52 kDa**. The 60 kDa proform MMP-13 was significantly decreased by 2.8-fold (mean±SE with respect to empty vector cells set at 1: 2.8±0.07, n=3, Student's t-test, *P*=0.004) in the CM from R37-S100P and by 8.4-fold (8.4±0.2, n=3, *P*<0.0001) in the CM from R37-S100A4. In contrast, the 52 kDa active MMP-13 was significantly increased by about 5.3-fold (5.27±0.29, n=3, *P*<0.0001) in the CM from R37-S100P and by 1.6-fold (1.6±0.005, n=3, *P*=0.012) in the CM from R37-S100A4 compared to R37 empty vector control cell lines (**Figure 3.6. B1 & B2**).

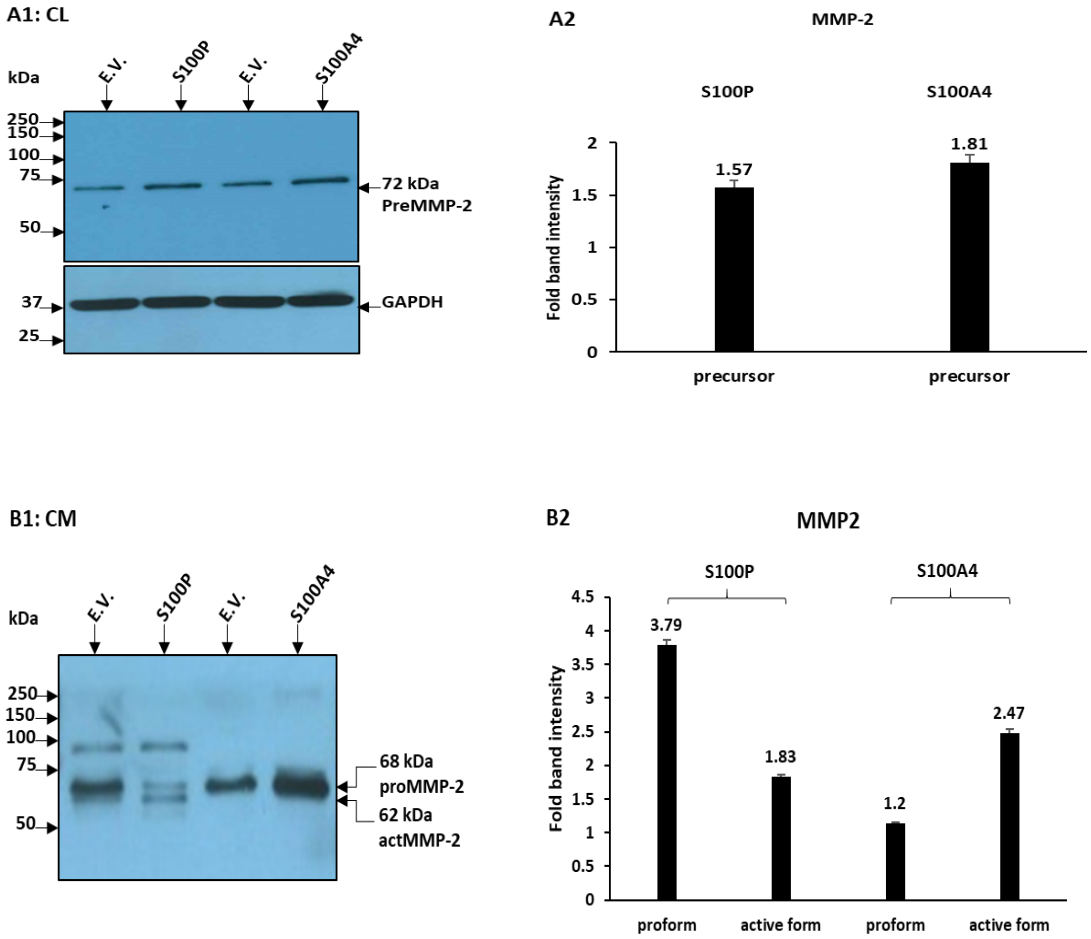

Figure 3.4. Western blot for MMP-2 forms in the cell lysate (CL) and conditioned media (CM) from rat mammary cell lines.

Ten micrograms (10 µg) of protein for CL or 10 µL volume for CM were loaded on 10 % (w/v) SDS-PAGE gels. The total protein concentrations were quantified using BCA. The quantities of CM loaded were adjusted according to the amount of protein in the CL estimated by BCA (Section **2.5**) (**A1:CL**) Representative Western blot showed the precursor MMP-2 (preMMP-2) at 72 kDa in the cell lysate (CL) from R37 empty vector (E.V.), R37-S100P (S100P) and R37-S100A4 (S100A4) cell lines. (**A2**) Histogram of three independent experiments of **A1** showing that the level of preMMP-2 (precursor) was increased significantly in the CL from R37-S100P and from R37-S100A4 by 1.57±0.06-fold (Student's t-test, *P*=0.004) and by 1.81±0.07-fold (*P*=0.004), respectively, compared to their E.V. control cell lines. (**B1:CM**) Representative Western blot showed the proform MMP-2 (proMMP-2) at 68 kDa and active MMP-2 (actMMP-2) at 62 kDa in the CM from R37 empty vector (E.V.), R37-S100P (S100P) and R37-S100A4 (S100A4) cell lines. (**B2**) Histogram of three independent experiments from **B1** showed proMMP-2 (proform) was significantly decreased by 3.8±0.07-fold (*P*<0.0001), but actMMP-2 (active form) was increased significantly by 1.83±0.03-fold (*P*<0.0001) in the CM from R37-S100P over that in empty vector control cell line. The CM from R37-S100A4 cell line showed proMMP-2 (proform) was also decreased significantly by 1.14±0.02-fold (*P*<0.0001), but actMMP-2 (active form) was increased significantly by 2.47±0.06-fold (*P*<0.0001) over that in empty vector control cell line. There is a band observed at 90 kDa which only appeared

during longer exposures with ECL Select Reagent but did not correspond to any seen by zymography. Therefore, it was excluded in reporting quantitative results for MMP-2. E.V. was different for empty vector control for R37-S100P and for R37-S100A4 cells (**Section 2.2.2**).

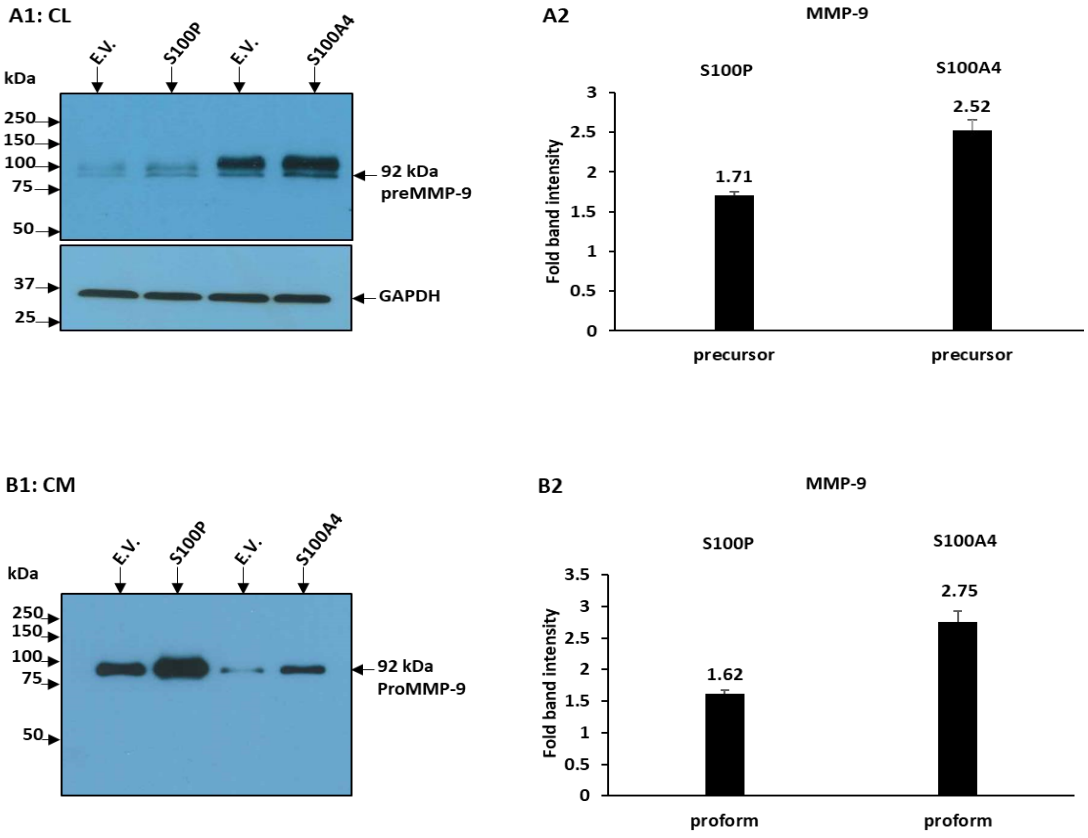

Figure 3.5. Western blot for MMP-9 forms in the cell lysate (CL) and conditioned media (CM) from rat mammary cell lines.

Ten micrograms (10 µg) of protein for CL or 10 µL for CM was loaded on 10 % (w/v) SDS-PAGE gels. The total protein concentrations in CL were quantified using BCA. The quantity of CM loaded was adjusted according to the amount of protein in the CL estimated by BCA (Section **2.5**). (**A1:CL**) Representative Western blot showed the precursor MMP-9 (preMMP-2) as a double band at 92 kDa in the cell lysate (CL) from R37 empty vector (E.V.), R37-S100P (S100P) and R37-S100A4 (S100A4) cell lines. (**A2**) Histogram of three independent experiments from **A1** showing that the level of preMMP-9 (precursor) was increased significantly in the CL from R37-S100P and R-37-S100A4 cell lines by 1.7±0.03-fold (Student's t-test, *P*=0.035) and about 2.5±0.14-fold (*P*=0.001), respectively, compared to their E.V. control cell lines. (**B1:CM**) Representative Western blot shows the proform MMP-9 (proform) at 92 kDa in the CM from R37 empty vector (E.V.), R37-S100P (S100P) and R37-S100A4 (S100A4) cell lines. (**B2**) Histogram of three independent experiments from **B1** showing that proform MMP-9 (proform) was significantly increased by 1.62±0.05-fold (*P*<0.0001) and by 2.75±0.17-fold (*P*<0.0001) in the CM from R37-S100P and R37-S100A4 cell line, respectively, over empty

vector cells. E.V. was different for empty vector control for R37-S100P and for R37-S100A4 cells (**Section 2.2.2**).

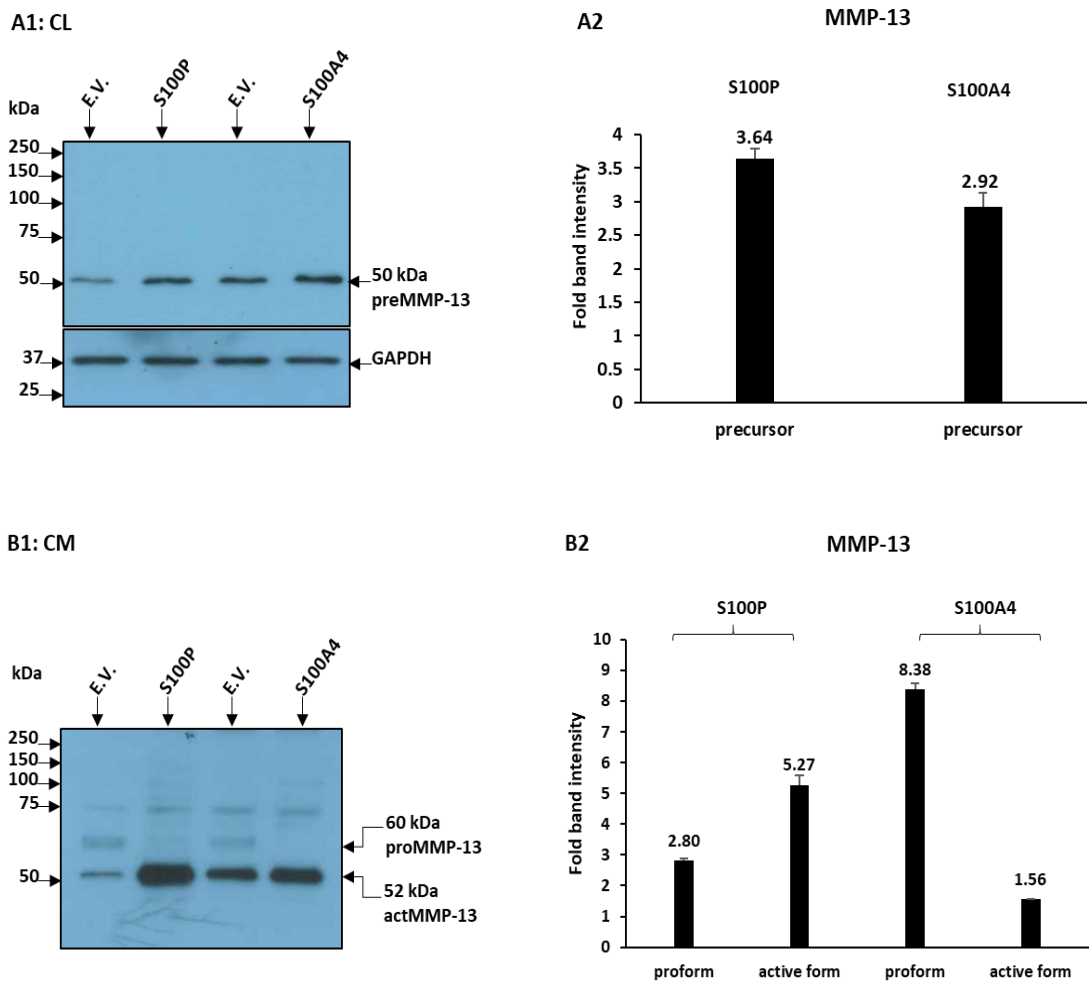

Figure 3.6. Western blot for MMP-13 forms in the cell lysate (CL) and conditioned media (CM) from rat mammary cell lines.

Ten micrograms (10 µg) of protein for CL or 10 µL for CM were loaded on 10 % (w/v) SDS-PAGE gels. The total protein concentrations were quantified using BCA. The quantity of CM loaded was adjusted according to the amount of protein in the CL estimated by BCA. (**A1:CL**) Representative Western blot showed the precursor MMP-13 (preMMP-13) at 50 kDa in the cell lysate (CL) from R37 empty vector (E.V.), R37-S100P (S100P) and R37-S100A4 (S100A4) cell lines. (**A2**) Histogram of three independent experiments from **A1** showing that the level of precursor MMP-13 (precursor) was increased significantly in the CL from R37-S100P and R37-S100A4 cell lines by 3.6±0.14-fold (Student's t-test, *P*=0.001) and by 2.9±0.21-fold (*P*=0.005), respectively, compared to their E.V. control cell lines. (**B1:CM**) Representative Western blot showed the proform MMP-13 (proMMP-13) at 60 kDa and active MMP-13 (actMMP-13) at 52 kDa in the CM from R37 empty vector (E.V.), R37-S100P (S100P) and R37-

S100A4 (S100A4) cell lines. (**B2**) Histogram of three experiments from **B1** showing that the proform MMP-13 (proform) was significantly decreased by 2.8±0.07-fold (Student's t-test, *P*<0.004), but active MMP-13 (active form) was increased significantly by 5.27±0.29-fold (*P*<0.0001) in CM from the R37-S100P cell line. The CM from S100A4 cell line showed proform MMP-13 (proform) was also decreased significantly by 8.38±0.21-fold (*P*<0.0001), while active MMP-13 (active form) was increased significantly by 1.6±0.005-fold (*P*=0.012) compared to empty vector cells. There was a band observed at 75 kDa which appeared only during longer exposures with ECL Select Reagent, but which did not correspond to any seen by zymography. Therefore, it was ignored in reporting quantitative results for MMP-13. E.V. was different for empty vector control for R37-S100P and for R37-S100A4 cells (**Section 2.2.2**).

3.3 Discussion

The apparent molecular weights of intracellular S100P and S100A4 of (mean±SE) 7.4±0.2 and 8.5±0.3 kDa, respectively, were consistent with Wang et al., (2015) and Zhuang et al., (2016). S100A4 has a longer C-terminal region than S100P of 5 amino acid residues corresponding to an increase of about 1 kDa in apparent molecular weight (Gross et al., 2014). In addition, we detected S100P and S100A4 proteins in the CM from the same transfected rat mammary cell lines. These proteins had the same molecular weights as those in the cytoplasm, but they showed very large increases of about (mean±SE) 34.3±3.0 and 76±13-fold, respectively, compared to their empty vector control cell lines (**Figure 3.1. B2, D2**). Although S100P can be detected extracellularly, whether they are secreted from living cells or released from floating, potentially dying cells *in vitro* is still debated (Bresnick et al., 2015; Donato et al., 2013; Leclerc, 2011). The amounts of S100P or S100A4 proteins inside cells (CL) were 16.6±3.8 ng or 18.1±0.5 ng per 20 µg CL and outside in the CM were 8.6±2.3 ng or 8.0±0.4 ng per 10 µL CM. Thus, approximately 14.4 **%** for S100P and 13.1 **%** for S100A4 was found in the conditioned media over the same time period. How these

S100 proteins were released from cells is unknown, since they contain no secretory signal sequence (Gross et al., 2014).

The human array used here can detected 7 MMPs and 3 TIMPs: MMP-1, -2, -3, -8, -9, -10 & -13, and TIMP-1, -2 & 4. This experiment showed that all these MMPs were increased, but not significantly except for MMP-10 and MMP-13 in the CM from R37-S100P or R37-S100A4 cells over the empty vector cell lines (**Figure 3.2, Appendix 2**). Moreover, the most common MMP proteins which showed an increase between S100P-induced HeLa-A3 and R37-S100P/A4 cells were MMP-2, -9, -10 and -13. The S100P-induced HeLa cells were included in case the antibodies showed preferential specificity for human MMPs. The results using zymography showed that CM from R37-S100P and S100A4, when chemically activated after running the gels, produced bands corresponding to only MMP-2 and MMP-9 on gelatin-gels and to only MMP-13 on casein-gels, so eliminating MMP-10 as an activatable MMP (Wu et al., 2012) in the cell lines under study. The reason why overexpression of S100P and S100A4 stimulated only MMP-2, -9 and -13, at least, in Rama 37 cells is unknown.

The measured molecular weights in the CM for the higher molecular weight forms of MMP-2 and -13 of 68 and 60 kDa and for the next lowest forms of 62 and 52 kDa, respectively, are identical when detected by chemically-activated enzymatic activity (zymography) (**Figures 3.3.A1, B1, C1**) or by specific antibodies (Western blotting) (**Figures 3.4.B1, 3.5.B1, 3.6.B1**). These molecular weight forms correspond to the reported values for the activated forms and the proforms of the MMPs (da Silva et al., 2014; Nair et al., 2006; Orgaz et al., 2014; Peeters-Joris et al., 1998; Roomi et al., 2010; Schröpfer et al., 2010; Shimokawa Ki et al., 2002), except for MMP-9 where our gels identified only that corresponding to the proform and not the

reported active form of 82 kDa (Zeng et al., 1999). Moreover, the molecular weights forms of MMP-2, MMP-9 and MMP-13 identified by Western blot of CLs (cell lysates) of 72, 92 and 50 kDa, respectively, corresponded to those of the reported precursor forms which occur within cells (da Silva et al., 2014; Nair et al., 2006; Orgaz et al., 2014; Peeters-Joris et al., 1998; Roomi et al., 2010; Schröpfer et al., 2010; Shimokawa Ki et al., 2002). Presumably preMMP-2 at 72 kDa is successively cleaved into proMMP-2 at 68 kDa and activated MMP-2 at 62 kDa (Takino et al., 1995); the cleavage pathway for MMP-9 (Orgaz et al., 2014) does not occur in our cells. In contrast, there is an increase in apparent molecular weight in going from preMMP-13 at 50 kDa to proMMP-13 at 60 kDa and then a reduction to activate MMP-13 at 52 kDa presumably due to post-translation modifications and zymogen activation, respectively (Boon et al., 2016; Knäuper et al., 1996).

When the quantitative results are compared between those obtained by zymography and by Western blots, there is complete agreement of direction of change for all 3 MMPs in R37-S100P and R37-S100A4 cells (**Table 3.1.**). In the CM for MMP-2 and MMP-13 where cleavage occurs, the proform is significantly reduced and the activated form is significantly increased (Student's t-test $P \leq 0.004$). Since no activated form of MMP-9 is produced, the proforms showed significant accumulation in the CM over the empty vector cell lines ($P \leq 0.035$) (**Table 3.1**). The production of precursors in the CL measured by Western blotting alone all showed an increase ranging from 1.6 to 3.6-fold and these increases were similar to the range of increases in activated forms for MMP-2 and MMP-13 of 1.6 to 5.3-fold, with individual paired fold changes showing similar differences (CL precursor vs CM active form in the R37-S100P and S100A4 cells using Western blot) MMP-2: 1.6 vs 1.83 and 1.81 vs 2.47, and

MMP-13: 3.64 vs 5.27 and 2.92 vs 1.56, respectively. Since the input of both the CM and CL have been normalised to the total protein in the cell (section **2.5**), these results suggested that all the increase seen in the active forms of MMP-2 and MMP-13 in the CM could be accounted for by the increase in production of the precursor forms within the cell, and even in the case of MMP-9 where no active form is produced, the increases in proMMP-9 in CM are not significantly different from those in precursor MMP-9 in the cells (CL vs CM: 1.71±0.035 vs 1.62±0.05; 2.52±0.14 vs 2.75±0.17 for S100P and S100A4-containing cells) (**Table 3.1**).

Table 3.1. Conclusion of comparative changes in MMPs.

MMP [a]	CL/CM [b]	Fold changes in S100P±SE [c]		Fold changes in S100A4±SE [c]	
		Zymography [d]	Westerns [d]	Zymography [d]	Westerns [d]
preMMP-2	CL	n.d.	+ 1.6±0.06	n.d.	+ 1.8±0.07
proMMP-2	CM	- 2.9±0.36	- 3.8±0.07	- 2.5±0.14	- 1.2±0.02
actMMP-2	CM	+1.9±0.16	+ 1.8±0.03	+ 2.4±0.25	+ 2.5±0.06
preMMP-9	CL	n.d.	+ 1.7±0.03	n.d.	+ 2.5±0.14
proMMP-9	CM	+ 1.9±0.16	+ 1.6±0.05	+ 2.3±0.17	+ 2.8±0.17
preMMP-13	CL	n.d	+ 3.6±0.14	n.d	+ 2.9±0.21
proMMP-13	CM	- 1.9±0.05	- 2.8±0.07	- 1.4±0.02	- 8.4±0.2
actMMP-13	CM	+ 5.3±0.20	+ 5.3±0.2	+ 2.2±0.06	+ 1.6±0.005

[a] Matrix metalloproteinase (MMP): pre, precursor; pro, proform; act, active form.
[b] Cell lysate (CL) or conditioned media (CM).
[c] Mean fold changes in levels of MMPs in S100P/S100A4 either increased (+) or decreased (-) ± standard error of mean (SE).
[d] All significantly different between Zymography and Western determinations.

Our results of increases in MMP-2, -9 and -13 in malignant over non-malignant cell lines are broadly in agreement with those previously published in different cell system (Johansson et al., 1999; Li et al., 2017). Thus in the breast cancer cell lines

MDA-MB-231 and MCF-7 there is an increase in MMP-2 mRNA or protein compared to the normal human breast Hs578Bst cell line (Li *et al.*, 2017), although an earlier publication suggested that it was produced only in the stromal cells and not from the breast cancer cells in cell lines and primary cultures from breast cancer biopsies (Singer et al., 2002). For MMP-9 Mehner et al. (2014) showed that expression of MMP-9 mRNA was elevated in the media of the more malignant breast cancer MDA-MB-435 cell line. A further study showed that more inactive proform of MMP-9 was produced in rounded-amoeboid melanoma cells than in elongated mesenchymal-like melanoma cells. More importantly, addition of inactive proform MMP-9 could enhance rounded-amoeboid cell migration in three dimensions due to an increase in actomyosin contractility triggered via the CD44 receptor (Orgaz et al., 2014). Thus, it is possible that overproduction and release of proform MMP-9 from R37-S100P/A4 cells may still have a significant role in cell migration independent of its gelatinase activity. For MMP-13, it was found to be highly expressed as mRNA or protein in highly invasive MDA-MB-231 cells compared to other less invasive cell lines (Balduyck et al., 2000). Moreover, a study on specimens from breast cancer *in vivo* showed that the level of MMP-13 protein was significantly higher in breast cancer than in normal breast cells (Kotepui et al., 2016), confirming earlier reports in colorectal cancer (M. F. Leeman et al., 2002) and papillary thyroid carcinoma (Wang et al., 2013). Whether the increased levels of these MMPs play a biological role in the development of the S100-transfected cells' malignant phenotype is the subject of the next chapter.

3.4 Summary

Benign rat mammary (R37) cell lines previously transfected with expression vectors for S100P or S100A4 produced 22 to 128-fold more of these proteins inside cells in comparison with empty vector-containing R37 cells and for the first time were shown to secrete substantial amounts of 8.6 ng and 8.03 ng in 10 µL CM, respectively. When screened with antibody arrays these transfected and S100-overexpressing cell lines produced increased levels of MMPs in their CM, but on chemically-activated zymography only MMP-2, MMP-9 and MMP-13 showed significant increases in proteolytic activity on gelatin (MMP-2 and MMP-9) or casein (MMP-13) containing polyacrylamide gels. Western blotting confirmed significantly increased levels of 1.6 to 5.3-fold of active forms of MMP-2 and MMP-13 in the CM were probably produced by similar increases of 1.6 to 3.6-fold in their precursors inside the cells (CL). MMP-9, in contrast, produced only its proform in the CM in 1.6 to 2.7-fold higher levels than that in empty vector-containing cells and these values were matched by a similar increases in precursor MMP-9 of 1.7 to 2.3-fold inside the cells.

Chapter 4

Role of specific MMPs in induction of migration and invasion in S100P/S100A4 overexpressing rat mammary cell lines

4.1 Introduction

Among many proteins reported to be involved in breast cancer are S100P and S100A4, and their levels correlate significantly with poor outcome for breast cancer patients' survival (Ismail et al., 2017; Rudland et al., 2000; Wang et al., 2006; Zhang et al., 2017). S100P and S100A4 have been shown to promote metastasis in breast cancer models (Ambartsumian et al., 1996; Davies et al., 1993, 1996; Wang et al., 2006) by increasing cell motility and invasion (Du et al., 2012; Jenkinson et al., 2004). Degradation of the ECM is involved in both cell migration and cell invasion and both processes are promoted by MMPs in tissue cultured cells (Maletzki et al., 2012). MMPs also can enhance cancer cell metastasis, presumably by stimulating cell migration and/or invasion (Mishra et al., 2012), possibly by cleavage of fibronectin and collagen I, respectively (Sen et al., 2010). On particular example is when S100P inhibition is reduced in nasopharyngeal carcinoma cell lines a series of intracellular alterations are generated, these include suppression of expression of MMP-2 and MMP-9 (Liu et al., 2017). Moreover in the pancreatic carcinoma BxPC3 cell line, S100P can stimulate invasion by inducing IκBα and the secretion of MMP-9 (Dakhel et al., 2014).

In thyroid cancer and in rat C6 glioma cell lines, overexpression and suppression of the S100A4 gene intracellularly has led to increases and decreases, respectively, in the expression of MMP-9 (Jia et al., 2013; Takenaga and Kozlova, 2006). Moreover, in MDA-MB-231 and MDA-MB-468 breast cancer cell lines, S100A4 can induce epithelial-mesenchymal transition (EMT), in part, through increased expression of MMP-2 (Xu et al., 2016). Thus, in order to investigate the effects of MMPs on cell migration and invasion *in vitro*, we shall knock-down the selected MMPs identified in Chapter 3 in S100P/S100A4-overexpressing rat mammary cell lines and observe the resultant effects on cell migration and invasion *in vitro*.

For knock-down experiments in mammalian cells, double stranded RNAs (21-23 nucleotides), also called short or small interfering RNAs (siRNA), can be used to inhibit specific sequences in protein-coding genes (Elbashir et al., 2001). Thus, transient transfection of siRNAs into living cells can inhibit, for a short-term, specific gene expression, and hence the effect of this gene on cellular processes (Ameyar-Zazoua et al., 2005). There are several examples of this type of experiment in cancer cells. Thus, when Badiga et al., (2011) inhibited MMP-2 expression using siRNA techniques, this caused a significant reduction in glioma cell migration, invasion, angiogenesis and tumour growth compared to non-inhibited control cells.

To study cell migration, there are a number of methods, e.g., scratch or wound healing assays in 2D,transwell migration and invasion assays by squeezing through pores in membranes, 3D cell migration in gels *in vitro* and cell movement in organs *in vivo* (Moutasim et al., 2011; Su et al., 2017). These assays all have their own advantages and disadvantages. The most common method to study cancer cell

migration and invasion is through pores in membranes along a concentration gradient (Moutasim et al., 2011).

4.1.1 Chapter aims

To examine the transient effect of siRNAs directed against specific MMPs on the migration and invasion of S100P/A4 overexpressing cell lines.

4.2 Results

4.2.1 Knock-down of MMP proteins

The R37-S100P and R37-S100A4 cell lines were cultured routinely and then processed to knock-down MMP-2, MMP-9 and MMP-13 individually or a combination of all 3 MMPs as described in Materials and Methods (Section **2.15**).

4.2.1.1 Treatment with siRNA for MMP-2

Upon transient transfection of siRNA directed at MMP-2 mRNA, the level of precursor intracellular MMP-2 at 72 kDa was significantly decreased in the R37-S100P and R37-S100A4 cell lines by 9-fold (mean±SE:9.02±0.19, n=3, Student's t-test, $P<0.0001$), and by 6.5-fold (6.5±1.6, n=3, $P=0.020$), respectively. The levels of intracellular precursor MMP-9 or MMP-13 were not significantly affected ($P\leq0.460$) when MMP-2 alone was knocked-down by siRNA MMP-2 compared to si-scrambled control (**Appendix 3**). In addition, the R37-S100P and R37-S100A4 cells treated simultaneously with the combined siRNA to MMP-2, 9 and 13 showed a significant decrease in the level of MMP-2 by about 1.4-fold (1.4±0.01, n=3, $P=0.014$) and by about 3.8-fold (3.8±1.0, n=3, $P=0.037$), respectively (**Figure 4.1**). Since MMP-2 levels

failed to change between untreated R37-S100P (mean±SE, 0.321±0.04) or R37-S100A4 (0.4±0.1) cells and treated R37-S100P (0.4±0.02) or R37-S100A4 (0.4±0.08) cells with scrambled siRNA (P≥0.51), there was no toxicity due to siRNA transfection.

4.2.1.2 Treatment with siRNA for MMP-9

When transiently transfected with siRNA to MMP-9, the R37-S100P and R37-S100A4 cell lines showed a significant decline in the level of intracellular precursor MMP-9 at 92 kDa by about 5-fold (mean±SE:5.2±0.8, n=3, Student's t-test, P=0.005), and by about 6-fold (5.8±0.2, n=3, P<0.0001), respectively. Moreover, when the R37-S100P and R37-S100A4 cells were simultaneously treated with siRNA to MMP-2, 9 and 13 the level of MMP-9 was also significantly reduced by nearly 3.5-fold (3.5±0.7, n=3, P=0.011) and by nearly 2.6-fold (2.6±0.08, n=3, P<0.0001), respectively (**Figure 4.2**). The levels of intracellular precursor MMP-2 or MMP-13 were not obviously affected when MMP-9 alone was knocked-down by siRNA MMP-9 (data not shown). Since MMP-9 levels failed to change between untreated R37-S100P (mean±SE, 0.55±0.14) or R37-S100A4 (0.14±0.004) cells and treated R37-S100P (0.38±0.05) or R37-S100A4 (0.13±0.002) cells with scrambled siRNA (P≥0.27), there was no toxicity due to siRNA transfection.

4.2.1.3 Treatment with siRNA for MMP-13

When both R37-S100P and R37-S100A4 cell lines were treated with siRNA to MMP-13, they showed a considerable decline in the level of intracellular precursor MMP-13 at 50 kDa by about 3.7-fold (mean±SE:3.7±0.2, n=3, Student's t-test, P<0.0001), and by nearly 3.6-fold (3.6±0.2, n=3, P=0.003), respectively. Additionally,

when R37-S100P and R37-S100A4 cell lines were simultaneously treated with siRNA to MMP-2, 9 and 13, they both showed a significant decrease in the level of MMP-13 by about 1.7-fold (1.72±0.048, n=3, $P<0.0001$) and about 1.9-fold (1.95±0.077, n=3, $P=0.019$), respectively (**Figure 4.3**). The levels of intracellular precursor MMP-2 or MMP-9 were not obviously affected when MMP-13 alone was knocked-down by siRNA MMP-13 (data not shown). Since MMP-13 levels failed to change between untreated R37-S100P (mean±SE, 0.83±0.01) or R37-S100A4 (0.22±0.03) cells and treated R37-S100P (0.70±0.01) or R37-S100A4 (0.21±0.02) cells with scrambled siRNA ($P\geq0.152$), there was no toxicity due to siRNA transfection.

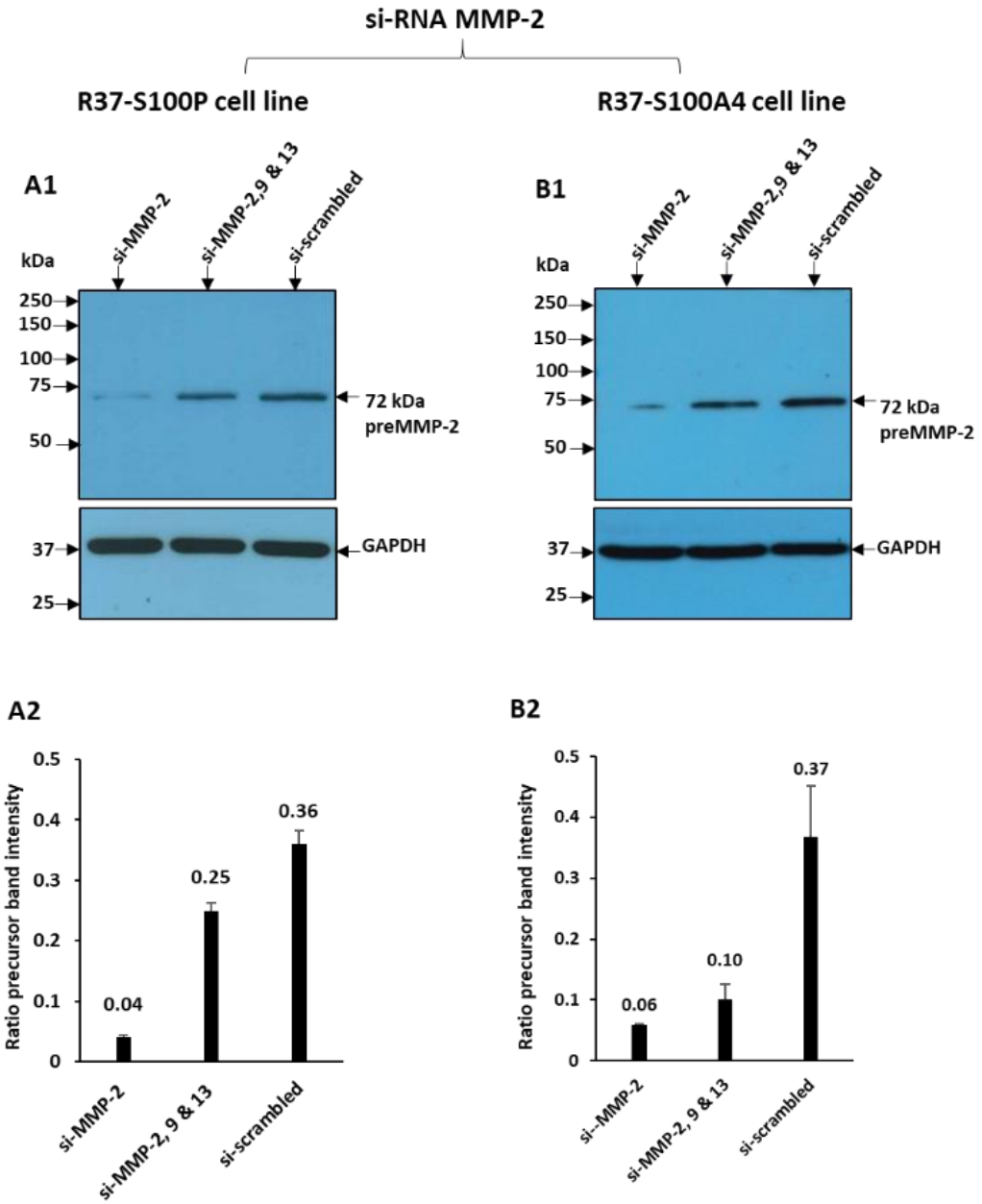

Figure 4.1. Western blots for MMP-2 in the R37-S100P and R37-S100A4 cell lines treated with siRNA to MMP-2 alone or siRNA to MMP-2, 9 and 13.

Ten µg of protein was loaded on 10 % (w/v) SDS-PAGE gels after total protein concentrations in cell lysates (CL) were quantified using BCA. (**A1 & B1**) Representative Western blots show the level of intracellular precursor MMP-2 (preMMP-2) at 72 kDa in the Rama 37-S100P (R37-S100P) and in the Rama 37-S100A4 (R37-S100A4) cells after 72 h treatment with siRNA MMP-2 (si-MMP-2) alone, siRNA MMP-2, 9 and 13 simultaneously (siMMP-2, 9 and 13), and siRNA scrambled control (si-scrambled). GAPDH was used as a loading control. The MMP-2 band chemiluminescence was detected using ECL Select Reagents, whilst that of GAPDH was detected using standard ECL Reagents (Materials and Methods). (**A2**) Histogram of the mean±SE of three independent experiments from **A1** showing ratio precursor band intensity of MMP-2 to that of GAPDH in the R37-S100P cells treated with si-MMP-2 individually; si-

MMP-2, 9 and 13 simultaneously; or si-scrambled control. Level of MMP-2 was significantly decreased in the R37-S100P cells treated with si-MMP-2 alone by 9-fold (Student's t-test, $P<0.0001$) and in R37-S100P cells treated with si-MMP-2, 9 and 13 simultaneously by 1.42-fold ($P=0.014$) compared to si-scrambled control. (**B2**) Histogram of the mean±SE of three independent experiments from **B1** showing ratio precursor band intensity of MMP-2 to that of GAPDH in the R37-S100A4 cells treated with si-MMP-2 individually, si-MMP-2, 9 and 13 simultaneously, or si-scrambled control. Level of MMP-2 was also significantly decreased in R37-S100A4 cells treated with si-MMP-2 alone by 6.5-fold ($P=0.020$) and in R37-S100A4 cells treated with si-MMP-2, 9 and 13 simultaneously by 3.8-fold ($P=0.037$) compared to si-scrambled control.

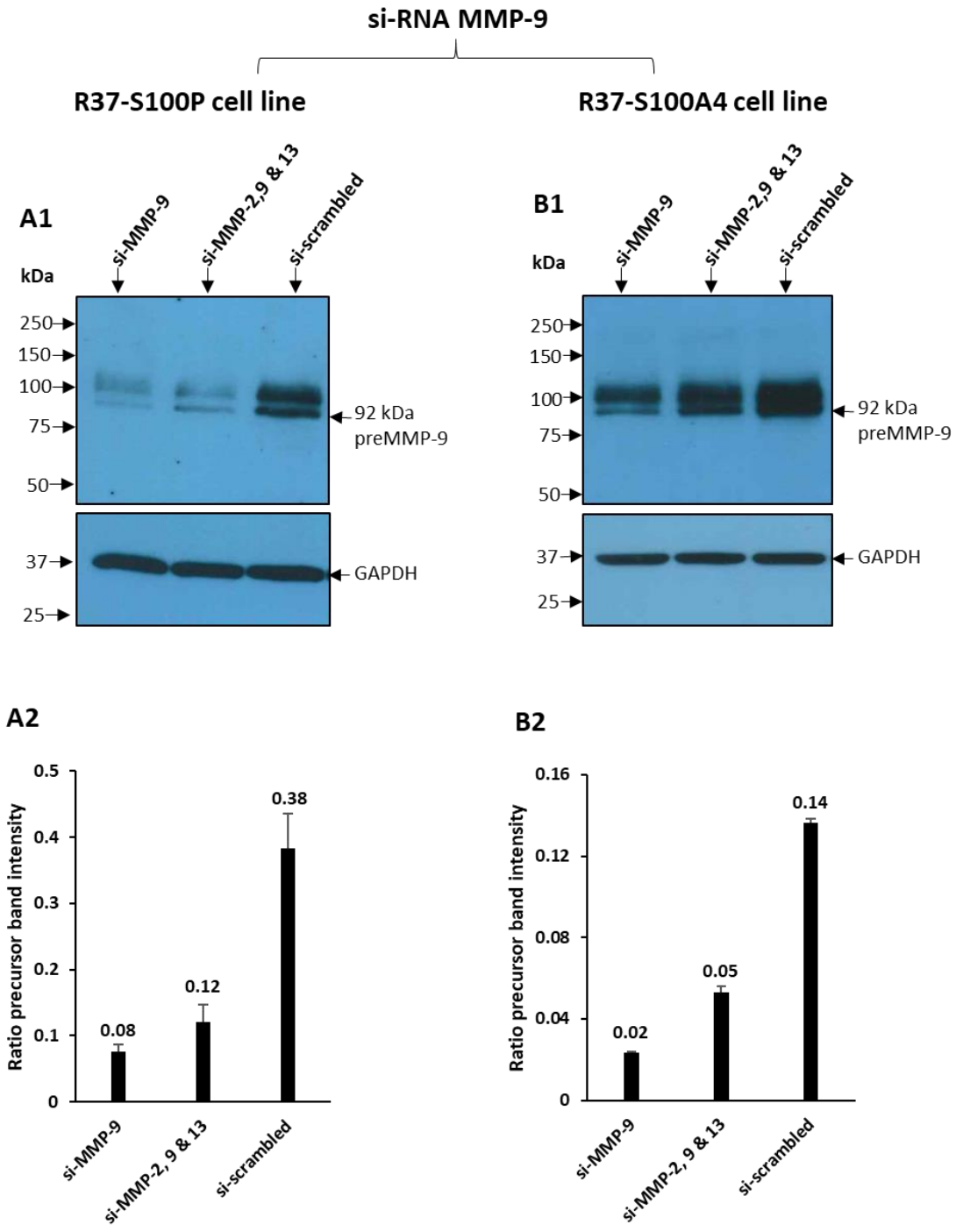

Figure 4.2. Western blots for MMP-9 in the Rama 37-S100P (R37-S100P) and Rama 37-S100A4 (R37-S100A4) cell lines treated with siRNA to MMP-9 or MMP-2, 9 and 13.

Ten µg of protein was loaded on 10 % (w/v) SDS-PAGE gels after total protein concentrations in cell lysates (CL) were quantified using BCA. (**A1 & B1**) Representative Western blots showed the level of intracellular precursor MMP-9 (preMMP-9) at 92 kDa in R37-S100P or R37-S100A4 cell lines after 72 h treatment with siRNA MMP-9 (si-MMP-9) alone, siRNA MMP-2, 9 and 13 simultaneously (siMMP-2, 9 and 13), or siRNA scrambled (si-scrambled) control. GAPDH was used as a loading control. The MMP-9 band chemiluminescence was detected

using ECL Select Reagents, whilst that of GAPDH was detected using standard ECL Reagents (Material and Methods). (**A2**) Histogram of the mean±SE of three independent experiments from **A1** showing ratio precursor band intensity of MMP-9 to that of GAPDH in R37-S100P cells treated with si-MMP-9 alone; si-MMP-2, 9 and 13 simultaneously or si-scrambled control. Level of MMP-9 was significantly decreased in R37-S100P cells treated with si-MMP-9 alone by 5-fold (Student's t-test, *P*=0.005) and in R37-S100P cells treated with si-MMP-2, 9 and 13 simultaneously by 3.5-fold (*P*=0.011) compared to si-scrambled control. (**B2**) Histogram of mean±SE of three independent experiments from **B1** showing ratio precursor band intensity of MMP-9 to that of GAPDH in R37-S100A4 cells treated with si-MMP-9 alone, si-MMP-2, 9 and 13 simultaneously or si-scrambled control. Level of MMP-9 was also significantly decreased in R37-S100A4 cells treated with si-MMP-9 alone by 5.8-fold (*P*<0.0001) and in R37-S100A4 cells treated with si-MMP-2, 9 and 13 simultaneously by 2.6-fold (*P*<0.0001) compared to si-scrambled control.

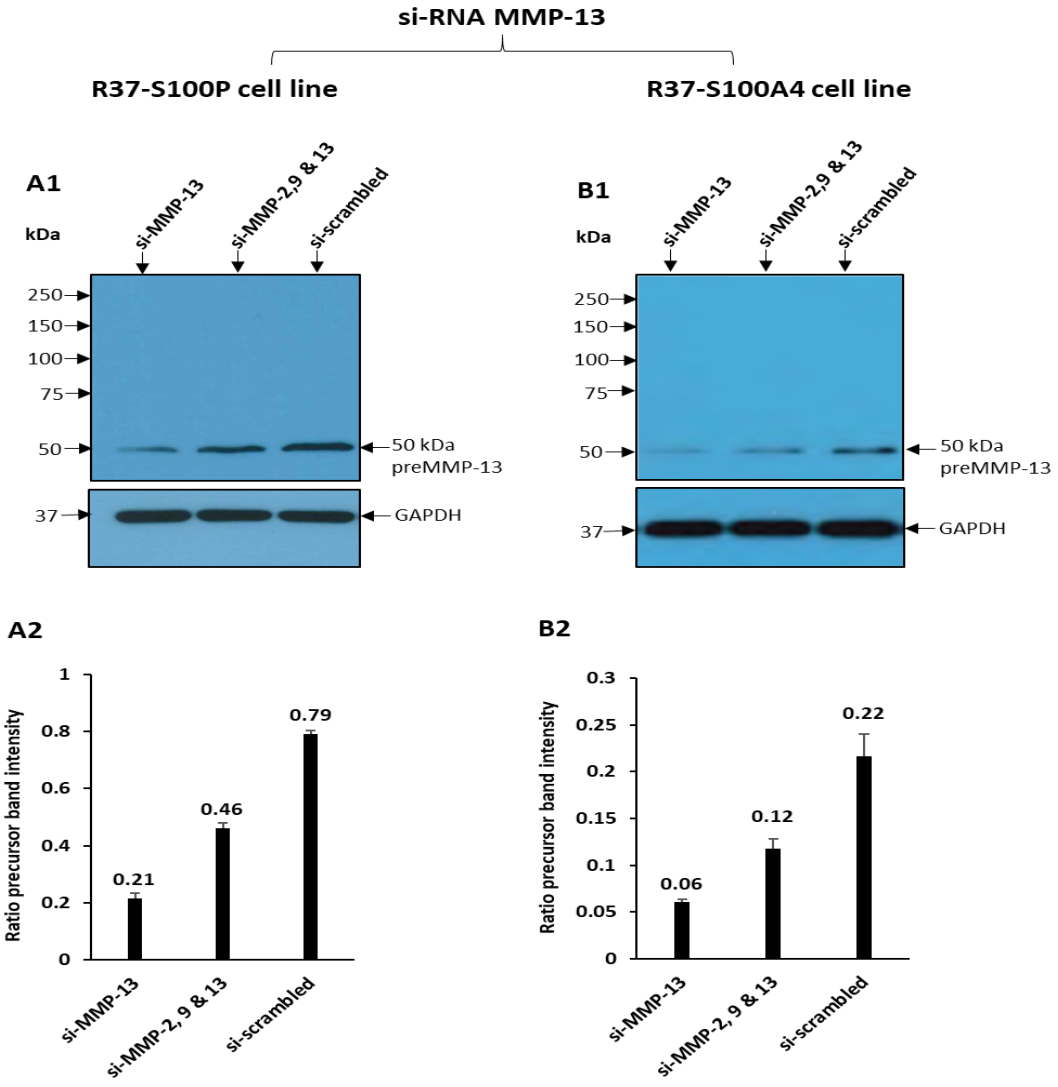

Figure 4.3. Western blots for MMP-13 in Rama 37-S100P (R37-S100P) and Rama 37-S100A4 (R37-S100A4) cell lines treated with siRNA to MMP-9 or siRNA to MMP-2, 9 and 13 simultaneously.

Ten µg of protein was loaded on 10 % (w/v) SDS-PAGE gels after total protein concentrations in cell lysates (CL) were quantified using BCA. (**A1 & B1**) Representative Western blots showed the level of intracellular precursor MMP-13 (preMMP-13) at 50 kDa in R37-S100P or R37-S100A4 cells after treatment for 72 h with siRNA MMP-13 (si-MMP-13) alone; siRNA MMP-2, 9 and 13 simultaneously (siMMP-2, 9 and 13); or siRNA scrambled (si-scrambled) control. The GAPDH was used as a loading control. The MMP-13 band chemiluminescence was detected using ECL Select Reagents, whilst GAPDH band chemiluminescence was detected using standard ECL Reagents. (**A2**) Histogram of mean±SE of three independent experiments from **A1** showing that the ratio precursor band intensity of MMP-13 to that of GAPDH in R37-S100P cells treated with si-MMP-13 alone; si-MMP-2, 9 and 13 simultaneously, or si-scrambled control. Level of MMP-13 was significantly decreased in R37-S100P cells treated with the si-MMP-13 alone by 3.7-fold (Student's t-test, $P<0.0001$) and in R37-S100P cells treated with si-MMP-2, 9 and 13 simultaneously by 1.7-fold ($P<0.0001$) compared to si-scrambled control. (**B2**) Histogram of mean±SE of three independent experiments from **B1** showing ratio precursor band intensity of MMP-13 to that of GAPDH in R37-S100A4 cells treated with si-MMP-13 alone; si-MMP-2, 9 and 13 simultaneously, or si-scrambled control. Level of the MMP-13 was also significantly decreased in R37-S100A4 cells treated with si-MMP-13 alone by 3.6-fold ($P=0.003$) and in R37-S100A4 cells treated with the si-MMP-2, 9 and 13 simultaneously by 1.9-fold ($P=0.019$) compared to si-scrambled control.

4.2.2 Migration and invasion assays in the Rama 37-S100P/S100A4 cell lines

For the R37-S100P and R37-S100A4 cell lines, 6 x 10^3 cells for the migration, and 12 x 10^3 cells for the invasion assays were seeded and grown for 24 h in Boyden chambers without or with membranes coated with Matrigel (Section **2.13** and **2.14**) (**Appendix Figure 4**). Results from the migration assays showed that there was an increase of about 7-fold (mean±SE:7.4±0.7, n=3, Student's t-test, $P=0.006$) in the R37-S100P, and about 2-fold (2.1±0.2, n=3, $P=0.006$) in the R37-S100A4 cell line compared to the R37 empty vector control (**Figure 4.4A**). Moreover, results from the invasion assays showed even greater increases of about 20-fold (mean±SE:20.3±7.6, n=3,

Student's t-test, *P*=0.014) in the R37-S100P, and about 3-fold (3.3±0.6, n=3, *P*=0.03) in the R37-S100A4 cell line compared to Rama 37 empty vector control (**Figure 4.4B**).

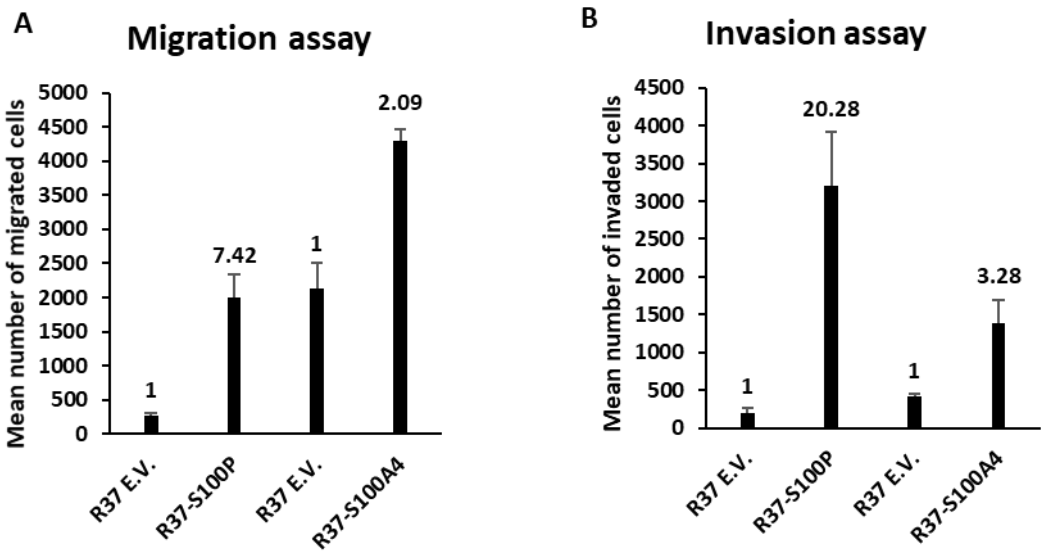

Figure 4.4. Migration and invasion assays in the Rama 37-S100P (R37-S100P) and Rama 37-S100A4 (R37-S100A4) cell lines.

(**A**) Histogram shows the mean±SE increase in migrated cells for R37-S100P and R37-S100A4 in comparison with the empty vector control cell lines. There was a significant increase of about 7-fold (Student's t-test, *P*=0.006) and about 2-fold (*P*=0.006), respectively, compared to R37 empty vector control cells. (**B**) Histogram shows the mean±SE fold increase in invaded cells for R37-S100P and R37-S100A4 in comparison with the empty vector control cell lines. There was a significant increase of about 20-fold (*P*=0.014) and about 3-fold (*P*=0.034), respectively, compared to R37 empty vector control cells. Migration and invasion experiments were recorded from 3 wells repeated 3 times with different batches of cells (n=3). The Bars refer to mean±SE and the numbers above them refer to fold differences compared to empty vector control (R37 E.V.) cells. Micrographs of migration and invasion assays are recorded in **Appendix 4**.

4.2.3 Effect of knock-down of MMPs on migration or invasion of S100P/S100A4 overexpressing rat mammary cells

The R37-S100P or S100A4 cells were divided into 5 groups and then each group was treated with one of the following: siRNA to MMP-2; siRNA to MMP-9; siRNA to MMP-13; siRNAs to MMP-2, 9 and 13 simultaneously, or siRNA to scrambled

control (Section **2.15**). After 48 h transfection time, all cells were removed and seeded in Boyden chambers without or with Matrigel (Sections **2.13** and **2.14**) (**Appendix 5**). R37-S100P cells showed a significant decrease in cell migration for all knocked-down groups compared to siRNA scrambled control. Results were a decrease of 1.8-fold (mean±SE:1.82±0.05, n=2, Student's t-test, *P*=0.001) in the siRNA MMP-2-treated group; 1.7-fold (1.72±0.10, n=2, *P*=0.008) in the group treated with siRNA MMP-9-treated group; 1.4-fold (1.44±0.07, n=2, *P*=0.010) in the siRNA MMP-13-treated group; and 2.8-fold (2.75±0.07, n=2, P<0.0001) in the siRNAs MMP-2, 9 and 13 simultaneously-treated group. Moreover, R37-S100A4 cells after MMP's knock-down also showed significant decreases in cell migration as follows: 2-fold (mean±SE: 2.1±0.05, n=2, Student's t-test, *P*=0.002) in the siRNA MMP-2-treated group; 2-fold (2.5±0.01, n=2, *P*=0.002) in the siRNA MMP-9-treated group; 2-fold (2.4±0.02, n=2, *P*=0.002) in the MMP-13-treated group; and 2-fold (2.1±0.04, n=2, *P*=0.002) in the siRNAs MMP-2, 9 and 13 simultaneously-treated group compared to siRNA scrambled control groups (**Figure 4.5A**).

Results for invasion were decreased even more significantly than those for migration in the R37-S100P cells after MMPs knock-down as follows: 3-fold (mean±SE: 3.3±0.2, n=2, Student's t-test, *P*=0.002) in the siRNA MMP-2-treated group; 2-fold (2.3±0.1, n=2, *P*=0.004) in the siRNA MMP-9-treated group; 9-fold (9.4±0.7, n=2, *P*=0.001) in the siRNA MMP-13-treated group; and 5-fold (5.0±0.5, n=2, *P*=0.002) in the siRNA MMP-2, -9 and -13 simultaneously-treated group compared to siRNA-A scrambled control group. Moreover, results for knock-down of MMPs in R37-S100A4 cells showed an even more significant decrease in invasion as follows: 21-fold (mean±SE: 21.17±0.54, n=2, Student's t-test, *P*=0.009) in the siRNA MMP-2-treated

group; 11-fold (11.24±1.04, n=2, *P*=0.010) in the siRNA MMP-9-treated group; 18-fold (18.18±4.78, n=2, *P*=0.009) in the siRNA MMP-13-treated group; and 38-fold (37.95±3.21, n=2, *P*=0.009) in the siRNA MMP-2, -9 and -13 simultaneously-treated group in comparison with siRNA-A scrambled control (**Figure 4.5B**).

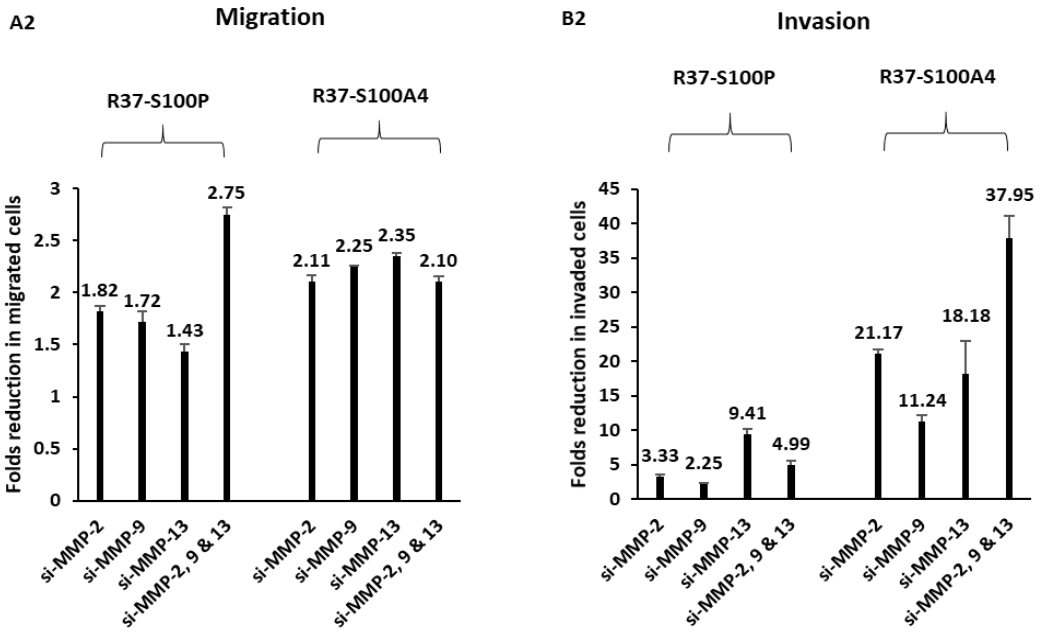

Figure 4.5. Migration and invasion of S100P/S100A4 overexpressing rat mammary cell lines after knock-down by MMPs.

(**A**) Histogram shows mean±SE fold reduction in migrated cells for R37-S100P and R37-S100A4 cell lines treated for 48 hours with siRNAs to different MMPs relative to scramble siRNA. R37-S100P cells showed significant decreases in cell migration after MMP's knock-down by the following: 1.8-fold (Student's t-test, n=2, *P*=0.001) in the siRNA MMP-2 (si-MMP-2)-treated group; 1.7-fold (*P*=0.008) in the siRNA MMP-9 (si-MMP-9)-treated group; 1.4-fold (*P*=0.010) in the siRNA MMP-13 (si-MMP-13)-treated group; and 2.7-fold (*P*<0.0001) in the siRNAs MMP-2, -9 and -13 simultaneously (si-MMP-2, -9 and -13)-treated group compared to siRNA-A scrambled control. Moreover, R37-S100A4 cells showed a significant similar decrease in cell migration by 2-fold (Student's t-test, n=2, *P*=0.002) in the siRNA MMP-2 (si-MMP-2)-treated group; 2.3-fold (*P*=0.002) in the siRNA MMP-9 (si-MMP-9)-treated group; 2.4-fold (*P*=0.002) in the siRNA MMP-13 (si-MMP-13)-treated group; and 2-fold (*P*=0.002) in the siRNAs MMP-2, -9 and -13 simultaneously (si-MMP-2, -9 and -13)-treated group compared to siRNA-A scramble control. (**B2**) Histogram shows mean±SE fold reduction in invaded cells for R37-S100P and R37-S100A4 cell lines treated for 48 hours with siRNA to different MMPs relative to scrambled siRNA. R37-S100P cells showed significant decreases in cell invasion after MMPs were knocked-down by the following: 3-fold (Student's t-test,

n=2, *P*=0.002) in the siRNA MMP-2 (si-MMP-2)-treated group; 2.3-fold (*P*=0.004) in the siRNA MMP-9 (si-MMP-9)-treated group; 9-fold (*P*=0.001) in the siRNA MMP-13 (si-MMP-13)-treated group; and 5-fold (P=0.002) in the siRNAs MMP-2, -9 and -13 simultaneously (si-MMP-2, -9 and -13)-treated group compared to siRNA-A scramble control. Moreover, R37-S100A4 cells showed even more significant differences than the R37-S100P cells in cell invasion after MMP's knock-down by the following: 21-fold (Student's t-test, n=2, *P*=0.009) in the siRNA MMP-2 (si-MMP-2)-treated group; 11-fold (*P*=0.01) in the siRNA MMP-9 (si-MMP-9)-treated group; 18-fold (*P*=0.009) in the siRNA MMP-13 (si-MMP-13)-treated group; and 38-fold (*P*=0.009) in the siRNAs MMP-2, -9 and -13 simultaneously (si-MMP-2, -9 and -13)-treated group compared to siRNA-A scramble control. Migration and invasion experiments were recorded from 3 wells repeated 2 times with different batches of cells (n=2). Micrographs of migration and invasion assays are shown in **Appendix 5**.

4.3 Discussion

S100P/S100A4 overexpressing rat mammary cell lines showed a significant decrease ranging from 3.6 to 9-fold (Student's t-test, *P*≤0.02) (**Table 4.1.)** in protein expression of intracellular preMMP-2, -9 and -13 after separate treatment with each siRNA for MMP-2, -9 or -13 (**Figure 4.1-3**). Treatment of cell lines with the noncognate MMP siRNA showed no significant difference (*P*≥0.380) for MMP-9 or MMP-13 (**Appendix 3**). Moreover, knock-down of MMP-2, -9 and -13 at the same time (i.e. simultaneously) showed a significant decrease ranging from 1.4 to 3.9-fold (Student's t-test, *P*≤0.037) in the protein levels for these MMPs in R37-S100P/A4 cell lines as summarised in **Table 4.1**. A possible reason for the lower fold decreases in the triple siRNA to single siRNA levels of individual MMPs is the fact that the input was 3.5 pmol for each MMP in the triple siRNA and 7 pmol for each MMP in the single siRNA (Section **2.15.5**). The siRNA depletion was specific for its target MMP, since there was no effect on unrelated MMPs (**Appendix 3**). Moreover, siRNA caused no reduction in the control protein GAPDH which showed that such house-keeping proteins are

unaffected. Although, both cell lines showed a reduction in specific MMP when transfected with its cognate siRNA and a concomitant reduction in both cell migration and cell invasion, there was no simple linear relationship between level of MMP and cell migration/invasion. However, the fold decreases in cell migration were usually less than those in cell invasion (**Table 4.1 and 4.2**). These results suggest that the major effect of the MMPs was in promoting cell invasion, probably by digesting the ECM in Matrigel, predominantly collagen I, and that they exerted a smaller effect on cell migration possibly by digesting proteins connected to focal adhesions (e.g. fibronectin) (Sen et al., 2010). This conclusion is consistent with that obtained in the R37-S100P and R37-S100A4 transfected cell lines where fold increases in invasion were invariably greater than fold increases in migration over those of the empty vector transfected control cell lines (**Figure 4.4**). The results are also consistent with these MMPs being one of the effectors of S100P/A4.

Table 4.1. Effect of MMP knock-down on MMP protein levels in S100P/A4 overexpressing rat mammary cell lines.

Cell line	Mean±SE fold decrease in MMP protein [a]					
	MMP-2 [b]		MMP-9		MMP-13	
	siRNA MMP-2 [c]	siRNA MMP-2, -9 & -13 [d]	siRNA MMP-9 [c]	siRNA MMP-2, -9 & -13 [d]	siRNA MMP-13 [c]	siRNA MMP-2, -9 & -13 [d]
R37-S100P	9.0±0.2, *P*<0.0001	1.4±0.01, *P*=0.014	3.2±0.1, *P*<0.0001	1.6±0.1, *P*<0.0001	3.7±0.2, *P*<0.0001	1.7±0.04, *P*<0.0001
R37-S100A4	6.5±1.6, *P*=0.020	3.9±1.0, *P*=0.037	5.8±0.1, *P*<0.0001	2.6±0.1, *P*<0.0001	3.6±0.2, *P*=0.003	2.0±0.1, *P*=0.019

[a] Mean fold decrease±SE, n=3, Student's t-test, P value.

[b] Matrix metalloproteinase-2.

[c] Cell line transfected with particular siRNA to MMP (7 pmol).

[d] Cell line transfected with a combination of all 3 MMPs (3.5 pmol each).

Migratory and invasive potential of malignant R37-S100P/S100A4 cells have been previously reported (Lloyd et al., 1998; Wang et al., 2006). Our data for R37-S100P and R37-S100A4 cell migration showed significant increases by 7.4- and 2-fold (Student's t-test, n=3, $P \leq 0.006$), respectively, over the non-malignant R37 empty vector control cell line. However, the difference between the two empty vector controls in the migration assay (**Figure 4.4A**) is of the order of 7-fold. This highlights the potential problem of using clonal cell lines for biological assays; these clones may at times exhibit substantial differences from the original cell population from which they were derived. Therefore, the differences between the results of transfectants and their respective empty vector controls may also include effects (positive or negative) due to their clonal origin.

In addition, the malignant S100P/S100A4 overexpressing cell lines showed even higher increases of 20- and 3-fold ($P \leq 0.03$), respectively, over non-malignant empty vector control cell lines, these results are in agreement with those previously reported for S100P or S100A4 transfected rat mammary cell lines (Du et al., 2012; Gross et al., 2014; Jenkinson et al., 2004).

When MMPs in malignant, overexpressing S100P or S100A4 rat mammary cells were knocked-down, they showed a significant decrease in the number of cells migrating ranging from 1.4- to 2.8-fold ($P \leq 0.01$) and 2.1- to 2.4-fold ($P \leq 0.002$), respectively, and an even greater fold reduction in invading cells ranging from 2.3- to 9.4-fold and 11.2- to 38-fold, respectively (**Table 4.2**), since siRNA transfection introduced no toxicity on nontarget proteins (**Appendix 3**).

Table 4.2. Conclusion of MMP knock-down and effect on R37-S100P/A4 cell migration and invasion.

Exper.	Cell line	MMP knock-down [a] (*P*) [b]			
		siRNA MMP-2	siRNA MMP-9	siRNA MMP-13	siRNA MMP-2, -9 & -13
Migration assay	R37-S100P	1.8±0.04, (0.001)	1.7±0.10, (0.0080)	1.4±0.1, (0.010)	2.8±0.1, (<0.0001)
	R37-S100A4	2.1±0.05, (0.002)	2.3±0.01, (0.002)	2.4±0.02, (0.002)	2.1±0.04, (0.002)
Invasion assay	R37-S100P	3.3±0.2, (0.002)	2.3±0.1, (0.004)	9.41±0.73, (0.001)	5±0.6, (0.002)
	R37-S100A4	21.2±0.5, (0.009)	11.2±1.0, (0.010)	18.2±4.8, (0.009)	38±3.2, (0.009)

[a] Mean fold decrease±SE after transient transfection of siRNAs to different MMPs in relation to scrambled siRNA controls.
[b] Probability *P* of difference from scrambled controls (Student's t-test, n=2).

The R37-S100P cell line showed higher fold increases in migrating and invading cells (7.4- and 20-fold) (**Figure 4.4**), respectively, than that for knock-down by various siRNA MMPs (1.4 to 2.8 and 2.3 to 9.4-fold decreases, respectively) (**Table 4.2**) over the R37 empty vector control cells. Assuming siRNA inhibition is complete, this result suggests that there are additional changes induced by S100P which contribute to the S100P-induced increase in migration and invasion other than those produced by MMP-2, MMP-9 and MMP-13. One example could be increases in plasminogen activator/plasmin (Clarke et al., 2017). In contrast, the lower increases induced by S100A4 (2 and 3-fold) (**Figure 4.4**) are largely matched (2-fold in migration) or even exceeded (11- to 38-fold in invasion) (**Table 4.2**) by the decreases caused by siRNA MMPs in R37-S100A4 cells. Thus, it would seem that no extra changes need to be suggested to account for the increase in cell migration and invasion in R37-S100A4 cells.

Moreover, knocking-down MMP-2, -9 and -13 simultaneously in R37-S100P cells showed higher fold decreases in number of migrating cells by 2.8-fold (P<0.0001) compared to knock-down of MMPs individually which showed decreases ranging from 1.4- to 1.8-fold. In contrast, R37-S100A4 showed almost similar impacts on cell migration when siRNAs to MMPs were added either individually or when added simultaneously, producing decreases ranging from 2.1- to 2.4-fold. Since roughly equal amounts of total single and triple siRNA were added (Materials and Methods), it may be that there is a requirement for more than one MMP to be active in promoting cell migration in R37-S100P, but not in R37-S100A4 cells.

The relative effect on cell invasion of individually knocking-down MMPs in the R37-S100P cells showed that the most effective siRNA was that due to MMP-13. This result may due to the requirement of MMP-13 for stimulation and activation of MMP-2 and/or MMP-9 (Knauper et al., 1997, 1996; Leeman et al., 2002), as described in Section **1.3.2**. This conclusion would suggest that more than one MMP is required to promote invasion effectively in R37-S100P cells, similar to the conclusion reached for migration. In contrast, siRNA to MMP-2 was the most effective in decreasing invasion of R37-S100A4 cells followed by siRNA to MMP-13. These results suggest that the collagen IV/collagen I matrix laid down by R37-S100P and R37-S100A4 cells may be slightly different requiring different MMPs to digest it successfully (Warburton et al., 1987a, 1987b), and thereby allow cells to pass through the pores in the membrane.

The results from knocking-down MMP-2 and MMP-13 on cell migration and invasion in both cell lines are consistent with their significant activities observed using zymography (Section **3.2.3**). The stronger effect of siRNA to MMP-2 in R37-S100A4 over R37-S100P cells may be because the level of precursor MMP-2 (in CL) and active

form MMP-2 (in CM) is always higher in the R37-S100A4 compared to the R37-S100P cells over empty vector control cell lines.

The knock-down of R37-S100P/S100A4 cells with siRNA to MMP-9 showed that MMP-9 has more effect on cell migration and invasion in the R37-S100A4 compared to the R37-S100P cell lines. This difference may due to the fact that MMP-9's levels in the CL and CM were higher in the R37-S100A4 compared to the R37-S100P cells over empty vector control cell lies. Although, MMP-9 appeared only as its proform in CM of both cell lines using zymography (Section **3.2.3**), it still showed a highly significant effect on the cells' migration or invasion in both cell lines. Since MMP-9 appeared incapable of proteolytic digestion in our systems, it must produce its effects via another system or pathway. One suggested alternative is for proMMP-9 to regulate the actomyosin cytoskeleton, thereby increasing cell migration via CD44 receptors and eventually cell invasion via remodelling of the ECM via gelatinases and collagenases, such as MMP2/MMP-9 and MMP-13 (Orgaz et al., 2014).

Intracellularly-overexpressed S100P has been found in many types of cultured cancer cell lines, such as those from breast (Guerreiro Da Silva et al., 2000), colon (Dong et al., 2014), pancreas (Dong et al., 2014) and lung (Dong et al., 2014). These cell lines have been usually manipulated by knockout experiments to demonstrate the crucial role of S100P in enhancing metastasis. These results *in vitro* are consistent with the finding in this thesis and that of others (Arumugam and Logsdon, 2011; Gross et al., 2014) that overexpression of S100P in rat mammary cell lines caused a significant increase in migration and invasion. Similarly, overexpression of S100A4 in our rat mammary cells shows enhanced cell migration and invasion, a result consistent with many previous reports in cancer cell lines from breast, colorectal,

pancreas, and lung (Bowers et al., 2012; Chen et al., 2012; Goh Then Sin et al., 2011; Huang et al., 2012; Jenkinson et al., 2004; Li et al., 2012; Sack et al., 2011; Wang et al., 2012; Zhang et al., 2012). In contrast, a study on brain white matter showed that siRNA depletion of S100A4 in cultured astrocytes caused increased cell migration (Takenaga and Kozlova, 2006). However, astrocytes are themselves migratory in the brain white matter, and it may be that suppression of S100A4 can interfere with the normal machinery of this cell to cause a stimulation of cell migration. Moreover, when a nasopharyngeal carcinoma C666-1 cell line was transfected with siRNA to S100P, this led to inhibition of cell migration and wound healing via suppression of MMP-2 and MMP-9 expression, downregulation of epidermal growth factor, cluster of differentiation CD 44 and RAGE receptor expression (Liu et al., 2017). When prostate cancer cell lines overexpressed S100P or suppressed expression of S100P, this led to increases or decrease, respectively, in cell growth and expression of several genes related to proliferation and angiogenesis including MMP-13 by (3.7-fold) compared to control cells *in vitro* (Basu et al., 2008). When anaplastic thyroid 8505C and SW1736 cell lines were transfected with siRNA to TGF-β (transforming growth factor-beta), the resultant cells coordinately downregulated S100A4, MMP-2 and MMP-9 which, in turn, caused an inhibition of cell migration and invasion. Furthermore, when siRNA to S100A4 was transfected into the same parental cells, this experiment produced a significant reduction in MMP-2 and MMP-9 which, in turn, inhibited migration and invasion in these cell lines. Finally, when MMP-2 and MMP-9 were blocked with BB-94 MMP inhibitors (Batimastat), these same cells showed a significant reduction in mRNA and protein for S100A4 either with or

without treatment by TGF- β (Zhang et al., 2016). These conclusions suggest the complex way that S100 proteins and MMPs may interact.

Similar types of results were obtained in the breast cancer cell line MDA-MB-231 (Wang et al., 2012). When they were transfected with cDNA for S100A4, the cells upregulated MMP-13 expression and caused an increase in cell migration. When transfected with siRNA to S100A4, these cells had a reduced level of MMP-13, cell migration and angiogenesis. Moreover, when MMP-13 was blocked with specific antibodies, the levels of cell migration and angiogenesis were reduced in these S100A4 expressing MDA-MB-231 cells (Wang et al., 2012). These results connected S100A4, MMP-13, cell migration and angiogenesis. Thus, our own results and those in the literature have established a causal link between elevated intracellular levels of two S100 proteins, S100P and S100A4, three MMPs: MMP-2, -9, -13 and an increase in cell migration and invasion in tissue cultured cells. However, whether the S100 proteins act inside the cell to induce these biological changes or whether they can act outside the cell in a paracrine fashion is still not yet clear, and will provide the focus for the next chapter.

4.4 Summary

The malignant R37-S100P/S100A4 cell lines showed increases in cell migration and invasion in Boyden chambers without and with Matrigel, respectively, compared to their empty vector-transfected control cell lines. The R37-S100P and S100A4 cell lines demonstrated reductions in levels of specific MMPs after transient transfections with siRNA to MMP-2, MMP-9 or MMP-13 individually or simultaneously all together, compared to scrambled transfected control cells. These transient knocked-down cells

showed significant decreases in cell migration and even more in cell invasion. siRNA silencing of MMP-2 reduced cell migration and invasion more in R37-S100A4 cells and silencing MMP-13 relatively more in R37-S100P cells. These data suggest that the two S100 proteins target different MMPs, and that these three MMPs simultaneously can account for the invasive changes in R37-S100A4 cells, but not in R37-S100P cells.

Chapter 5

Effect of exogenously-added S100P/S100A4 on MMPs and migration/invasion of parental rat mammary cells

5.1 Introduction

Despite being widely involved in broad intracellular signalling pathways that promote metastasis in many types of cancer cells, metastasis-inducing proteins S100P/S100A4 have also been reported to enhance metastasis in different types of cancer cells through extracellular functions (Leclerc and Vetter, 2015). Thus, addition of extracellular S100P can stimulate proliferation of pancreatic carcinoma BxPC3 cell line via phosphorylation of IκBα and activation MMP-9 (Dakhel et al., 2014), can contribute to the development of lung adenocarcinoma through its interaction with the receptor for advanced glycation end-products (RAGE) (Rehbein et al., 2008), and can stimulate cultured human colon cancer cell invasion through activation of RAGE (Mercado-Pimentel et al., 2015). In addition, direct binding between the V domain of RAGE and S100P was found to require Ca^{+2} ions and to lie in the micromolar range (K_d of ~6μM) (Penumutchu et al., 2014).

Moreover, addition of extracellular S100A4 has also been reported to stimulate invasive growth and angiogenesis of mouse microvascular endothelial cells via MMP-13 production and activation (Schmidt-Hansen et al., 2004), and prometastatic activation of human melanoma cell line A375 via interaction with RAGE (Herwig et al., 2016). Downregulation of S100A4 in osteosarcoma cultured cells

resulted in reduced expression and activation of MMP-2 which led to diminished cell migration (Bjornland *et al.*, 1999). Finally, addition of S100A4 to chondrocytes, synovial fibroblasts or endothelial cells enhanced cell invasion through elevated levels and activation of MMP-13 (Boye and Maelandsmo, 2010). In summary, although S100P/A4 are involved in many intracellular signalling pathways which promote tumour motility, when added extracellularly it seems that the RAGE receptor is the most frequent target employed to transduce the signal inside the cell.

RAGE receptors have been reported to interact with a variety of ligands including some of the S100 protein family (Heizmann et al., 2007), as already outlined in Section **1.5**. RAGE has been reported to be overexpressed in several cancer types and its signalling pathway may help to drive tumorigenesis and metastasis in multiple cancers including breast cancer (Kalea et al., 2010; Kang et al., 2010; Kwak et al., 2017; Taguchi et al., 2000). When detected by immunohistochemistry, RAGE protein is highly expressed in breast (63%) and lung (47%) cancer, whereas low or no RAGE expression was observed in brain, lymphoma, prostate, ovarian, melanoma and colon cancers (Hsieh et al., 2003). Moreover, immunostaining, Western blot or RT-PCR showed that RAGE protein is expressed in breast adenocarcinoma MDA-MB-231 and lung cancer cell lines, but at higher levels in breast cancer than in lung cancer cells (Hsieh et al., 2003). A study on breast cancer showed that RAGE protein was expressed at a higher level in the aggressively malignant human triple negative breast cancer (TNBC) cell lines than in the weakly metastatic breast cancer cell lines such as MCF-7, T47D and BT474. Moreover, RAGE was also expressed at a significantly higher level in basal type human breast cancer (majorly TNBC) than in non-basal type tumours (majority $ER\alpha^{+}$) (Nasser et al., 2015). Also, the latter study showed that when

highly metastatic MDA-MB-231 cell lines were injected intracardially into nude mice and RAGE activity was blocked with neutralising antibody, there was a significant reduction in the metastatic potential of these cells compared to IgG control-treated mice (Nasser et al., 2015). In addition, when RAGE $^{-/-}$ model mice were injected with TNBC cells, they showed a significant inhibition in tumour growth compared to RAGE $^{+/+}$ model mice. To show the signalling molecules involved, this study found that MMP-2 and MMP-9 immunofluorescent expression was also decreased in TNBC cells obtained from RAGE $^{-/-}$ mice compared to tissue obtained from RAGE $^{+/+}$ mice (Nasser et al., 2015). Silencing RAGE or its ligands such as S100P, S100A4 and high-mobility group box 1 (HMGB-1) led to inhibition of growth and migration of pancreatic ductal adenocarcinoma (PDAC) cells *in vitro* (Arumugam et al., 2012). Moreover, blocking RAGE contributes to a reduction in expression of MMPs such as MMP-2 /-9 and in carcinogenic properties of C6 glioma cell line *in vitro* (Taguchi et al., 2000). In parallel studies, antiallergic drugs such as olopatadine, amlexanox and cromolyn which can bind to S100 proteins such as S100A1, S100A12, S100A13 and an 8 kDa unknown protein, have been shown to inhibit the IgE-mediated degranulation of immune cells such as mast cells (Okada et al., 2002; Oyama et al., 1997). Moreover, the anti-allergic drug cromolyn can bind to S100P, prevent RAGE activation and can inhibit pancreatic tumour growth *in vivo* when pancreatic cancer cells are injected into mouse models (Arumugam et al., 2006), but how specific cromolyn was for inhibition of S100P was not determined. Cromolyn has a broad activity which appears to inhibit activities associated with RAGE activation (Arumugam et al., 2006)

5.1.1 Chapter aims

To examine the effect of exogenously-added S100P/S100A4 on specific MMPs and migration/invasion of the parental rat mammary cell lines.

5.2 Results

5.2.1 Effect of adding S100P to parental Rama 37 wild type cells on level of MMP-9 protein

Recombinant S100P protein at different concentrations (0, 0.001, 0.01, 0.1, 1, 5 μM) was added to the conditioned medium of the parental S100P/A4-negative rat mammary wild type cells (R37 wt) to study its effect on intracellular precursor MMP-9) and extracellular proform MMP-9 production. The level of intracellular precursor MMP-9 (preMMP-9) was increased dramatically, initially in a dose-dependent manner (**Figure 5.1**). Thus, preMMP-9 showed a significant increase no addition when set at 1.0 (mean fold±SE, n=3, one-way ANOVA, with overall $P<0.0001$) of 1.3±0.10, 4.6±0.3, 5.6±0.2, 6.8±0.2 and 6.4±0.1-fold after addition of 0.001, 0.01, 0.1, 1 and 5 μM S100P, respectively. The maximal response was achieved at 1 μM and plateaued out at 5 μM, since there was no further significant increase (One-way ANOVA, 1 μM vs 5 μM $P=99$). Similar dose-dependent increases were seen in the level of extracellular proform MMP-9 (proMMP-9) in the CM when the proMMP-9 level for 0 μM set at 1.0 (mean fold±SE, n=3, one-way ANOVA, with overall $P<0.0001$) of 2.1±0.08, 4.36±0.13, 4.99±0.18, 6.07±0.11 and 5.28±0.17-fold after extracellular addition of 0.001, 0.01, 0.1, 1 and 5 μM S100P, respectively, plateauing out at 1 μM (Student's t-test, 1 μM vs 5 μM $P=70$) (**Figure 5.1**).

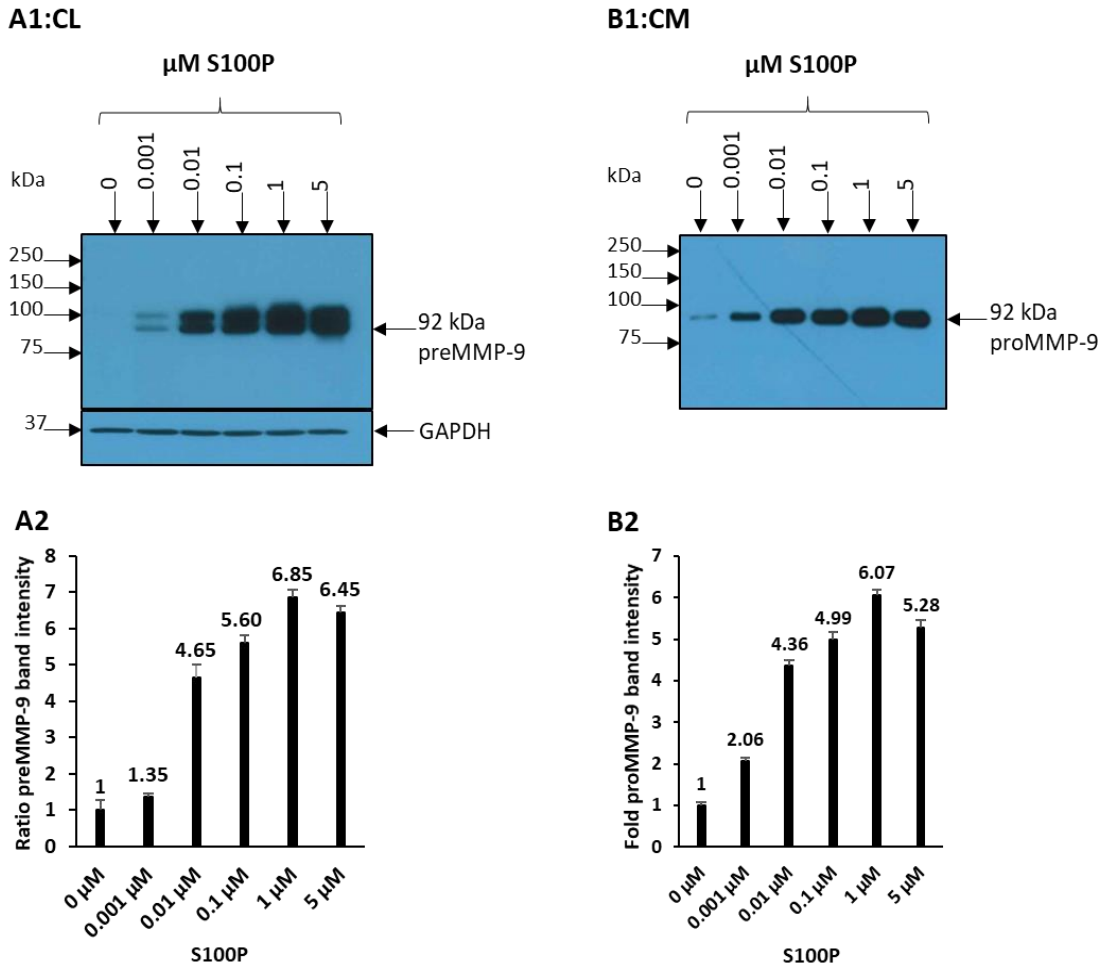

Figure 5.1. Effect of adding extracellularly different doses of S100P on the level of intracellular and extracellular MMP-9.

Different doses of recombinant S100P protein yielding the final concentrations shown were added to the medium of Rama 37 wild type cells which were then incubated for a further 24 h. Ten micrograms (10 µg) of protein for CL or suitably adjusted µL for CM were loaded on 10 % (w/v) SDS-PAGE gels. The total protein concentrations in CL were quantified using a BCA assay. The quantity of CM loaded was adjusted according to the amount of protein in the CL estimated by BCA (Section **2.5**) (**A1:CL**) Representative Western blot showing the precursor MMP-9 (preMMP-9) as a double band at 92 kDa in the cell lysate (CL) from R37 wt cells. GAPDH was used as a loading control. The preMMP-9 bands were detected using ECL Select Reagents, while GAPDH bands were detected used standard ECL Reagents. (**A2**) Histogram of three independent experiments from **A1** showing that the level of preMMP-9 increased dramatically up to 6.85-fold for 1 µM S100P, and then plateaued at 5 µM S100P. (**B1:CM**) Representative Western blot shows the proMMP-9 (proform MMP-9) at 92 kDa in the CM from R37 wt cells. (**B2**) Histogram of three independent experiments from **B1** showing that proMMP-9 (proform MMP-9) in the CM also increased dramatically up to 6.07-fold for 1 µM S100P, while its level started to fall to 5.28-fold with 5 µM S100P. Dose response in a log scale is shown in **Figure 5.9**.

5.2.2 Effect of adding fixed concentrations of S100P or S100A4 to Rama 37 wild type cells on levels of MMP-2, MMP-9 and MMP-13

The dose-response experiment above showed that 1µM S100P when added extracellularly to R37 wt cells was saturating for the production of MMP-9. Therefore, in subsequent experiments 1µM S100P or S100A4 was added extracellularly to R37 wt cells and its effects on levels of MMP-2, -9 and -13 in the CL and CM was measured by Western blotting.

5.2.2.1 MMP-2

When recombinant S100P or S100A4 were separately added to R37 cells to a final concentration of 1µM, precursor MMP-2 inside the cells was significantly increased by 2.8-fold (mean fold±SE: 2.75±0.05, n=2, Student's t-test, *P*=0.007) and by 2.5-fold (2.5±0.02, *P*=0.001), respectively, over its level inside the cells without adding S100 proteins (**Figure 5.2A**). Moreover, the pro and active forms of MMP-2 outside the cells were also increased significantly after addition of 1µM S100P or S100A4 by 7.5-fold (mean fold±SE: 7.5±0.12, n=2, Student's t-test, *P*<0.0001) and by 6.9-fold (6.87±0.57, *P*=0.005), respectively (**Figure 5.2B)**.

5.2.2.2 MMP-9

Levels of MMP-9 were increased significantly for both intracellular precursor MMP-9 and extracellular proform MMP-9. Adding 1µM S100P or S100A4 extracellularly to the R37 wt cells caused the level of precursor MMP-9 to increase significantly by 2.6-fold (mean fold±SE: 2.58±0.03, n=2, Student's t-test, *P*=0.026) and 3-fold (3.2±0.01, *P*=0.004), respectively inside cells (**Figure 5.3A**). The extracellular

form of MMP-9 protein showed only proform MMP-9 consistent with our previous result in **Figure 5.1**. Adding 1μM of S100P or S100A4 to the R37 wt cells caused a significant increase in proform MMP-9 by 3.6-fold (mean fold±SE: 3.57±0.18, n=2, Student's t-test, *P*=0.003) and by 4-fold (4.1±0.22, *P*=0.002), respectively (**Figure 5.3B**) outside the cells.

5.2.2.3 MMP-13

One micromolar of S100P or S100A4 added extracellularly to the R37 wt cells caused the levels of precursor MMP-13 to increase significantly by 3-fold (mean fold±SE: 3.1±0.02, n=2, Student's t-test, *P*=0.003) and by 3.4-fold (3.38±0.003, *P*=0.001), respectively (**Figure 5.4A**) inside the cells. MMP-13 occurred outside the cells in both pro and active forms. When 1μM S100P or S100A4 was added to the R37 wt cells, the levels of both pro and active forms of MMP-13 increased by 3-fold (mean fold±SE: 3.1±0.27, n=2, Student's t-test, *P*=0.006) and by 5.7-fold (5.66±0.65, *P*=0.007), respectively (**Figure 5.4B**), outside the cells.

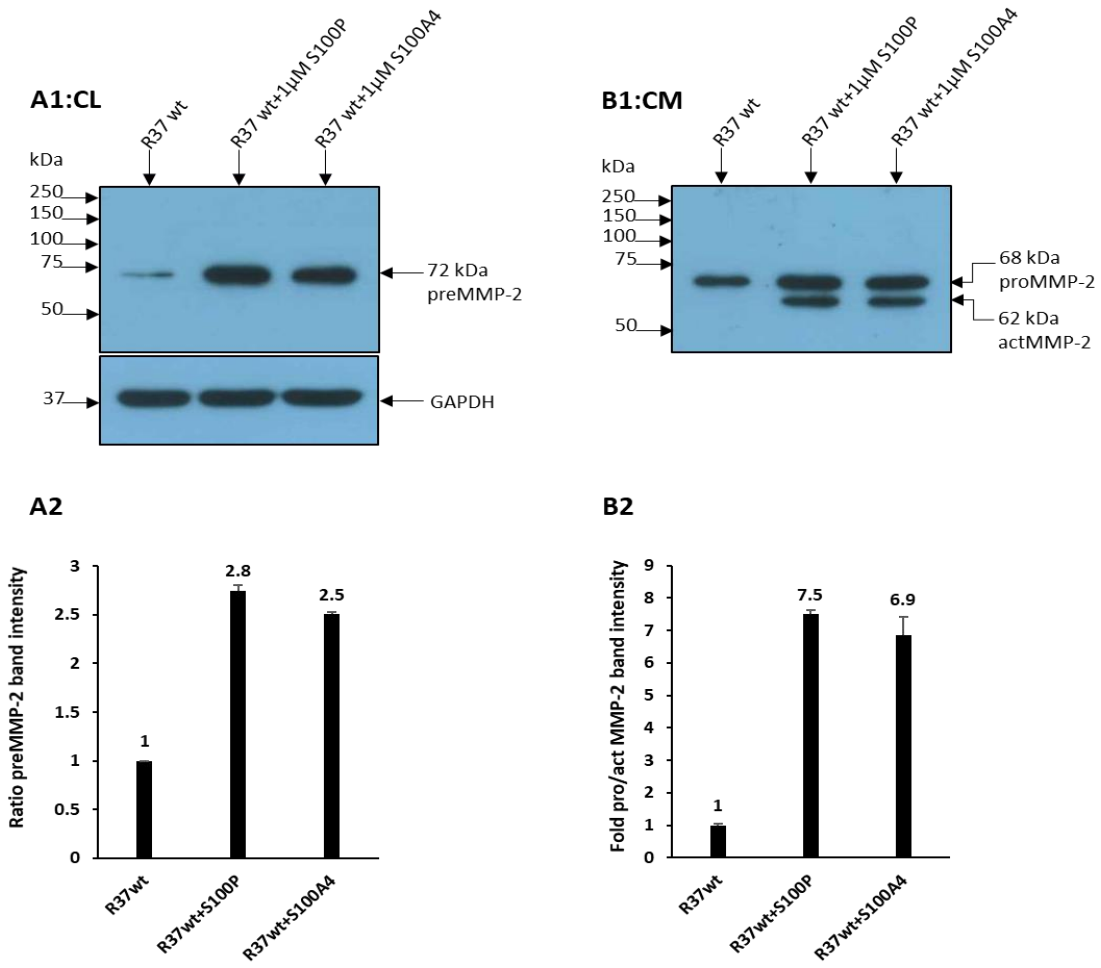

Figure 5.2. Effect of adding 1 μM S100P or S100A4 to R37 wt cells on levels of intracellular and extracellular MMP-2.

Ten μg of CL proteins or suitably adjusted μL for CM were loaded on 10 % (w/v) SDS-PAGE gels. The total protein concentrations in CL were quantified using BCA. The quantity of CM loaded was adjusted according to the amount of protein in the CL estimated by BCA (Section **2.5**) (**A1:CL**) Representative Western blot shows the intracellular precursor MMP-2 (preMMP-2) at 72 kDa in R37 wild type cells (R37 wt) treated with 1μM S100P (R37 wt + S100P) or S100A4 (R37 wt + S100A4) compared to R37 wt untreated control cells. MMP-2 bands were detected using ECL Select Reagents, while GAPDH bands were detected using standard ECL Reagents. (**A2**) Histogram of two independent experiments from **A1** showing the preMMP-2 band intensity firstly ratioed to GAPDH in the S100P or S100A4-treated R37 wt cells and then compared to that in R37 wt untreated control which has been set at 1.0. The preMMP-2 level inside cells was increased significantly by 2.8-fold or 2.5-fold (Student's t-test, $P \leq 0.007$) when 1 μM S100P or S100A4, respectively, were added to the R37 wt cells. (**B1:CM**) Representative Western blot shows both the pro (at 68 kDa) and active (at 62 kDa) forms of MMP-2 in the CM of untreated R37 wt or cells treated with 1 μM S100P or S100A4. (**B2**) Histogram of two independent experiments from **B1** showing the combined fold changes in pro and active MMP-2 band intensities in the CM of R37 wt cells treated with 1 μM S100P or S100A4 compared to those in R37 wt cells untreated control which has been set at 1.0. The levels of both forms of MMP-2 increased significantly by 7.5-fold or 6.9-fold ($P \leq 0.005$) in

the CM of R37 wt cells treated with 1 µM S100P or S100A4, respectively, compared to untreated R37 wt cells.

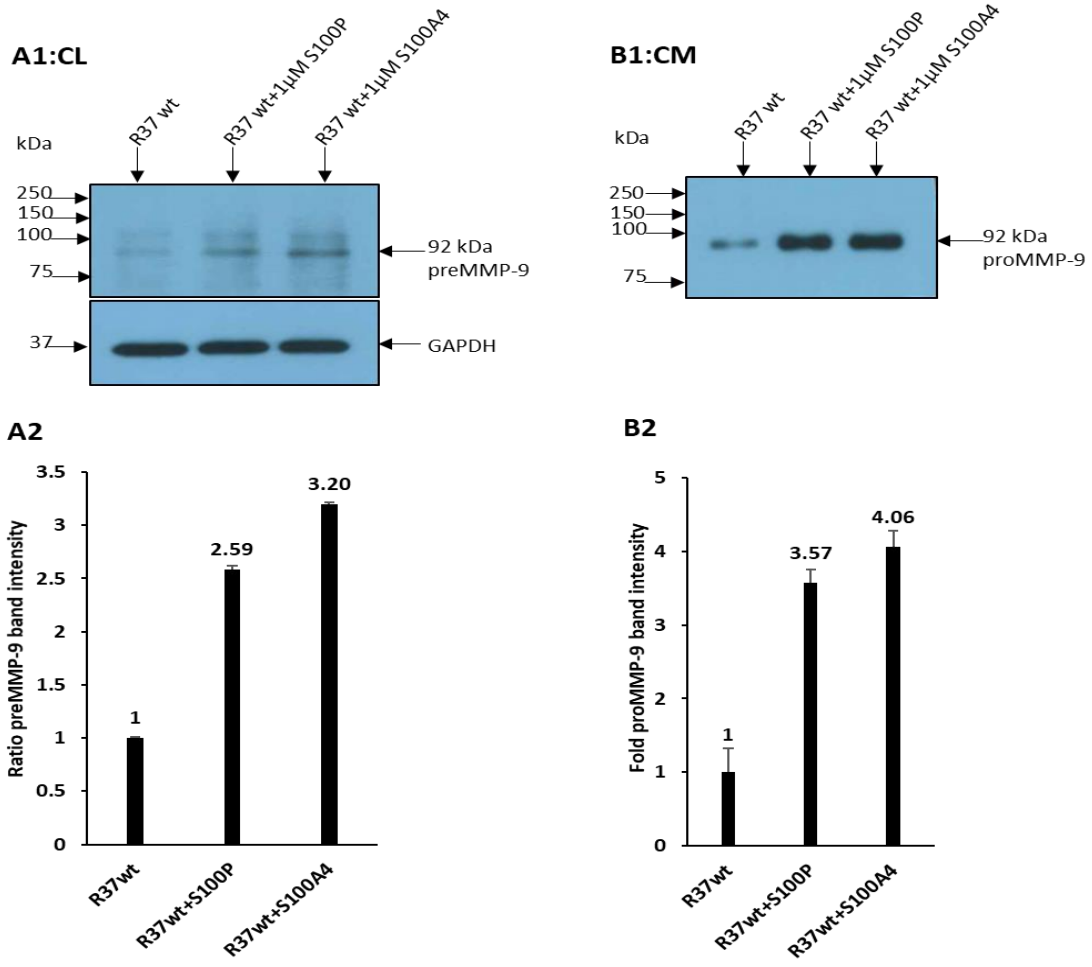

Figure 5.3. Effect of adding 1 µM S100P or S100A4 to R37 wt cells on levels of intracellular and extracellular MMP-9.

Ten µg of CL proteins or suitably adjusted µL for CM were loaded on 10 % (w/v) SDS-PAGE gels. The total protein concentrations in CL were quantified using BCA. The quantity of CM loaded was adjusted according to the amount of protein in the CL estimated by BCA (Section **2.5**) (**A1:CL**) Representative Western blot shows the intracellular precursor MMP-9 (preMMP-9) at 92 kDa in R37 wild type (R37 wt) treated with 1µM S100P (R37 wt + S100P) or S100A4 (R37 wt + S100A4) compared to R37 wt untreated control cells. MMP-9 bands were detected using ECL Select Reagents, while GAPDH bands were detected using standard ECL Reagents. (**A2**) Histogram of two independent experiments from **A1** showing the preMMP-9 band intensity ratioed to GAPDH in the S100P or S100A4-treated R37 wt cells and then compared to that in R37 wt untreated control, which has been set at 1.0. The preMMP-9 level inside cells was increased significantly by 2.8-fold or 2.5-fold (Student's t-test, $P \leq 0.007$) when 1µM S100P or S100A4, respectively, was added to the R37 wt cells. (**B1:CM**) Representative Western blot shows only the proform MMP-9 (proMMP-9) at 92 kDa in the CM of untreated R37 wt or cells treated with 1 µM S100P or S100A4. (**B2**) Histogram of two

independent experiments from **B1** showing the ratio of proMMP-9 band intensities in the CM of R37 wt cells treated with 1 µM S100P or S100A4 compared to those in R37 wt untreated control, which has been set at 1.0. The levels of proMMP-9 increased significantly by 3.6-fold or 4-fold ($P \leq 0.003$) in the CM of R37 wt cells treated with 1 µM S100P or S100A4, respectively, compared to untreated R37 wt cells.

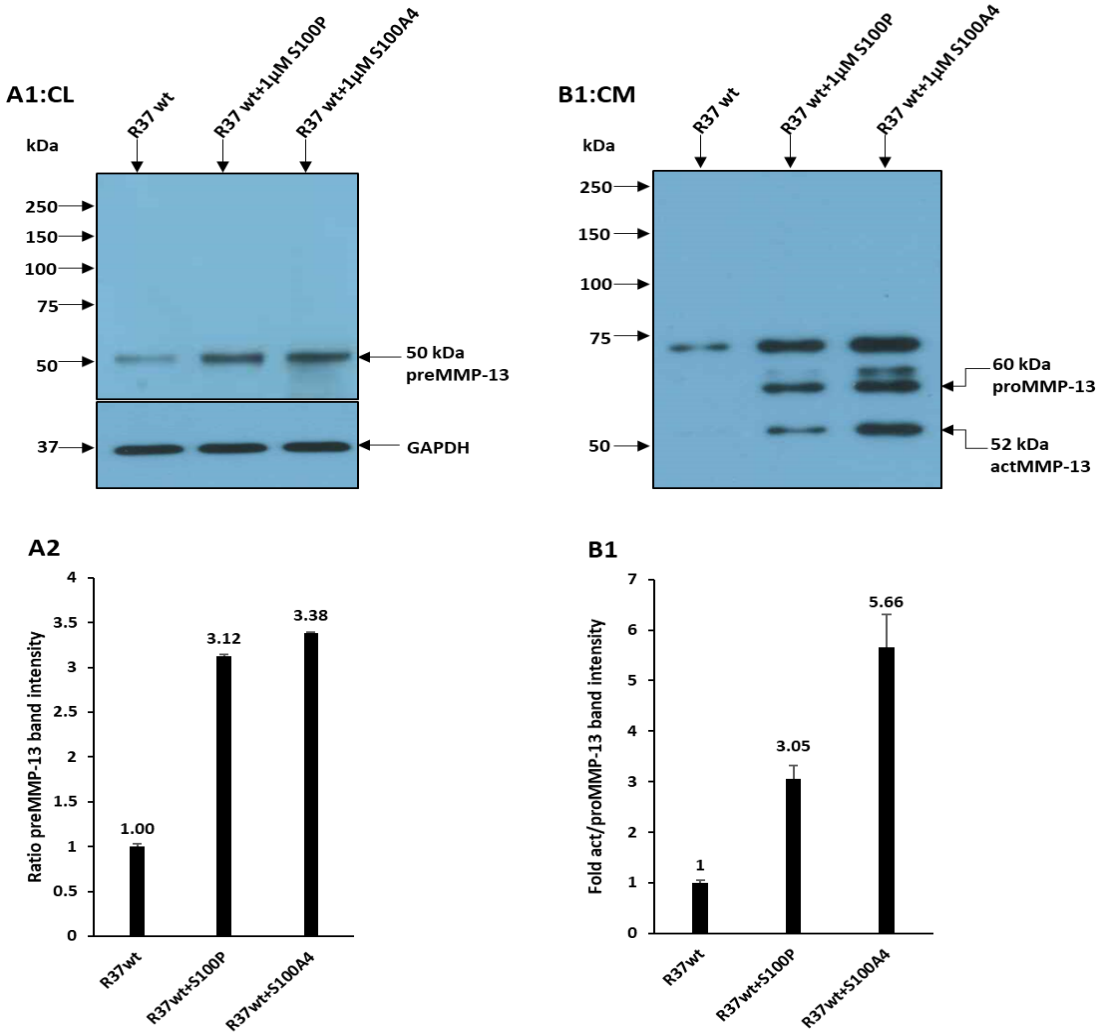

Figure 5.4. Effect of adding 1 µM S100P or S100A4 to R37 wt cells on levels of intracellular and extracellular MMP-13.

Ten µg of CL proteins or suitably adjusted µL for CM were loaded on 10 % (w/v) SDS-PAGE gels. The total protein concentrations in CL were quantified using BCA. The quantity of CM loaded was adjusted according to the amount of protein in the CL estimated by BCA (Section **2.5**) (**A1:CL**) Representative Western blot shows the intracellular precursor MMP-13 (preMMP-13) at 50 kDa in the R37 wild type (R37 wt) treated with 1µM S100P (R37 wt + S100P) or S100A4 (R37 wt + S100A4) compared to R37 wt untreated control cells. MMP-13 bands were detected using ECL Select Reagents, while GAPDH bands were detected used

standard ECL Reagents. (**A2**) Histogram of two independent experiments from **A1** showing preMMP-13 band intensity ratioed to GAPDH in the S100P or S100A4-treated R37 wt cells and then compared to that in R37 wt untreated control, which has been set at 1.0. The preMMP-13 level inside the cells was increased significantly by 3-fold or 3.4-fold (Student's t-test, $P \leq 0.003$) when 1µM S100P or S100A4, respectively, was added to the R37 wt cells. (**B1:CM**) Representative Western blot shows both the pro (at 60 kDa) and active (at 52 kDa) forms of MMP-13 in the CM of untreated R37 wt or cells treated with 1 µM S100P or S100A4. (**B2**) Histogram of two independent experiments from **B1** showing the ratio of combined pro and active MMP-13 band intensities in the CM of R37 wt cells treated with 1 µM S100P or S100A4 compared to that in R37 wt untreated control, which has been set at 1.0. The combined levels of both forms of MMP-13 were increased significantly by 3-fold or 5.7-fold ($P \leq 0.007$) in the CM of R37 wt cells treated with 1 µM S100P or S100A4, respectively, compared to untreated R37 wt cells. The two bands at 73 and 64 kDa were considered to be nonspecific and unrelated to MMP-13, since they appeared with only one batch of MMP-13 antibody and were not observed in our previous blots in zymography or Western blotting for pro and actMMP-13.

5.2.3 RAGE receptor levels in the S100P or S100A4 overexpressing rat mammary cell lines

Several reports have suggested that extracellular S100P/A4 can interact with the Receptor for Advanced Glycation End Products (RAGE) in the plasma membrane (Arumugam et al., 2004; Boye et al., 2008; Herwig et al., 2016; Penumutchu et al., 2014; Zhu et al., 2013), which could be consistent with our results in **Figure 5.1.** We investigated whether this receptor was present in the Rama 37 cells using a specific antibody directed at the RAGE receptor. RAGE protein was detected in the cell lysates (CL) of Rama 37 wild type (R37 wt), Rama 37-S100P (R37-S100P) and Rama 37-S100A4 (R37-S100A4) cells using Western blotting. The apparent molecular weight of 45 kDa is consistent with reports in other system (Taguchi et al., 2000). The lower molecular weight band observed at 39 kDa (**Figure 5.5**) is thought to be nonspecific and unrelated to RAGE because it was not blocked by immunizing peptide (Section **2.17**). The level of RAGE receptor was increased significantly by 2.2-fold (mean fold±SE:

2.18±0.07, n=3, Student's t-test, *P*=0.015) and by 1.7-fold (1.65±0.04, *P*=0.027) in the CL of R37-S100P and R37-S100A4 cells, respectively, over the R37 wt control cell line (**Figure 5.5**). There was no change in GAPDH showing that increase in RAGE was a specific effect.

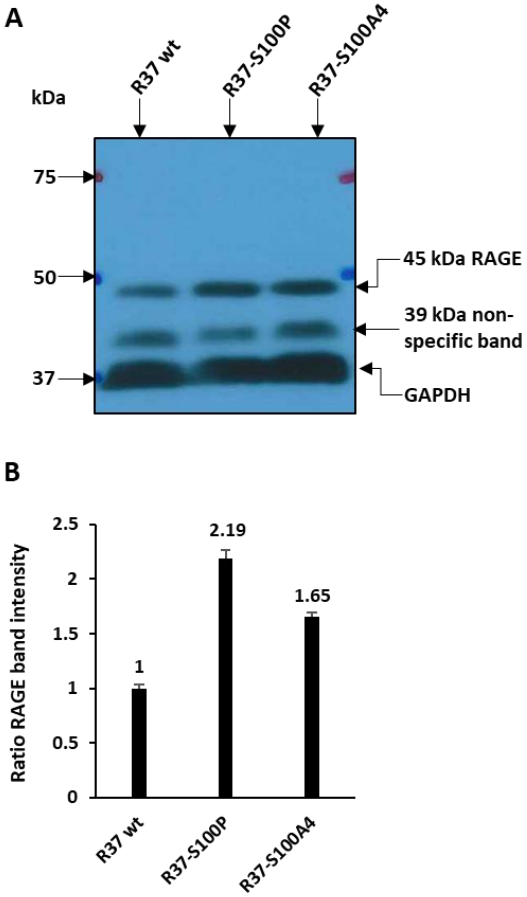

Figure 5.5. Detection of RAGE in cell lysates of Rama 37 wild type and S100P/S100A4 overexpressing cell lines.

Total protein concentrations in cell lysates (CL) were quantified using BCA and 10 µg of CL proteins were loaded on 10 % (w/v) SDS-PAGE gels. (**A**)Representative Western blot shows the level of RAGE at 45 kDa in the CL of Rama 37 wild type (R37 wt), Rama 37-S100P (R37-S100P) and Rama 37-S100A4 (R37-S100A4) cell lines. A band at 39 kDa was considered to be nonspecific as describe in Section **2.17**. GAPDH at 37 kDa was used as a loading control. RAGE and GAPDH bands were detected using standard ECL Reagents. (**B**) Histogram of three independent experiments showing RAGE band intensities in the CL of R37 wt, R37-S100P and R37-S100A4 ratioed to that in GAPDH and normalized to that in R37 wt. which was set at 1. The levels of RAGE receptor were increased significantly by 2-fold or 1.7-fold (Student's t-test, *P*≤0.027) in the CL of R37-S100P or R37-S100A4 cell lines, respectively, compared to that in R37 wt control cell line.

5.2.4 Effect of adding S100P or S100A4 on migration and invasion activities of parental rat mammary wild type cells

The Rama 37 wild type (R37 wt) are benign tumour cells, which migrate and invade at low frequency (Jenkinson et al., 2004). In this experiment 1 µM of S100P or S100A4 was added extracellularly to Rama 37 wt cells (Section **2.17.2**) growing in three Boyden migration chambers or three Matrigel invasion chambers for each set of additions and each experiment was repeated twice. When 1 µM S100P or S100A4 was added to R37 wt cells, the cells showed a significant increase in migration of 2.5-fold (mean fold± SE: 2.49±0.23, n=2, Student's t-test, *P*=0.03) or by 2.1-fold (2.07±0.05, *P*=0.017), respectively, compared to control R37 wt cells without any additions (**Figure 5.6A**). Higher increases were observed in cell invasion. Thus, when 1µM S100P or S100A4 was added extracellularly to R37 wt cells, their invasion was significant increased by about 4-fold for both S100 proteins (S100P; mean fold ±SE: 4.06±2.38, n=2, Student's t-test, *P*=0.025 and S100A4; 4.33±0.016, *P*=0.005) compared to R37 wt cells without any additions (**Figure 5.6B**).

The amount of S100P or S100A4 (1 µM) was estimated from a dose response curve of addition of S100P to stimulate production of MMP-9 and this was found to saturate at 1 µM (**Figure 5.1**). Therefore, 1 µM was used throughout on the assumption that additions of S100 proteins and production of other MMPs were the same.

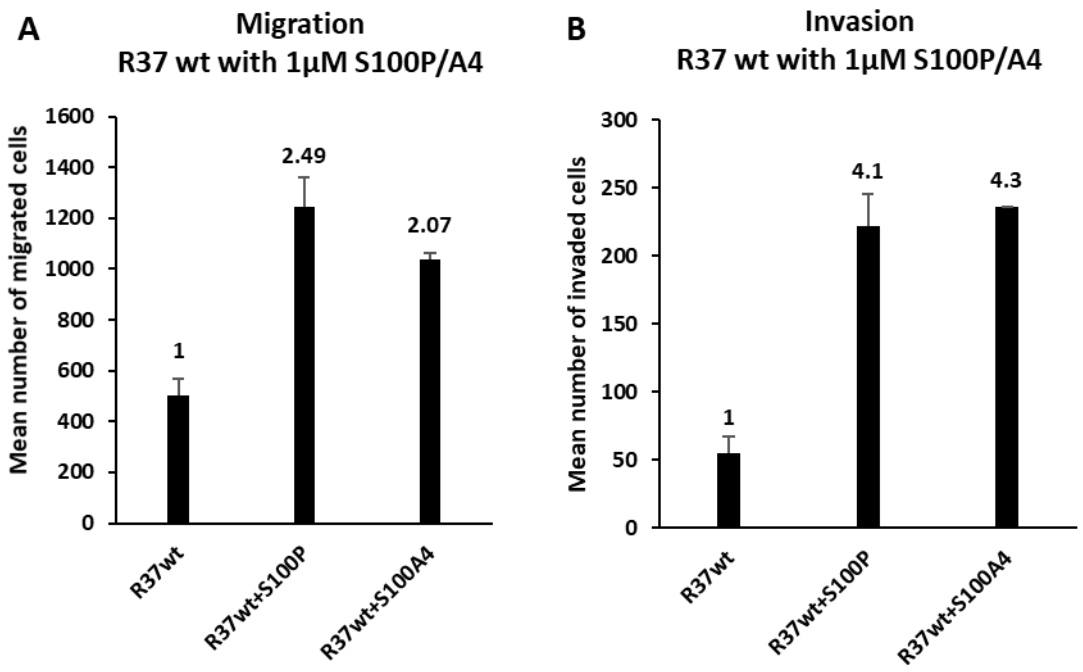

Figure 5.6. Effect of addition of S100P and S100A4 on migration and invasion of benign Rama 37 wild type cells.

(**A**) Histogram of two independent experiments showing the ability of benign Rama 37 wild type (R37 wt) cells to migrate through Boyden migration chambers. The migration rates of R37 wt cells were significantly increased after extracellular addition of 1µM S100P or S100A4 by 2.5-fold (mean fold±SE: 2.49±0.23, n=2, Student's t-test, *P*=0.03) or by 2-fold (2.07±0.05, *P*=0.017) over R37 wt control cells without additions. (**B**) Histogram of two independent experiments showing the ability of benign R37 wt cells to invade through Matrigel invasion chambers. The invasion rates of R37 wt cells were significantly increased after extracellular addition of 1µM S100P or S100A4 by about 4-fold for both S100P (mean fold±SE: 4.06±2.38, n=2, *P*=0.02) or S100A4 (4.33±0.016, *P*=0.005) over R37 wt control cells without additions. Invasion experiments were recorded from 3 wells repeated 2 times with different batches of cells (n=2). The Bars refer to mean±SE and the numbers above them refer to fold differences compared to empty vector control (R37 E.V.) cells.

5.2.5 Effect of adding S100P/S100A4 with RAGE inhibitors on invasion of parental rat mammary cells

To investigate whether the biological effects of S100P/A4 was exerted through RAGE, two of its inhibitors were also added to R37 wt cells. The two inhibitors used were a RAGE neutralising antibody (Namba et al., 2009) and the anti-allergy

drug, Cromolyn, which can bind to members of the S100 protein family such as S100P at the site of the S100P-RAGE interaction (Arumugam et al., 2006; Penumutchu et al., 2014).

Firstly, we tested the effects of adding RAGE inhibitors extracellularly alone on the invasive ability of R37 wt cells using concentrations reported to be completely inhibitory in a human gastric carcinoma cell line (Namba et al., 2009). Rama 37 wild type (R37 wt) cells were divided into three groups: Group 1: R37 wt cells were seeded alone inside the Matrigel chambers as a negative control. Group 2: R37 wt with 1/200 diluted anti-RAGE antibody inside and outside the Matrigel chambers. Groupe 3: R37wt with 100 µM Cromolyn inside and outside the Matrigel chambers (Section **2.17.3**). The results showed that at the concentrations of inhibitors used, the RAGE antibody or Cromolyn alone had no significant effect on invasive ability of R37 wt cells compared to R37 wt control without additions (mean fold decrease±SE: 1.16±0.25, n=2, Student's t-test, *P*=0.456 and 0.92±0.05, *P*=0.219, respectively) (**Figure 5.7A**).

Secondly, The Rama 37 wild type (R37 wt) cells were divided into three groups: Group 1: R37 wt with final concentration of 1 µM S100P or S100A4 inside and outside the Matrigel chamber. Group 2: R37 wt with final concentration of 1 µM S100P or S100A4 and 1/200 µL anti-RAGE antibody inside and outside the Matrigel chamber. Groupe 3: R37 wt with 1 µM S100P or S100A4 and 100 µM Cromolyn inside and outside the Matrigel chamber (Section **2.17.4**). The results showed that addition of RAGE antibody or Cromolyn with S100P to R37 wt cells significantly decreased their rate of invasion by 4-fold (mean fold decrease±SE: 3.96±0.13, n=2, Student's t-test, *P*=0.02) or by 2.5-fold (2.51±0.09, *P*=0.03), respectively, compared to R37 wt cells

with only S100P (**Figure 5.7B**). Indeed, the inhibitions were able to reduce the invasion of the cells to at least below basal levels (**Figures 5.7A, B**).

Moreover, the results showed that addition of RAGE antibody or Cromolyn with S100A4 to R37 wt cells also significantly decreased their rate of invasion by 1.9-fold (mean fold decrease±SE: 1.88±0.13, n=2, Student's t-test, *P*=0.037) or by 2-fold (2.04±0.104, *P*=0.03), respectively, over the R37 wt cells with only S100A4 (**Figure 5.7C**). In contrast to S100P-stimulated cells, the 2-fold reduction in invasion in S100A4-stimulated cells remained well above basal levels (**Figures 5.7A**, **C**).

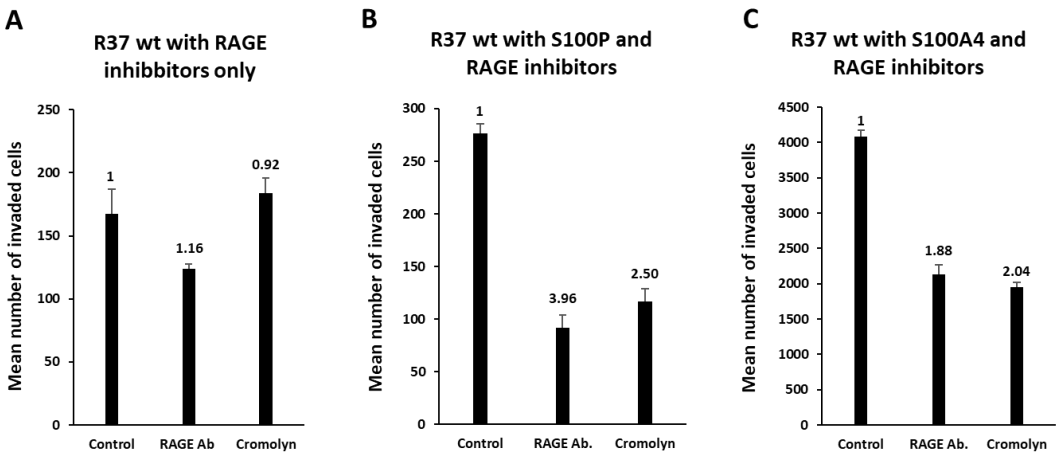

Figure 5.7. Effect of addition of S100P/S100A4 and RAGE inhibitors on invasion of Rama 37 wild type cells.

(**A**) Histogram of two independent experiments of 3 chambers each shows that 1/200 diluted RAGE antibody or 100 µM Cromolyn drug had no significant effect (RAGE Ab mean fold decrease±SE: 1.16±0.25, n=2, *P*=0.456; Cromolyn: 0.92±0.05, *P*=0.219) on rate of invasion of Rama 37 wild type (R37 wt) compared to R37 wt cells alone (control). (**B**) Histogram of two independent experiments of 3 chambers each shows that the R37 wt with 1 µM S100P and 1/200 diluted RAGE antibody (RAGE Ab.) or 100 µM Cromolyn produced significant decreases in R37 wt cells rate of invasion by 4-fold (mean fold decrease: 3.96±0.13, n=2, *P*=0.02) or 2.5-fold (2.51±0.09, n=2, *P*=0.03), respectively, compared to R37 wt cells with 1 µM S100P (control). (**C**) Histogram of two independent experiments of 3 chambers each showing that R37 wt with 1 µM S100A4 and 1/200 diluted RAGE antibody (RAGE Ab.) or 100 µM Cromolyn produced significant decreases in R37 wt cells rate of invasion by 1.9-fold (mean fold decrease: 1.88±0.13, n=2, *P*=0.037) or 2-fold (2.04±0.104, n=2, P=0.03), respectively, compared to R37 wt cells with 1 µM S100A4 (control). Invasion experiments were

recorded from 3 wells repeated 2 times with different batches of cells (n=2). The Bars refer to mean±SE and the numbers above them refer to fold differences compared to empty vector control (R37 E.V.) cells.

5.2.6 Effect of adding RAGE inhibitors on invasion of S100P/S100A4 overexpressing rat mammary cells

RAGE inhibitors were added to the Rama 37-S100P and Rama 37-S100A4 cells to observe their effects on the rate of invasion, when the S100 proteins were expressed inside the cells. Both cell lines were divided into three groups: Group 1: R37-S100P or R37-S100A4 cells alone (control). Group 2: R37-S100P or S100A4 cells with 1/200 diluted anti-RAGE antibody inside and outside the Matrigel chamber. Groupe 3: R37-S100P or S100A4 with 100 µM Cromolyn inside and outside the Matrigel chamber (Section **2.17.5**). The results showed that addition of RAGE antibody or Cromolyn to R37-S100P cells significantly decreased their rate of invasion by 1.6-fold (mean fold decrease±SE: 1.60±0.02, n=2, Student's t-test, *P*=0.003) or by 1.5-fold (1.49±0.06, *P*=0.007), respectively, compared to R37-S100P cells alone (control) (**Figure 5.8A**). However, inhibition was still 2-3 fold above basal levels showing that the inhibition was incomplete (**Figure 5.8A, 4.4B**). Moreover, the results showed that addition of 1/200 diluted RAGE antibody or 100 µM Cromolyn to R37-S100A4 cells significantly decreased their rate of invasion by 3-fold (mean fold decrease±SE: 2.99±0.55, n=2, Student's t-test, *P*=0.006) or by 2.4-fold (2.44±0.12, *P*=0.005), respectively, over the R37-S100A4 cells alone (control) (**Figure 5.8B**). The 3-fold reduction in invasion in R37-S100A4 cells approached basal levels showing that inhibition was complete (**Figures 5.8B, 4.4B**).

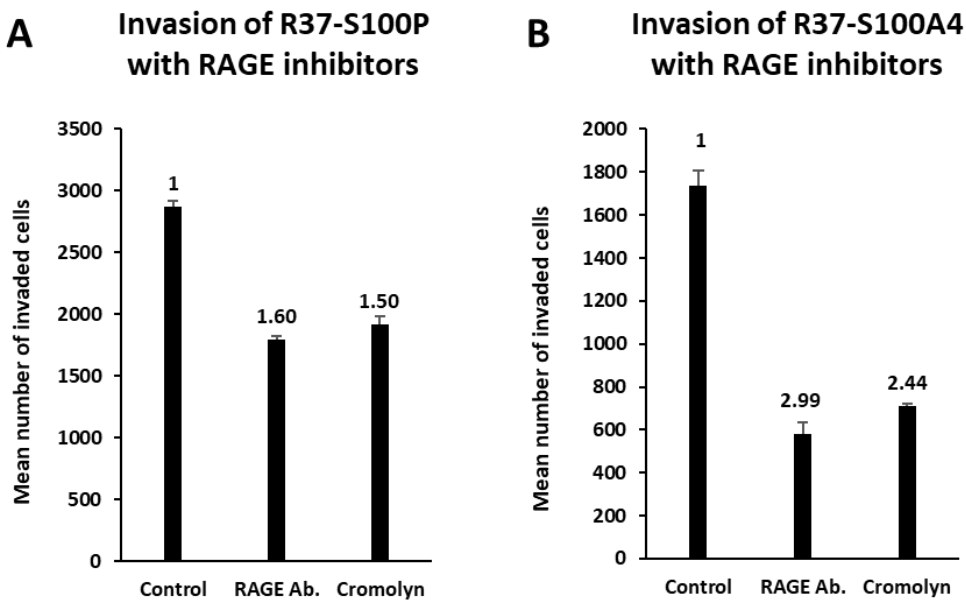

Figure 5.8. Effect of addition of RAGE inhibitors on invasion of Rama 37-S100P/S100A4 cells.

(**A**) Histogram of two independent experiments of 3 chambers each shows that R37-S100P with 1/200 diluted RAGE antibody (RAGE Ab.) or 100 µM Cromolyn produced a significant decrease in their rate of invasion by 1.6-fold (mean fold decrease±SE: 1.60±0.02, n=2, *P*=0.003) or 1.5-fold (1.49±0.06, *P*=0.007), respectively, compared to R37-S100P cells alone (control). (**B**) Histogram of two independent experiments of 3 chambers each shows that R37-S100A4 with 1/200 diluted RAGE antibody (RAGE Ab.) or 100 µM Cromolyn produced significant decrease in their rate of invasion by 3-fold (mean fold decrease±SE: 2.99±0.55, n=2, Student's t-test, *P*=0.006) or by 2.4-fold (2.44±0.12, *P*=0.005), respectively, compared to R37-S100P cells alone (control). Invasion experiments were recorded from 3 wells repeated 2 times with different batches of cells (n=2). The Bars refer to mean±SE and the numbers above them refer to fold differences compared to empty vector control (R37 E.V.) cells.

5.3 Discussion

When S100P or S100A4 was added to R37 wt cells the same molecular weight forms of MMP-2 (intracellular at 72 kDa, extracellular at 68 kDa and 62 kDa), MMP-9 (intracellular and extracellular at 92 kDa) and MMP-13 (intracellular at 50 kDa,

extracellular at 60 kDa and 52 kDa) were seen as in parental R37 wt and S100P/S100A4-transfected cells and hence the same designations of pre/pro and active forms of each of the MMPs can be utilised in this chapter as in chapter 3.

Our data showed that addition of S100P resulted in a gradual increase in the level of MMP-9 in a dose-dependent manner, both inside and outside the R37 wt cells and then plateaued off. These points lie on sigmoidal curves with initial slopes approximating to straight lines and the response plateaus off at 100 nM corresponding to an increase of roughly 6-fold for preMMP-9 and 5.6-fold for proMMP-9. The initial slopes occurred between 1 and 10 nM, plateau values at 100M, and half maximal effective concentration (EC_{50}) at 4.33 nM for intracellular preMMP-9 and 3.99 nM for extracellular proMMP-9 (**Figure 5.9**).

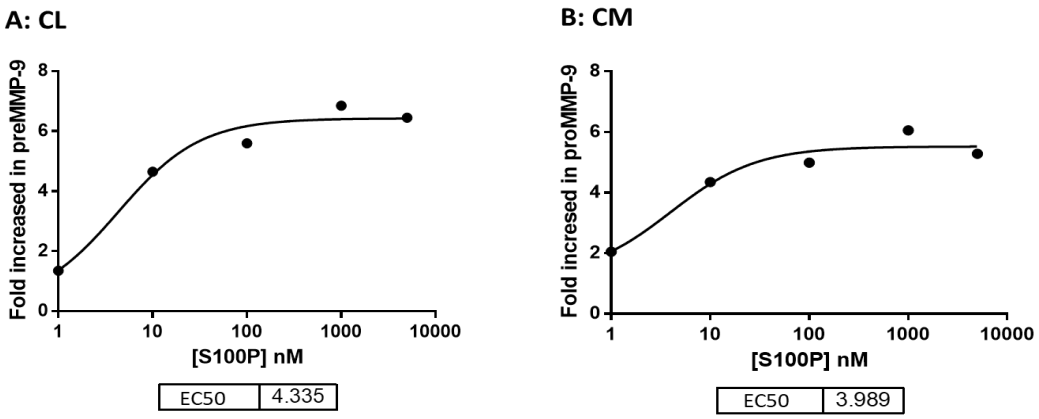

Figure 5.9. Effect of adding increasing concentrations of S100P to R37 wt cells on fold increase in MMP-9.
(**A**) Dose-response of addition of S100P that stimulates fold increase in intracellular precursor MMP-9 (preMMP-9). The effective concentration at half maximum stimulation EC_{50} = 4.335. (**B**) Dose-response of addition of S100P that stimulates fold increases in extracellular proform MMP-9 (proMMP-9). The effective concentration at half maximum stimulation EC_{50} = 3.984. These graphs were plotted using GraphPad Prism software version 6.00 (GraphPad, San Diego, CA, USA).

The simplest interpretation of the results is that S100P was binding to saturable receptors with EC50 of about 4 nM. This value is consistent with that of Arumugam et al. (2004), which showed that addition of S100P to NIH3T3 cells (mouse embryo fibroblasts) stimulated NF_kB, ERKs and cell proliferation, over a wide range of concentrations from 0.01 to 100nM with EC50 of roughly 4 nM. However, Boye et al., (2008), showed that addition of S100A4 to the human osteosarcoma cell line (II-11b) stimulated NFκB activation, angiogenesis, reduced cell death and increased cell invasion also in a dose-dependent manner, but this activation showed an EC50 of about 1 μM, suggesting a weaker binding for S100A4.

These results also suggest that the increase in MMP-9 outside was matched by its increase inside the cells. This result is consistent with little or no processing of the protein and suggests that the binding of S100P to its receptors stimulates increased expression of intracellular preMMP-9, which governs the level of this protein outside the cells. Since 1 μM S100P was well in excess of saturating concentrations for production of maximum MMP-9 in R37 wt cells, this concentration was adopted for all subsequent experiments investigating levels of MMPs and their biological effects on R37 wt cells.

Our results show that addition of S100P or S100A4 to the outside of R37 wt cells produced increases in all three MMPs and in cell migration and invasion. There were no increases in a standard housekeeping protein GAPDH showing that the increases were restricted to specific proteins. However, the results show slightly different fold changes in MMP-9 between cells of different passage number e.g MMP-9 production yielded a 6.85-fold increase in CL and a 6.07-fold increase in CM in **Figure 5.1** compared to 3 and 4-fold increases, respectively, in **Figure 5.3**. This may

reflect the stem cell nature of the parental R37 wt cells, since the cuboidal epithelial cells produce at low frequency (< 1 %) more-elongated, myoepithelial-like cells the proportion of which can increase with passage number (Dunnington et al., 1983). These myoepithelial-like cells produce considerably more S100A4 than the R37 wt cells (Barraclough et al., 1984) and hence increases in these cells with increased passage number would lead to increases in the overall basal levels of MMP-9 in the cell population (Chapter 3: **Figure 3.3B** and **3.5**)

Although, S100P and S100A4 increased all three MMPs by similar folds inside the cells (2.5 to 3.4-fold), MMP-2 outside the cells was increased by higher levels to 7.5-fold and 6.9-fold, respectively, and similarly levels of MMP-13 were increased by 5.7-fold for addition of S100A4, but not S100P (3.1-fold). In the case of MMP-2, the actMMP-2 at 62 kDa was relatively increased much more than proMMP-2 at 68 kDa over the non-stimulated R37 wt cells (**Figure 5.2B**). In the case of MMP-13, the active form at 52 kDa was increased relatively much more for addition of S100A4 than addition of S100P (**Figure 5.4B**). These results suggest that although both S100P/A4 increase production of all three MMPs, they have different effects on MMP processing, and these can even be different between S100P and S100A4 in processing the same MMP, in this case MMP-13. Thus, although there have been several reports of addition of S100P/A4 to cells causing increases in certain MMPs (Dakhel et al., 2014; Schmidt-Hansen et al., 2004), this is the first report of differential effects on particular MMPs and by different S100 proteins.

In addition to effects on MMPs, addition of 1μM S100P or S100A4 significantly increased the migration of R37 wt cells by 2.5- or 2-fold ($P \leq 0.03$), respectively, and invasion by 4-folds ($P \leq 0.025$). The fold increases in migration were less than the

general fold increases in MMPs, but the fold increases in invasion were higher than in migration and more similar to the fold increases in intracellular MMPs. These results suggest that there is a closer link between MMPs and cell invasion than with cell migration when S100 proteins are added to cells, consistent with previous reports (Dakhel et al., 2014; Schmidt-Hansen et al., 2004).

Since we had identified saturation effects of addition of S100P to R37 wt cells on both intracellular and extracellular MMP-9 production, we investigated whether the most widely reported cell surface receptor linked to S100 proteins, RAGE (Herwig et al., 2016; Rehbein et al., 2008) could play a role in promoting the effects of S100P/A4 on R37 wt cells. Our experiments showed that addition of 1 µM S100P or S100A4 with neutralising antibody to RAGE caused significant decreases by 3.96-fold (P=0.02) or 1.88-fold (P=0.03), respectively. Furthermore, addition of Cromolyn, which inhibits S100P binding to the RAGE receptor, also caused significant decreases by 2.5-fold (P=0.03) or 2.04-fold (P=0.03), respectively. There were no significant effects of either inhibitor alone on R37 wt cells showing that inhibition was specific to the stimulation produced by S100 proteins (**Figure 5.7**). The overall effect of both inhibitors on cell invasion was to suppress the approximate 4-fold stimulatory effect of the S100 proteins by just over a half (2.6-fold). Although, it is possible that these partial inhibitory effects could be due to use of too low a concentration of inhibitors, this is unlikely, since we used the optimum recommended 5 µg/mL dilution of anti-RAGE (Arumugam et al., 2006; Taguchi et al., 2000) and 100 µM of Cromolyn. Even when RAGE neutralizing antibody was used at higher concentrations of 10 µg/mL (Nasser et al., 2015) or 20 µg/mL (L. Zhou et al., 2012), there was still only about a 50 % reduction in invasion. Moreover, 100 µM Cromolyn caused inhibition of cell

invasion stimulated by S100P by a variable amount of 50 % or more in different cell lines (Arumugam et al., 2006; Weng et al., 2012). Taken at face value, this result suggests that not all the effects of the S100 proteins on cell invasion involves RAGE and that the S100P/A4 could interact with other targets, presumably still on the surface of the cell. One such reported target is Annexin II (Liu et al., 2015). When we used the same inhibitors on the stably-transfected R37-S100P or R37-S100A4 cell lines, the RAGE antibody significantly decreased invasion by 1.6-fold (P=0.003) or 2.99-fold (P=0.006), respectively, and Cromolyn by 1.5-fold (P=0.007) or 2.44-fold (P=0.005), respectively. These results suggest that the original overall 11-fold stimulation for R37-S100P and R37-S100A4 (Chapter 4) caused by intracellularly produced S100 proteins on cell invasion was suppressed overall by about a half (2.2-fold) and hence once again, other interactions could also play a role.

If we compare the fold increases for production of MMP-9 after addition of different concentrations of S100P to R37 wt cells with the published binding of S100P to the RAGE-V domain (~6µM) (Penumutchu et al., 2014), there are differences of at least three orders of magnitude. Thus, even if all the effects of S100P on MMP-9 could have been inhibited by neutralising antibody, the large difference in these values would suggest that there are at least 2 forms of the RAGE receptor, either with different affinities like the epidermal growth factor receptor (EGFR) (McAndrew et al., 1994), or two different receptors as seen with the FGF dual receptor system with two different subunits synergising together to yield receptor binding of high affinity (Xu et al., 2013).

Thus, we have shown that addition of extracellular S100P or S100A4 can stimulate cell migration and particularly cell invasion of benign rat mammary cells, in

part, via the RAGE receptor (Herwig et al., 2016; Mercado-Pimentel et al., 2015) probably by their ability to increase production and activation of certain MMPs, in general agreement with reports in other cell systems (Dakhel et al., 2014; Schmidt-Hansen et al., 2004). The overall relevance of our finding to the human situation is discussed in Section 7.

5.4 Summary

Our data showed that when S100P or S100A4 was added externally to Rama 37 wild type cells (R37 wt), they increased production of intracellular MMP-2, MMP-9 and MMP-13 by 2.5- to 3.4-fold, both increased extracellular MMP-2 by 7-fold, MMP-9 by only 3.5- to 4-fold, and S100A4 increased extracellular MMP-13 by about 6-fold, whilst S100P increased it by only about 3-fold. These changes were accompanied by 2- to 2.5-fold increases in cell migration and 4-fold increases in cell invasion. Inhibition of these increases in invasion produced by S100 proteins with RAGE neutralizing antibody or Cromolyn caused a very approximate 50 % reduction in R37 wt cells with added S100P/A4 or in S100P/A4 transfected cells. These results suggest that S100P/A4 act in part through RAGE to stimulate MMP production and sometimes activation so as to increase invasion rates in these rat mammary cells. Whether changes in S100 proteins are related to changes in MMPs and death from metastatic disease in human breast cancer is the subject of the next chapter.

Chapter 6

Relationship of specific MMPs to S100P/A4 in primary tumours and to patients' survival times in human breast cancer

6.1 Introduction

The most common cause of cancer deaths amongst females in the Western and now Eastern world is breast cancer (Egeland et al., 2017; Makoukji et al., 2016). S100P and S100A4 are members of the S100 family of Ca^{2+} - binding proteins and have been reported to be associated with early patient death in many cancer types for example lung, prostate, colorectal, pancreas and breast cancer (Ambartsumian et al., 2001; Basu et al., 2008; Bresnick et al., 2015; Bulk et al., 2008; Dahlmann et al., 2012; Dakhel et al., 2014; Ding et al., 2011; Gross et al., 2014; Jiang et al., 2011; Rudland et al., 2000; Salama et al., 2008; Siddique et al., 2013; Takenaga et al., 1997), presumably due to their propensity to induce metastasis, at least in experimental animals (Davies et al., 1993, 1996). Recent studies on breast cancer specimens with different histological grades (I, II & III) showed a significant increase in many mRNAs compared to non-tumour samples, including mRNAs for S100P and some MMPs, e.g MMP-13. Increases in S100P and MMP-13 mRNAs were correlated with reduced patient survival times (Makoukji et al., 2016). S100A4 has also been reported to be associated with MMPs, e.g. MMP-13, and to encourage metastasis in many cancer types *in vivo* including those from breast cancer (Ambartsumian et al., 2001; Basu et

al., 2008; Bulk et al., 2008; Dahlmann et al., 2012; Dakhel et al., 2014; Ding et al., 2011; Egeland et al., 2017; Fei et al., 2017; Gross et al., 2014; Jiang and Lai, 2011; Rudland et al., 2000; Salama et al., 2008; Siddique et al., 2013; Takenaga et al., 1997; Wang et al., 2012), MMPs have been reported to be associated with breast cancer patients' survival times, either individually or in the presence of an S100 protein such as S100A4 in breast cancer specimens (Ismail et al., 2017). Moreover, protein levels and activities of MMP-2 and MMP-9 were increased in malignant tumours compared to normal breast tissues (Jinga et al., 2006). MMP-13 was also reported to be frequently detected in breast tumours, especially in lymph node metastases (Kotepui et al., 2016). Although, protein levels can be quantified using Western blots of whole specimens, they do not allow separate estimation of the important carcinoma cells from the reactive host stromal cells, which can be often 50% of the tumour mass (Rudland et al., 2000). For this aspect, immunohistochemical staining is undertaken and usually the percentage of stained tumour cells is related to the overall levels of the protein determined by Western blotting (Zhao et al., 2014). However, the detailed relationship between S100 proteins, MMPs and patient survival times in breast cancer has not yet been investigated.

6.1.1 Chapter aims

To examine the relationship between specific MMPs and S100P/A4 in primary tumours and their relationship to survival times of breast cancer patients using immunohistochemical staining of primary breast carcinomas.

6.2 Results

6.2.1 Immunohistochemistry (IHC) staining

IHC was performed on 183 specimens of primary tumours from unselected breast cancer patients (Section **2.18.1**). IHC staining with a single chromophore was used for monoclonal antibodies against S100P, S100A4, MMP-2, MMP-9 and MMP-13, or double staining with antibodies directed against S100 proteins and directed against MMPs but with different chromophores for each family of proteins (**Figure 6.1**). Histologically all sections showed lobules with some ducts. IHC staining for MMPs on 183 patients showed 32% to 67% with positively stained carcinoma cells (**Figure 6.1**). According to the IHC staining results of the carcinoma cells, the breast cancer specimens were divided into 5 staining categories: negative – (<1%), borderline ± (1-5%), intermediate + (5-25%), moderated ++ (25-50%) and strong +++ (>50%) staining groups (Section **2.18.2**). IHC staining of the host stromal cells was ignored. Using Wilcoxon and Cox's univariate analyses the most significant and greatest difference in relative risk (RR) of patients' survival times between adjacent staining groups occurred between borderline (±) and moderately (+) staining categories for each of MMP-2, 9 and 13 (Ismail et al., 2017) (**Table 6.1**). Accordingly, we used a 5% cutoff to separate the patients into two categorical staining groups for ease of further statistical manipulations: the new negatively stained (- and ±) with about 19% to 26% of tumours and the overall positively stained group (+, ++ and +++) with about 15% to 47% of staining tumours (Ismail *et al.*, 2017).

Previously IHC staining of the same human breast cancer specimens for S100P or S100A4 showed highly significant reductions in patients' survival times when

sections were positively stained for S100P or for S100A4 over those that were not stained (Rudland *et al.*, 2000; Wang *et al.*, 2006; de Silva Rudland *et al.*, 2011; Ismail *et al.*, 2017).

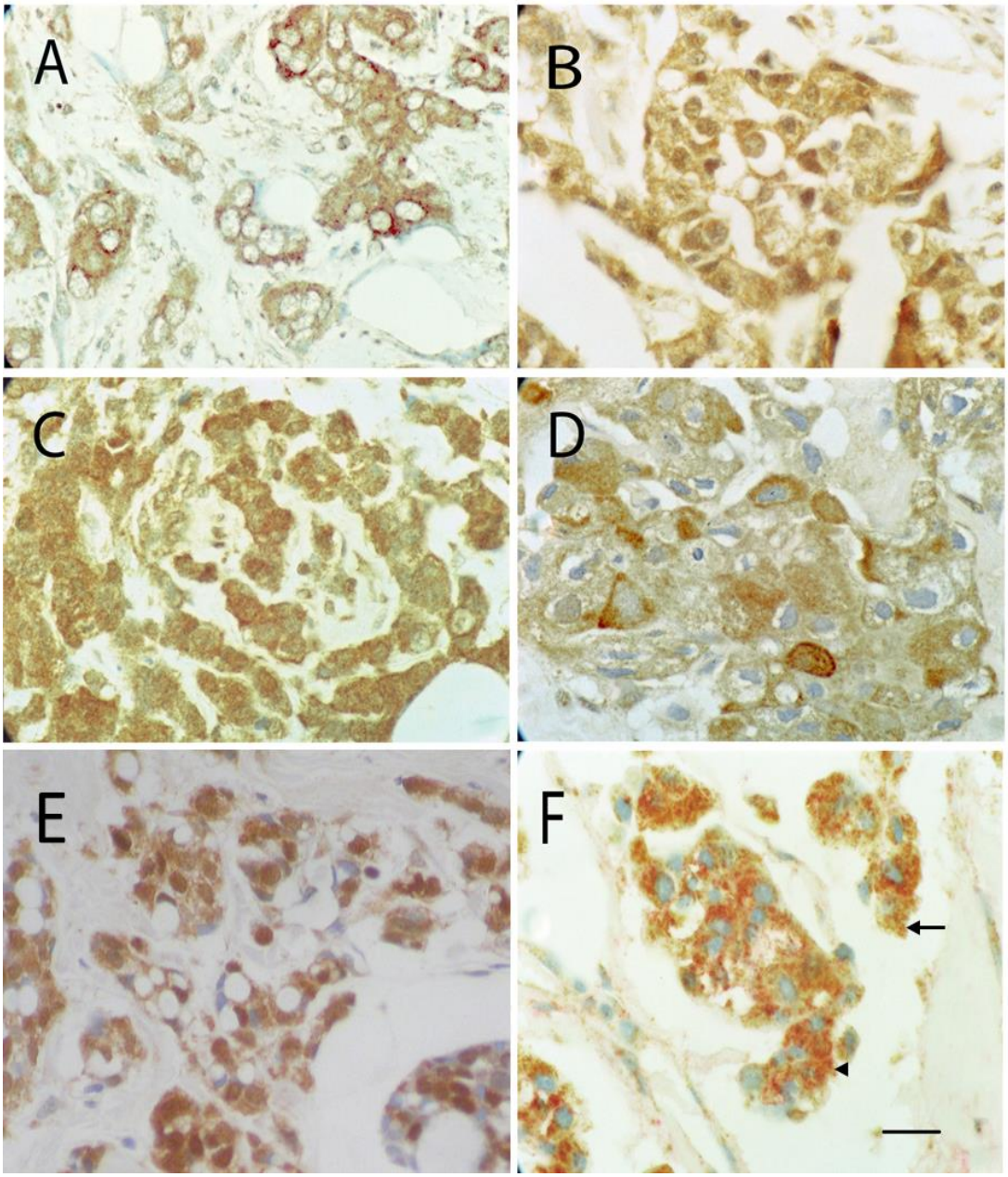

Figure 6.1. Immunohistochemical staining of human breast carcinoma specimens for MMPs and S100 proteins.

(**A, B** and **C**) Monoclonal antibody staining against MMP-2, MMP-9 and MMP-13, respectively, showing brown staining of the carcinoma cell cytoplasm. (**D** and **E**) Monoclonal antibody staining for S100P or S100A4, respectively, showing bead-like, nuclear and mostly cytoplasmic brown staining. (**F**) Serial sections from the same tumour as in **E** stained for S100A4 (red) and for MMP-2 (brown). Most breast carcinoma cells were stained both red for

S100A4 and brown for MMP-2, but some cells were stained either red for S100A4 (arrow head) or brown for MMP-2 (arrow). Magnification x 180; scale bar 20 µM. Taken from Ismail et al., 2017.

Table 6.1. Comparisons between pairwise IHC staining groups for MMPs to show the relative risk between each MMP group.

MMP identity	Staining group for MMP [a]	X^2 [b]	P [c]	RR [d]
MMP-2	- vs ±	3.7	0.055	2.44
	± vs +	16.6	<0.001	4.75
	+vs ++	0.008	0.93	1.1
	++ vs +++	1.7	0.19	1.65
MMP-9	- vs ±	4.7	0.030	1.84
	± vs +	6.3	0.012	2.94
	+vs ++	0.2	0.63	0.99
	++ vs +++	0.09	0.77	1.22
MMP-13	- vs ±	0.06	0.81	0.97
	± vs +	3.9	0.049	2.61
	+vs ++	4.1	0.042	2.25
	++ vs +++	2.1	0.150	1.77

[a] Staining group for each MMP, see **Table 2.3**.
[b] Wilcoxon statistic X^2.
[c] Statistical significance from Wilcoxon-Gehan analysis.
[d] Relative risk (RR) of survival from Cox's univariate analysis.

6.2.2 Association between MMPs and patients' survival times

The association between staining for each of MMP-2, -9 and -13 and patient survival times was checked by plotting Kaplan Meier survival curves for each of the staining groups in **Table 2.3** followed by analysis using Wilcoxon and Cox's univariate statistics, as described for S100A4 and S100P alone (de Silva Rudland et al., 2011). The most significant differences and greatest relative risks (RR) for all three MMPs occurred between the ± and + staining groups (**Table 6.1**). Therefore, for ease of

computation the staining groups were recategorized into two categorical staining groups of negative (-,±) and positive (+, ++, +++) groups using a 5 % cutoff of stained carcinoma cells to separate them (Section **2.18.2**). When survival times for each of MMP-2, MMP-9 and MMP-13 or all 3 MMPs were compared between negative (-, ±) and positive (+, ++, +++) groups, there was a highly significant reduction in patient survival times for each of the 3 different MMPs or for their combination (Wilcoxon Gehan statistics, *P*<0.001) (**Figure 6.2-3**). In more individual detail for MMP-2, the cumulative proportion of patients surviving at the end for MMP-2 negative group (-, ±) was 0.81 (number starting was 106 patients) and 0.11 (number starting was 77 patients) for positive group (+, ++ and +++) with relative risk (RR) of 9.04 (**Figure 6.2A)**. For MMP-9, the cumulative proportion surviving at the end for MMP-9 negative group (-, ±) was 0.58 (number starting was 156 patients) and 0.10 (number starting was 27 patients) for the positive group (+, ++ and +++) with relative risk (RR) of 4.7 (**Figure 6.2 B)**. For MMP-13, the cumulative proportion surviving at the end for MMP-13 negative group (-, ±) was 0.75 (number starting was 96 patients) and 0.22 (number starting was 87 patients) for the positive group (+, ++ and +++) with relative risk (RR) of 4.9 (**Figure 6.3 A)**. For the 3 MMPs together, the cumulative proportion surviving at the end for 3 MMPs combined negative group (-, ±) was 0.57 (number starting was 160 patients) and 0.07 (number starting was 23 patients) for the positive group (+, ++ and +++) with relative risk (RR) of 4.96 (**Figure 6.3B)**.

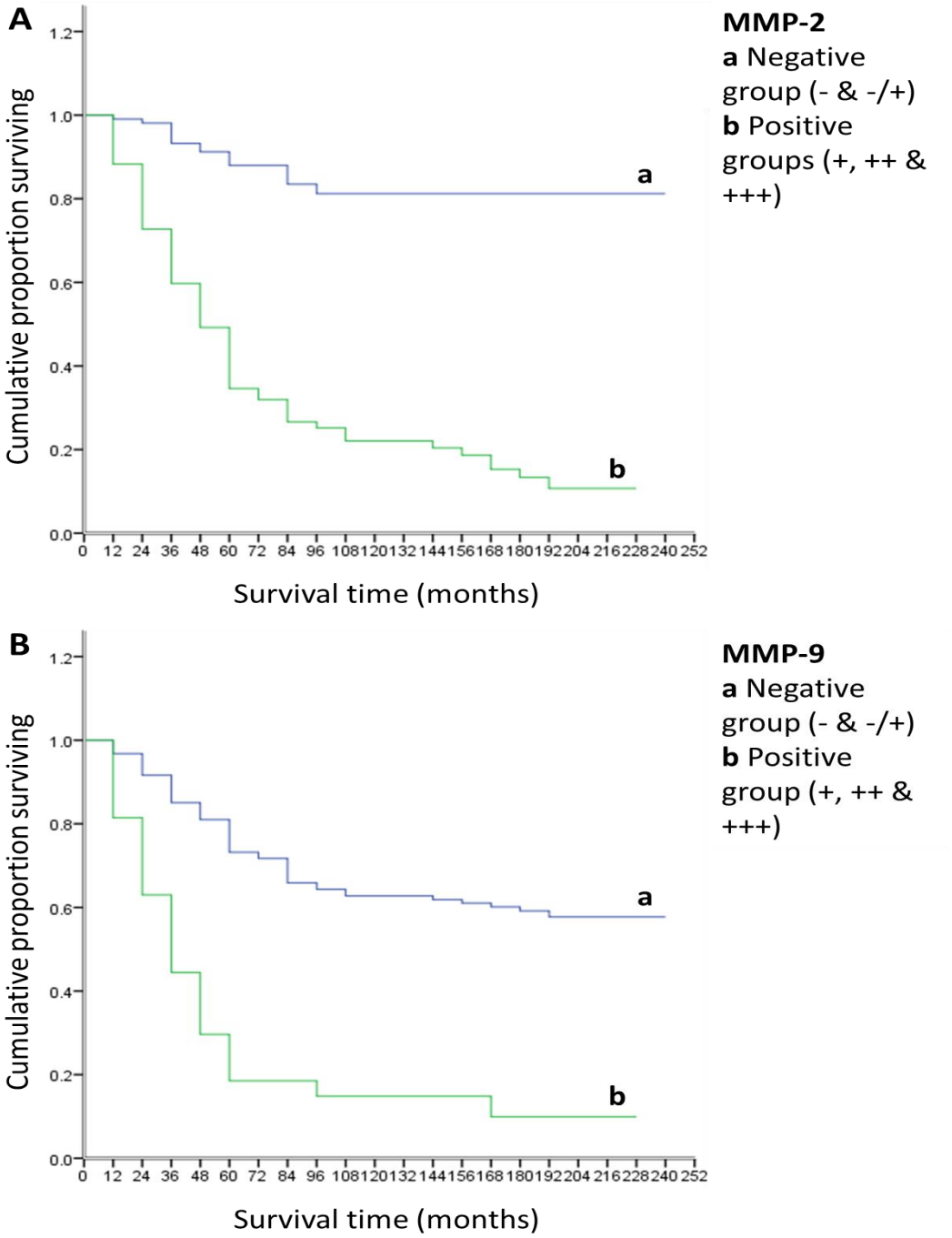

Figure 6.2. (A) MMP-2 or (B) MMP-9 survival curves.

Kaplan Meier plots to show the difference in survival time between patients with tumour (**a**) ≤ 5% stained (-, ±) group and (**b**) ≥ 5% stained (+, ++ and +++) group for mAb to MMP-2 or MMP-9 (see **Tables 2.3, 6.1 and Figure 6.1**). The data from 183 patients with invasive breast carcinoma was collected every 12 months for 20 years. (**A**) The median survival time was 228 months for (**a**) and 47.1 months for (**b**), there was a significant difference between the two groups (Wilcoxon Gehan statistic, *P*<0.001). (**B**) The median survival time was 228 months for (**a**) and 32.4 months for (**b**), there was a significant difference between the two groups (Wilcoxon Gehan statistic, *P*<0.001).

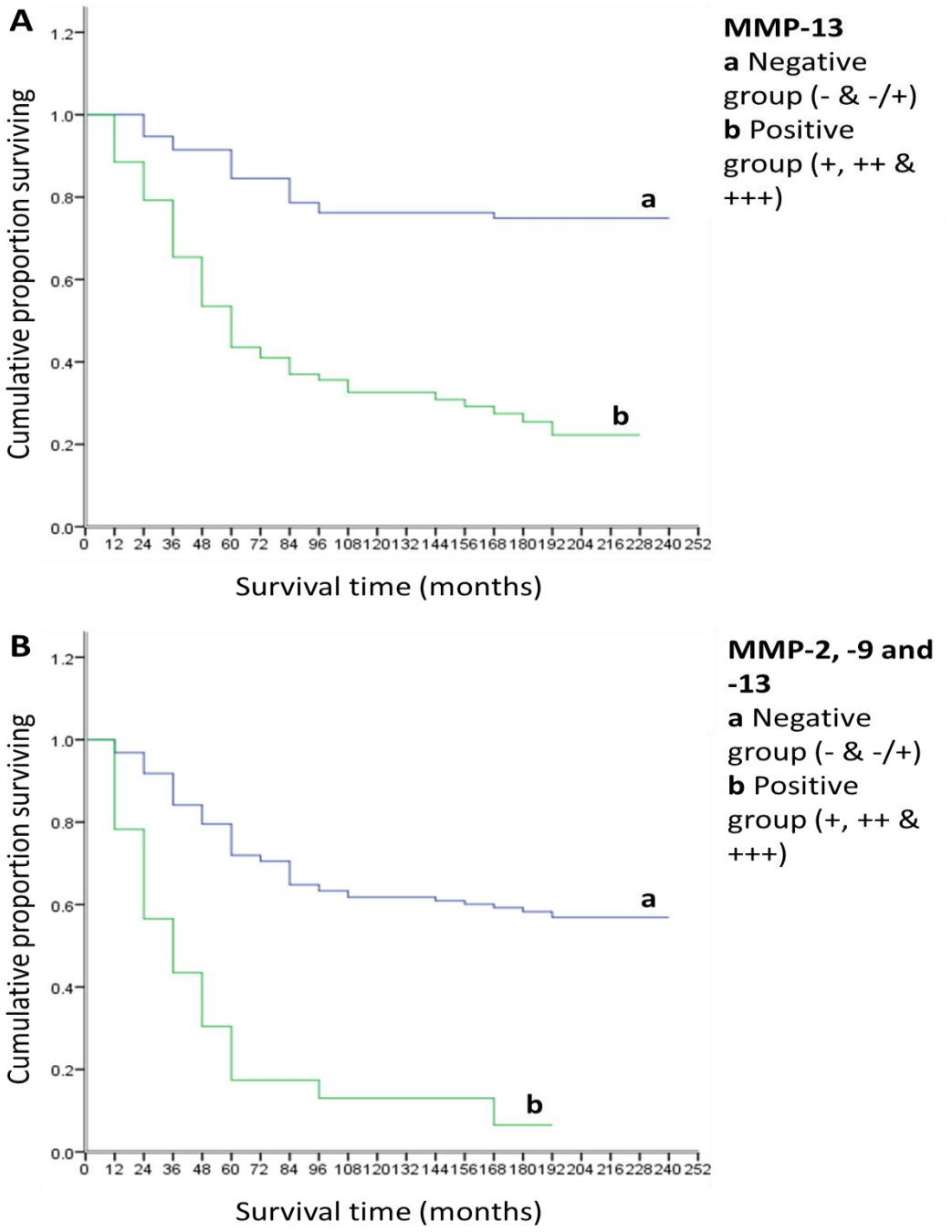

Figure 6.3. (A) MMP-13 or (B) MMP-2, -9 and -13 together survival curves.
Kaplan Meier plots to show the difference in survival time between patients with tumour (**a**) ≤ 5% stained (-, ±) group and (**b**) ≥ 5% stained (+, ++ and +++) group for mAb to MMP-13 or mAbs for 3 MMPs together (see **Tables 2.3, 6.1 and Figure 6.1**). The data from 183 patients with invasive breast carcinoma was collected every 12 months for 20 years. (**A**) The median survival time was 228 months for (**a**) and 52.3 months for (**b**), there was a significant difference between the two groups (Wilcoxon Gehan statistic, *P*<0.001). (**B**) The median survival time was 228 months for (**a**) and 30 months for (**b**), there was a significant difference between the two groups (Wilcoxon Gehan statistic, *P*<0.001).

6.2.3 Association of IHC staining for MMPs with that for S100 proteins using cross-tabulations

Comparisons of positive IHC staining of 183 patients for each one of MMP-2, -9 and -13 using 5% cutoffs with that for S100P or S100A4 from the same set of patients (Rudland et al., 2000; Wang et al., 2006) using cross-tabulations and significance computed by Fisher's Exact test are shown in **Table 6.2**.

Staining for each MMP and for the combination of all 3 MMPs was highly significantly associated with staining for either S100P or S100A4 (Fishers Exact test, *P*<0.001) (**Table 6.2**).

Table 6.2. Cross-tabulations showing the association of IHC staining for MMPs with S100 proteins.

S100 proteins [a]	MMP-2 {no (%)} [b]			MMP-9 {no (%)} [b]			MMP-13 {no (%)} [b]			MMP-2, -9 & -13 {no (%)} [c]		
	-	+	*P* [d]	-	+	*P* [d]	-	+	*P* [d]	-	+	*P* [d]
S100P -	63(68.5)	17(23.9)		76(55.5)	4(15.4)		59(71.1	21(26.3)		76(54.3)	4(17.4)	
S100P +	29(31.5)	54(76.1)	<0.001	61(44.5)	22(84.6)	<0.001	24(28.9)	59(73.8)	<0.001	64(45.7)	19(82.6)	=0.001
S100A4 -	84(79.2)	26(33.8)		104(66.7)	6(22.2)		75(78.1)	35(40.2)		105(65.6)	5(21.7)	
S100A4 +	22(20.8)	51(66.2)	<0.001	52(33.3)	21(77.8)	<0.001	21(21.9)	52(59.8)	<0.001	55(34.4)	18(78.3)	<0.001

[a] S100 protein family members.

[b, c] Patient number and percentage for classifying carcinoma cells IHC-stained negatively (-) or positively (+) for each of MMP-2 [b], -9 [b] and -13 [b] or for all MMPs simultaneously [c] using 5% cutoff for each case.

[d] Significance *P* value for Fisher's Exact test, 2-sided.

6.2.4 Relative probability of association of MMPs with S100 proteins using logistic regression

Binary logistic regression analysis of 183 breast carcinoma specimens was performed to show the relative association (RA) of one variable with a set of other tumour variables in the same patients. Thus, in **Set 1**, when staining for S100P was tested with that for the MMPs, the association of S100P was only significant with MMP-2 (RA 3.31, *P*=0.004) and MMP-13 (RA 3.45, *P*=0.002), but not with MMP-9 (RA 1.836, *P*=0.341) or all 3 MMPs together (RA<0.001, *P*=1.0). Similarly staining for S100A4 was only significantly associated with that for MMP-2 (RA 4.21, *P*<0.001) and borderline associated with MMP-13 (RA 2.17, *P*=0.051), but not with MMP-9 (*P*=0.11) nor all three MMPs (*P*=0.31) (**Table 6.3**).

When the converse testing was undertaken for an individual staining MMP, with that for S100P and S100A4 together, then MMP-2 was more strongly associated with S100A4 (RA 5.18, *P*<0.001) than S100P (RA 3.71, *P*=0.001). MMP-9 was similarly more strongly associated with S100A4 (RA 4.52, *P*=0.006) than S100P (RA 3.4, *P*=0.049). MMP-13, in contrast to MMP-2 and MMP-9, was more strongly associated with S100P (RA 4.22, *P*<0.001) than with S100A4 (RA 3.56, *P*=0.002). Staining for all 3 MMPs was only significantly associated with that for S100A4 (RA 5.16, *P*=0.005) and not for S100P (RA 2.62, *P*=0.13) (**Table 6.3**).

Table 6.3. Relative association between test variable and other tumour variables.

Test variable [a]	Other variables [b]	X^2 [c]	SE [d]	P [e]	RA [f]
Set 1					
S100P	MMP-2	8.232	0.417	0.004	3.309
	MMP-9	0.907	0.638	0.341	1.836
	MMP-13	9.276	1.238	0.002	3.449
	MMP-2, -9 & -13	0.000	23204	0.999	0.000
S100A4	MMP-2	13.61	0.389	<0.001	4.207
	MMP-9	2.587	0.547	0.108	2.412
	MMP-13	3.819	0.398	0.051	2.175
	MMP-2, -9 & -13	0.819	1.308	0.365	0.306
Set 2					
MMP-2	S100P	10.96	0.396	0.001	3.715
	S100A4	16.74	0.402	<0.001	5.185
MMP-9	S100P	3.861	0.626	0.049	3.420
	S100A4	7.620	0.546	0.006	4.520
MMP-13	S100P	14.12	0.383	<0.001	4.225
	S100A4	9.921	0.403	0.002	3.558
MMP-2, -9 & -13	S100P	2.253	0.641	0.133	2.619
	S100A4	7.748	0.589	0.005	5.158

[a] Test variable, **Set 1**, staining for S100P or S100A4 compared with the staining for each one of the three MMPs. **Set 2**, staining for each one of the 3 MMPs compared with staining for both S100P and S100A4 together.

[b] Other variables; **Set1**: MMPs and **Set 2**: S100 proteins.

[c] Logistic Regression statistic X^2.

[d] Standard error in binary Logistic Regression.

[e] *P* from Logistic Regression statistic X^2.

[f] Relative Association (RA) from binary Logistic Regression analysis.

6.2.5 Association of patient survival times with MMPs without and with S100 proteins

Cox's univariate analyses were performed on the 183 patients to determine whether staining for each one of MMP-2, -9, -13, S100P and S100A4 has a separate effect on patient survival times (**Table 6.4, Set 1**). Moreover, to determine whether staining for each of MMP-2, -9, -13 or for 3 MMPs simultaneously were significantly independent of staining for S100P or for S100A4 when related to patient survival times, Cox's bivariate analyses were conducted (**Table 6.4, Set 2 and 3**).

Data analysis showed that the individual risk of death significantly ($P \leq 0.002$) increased with staining for MMP-2, -9, -13, S100P or S100A4 when treated separately (univariate analysis). The relative risk (RR) of patient death was highly significant for all variables ($P < 0.001$) and greater for patients with breast cancer stained for S100A4 (9.961) than stained for S100P (7.076). The RR of positive staining for each MMP on patient death was also highly significant ($P < 0.001$) for all MMPs and greater for staining for MMP-2 (9.041), followed by staining for MMP-13 (4.870) and then for MMP-9 (4.694) (**Table 6.4, Set 1**).

When analyses with staining for one MMP and one S100 protein were conducted together (bivariate analysis), staining for MMP-2 with that for S100P or for S100A4 remained the greatest RR (6.5 or 5.1, respectively) compared to that for MMP-9 or MMP-13, the latter two MMPs had similar RRs in the presence of S100P or S100A4. These results may suggest that the pathway to patient death for MMP-2 overlap those of S100P and S100A4 less well than those of MMP-9 and MMP-13. (**Table 6.4 Set 2, 3**).

Table 6.4. Cox's bivariate analyses to show whether MMPs are significantly independent of S100 proteins when related to patient survival times.

Tumour variable [a]	X^2 [b]	SE [c]	*P* [d]	RR [e]
Set 1				
S100P	41.0	0.306	<0.001	7.076
S100A4	72.473	0.270	<0.001	9.961
MMP-2	66.225	0.271	<0.001	9.041
MMP-9	39.071	0.247	<0.001	4.694
MMP-13	39.681	0.251	<0.001	4.870
Set 2				
S100P	9.447	0.337	0.002	2.817
MMP-2	29.98	0.343	<0.001	6.547
S100P	30.853	0.315	<0.001	5.737
MMP-9	15.761	0.264	<0.001	2.855
S100P	21.225	0.329	<0.001	4.546
MMP-13	11.866	0.301	0.001	2.818
S100P	32.679	0.313	<0.001	5.973
MMP-2,9&13	20.881	0.271	<0.001	3.452
Set 3				
S100A4	37.184	0.287	<0.001	5.765
MMP-2	31.814	0.287	<0.001	5.054
S100A4	61.849	0.277	<0.001	8.822
MMP-9	16.140	0.257	<0.001	2.811
S100A4	50.180	0.281	<0.001	7.298
MMP-13	14.984	0.262	<0.001	2.757
S100A4	62.132	0.276	<0.001	8.835
MMP-2,9&13	15.157	0.266	<0.001	2.819

[a] **Set 1**: Set of stains for one tumour variable using cutoff of 5% carcinoma cells stained to separate the two categorical groups. **Set 2** and **Set 3**: Set of stains for two tumour variables. To test their simultaneous effects on patient survival times, the calculations involved entering 2 variables into Cox's Multiple Regression Analysis in order to compare their individual contribution to patient survival times in the presence of the other variable.

[b] Cox's statistic X^2.

[c] Standard error (SE) of X^2.

[d] *P* value, df = 1 in each case.

[e] Relative risk (RR).

In addition, when serial sections from three breast carcinomas strongly-staining for MMP2 were doubly IHC-stained for S100A4 (red) and for MMP2 (brown) on the same section, there were (mean ± SE) 80.2% ± 2.2% doubly stained cells, 6.9% ± 0.9% cells stained red for S100A4, 2.9% ± 0.4% cells stained brown for MMP2 and 9.1% ± 1.5% unstained cells (ANOVA, F = 669.3, 3 df, P<0.001) (**Figure 6.1**). Thus, S100A4 is associated with and partially confounded for patient survival by the three MMPs to varying degrees (Ismail et al., 2017).

6.3 Discussion

IHC staining for both S100 proteins, S100P and S100A4 and for all three MMPs was located both in the carcinoma cells as well as in the host cells of the primary tumours. Here we considered only staining of the carcinoma cells, since the percentage of stained carcinoma cells has previously been shown to be directly related to the level of particular proteins in the primary tumour (Rudland et al., 2002, 2000). That our antibodies recognized the correct proteins is shown by the fact that the same antibodies used in Western blots in **Chapter 3**, yielded the correct size bands on SDS-containing polyacrylamide gels. Moreover, prior incubation of the specific antibodies with the correct immunizing peptide/protein for both the S100 proteins (Rudland et al., 2002, 2000) and the MMPs (Ismail et al., 2017) abolished completely all the immunohistochemical staining.

Staining for the S100 proteins in previous publications (Ismail et al., 2010; Wang et al., 2006), and for each of the three MMPs as well as that for the combined set of MMPs (**Figure 6.2** and **6.3**) showed a highly significant association with reduced patient survival times. Our results for the MMPs and patient survival times with

breast cancer are consistent with those previously reported for only one of MMP-2 (Chen et al., 2015; Li et al., 2017), for MMP-9 (Li et al., 2017) and for MMP-13 (Zhang et al., 2008).

That staining for the MMPs usually occurred in the same tumours as that for either of the two S100 proteins can be inferred from the high level of significance of association determined from Fisher's Exact tests of the relevant paired cross tabulations (**Table 6.2**). Moreover, in at least one case where antibodies for S100A4 and to MMP-2 were labelled with different chromophores, most of the carcinoma cells were doubly stained by both antibodies, whereas relatively few were stained by only one or the other antibody (**Figure 6.1F**). This result demonstrated that S100A4 and MMP-2 were produced in the same cell, which is consistent with the idea that S100A4 triggered, either directly or indirectly the production of MMP-2 in the human cancer cells.

The relative association of staining for one S100 protein was tested against staining for the 3 MMPs together and one MMP was tested against the two S100 proteins together using logistic regression analysis (**Table 6.3**). Staining for S100A4 showed a greater propensity to associate with that for MMP-2, whilst that for S100P showed a greater propensity to associate with MMP-13. Moreover, staining for MMP-9 associated significantly with that for S100A4 and S100P (**Table 6.3**). These results suggest that S100 proteins may target the induction of different combinations or even different MMPs and that both S100P and S100A4 may be required to induce effectively all 3 MMPs. This differential targeting of MMPs by S100P and S100A4 may be one reason for the finding that the occurrences of both S100P and S100A4 in a breast tumour significantly enhances the rate of patient death over those patients

with only one or the other of the S100 proteins present (Wang et al., 2006). Moreover, there would be a requirement for S100P to induce MMP-13 to initiate collagen I digestion before S100A4 was required to induce MMP-2 and/or MMP-9 so as to complete the digestion of collagen I (Section **1.3.2**). If a major metastasis – inducing property of S100A4/P is to induce the MMPs, then it would be anticipated that S100P should be induced before S100A4 in the development of metastatic breast cancer. Preliminary results of immunohistochemical staining for X-ray detected premalignant and malignant breast cancer lesions suggest that this is indeed the case (Mr. J. Winstanley and Prof. P. S. Rudland, unpublished results).

6.4 Summary

The effect of S100P and S100A4 on patient survival times was reduced the most by MMP-2 in both cases, but MMP-13 reduced the effect of S100P more than that of S100A4. The decrease in RR probably reflects the extent of overlap of pathways leading to patient death (Ismail et al., 2017). This result would then suggest that S100P and MMP-13 pathway overlap more than those of S100A4 and MMP-13 consistent with the idea advanced in **Chapter 3**, that S100P and S100A4 promote some unique nonoverlapping pathways which lead to patient death and that both therefore could work synergistically in promoting patient demise.

Chapter 7

General Discussion

7.1 Insight and purpose of the Project

The most common mortality amongst females caused by cancer is metastatic breast cancer (Egeland et al., 2017; Makoukji et al., 2016). Amongst the most common tumour markers in humans involved in stimulating cancer cells to metastasise in rodent models are S100P and S100A4 (Egeland et al., 2017; Fei et al., 2017; Ismail et al., 2017; Makoukji et al., 2016). Cancer cells metastasise, in part, by passing though the extracellular matrix (ECM) by a combination of migration and invasion. The first component of the ECM encountered by the cancer cells is the basement membrane (collagen IV, laminin) and the remaining bulk is an insoluble interstitial matrix consisting of components such as collagen I, gelatin, proteoglycan and glycoproteins (McCuaig et al., 2017). Thus, cancer cells are required to recruit degradative systems to facilitate their passage through this insoluble barrier, these systems include degradative proteases such as serine, aspartic, cysteine, threonine and metalloproteinases (Brünner et al., 1994) (**Chapter 1**). Matrix metalloproteinases (MMPs) have been reported to be the most common proteases associated with and involved in human cancers (Mason and Joyce, 2011). Amongst the many members of the family of MMPs involved in cancer, the most commonly reported in breast cancer are MMP-2, -9 and -13. These have been reported to be expressed in either the host stromal cells of malignant tumours (Singer et al., 2002; Uría et al., 1997), or by the

malignant cancer cells themselves, both *in vivo* and *in vitro* (Li et al., 2017; Uría et al., 1997).

When expression of S100 metastasis-inducing proteins (e.g S100P) have been induced in rat mammary and human HeLa cells, their induction causes increased cell migration and invasion (Du et al., 2012). Moreover, when stromal cells such as fibroblasts have been incubated with conditioned medium from breast cancer cells such as MCF-7, they produce MMP-13 (Uría et al., 1997). These facts suggest that tumour factors such as S100P or S100A4 produced in breast cancer cells or in adjacent host stromal cells could stimulate expression of MMPs, either in the cancer cells themselves or in the adjacent stromal cells. The production of these MMPs, in turn, could assist the cancer cells to digest the basement membrane (mostly collagen IV) (Li, 2003; Yue, 2014) and ECM (mostly collagen I) to encourage cell migration and, particularly, cell invasion. Based on these considerations, we started our investigations to see whether breast cancer cells, which have raised levels of tumour factors like S100P/A4, could stimulate the production of MMPs to facilitate migration/invasion of carcinoma cells, as part of the overall process of metastasis.

7.1.1 Selection of members of MMPs *in vitro*

A human MMP antibody array was used to scan for MMP expression in R37-S100P/A4 and S100P-induced HeLa-A3 cell lines. This array consisted of antibodies to 7 MMPs (MMP-1, -2, -3, -8, -9, -10 and -13) and to 3 TIMPs (TIMP-1, -2 and -4). The first investigation showed that all MMPs tested were increased, but only MMP-10 and MMP-13 were increased significantly in R37-S100P/A4 cell lines (**Chapter 3**). Zymography assay was then used to show which MMP had proteolytic function when

released outside the cells. This experiment showed that CM from R37-S100P/A4 cell lines produced only MMP-2, -9 and -13 in significantly higher amounts than empty vector control cells. Both MMP-2 and MMP-13 released both pro and active forms, whilst MMP-9 released only the proform into the culture medium (**Chapter 3**). Thus, from these two experiments, we confined our investigations to these three MMPs, MMP-2, MMP-9 and MMP-13, and their relationship with S100P/A4 in model cancer cells *in vitro* and in human breast cancer specimens *in vivo*.

7.1.2 Comparison of the effect of intracellular or extracellular S100 proteins on the expression of MMPs *in vitro*

Both extracellular addition of or intracellularly-produced S100P/S100A4 significantly stimulated the levels of MMP-2, -9 and -13 in CL and CM (**Chapter 3** and **5**). Moreover, expression of MMP-2, -9 and -13 depended on the presence of S100P or S100A4 in our rat mammary cell lines (**Chapter 5**). Thus, levels of MMP-2, -9 and -13 increased significantly ($P \leq 0.026$) when 1 µM of S100P or S100A4 was added extracellularly to these rat mammary cells. These results are consistent with our data in **Chapter 3**, which showed that levels of these MMPs in CL and CM were increased significantly ($P \leq 0.035$) when S100P/A4 was expressed inside the cells using suitably-transfected R37-S100P or S100A4 cell lines (**Table 7.1**).

The combination of both pro and active forms of MMP-13 or proform of MMP-9 showed greater increases under the influence of S100A4 when produced by the cells or added extracellularly than the influence of S100P. In contrast, the combination of both pro and active forms of MMP-2 showed greater increases under the influence of S100P produced from either intracellularly or added extracellular than those of S100A4 (**Table 7.1**). These results suggest firstly that earlier steps for

stimulation of production of MMPs by S100 proteins inside and outside cells are similar. Secondly, since there are different quantitative changes in the levels of the 3 MMPs produced by either S100P or S100A4, these results suggest that particular S100 proteins can selectively stimulate production of different MMPs. Thus, the finding that S100P and S100A4 stimulate different quantitative changes in the MMPs in the same cell system represents a novel conclusion in the field.

In the S100P and S100A4 overexpressing R37 cells (R37-S100P, R37-S100A4), the amount of S100P or S100A4 released was 0.215 µg or 0.203 µg, respectively into 7 mL of CM /10 centimeter diameter dish. This represents concentrations of ~ 3 nM and 2.5 nM, respectively. Thus, the concentrations of S100 proteins released from R37 cells (**Figure 3.1)** are sufficient to stimulate appreciable production of MMPs reported in **Table 7.1.** Thus, even in this simple system, there is sufficient amount of S100P/A4 generated internally to produce an external effect on the increase in MMP production.

Table 7.1. Influence of different sources of S100P/S100A4 on levels of MMP-2, -9 and -13 *in vitro*.

Source of S100 proteins [a]	MMP-2 [b]		MMP-9 [b]		MMP-13 [b]	
	CL [c]	CM [d]	CL [c]	CM [d]	CL [c]	CM [d]
Intra. S100P	1.6±0.1	5.6±0.1	1.7±0.1	1.6±0.1	3.6±0.1	8.1±0.1
Extra. S100P	2.8±0.1	7.5±0.1	2.6±0.0	3.6±0.2	3.2±0.0	3.1±0.3
Intra. S100A4	1.8±0.1	3.7±0.04	2.5±0.1	2.8±0.2	2.9±0.2	9.9±0.1
Extra. S100A4	2.5±0.1	6.9±0.6	3.2±0.1	4.1±0.2	3.4±0.0	5.7±0.6

[a] Source of S100 proteins; either overexpression inside the R37 cells (intra S100P/A4) or added extracellularly to R37 wt cells (extra).
[b] Matrix metalloproteinase-2, -9 or -13.
[c, d] Fold increase for MMP protein level in cell lysate (CL)[c] and conditioned medium (CM)[d] compared to either control of R37 empty vector for intra S100P/A4 cell lines, or control of

R37 wild type without addition of S100P/A4 for extra S100P/A4 cell lines. All significantly different $P \leq 0.035$.

7.1.3 Effect of MMPs on cell biological activity produced by S100 proteins inside or added outside cells *in vitro*

In this thesis, expression and activation of MMPs can be stimulated by the presence of S100P or S100A4 either from inside or added from outside the cells (**Chapters 3** and **5**). Moreover, the presence of S100P and S100A4 inside or added outside the R37 cells showed significant increases in cell migration and invasion with an approximate ratio of 1:2, respectively (**Chapters 4** and **5**). Since MMPs have been reported to be involved in controlling focal adhesion sites and thereby cell migration *in vitro* (Jessen and Jessen, 2017), one interpretation of this ratio may be that cancer cells use the MMPs more for degradation of Matrigel in invasion than use them to reduce the number of focal adhesion sites and hence reduce cell migration *in vitro*. Thus, since S100P and S100A4 can also interact directly with myosin-IIA to stimulate breast cell migration in culture (Du et al., 2012; Li and Bresnick, 2006), the stimulatory effect of either S100 protein is likely to be more pronounced on cell migration than that of the MMPs, in agreement with results obtained in **Chapters 3** and **4**.

When MMPs were knocked-down in the R37-S100P or S100A4 cells, the resultant cells showed a significant reduction in both cell migration and invasion (**Chapter 4**). Similar to the S100 protein-overproducing cell lines, these knocked-down cell lines showed a much higher fold reduction in cell invasion compared to that in cell migration (**Figure 4.5**), one again suggesting that the effect of the MMPs was greater on cell invasion than on cell migration. Knock-down of each MMP

individually in R37-S100P or R37-S100A4 cell lines showed reductions in cell invasion in the following order: MMP-13/MMP-2 and then MMP-9 (**Figure 4.5**).

7.1.4 Association between staining for S100 proteins and MMPs on patients' survival times *in vivo* and their link to MMPs with S100 proteins *in vitro*

In the immunohistochemically-stained breast cancer specimens the relative association (RA) of MMPs with S100 proteins was significant (**Table 6.3**, **Set 2**) and showed higher RAs of MMP-2 and MMP-9 with S100A4, whilst RA of MMP-13 was higher with S100P. Our data in **Chapter 3** (**Table 3.1**) showed that the active form of MMP-2 and proform for MMP-9 were higher in overexpressing S100A4 cells than in overexpressing S100P cells, whilst the active form of MMP-13 showed higher levels in overexpressing S100P cells than in overexpressing S100A4 cells. These results for the overlapping of expression of S100P or A4 with that of individual MMPs are similar in the *in vivo* and *in vitro* systems and showed that S100A4 overlaps predominantly with MMP-2 and MMP-9 and that S100P overlaps predominantly with MMP-13 in either system.

The relative risk (RR) of patient survival for S100 proteins and MMPs taken together *in vivo* using a series of Cox's bivariate analyses showed significant reductions in patient survival times for all MMP/S100 paired combinations (**Table 6.4**). These confounding results showed that individual pathways leading to patient death for such pairings overlapped somewhat, but the extent of their overlap varied according to the identity of the pair. Thus, a comparison of RRs between anyone of MMP-2, MMP-9 and MMP-13 alone with that in the presence of either S100P or S100A4 showed that S100A4 had a greater confounding effect and hence overlap

than S100P on all 3 MMPs' pathways leading to patient death (**Table 7.2**). This conclusion is consistent with that obtained on cell invasion in the cell line studies, in that knock-down of any one MMP caused a greater reduction in cell invasion stimulated by S100A4 than by S100P (**Table 4.5**). Moreover, the RR for MMP-13 was confounded the most in the presence of S100P, and that for MMP-2 the most in the presence of S100A4 (**Table 7.2**), consistent with the knock-down studies on cell invasion *in vitro* (**Figure 4.5**). The consistency of results obtained on patient survival *in vivo* and cell invasion *in vitro* for the effect of S100 proteins on MMPs suggest that the two biological processes are strongly linked. Thus, a simple interpretation would be that a major rate–limiting step in patient death is indeed that of cell invasion, at least for the 5 molecules studied here.

Table 7.2. Decrease in relative risk of patient survival for each MMP with one or the other S100 protein.

Reduction in relative risk (%) [a]		
MMP [b]	**S100P [c]**	**S100A4 [c]**
MMP-2	27.5 %	44 %
MMP-9	38.3 %	40.4 %
MMP-13	42.1 %	43.4 %

[a] Percentage reduction in relative risk (RR) for patient survival time of a particular MMP when calculated in the presence of S100P or S100A4. Taken from Table 6.4.
[b] Matrix metalloproteinase: MMP-2, MMP-9 or MMP-13.
[c] Metastasis-inducing proteins S100P or S100A4.

7.1.5 Role of RAGE receptor in mediating S100 protein interaction with MMPs

The most common cell surface receptor reported to be involved with S100 proteins and their cell signalling is RAGE (**Section 1.5.2**). When different doses of S100P were added to R37 wt cells, they showed a corresponding response in MMP-9 in the range 0 – 1 μM with half maximum at 4 nM (**Figure 5.9**). These results raised the possibility that a cell surface receptor was involved, and it was found that R37-S100P or -S100A4 expressed significantly higher levels of RAGE than the still appreciable levels found in R37 wt cells (**Figure 5.5**). The reasons for this increase are unknown. When the RAGE receptor was inhibited by its neutralizing antibody, the S100P/A4 stimulatory effect on cell invasion was reduced somewhat, either when the S100 proteins were produced intracellularly or added extracellularly to the R37 transfectant or wt cells, respectively (**Figure 5.7** and **5.8**). This result suggested that the RAGE receptor was partially responsible for the S100-induced system that leads to increased cell invasion, either when the S100 proteins were produced intracellularly or added from the outside. When the RAGE receptor was inhibited in the R37 cells with S100P or S100A4 being added externally, cell invasion was reduced by about 80 % and 45 %, respectively (**Figure 5.6** and **5.7**). However, when the RAGE receptor was inhibited in stably transfected R37-S100P and R37-S100A4 cells, cell invasion was reduced by about 8 % and 83 %, respectively (**Figure 4.5** and **5.8**). These results suggested that the extent of interaction of RAGE with the S100 proteins was not the same for S100P and S100A4, and that the source of the S100 proteins was important in generating the increase in cell invasion. In general, the RAGE-S100A4 interaction was a stronger influence on cell invasion than that of RAGE-S100P, either

when the S100 proteins were added extracellularly or expressed inside the cells. The exception was the comparative lack of effect of the antibody to RAGE on R37-S100P cells, producing only an 8 % reduction in cell invasion. These results may suggest that intracellular S100A4 works via the RAGE receptor in stimulating cell invasion, but intracellular S100P does not. How intracellular S100P/A4 can stimulate the cell surface RAGE receptor is unknown. Moreover, since neutralising antibodies only suppress the effect of extracellularly-added S100 proteins on cell invasion by 45-80%, it is possible that certain S100 proteins can utilize other cell surface receptors to generate the extra signals required for maximum cell invasion (e.g. Annexin II; Liu et al., 2015).

7.2 Novel conclusions

In vitro we demonstrated that MMP-2, -9 and -13 were the only MMPs expressed which showed activatable proteolytic activity in the R37 rat mammary cell lines. The elevated levels of these MMPs were dependent on S100P/A4 being present. MMPs were capable, at least in part, of controlling the migratory and invasive abilities of these cultured cells. Both intracellularly synthesised and extracellularly-added S100P/A4 could be partially inhibited by anti-RAGE sera in their effect on cell invasion. This result suggests that the RAGE receptor was involved, as reported previously (**Section 1.5**), to vary degrees in delivering the intracellular signals for cell invasion. In primary breast tumours S100P/A4 and these 3 MMPs were individually associated with a higher risk of death of the breast cancer patients. The associations between individual S100 proteins and MMPs established in cultured cells was largely replicated in clinical specimens *in vivo*. The new confounding effect of

S100P/A4 on RR of individual MMPs suggested that the pathways associated with patient death for MMP-13 overlapped more with S100P and those for MMP-2 more with S100A4, consistent with MMP knock-down experiments on cell invasion in our cultured cells (**Chapter 5**). Since MMP-13 works more to unwind collagen I before the other MMPs can digest it further (eg. MMP-2 and MMP-9) (**Sections 1.3.2**and **3.1**), there may be a requirement for both types of MMP in human breast cancer, consistent with the synergistic effect of S100P and S100A4 on enhancing premature death of breast cancer patents (Wang et al., 2006).

7.3 Future work

- **Tubulin target in Cos-7 cells**

Since the major intracellular target for S100P/A4 proteins is nonmuscle myosin IIA (NMIIA) (Du et al., 2012; Kiss et al., 2016), it is not clear if S100P/A4 can initiate the changes in MMPs inside and even outside the cells, either in whole or in part, by binding solely to this component. To investigate whether this is a necessary first step, a monkey kidney Cos-7 cell line devoid of NMIIA will be utilised (Rai et al., 2017). In the past the S100P-NMIIA interaction has been studied *in vitro* using the inducible HeLa-A3 and R37-T25 cell lines (Du et al., 2012). In these systems, overexpression of S100P was shown to lead to a reduction in polymerised NMIIA (actomyosin fibers) and focal adhesions which, in turn, increased their ability to reduce anchoring forces and increase cell migration and invasion. Recently the equivalent S100P-inducible cell line has been produced from these NMIIA-deficient Cos-7 cells (Du et al., 2015). In these cells, S100P has been shown to interact with tubulin and to alter its dynamics of polymerisation, as well as stimulating cell migration (Du et al., 2015). The interaction between tubulin and S100P can be blocked by a specific peptide in the test tube. When this peptide is attached to a suitable signal sequence, it can penetrate these cells and inhibit cell migration, so demonstrating the importance of the S100P-tubulin interaction in promoting cell migration, independently of NMIIA, in these Cos-7 cells (Du et al., 2015).

My aim would be: firstly, to see if the same MMPs and cell invasion, as described in my thesis for the rat mammary cell line, are induced in these S100P-inducible Cos-7 cells. Secondly, to use the S100P-tubulin inhibitory peptide to

test whether both MMP production and cell invasion are inhibited. Thirdly, to see if addition of S100P/A4 extracellularly to Cos-7 parental cells also stimulates MMP production and invasion, and whether these events can be inhibited by the same tubulin-blocking peptide. If successful, these results should identify the same or different MMPs induced by S100P in the Cos-7 monkey kidney cells, and link them to cell invasion, so as to generalise my results obtained from rat mammary cells. Secondly, they would demonstrate that intracellular S100P can interact with tubulin rather than NMIIA, to induce MMPs and cell invasion in the Cos-7 cells. Thirdly, when applied from the outside to investigate whether S100P/A4 can still stimulate, or not as the case may be, induction of MMPs and cell invasion, and if they do, whether the extracellular addition of S100P/A4 still requires their binding to the cytoskeletal component, tubulin inside the cell, at least in Cos-7 cells.

In this way I should be able to dissect out in more detail S100P/A4-induced intracellular pathways that may lead to increases in MMPs and in cell invasion in Cos-7 cells. With further experimentation along similar lines in the original rat mammary cells, I should then be able to define the relative contribution of differing pathways involving NMIIA, tubulin, RAGE and indeed any other receptor which may further the S100P/A4 induction of MMPs and cell invasion, all in one cell system. In this way I should be able to clarify what are completely confusing studies reported in the literature at present regarding a plethora of targets for the S100 proteins in entirely different cell systems (Gross et al., 2014).

- **Stromal-epithelial interactions**

At a more general level, the abnormal **tumour microenvironment** (TME) which surrounds growing tumours can facilitate their development, progress and even their drug resistance (McCuaig et al., 2017). However, how these mechanisms work is still largely unknown (McCuaig et al., 2017). Moreover, patient profiling strategies for cancer-drug treatments, immunotherapy and the use of biomarkers requires a thorough understanding of both compartments of the tumour: the epithelial tissue and the TME, and how they interact in the development of the cancer. The TME contains cells of mesenchymal and haematopoietic origin, as well as noncellular components. Most mesenchymal cells in the TME are fibroblasts-myofibroblasts and the noncellular insoluble component is the extracellular matrix (ECM), largely consisting of collagens and to a lesser extent of proteoglycans and glycoproteins.

The purpose of possible future work would be to investigate the interactions between the surrounding TME and the carcinoma cells and how they facilitate cell invasion. I have recently been introduced to the chick embryo model, whereby cancer cells can be implanted on the chick chorioallantoic membrane and allowed to grow into a tumour and invade, while the embryo itself develops in a relatively immune-supressed environment (Ribatti, 2016). This could be an ideal model to study a reconstituted host cell and cancer cell interaction, since the development of the tumour as it invades can be followed for up to 14 days in the egg, using a variety of detection systems.

For example, I could transplant fibroblasts from different sources e.g. fibroblasts from normal breast tissue and myofibroblasts from breast cancer

(Chatterjee et al., 2018) with breast cancer cell lines, with the aim of determining whether the source of fibroblasts alters invasive capacity of the carcinoma cells. Once I have identified that there were differences in the fibroblasts from different sources as already recorded by others (Chatterjee et al., 2018), I could then screen for differentially-expressed mRNAs using standard high-through-put nucleotide-sequencing systems. I could then select those differentially expressed genes, that seemed appropriate for further study; in my case perhaps focussing on the degradative proteinases. By a combination of knock-in and knock-out experiments, I could then go on to identify invasion-enhancing genes for the carcinoma cells, first of all screening in a Matrigel/Boyden chamber assay, and then in the chick embryo system. In this way I should be able to identify invasion-stimulatory factors in the cancer fibroblasts, hopefully relating to collagen-degradative enzymes of the ECM, like the MMPs. A similar series of experiments could then identify the agents produced by the cancer cells that impinge on the fibroblasts to stimulate their release of invasion-stimulating factors like the MMPs. Since S100 proteins are some of the most abundant proteins produced by cancer cells (Bresnick et al., 2015), it is possible that their release from the carcinoma cell, may be the trigger, in turn, for the fibroblasts to release MMPs. In this way I may be able to identify some of the cross-talk necessary at the molecular level between the ECM and the carcinoma cells for cancer invasion that my studies of the extracellular effects of S100P/A4 on MMPs and cell invasion have suggested in the homogeneous rat mammary epithelial cell system used in this thesis.

References

Ahokas, K., Lohi, J., Lohi, H., Elomaa, O., Karjalainen-Lindsberg, M.L., Kere, J., Saarialho-Kere, U., 2002. Matrix metalloproteinase-21, the human orthologue for XMMP, is expressed during fetal development and in cancer. Gene 301, 31–41. https://doi.org/10.1016/S0378-1119(02)01088-0

Al-Mehdi, a B., Tozawa, K., Fisher, a B., Shientag, L., Lee, a, Muschel, R.J., 2000. Intravascular origin of metastasis from the proliferation of endothelium-attached tumor cells: a new model for metastasis. Nat. Med. 6, 100–102. https://doi.org/10.1038/71429

Ambartsumian, N., Klingelhöfer, J., Grigorian, M., Christensen, C., Kriajevska, M., Tulchinsky, E., Georgiev, G., Berezin, V., Bock, E., Rygaard, J., Cao, R., Cao, Y., Lukanidin, E., 2001. The metastasis-associated Mts1(S100A4) protein could act as an angiogenic factor. Oncogene 20, 4685–95. https://doi.org/10.1038/sj.onc.1204636

Ambartsumian, N.S., Grigorian, M.S., Larsen, I.F., Karlstrøm, O., Sidenius, N., Rygaard, J., Georgiev, G., Lukanidin, E., 1996. Metastasis of mammary carcinomas in GRS/A hybrid mice transgenic for the mts1 gene. Oncogene 13, 1621–30.

Ameyar-Zazoua, M., Guasconi, V., Ait-Si-Ali, S., 2005. siRNA as a route to new cancer therapies. Expert Opin. Biol. Ther. 5, 221–4. https://doi.org/10.1517/14712598.5.2.221

Andersen, K., Mori, H., Fata, J., Bascom, J., Oyjord, T., Mælandsmo, G.M., Bissell, M., 2011. The metastasis-promoting protein S100A4 regulates mammary branching morphogenesis. Dev. Biol. 352, 181–90. https://doi.org/10.1016/j.ydbio.2010.12.033

Armstrong, D.G., Jude, E.B., 2002. The role of matrix metalloproteinases in wound healing. J. Am. Podiatr. Med. Assoc. 92, 12–8.

Arumugam, T., Logsdon, C.D., 2011. S100P: A novel therapeutic target for cancer. Amino Acids 41, 893–899. https://doi.org/10.1007/s00726-010-0496-4

Arumugam, T., Ramachandran, V., Gomez, S.B., Schmidt, A.M., Logsdon, C.D., 2012. S100P-derived RAGE antagonistic peptide reduces tumor growth and metastasis. Clin. Cancer Res. 18, 4356–4364. https://doi.org/10.1158/1078-

0432.CCR-12-0221

Arumugam, T., Ramachandran, V., Logsdon, C.D., 2006. Effect of cromolyn on S100P interactions with RAGE and pancreatic cancer growth and invasion in mouse models. J. Natl. Cancer Inst. 98, 1806–1818. https://doi.org/10.1093/jnci/djj498

Arumugam, T., Simeone, D.M., Schmidt, A.M., Logsdon, C.D., 2004. S100P Stimulates Cell Proliferation and Survival via Receptor for Activated Glycation End Products (RAGE). J. Biol. Chem. 279, 5059–5065. https://doi.org/10.1074/jbc.M310124200

Avrameas, S., Ternynck, T., 1998. Enzyme-Linked Immunosorbent Assay (ELISA), in: Encyclopedia of Immunology. Elsevier, pp. 816–819. https://doi.org/10.1006/rwei.1999.0216

Badiga, A.V., Chetty, C., Kesanakurti, D., Are, D., Gujrati, M., Klopfenstein, J.D., Dinh, D.H., Rao, J.S., 2011. MMP-2 siRNA inhibits radiation-enhanced invasiveness in glioma cells. PLoS One 6, e20614. https://doi.org/10.1371/journal.pone.0020614

Baig, M.S., Yaqoob, U., Cao, S., Saqib, U., Shah, V.H., 2016. Non-canonical role of matrix metalloprotease (MMP) in activation and migration of hepatic stellate cells (HSCs). Life Sci. 155, 155–160. https://doi.org/10.1016/j.lfs.2016.04.031

Balduyck, M., Zerimech, F., Gouyer, V., Lemaire, R., Hemon, B., Grard, G., Thiebaut, C., Lemaire, V., Dacquembronne, E., Duhem, T., Lebrun, a, Dejonghe, M.J., Huet, G., 2000. Specific expression of matrix metalloproteinases 1, 3, 9 and 13 associated with invasiveness of breast cancer cells in vitro. Clin. Exp. Metastasis 18, 171–178. https://doi.org/10.1023/A:1006762425323

Barraclough, R., Kimbell, R., Rudland, P.S., 1984. Increased abundance of a normal cell mRNA sequence accompanies the conversion of rat mammary cuboidal epithelial cells to elongated myoepithellal-llke cells in culture. Nucleic Acids Res. 12, 8097–8114. https://doi.org/10.1093/nar/12.21.8097

Barry, S., Chelala, C., Lines, K., Sunamura, M., Wang, A., Marelli-Berg, F.M., Brennan, C., Lemoine, N.R., Crnogorac-Jurcevic, T., 2013. S100P is a metastasis-associated gene that facilitates transendothelial migration of pancreatic cancer cells. Clin. Exp. Metastasis 30, 251–64. https://doi.org/10.1007/s10585-012-9532-y

Barsky, S.H., Siegal, G.P., Jannotta, F., Liotta, L.A., 1983. Loss of basement membrane

components by invasive tumors but not by their benign counterparts. Lab. Invest. 49, 140–7.

Basu, G.D., Azorsa, D.O., Kiefer, J.A., Rojas, A.M., Tuzmen, S., Barrett, M.T., Trent, J.M., Kallioniemi, O., Mousses, S., 2008. Functional evidence implicating S100P in prostate cancer progression. Int. J. Cancer 123, 330–339. https://doi.org/10.1002/ijc.23447

Becker, T., Gerke, V., Kube, E., Weber, K., 1992. S100P, a novel Ca2+-binding protein from human placenta. cDNA cloning, recombinant protein expression and Ca2+ binding properties. Eur. J. Biochem. 207, 541–547. https://doi.org/10.1111/j.1432-1033.1992.tb17080.x

Bell, G., 2016. Quantifying western blots: None more black. BMC Biol. 14, 116. https://doi.org/10.1186/s12915-016-0339-1

Berge, G., Mælandsmo, G.M., 2011. Evaluation of potential interactions between the metastasis-associated protein S100A4 and the tumor suppressor protein p53. Amino Acids 41, 863–873. https://doi.org/10.1007/s00726-010-0497-3

Birkedal-Hansen, H., 1995. Proteolytic remodeling of extracellular matrix. Curr. Opin. Cell Biol. 7, 728–735. https://doi.org/10.1016/0955-0674(95)80116-2

Bjørnland, K., Winberg, J.O., Ødegaard, O.T., Hovig, E., Loennechen, T., Aasen, A.O., Fodstad, Ø., Mælandsmo, G.M., 1999. S100A4 involvement in metastasis: Deregulation of matrix metalloproteinases and tissue inhibitors of matrix metalloproteinases in osteosarcoma cells transfected with an anti-S100A4 ribozyme. Cancer Res. 59, 4702–4708. https://doi.org/10.1002/jcb.240560106

Boon, L., Ugarte-Berzal, E., Vandooren, J., Opdenakker, G., 2016. Glycosylation of matrix metalloproteases and tissue inhibitors: present state, challenges and opportunities. Biochem. J. 473, 1471–82. https://doi.org/10.1042/BJ20151154

Bopp, C., Bierhaus, A., Hofer, S., Bouchon, A., Nawroth, P.P., Martin, E., Weigand, M.A., 2008. Bench-to-bedside review: The inflammation-perpetuating pattern-recognition receptor RAGE as a therapeutic target in sepsis. Crit. Care 12, 201. https://doi.org/10.1186/cc6164

Bowers, R.R., Manevich, Y., Townsend, D.M., Tew, K.D., 2012. Sulfiredoxin redox-sensitive interaction with S100A4 and non-muscle myosin IIA regulates cancer cell motility. Biochemistry 51, 7740–7754. https://doi.org/10.1021/bi301006w

Boye, K., Grotterød, I., Aasheim, H.-C., Hovig, E., Maelandsmo, G.M., 2008. Activation of NF-κB by extracellular S100A4: Analysis of signal transduction mechanisms and identification of target genes. Int. J. Cancer 123, 1301–1310. https://doi.org/10.1002/ijc.23617

Boye, K., Maelandsmo, G.M., 2010. S100A4 and metastasis: a small actor playing many roles. Am. J. Pathol. 176, 528–35. https://doi.org/10.2353/ajpath.2010.090526

Bresnick, A.R., Weber, D.J., Zimmer, D.B., 2015. S100 proteins in cancer. Nat. Rev. Cancer 15, 96–109. https://doi.org/10.1038/nrc3893

Brett, J., Schmidt, A.M., Yan, S.D., Zou, Y.S., Weidman, E., Pinsky, D., Nowygrod, R., Neeper, M., Przysiecki, C., Shaw, A., 1993. Survey of the distribution of a newly characterized receptor for advanced glycation end products in tissues. Am. J. Pathol. 143, 1699–712.

Brünner, N., Pyke, C., Hansen, C.H., Rømer, J., Grøndahl-Hansen, J., Danø, K., 1994. Urokinase plasminogen activator (uPA) and its type 1 inhibitor (PAI-1): regulators of proteolysis during cancer invasion and prognostic parameters in breast cancer. Cancer Treat. Res. 71, 299–309.

Bulk, E., Hascher, A., Liersch, R., Mesters, R.M., Diederichs, S., Sargin, B., Gerke, V., Hotfilder, M., Vormoor, J., Berdel, W.E., Serve, H., Müller-Tidow, C., 2008. Adjuvant therapy with small hairpin RNA interference prevents non-small cell lung cancer metastasis development in mice. Cancer Res. 68, 1896–1904. https://doi.org/10.1158/0008-5472.CAN-07-2390

Cancer Facts & Figures 2014 [WWW Document], n.d. URL http://www.cancer.org/research/cancerfactsstatistics/cancerfactsfigures2014/ (accessed 5.27.15).

Cathcart, J., Pulkoski-Gross, A., Cao, J., 2015. Targeting matrix metalloproteinases in cancer: Bringing new life to old ideas. Genes Dis. 2, 26–34. https://doi.org/10.1016/j.gendis.2014.12.002

Chambers, A.F., Matrisian, L.M., 1997. Changing views of the role of matrix metalloproteinases in metastasis. JNCI J. Natl. Cancer Inst. 89, 1260–1270. https://doi.org/10.1093/jnci/89.17.1260

Chatterjee, S., Basak, P., Buchel, E., Safneck, J., Murphy, L.C., Mowat, M., Kung, S.K.,

Eirew, P., Eaves, C.J., Raouf, A., 2018. Breast Cancers Activate Stromal Fibroblast-Induced Suppression of Progenitors in Adjacent Normal Tissue. Stem Cell Reports 10, 196–211. https://doi.org/10.1016/j.stemcr.2017.11.002

Chen, D., Zheng, X.F., Yang, Z.Y., Liu, D.X., Zhang, G.Y., Jiao, X.L., Zhao, H., 2012. S100A4 silencing blocks invasive ability of esophageal squamous cell carcinoma cells. World J. Gastroenterol. 18, 915–922. https://doi.org/10.3748/wjg.v18.i9.915

Chen, Y., Tseng, S.H., 2012. The potential of RECK inducers as antitumor agents for glioma. Anticancer Res. 32, 2991–2998.

Chen, Y., Wang, X., Chen, G., Dong, C., Zhang, D., 2015. The impact of matrix metalloproteinase 2 on prognosis and clinicopathology of breast cancer patients: A systematic meta-analysis. PLoS One 10, e0121404. https://doi.org/10.1371/journal.pone.0121404

Chuah, Y.K., Basir, R., Talib, H., Tie, T.H., Nordin, N., 2013. Receptor for advanced glycation end products and its involvement in inflammatory diseases. Int. J. Inflam. 2013, 403460. https://doi.org/10.1155/2013/403460

Chung, L., Dinakarpandian, D., Yoshida, N., Layer-Fields, J.L., Fields, G.B., Visse, R., Nagase, H., 2004. Collagenase unwinds triple-helical collagen prior to peptide bond hydrolysis. EMBO J. 23, 3020–3030. https://doi.org/10.1038/sj.emboj.7600318

Cipollone, F., Iezzi, A., Fazia, M., Zucchelli, M., Pini, B., Cuccurullo, C., De Cesare, D., De Blasis, G., Muraro, R., Bei, R., Chiarelli, F., Schmidt, A.M., Cuccurullo, F., Mezzetti, A., 2003. The receptor RAGE as a progression factor amplifying arachidonate-dependent inflammatory and proteolytic response in human atherosclerotic plaques: Role of glycemic control. Circulation 108, 1070–1077. https://doi.org/10.1161/01.CIR.0000086014.80477.0D

Clarke, C., Gross, S.R., Ismail, T.M., Rudland, P.S., Al-Medhtiy, M., Santangeli, M., Barraclough, R., 2017. Activation of tissue plasminogen activator by metastasis-inducing S100P protein. Biochem. J. 474, 3227–3240. https://doi.org/10.1042/BCJ20170578

Clarke, C., Rudland, P., Barraclough, R., 2015. The metastasis-inducing protein AGR2 is O-glycosylated upon secretion from mammary epithelial cells. Mol. Cell.

Biochem. 408, 245–252. https://doi.org/10.1007/s11010-015-2502-3

Cowell, S., Knäuper, V., Stewart, M.L., D'Ortho, M.P., Stanton, H., Hembry, R.M., López-Otín, C., Reynolds, J.J., Murphy, G., 1998. Induction of matrix metalloproteinase activation cascades based on membrane-type 1 matrix metalloproteinase: associated activation of gelatinase A, gelatinase B and collagenase 3. Biochem. J. 331 (Pt 2, 453–458.

Crawford, H.C., Matrisian, L.M., 1996. Mechanisms controlling the transcription of matrix metalloproteinase genes in normal and neoplastic cells. Enzyme Protein 49, 20–37.

da Silva, F.S., Araujo, D.N., Lima, J.P.M.S., de Rezende, A.A., da Graça Azevedo Abreu, B.J., Dias, F.A.L., 2014. Análise da atividade enzimática de MMP-2 e 9 coletadas por swab em úlcera venosa de membro inferior. J. Vasc. Bras. 13, 229–234. https://doi.org/10.1590/jvb.2014.038

Dahlmann, M., Okhrimenko, A., Marcinkowski, P., Osterland, M., Herrmann, P., Smith, J., Heizmann, C.W., Schlag, P.M., Stein, U., 2014. RAGE mediates S100A4-induced cell motility via MAPK/ERK and hypoxia signaling and is a prognostic biomarker for human colorectal cancer metastasis. Oncotarget 5, 3220–33. https://doi.org/10.18632/oncotarget.1908

Dahlmann, M., Sack, U., Herrmann, P., Lemm, M., Fichtner, I., Schlag, P.M., Stein, U., 2012. Systemic shRNA mediated knock down of S100A4 in colorectal cancer xenografted mice reduces metastasis formation. Oncotarget 3, 783–97. https://doi.org/10.18632/oncotarget.572

Dakhel, S., Padilla, L., Adan, J., Masa, M., Martinez, J.M., Roque, L., Coll, T., Hervas, R., Calvis, C., Messeguer, R., Mitjans, F., Hernández, J.L., 2014. S100P antibody-mediated therapy as a new promising strategy for the treatment of pancreatic cancer. Oncogenesis 3, e92–e92. https://doi.org/10.1038/oncsis.2014.7

Davies, B.R., Davies, M.P., Gibbs, F.E., Barraclough, R., Rudland, P.S., 1993. Induction of the metastatic phenotype by transfection of a benign rat mammary epithelial cell line with the gene for p9Ka, a rat calcium-binding protein, but not with the oncogene EJ-ras-1. Oncogene 8, 999–1008.

Davies, M.P., Rudland, P.S., Robertson, L., Parry, E.W., Jolicoeur, P., Barraclough, R., 1996. Expression of the calcium-binding protein S100A4 (p9Ka) in MMTV-neu

transgenic mice induces metastasis of mammary tumours. Oncogene 13, 1631–7.

de Silva Rudland, S., Martin, L., Roshanlall, C., Winstanley, J., Leinster, S., Platt-Higgins, A., Carroll, J., West, C., Barraclough, R., Rudland, P., 2006. Association of S100A4 and osteopontin with specific prognostic factors and survival of patients with minimally invasive breast cancer. Clin. Cancer Res. 12, 1192–1200. https://doi.org/10.1158/1078-0432.CCR-05-1580

de Silva Rudland, S., Platt-Higgins, A., Winstanley, J.H.R., Jones, N.J., Barraclough, R., West, C., Carroll, J., Rudland, P.S., 2011. Statistical Association of Basal Cell Keratins with Metastasis-Inducing Proteins in a Prognostically Unfavorable Group of Sporadic Breast Cancers. Am. J. Pathol. 179, 1061–1072. https://doi.org/10.1016/j.ajpath.2011.04.022

Deane, R., Yan, S. Du, Submamaryan, R.K., LaRue, B., Jovanovic, S., Hogg, E., Welch, D., Manness, L., Lin, C., Yu, J., Zhu, H., Ghiso, J., Frangione, B., Stern, A., Schmidt, A.M., Armstrong, D.L., Arnold, B., Liliensiek, B., Nawroth, P., Hofman, F., Kindy, M., Stern, D., Zlokovic, B., 2003. RAGE mediates amyloid-β peptide transport across the blood-brain barrier and accumulation in brain. Nat. Med. 9, 907–913. https://doi.org/10.1038/nm890

Deloulme, J.C., Mbele, G.O., Baudier, J., 2002. S100 proteins. From purification to functions. Methods Mol. Biol. 172, 185–98. https://doi.org/10.1385/1-59259-183-3:185

Ding, Q., Chang, C.-J., Xie, X., Xia, W., Yang, J.-Y., Wang, S.-C., Wang, Y., Xia, J., Chen, L., Cai, C., Li, H., Yen, C.-J., Kuo, H.-P., Lee, D.-F., Lang, J., Huo, L., Cheng, X., Chen, Y.-J., Li, C.-W., Jeng, L.-B., Hsu, J.L., Li, L.-Y., Tan, A., Curley, S.A., Ellis, L.M., DuBois, R.N., Hung, M.-C., 2011. APOBEC3G promotes liver metastasis in an orthotopic mouse model of colorectal cancer and predicts human hepatic metastasis. J. Clin. Invest. 121, 4526–4536. https://doi.org/10.1172/JCI45008

Donato, R., 2003. Intracellular and extracellular roles of S100 proteins. Microsc. Res. Tech. 60, 540–551. https://doi.org/10.1002/jemt.10296

Donato, R., Cannon, B.R., Sorci, G., Riuzzi, F., Hsu, K., Weber, D.J., Geczy, C.L., 2013. Functions of S100 proteins. Curr. Mol. Med. 13, 24–57.

Dong, L., Wang, F., Yin, X., Chen, L., Li, G., Lin, F., Ni, W., Wu, J., Jin, R., Jiang, L., 2014.

Overexpression of S100P promotes colorectal cancer metastasis and decreases chemosensitivity to 5-FU in vitro. Mol. Cell. Biochem. 389, 257–264. https://doi.org/10.1007/s11010-013-1947-5

Du, M., Wang, G., Barraclough, R., Rudland, P., 2015. P0017 S100P regulates cytoskeleton dynamics to promote cell migration and metastasis. Eur. J. Cancer 51, e6–e7. https://doi.org/10.1016/j.ejca.2015.06.022

Du, M., Wang, G., Ismail, T.M., Gross, S., Fernig, D.G., Barraclough, R., Rudland, P.S., 2012. S100P dissociates myosin IIA filaments and focal adhesion sites to reduce cell adhesion and enhance cell migration. J. Biol. Chem. 287, 15330–15344. https://doi.org/10.1074/jbc.M112.349787

Dunnington, D.J., Hughes, C.M., Monaghan, P., Rudland, P.S., 1983. Phenotypic instability of rat mammary tumor epithelial cells. J. Natl. Cancer Inst. 71, 1227–40.

Dunnington, D.J., Hughes, C.M., Monaghan, P., Rudland, P.S., 1983. Phenotypic instability of rat mammary tumor epithelial cells. J. Natl. Cancer Inst. 71, 1227–1240. https://doi.org/10.1093/jnci/71.6.1227

Egeland, E.V., Boye, K., Park, D., Synnestvedt, M., Sauer, T., Sauer, T., Geisler, J., Hofvind, S., Bathen, T.F., Borgen, E., Børresen-Dale, A.L., Engebråten, O., Fodstad, Ø., Garred, Ø., Geitvik, G.A., Kåresen, R., Naume, B., Mælandsmo, G.M., Russnes, H.G., Schlichting, E., Sørlie, T., Lingjærde, O.C., Kristensen, V.N., Sahlberg, K.K., Skjerven, H.K., Fritzman, B., Naume, B., Borgen, E., Mælandsmo, G.M., 2017. Prognostic significance of S100A4-expression and subcellular localization in early-stage breast cancer. Breast Cancer Res. Treat. 162, 127–137. https://doi.org/10.1007/s10549-016-4096-1

Elbashir, S.M., Harborth, J., Lendeckel, W., Yalcin, A., Weber, K., Tuschl, T., 2001. Duplexes of 21 ± nucleotide RNAs mediate RNA interference in cultured mammalian cells. Nature 411, 494–498. https://doi.org/10.1038/35078107

Engelholm, L.H., Nielsen, B.S., Netzel-Arnett, S., Solberg, H., Chen, X.D., Lopez Garcia, J.M., Lopez-Otin, C., Young, M.F., Birkedal-Hansen, H., Danø, K., Lund, L.R., Behrendt, N., Bugge, T.H., 2001. The urokinase plasminogen activator receptor-associated protein/endo180 is coexpressed with its interaction partners urokinase plasminogen activator receptor and matrix metalloprotease-13

during osteogenesis. Lab. Invest. 81, 1403–14.

Fan, C., Oh, D.S., Wessels, L., Weigelt, B., Nuyten, D.S. a, Nobel, A.B., van't Veer, L.J., Perou, C.M., 2006. Concordance among gene-expression-based predictors for breast cancer. N. Engl. J. Med. 355, 560–569. https://doi.org/10.1056/NEJMoa052933

Fei, F., Qu, J., Zhang, M., Li, Y., Zhang, S., Fei, F., Qu, J., Zhang, M., Li, Y., Zhang, S., Fei, F., Qu, J., Zhang, M., Zhang, Y.L. and S., 2017. S100A4 in cancer progression and metastasis: A systematic review. Oncotarget 8, 73219–73239. https://doi.org/10.18632/oncotarget.18016

Feng, G., Xu, X., Youssef, E.M., Lotan, R., 2001. Diminished expression of S100A2, a putative tumor suppressor, at early stage of human lung carcinogenesis. Cancer Res. 61, 7999–8004.

Fernández-Resa, P., Mira, E., Quesada, A.R., 1995. Enhanced detection of casein zymography of matrix metalloproteinases. Anal. Biochem. 224, 434–5.

Freije, J.M., Díez-Itza, I., Balbín, M., Sánchez, L.M., Blasco, R., Tolivia, J., López-Otín, C., 1994. Molecular cloning and expression of collagenase-3, a novel human matrix metalloproteinase produced by breast carcinomas. J. Biol. Chem. 269, 16766–73.

Fuentes, M.K., Nigavekar, S.S., Arumugam, T., Logsdon, C.D., Schmidt, A.M., Park, J.C., Huang, E.H., 2007. RAGE Activation by S100P in Colon Cancer Stimulates Growth, Migration, and Cell Signaling Pathways. Dis. Colon Rectum 50, 1230–1240. https://doi.org/10.1007/s10350-006-0850-5

Gabriely, G., Wurdinger, T., Kesari, S., Esau, C.C., Burchard, J., Linsley, P.S., Krichevsky, A.M., 2008. MicroRNA 21 Promotes Glioma Invasion by Targeting Matrix Metalloproteinase Regulators. Mol. Cell. Biol. 28, 5369–5380. https://doi.org/10.1128/MCB.00479-08

Goh Then Sin, C., Hersch, N., Rudland, P.S., Barraclough, R., Hoffmann, B., Gross, S.R., 2011. S100A4 downregulates filopodia formation through increased dynamic instability. Cell Adh. Migr. 5, 439–447. https://doi.org/10.4161/cam.5.5.17773

Gongoll, S., Peters, G., Mengel, M., Piso, P., Klempnauer, J., Kreipe, H., Von Wasielewski, R., 2002. Prognostic significance of calcium-binding protein S100A4 in colorectal cancer. Gastroenterology 123, 1478–1484.

https://doi.org/10.1053/gast.2002.36606

Gross, S.R., Sin, C.G.T., Barraclough, R., Rudland, P.S., 2014. Joining S100 proteins and migration: For better or for worse, in sickness and in health. Cell. Mol. Life Sci. 71, 1551–1579. https://doi.org/10.1007/s00018-013-1400-7

Guerreiro Da Silva, I.D., Hu, Y.F., Russo, I.H., Ao, X., Salicioni, A.M., Yang, X., Russo, J., 2000. S100P calcium-binding protein overexpression is associated with immortalization of human breast epithelial cells in vitro and early stages of breast cancer development in vivo. Int. J. Oncol. 16, 231–240. https://doi.org/10.3892/ijo.16.2.231

Hapangama, D.K., Raju, R.S., Valentijn, A.J., Barraclough, D., Hart, A., Turner, M.A., Platt-Higgins, A., Barraclough, R., Rudland, P.S., 2012. Aberrant expression of metastasis-inducing proteins in ectopic and matched eutopic endometrium of women with endometriosis: implications for the pathogenesis of endometriosis. Hum. Reprod. 27, 394–407. https://doi.org/10.1093/humrep/der412

Heizmann, C.W., Ackermann, G.E., Galichet, a, 2007. Pathologies involving the S100 proteins and RAGE. Subcell. Biochem. 45, 93–138. https://doi.org/10.1007/s00432-011-1062-5

Hernández, J.L., Padilla, L., Dakhel, S., Coll, T., Hervas, R., Adan, J., Masa, M., Mitjans, F., Martinez, J.M., Coma, S., Rodríguez, L., Noé, V., Ciudad, C.J., Blasco, F., Messeguer, R., 2013. Therapeutic Targeting of Tumor Growth and Angiogenesis with a Novel Anti-S100A4 Monoclonal Antibody. PLoS One 8, e72480. https://doi.org/10.1371/journal.pone.0072480

Herwig, N., Belter, B., Wolf, S., Haase-Kohn, C., Pietzsch, J., 2016. Interaction of extracellular S100A4 with RAGE prompts prometastatic activation of A375 melanoma cells. J. Cell. Mol. Med. 20, 825–835. https://doi.org/10.1111/jcmm.12808

Hofmann, M.A., Drury, S., Fu, C., Qu, W., Taguchi, A., Lu, Y., Avila, C., Kambham, N., Bierhaus, A., Nawroth, P., Neurath, M.F., Slattery, T., Beach, D., McClary, J., Nagashima, M., Morser, J., Stern, D., Schmidt, A.M., 1999. RAGE mediates a novel proinflammatory axis: A central cell surface receptor for S100/calgranulin polypeptides. Cell 97, 889–901. https://doi.org/10.1016/S0092-8674(00)80801-6

Hofmann, M.A., Drury, S., Hudson, B.I., Gleason, M.R., Qu, W., Lu, Y., Lalla, E., Chitnis, S., Monteiro, J., Stickland, M.H., Bucciarelli, L.G., Moser, B., Moxley, G., Itescu, S., Grant, P.J., Gregersen, P.K., Stern, D.M., Schmidt, A.M., 2002. RAGE and arthritis: The G82S polymorphism amplifies the inflammatory response. Genes Immun. 3, 123–135. https://doi.org/10.1038/sj.gene.6363861

Hori, O., Brett, J., Slattery, T., Cao, R., Zhang, J., Jing Xian Chen, Nagashima, M., Lundh, E.R., Vijay, S., Nitecki, D., Morser, J., Stern, D., Schmidt, A.M., 1995. The receptor for advanced glycation end products (RAGE) is a cellular binding site for amphoterin. Mediation of neurite outgrowth and co-expression of RAGE and amphoterin in the developing nervous system. J. Biol. Chem. 270, 25752–25761. https://doi.org/10.1074/jbc.270.43.25752

Hornick, J.L., 2014. Novel uses of immunohistochemistry in the diagnosis and classification of soft tissue tumors. Mod. Pathol. 27, S47–S63. https://doi.org/10.1038/modpathol.2013.177

Hsieh, H.-L., Schäfer, B.W., Sasaki, N., Heizmann, C.W., 2003. Expression analysis of S100 proteins and RAGE in human tumors using tissue microarrays. Biochem. Biophys. Res. Commun. 307, 375–381. https://doi.org/10.1016/S0006-291X(03)01190-2

Hu, X., Beeton, C., 2010. Detection of Functional Matrix Metalloproteinases by Zymography. J. Vis. Exp. 1–5. https://doi.org/10.3791/2445

Huang, L., Xu, Y., Cai, G., Guan, Z., Cai, S., 2012. Downregulation of S100A4 expression by RNA interference suppresses cell growth and invasion in human colorectal cancer cells. Oncol. Rep. 27, 917–922. https://doi.org/10.3892/or.2011.1598

Ismail, T.M., Bennett, D., Platt-Higgins, A.M., Al-Medhity, M., Barraclough, R., Rudland, P.S., 2017. S100A4 elevation empowers expression of metastasis effector molecules in human breast cancer. Cancer Res. 77, 780–789. https://doi.org/10.1158/0008-5472.CAN-16-1802

Ismail, T.M., Fernig, D.G., Rudland, P.S., Terry, C.J., Wang, G., Barraclough, R., 2008. The basic C-terminal amino acids of calcium-binding protein S100A4 promote metastasis. Carcinogenesis 29, 2259–2266. https://doi.org/10.1093/carcin/bgn217

Ismail, T.M., Zhang, S., Fernig, D.G., Gross, S., Martin-Fernandez, M.L., See, V.,

Tozawa, K., Tynan, C.J., Wang, G., Wilkinson, M.C., Rudland, P.S., Barraclough, R., 2010. Self-association of Calcium-binding Protein S100A4 and Metastasis. J. Biol. Chem. 285, 914–922. https://doi.org/10.1074/jbc.M109.010892

Jenkinson, S.R., Barraclough, R., West, C.R., Rudland, P.S., 2004. S100A4 regulates cell motility and invasion in an in vitro model for breast cancer metastasis. Br. J. Cancer 90, 253–62. https://doi.org/10.1038/sj.bjc.6601483

Jessen, T.N., Jessen, J.R., 2017. VANGL2 interacts with integrin αv to regulate matrix metalloproteinase activity and cell adhesion to the extracellular matrix. Exp. Cell Res. 361, 265–276. https://doi.org/10.1016/j.yexcr.2017.10.026

Jia, W., Gao, X.J., Zhang, Z.D., Yang, Z.X., Zhang, G., 2013. S100A4 silencing suppresses proliferation, angiogenesis and invasion of thyroid cancer cells through downregulation of MMP-9 and VEGF. Eur. Rev. Med. Pharmacol. Sci. 17, 1495–1508.

Jiang, L., Lai, Y.-K., Zhang, J., Wang, H., Lin, M.C., He, M.-L., Kung, H.-F., 2011. Targeting S100P inhibits colon cancer growth and metastasis by Lentivirus-mediated RNA interference and proteomic analysis. Mol. Med. 17, 709–716. https://doi.org/10.2119/molmed.2011.00008

Jinga, D.C., Blidaru, A., Condrea, I., Ardeleanu, C., Dragomir, C., Szegli, G., Stefanescu, M., Matache, C., 2006. MMP-9 and MMP-2 gelatinases and TIMP-1 and TIMP-2 inhibitors in breast cancer: Correlations with prognostic factors. J. Cell. Mol. Med. 10, 499–510. https://doi.org/10.1111/j.1582-4934.2006.tb00415.x

Johansson, N., Vaalamo, M., Grénman, S., Hietanen, S., Klemi, P., Saarialho-Kere, U., Kähäri, V.M., 1999. Collagenase-3 (MMP-13) is expressed by tumor cells in invasive vulvar squamous cell carcinomas. Am. J. Pathol. 154, 469–80. https://doi.org/10.1016/S0002-9440(10)65293-5

Jones, G.T., 2014. Matrix Metalloproteinases in Biologic Samples, in: Advances in Clinical Chemistry. Elsevier, pp. 199–219. https://doi.org/10.1016/B978-0-12-800141-7.00007-3

Jung, N.R., 2016. Clarifying the legal ambiguity in article 2.2.2(III) of the anti-dumping agreement: A proposed set of interpretative guidelines for “Any other reasonable method.” Asian J. WTO Int. Heal. Law Policy 11, 369–394. https://doi.org/10.1088/1751-8113/44/8/085201

Kalea, A.Z., See, F., Harja, E., Arriero, M., Schmidt, A.M., Hudson, B.I., 2010. Alternatively sliced RAGEv1 inhibits tumorigenesis through suppression of JNK signaling. Cancer Res. 70, 5628–5638. https://doi.org/10.1158/0008-5472.CAN-10-0595

Kalluri, R., 2003. Basement membranes: Structure, assembly and role in tumour angiogenesis. Nat. Rev. Cancer 3, 422–433. https://doi.org/10.1038/nrc1094

Kang, R., Tang, D., Schapiro, N.E., Livesey, K.M., Farkas, A., Loughran, P., Bierhaus, A., Lotze, M.T., Zeh, H.J., 2010. The receptor for advanced glycation end products (RAGE) sustains autophagy and limits apoptosis, promoting pancreatic tumor cell survival. Cell Death Differ. 17, 666–676. https://doi.org/10.1038/cdd.2009.149

Ke, Y., Beesley, C., Smith, P., Barraclough, R., Rudland, P., Foster, C.S., 1998. Generation of metastatic variants by transfection of a rat non-metastatic epithelial cell line with genomic DNA from rat prostatic carcinoma cells. Br. J. Cancer 77, 287–296. https://doi.org/10.1038/bjc.1998.45

Kim, Y.H., Kwon, H.-J., Kim, D.-S., 2012. Matrix Metalloproteinase 9 (MMP-9)-dependent Processing of βig-h3 Protein Regulates Cell Migration, Invasion, and Adhesion. J. Biol. Chem. 287, 38957–38969. https://doi.org/10.1074/jbc.M112.357863

Kiss, B., Kalmár, L., Nyitray, L., Pál, G., 2016. Structural determinants governing S100A4-induced isoform-selective disassembly of nonmuscle myosin II filaments. FEBS J. 283, 2164–2180. https://doi.org/10.1111/febs.13728

Knäuper, V., López-Otin, C., Smith, B., Knight, G., Murphy, G., 1996. Biochemical characterization of human collagenase-3. J. Biol. Chem. 271, 1544–1550. https://doi.org/10.1074/jbc.271.3.1544

Knauper, V., Smith, B., Lopez-Otin, C., Murphy, G., 1997. Activation of Progelatinase B (proMMP-9) by Active Collagenase-3 (MMP-13). Eur. J. Biochem. 248, 369–373. https://doi.org/10.1111/j.1432-1033.1997.00369.x

Knauper, V., Will, H., Lopez-Otin, C., Smith, B., Atkinson, S.J., Stanton, H., Hembry, R.M., Murphy, G., 1996. Cellular Mechanisms for Human Procollagenase-3 (MMP-13) Activation. J. Biol. Chem. 271, 17124–17131. https://doi.org/10.1074/jbc.271.29.17124

Köhrmann, A., Kammerer, U., Kapp, M., Dietl, J., Anacker, J., 2009. Expression of matrix metalloproteinases (MMPs) in primary human breast cancer and breast cancer cell lines: New findings and review of the literature. BMC Cancer 9, 188. https://doi.org/10.1186/1471-2407-9-188

Kotepui, M., Punsawad, C., Chupeerach, C., Songsri, A., Charoenkijkajorn, L., Petmitr, S., 2016. Differential expression of matrix metalloproteinase-13 in association with invasion of breast cancer. Współczesna Onkol. 3, 225–228. https://doi.org/10.5114/wo.2016.61565

Kwak, T., Drews-Elger, K., Ergonul, A., Miller, P.C., Braley, A., Hwang, G.H., Zhao, D., Besser, A., Yamamoto, Y., Yamamoto, H., El-Ashry, D., Slingerland, J.M., Lippman, M.E., Hudson, B.I., 2017. Targeting of RAGE-ligand signaling impairs breast cancer cell invasion and metastasis. Oncogene 36, 1559–1572. https://doi.org/10.1038/onc.2016.324

Lamartina, S., Silvi, L., Roscilli, G., Casimiro, D., Simon, A.J., Davies, M.E., Shiver, J.W., Rinaudo, C.D., Zampaglione, I., Fattori, E., Colloca, S., Gonzalez Paz, O., Laufer, R., Bujard, H., Cortese, R., Ciliberto, G., Toniatti, C., 2003. Construction of an rtTA2s-M2/tTSkid-based transcription regulatory switch that displays no basal activity, good inducibility, and high responsiveness to doxycycline in mice and non-human primates. Mol. Ther. 7, 271–280. https://doi.org/10.1016/S1525-0016(02)00051-5

Lawrie, A., Spiekerkoetter, E., Martinez, E.C., Ambartsumian, N., Sheward, W.J., MacLean, M.R., Harmar, A.J., Schmidt, A.-M., Lukanidin, E., Rabinovitch, M., 2005. Interdependent serotonin transporter and receptor pathways regulate S100A4/Mts1, a gene associated with pulmonary vascular disease. Circ. Res. 97, 227–35. https://doi.org/10.1161/01.RES.0000176025.57706.1e

Leclerc, E., 2011. The importance of Ca2+/Zn2+ signaling S100 proteins and RAGE in translational medicine. Front. Biosci. S3, 1232. https://doi.org/10.2741/223

Leclerc, E., Fritz, G., Vetter, S.W., Heizmann, C.W., 2009. Binding of S100 proteins to RAGE: An update. Biochim. Biophys. Acta - Mol. Cell Res. 1793, 993–1007. https://doi.org/10.1016/j.bbamcr.2008.11.016

Leclerc, E., Vetter, S.W., 2015. The role of S100 proteins and their receptor RAGE in pancreatic cancer. Biochim. Biophys. Acta - Mol. Basis Dis. 1852, 2706–2711.

https://doi.org/10.1016/j.bbadis.2015.09.022

Leeman, M.F., Curran, S., Murray, G.I., 2002. The structure, regulation, and function of human matrix metalloproteinase-13. Crit. Rev. Biochem. Mol. Biol. 37, 149–166. https://doi.org/10.1080/10409230290771483

Leeman, M.F., McKay, J.A., Murray, G.I., 2002. Matrix metalloproteinase 13 activity is associated with poor prognosis in colorectal cancer. J. Clin. Pathol. 55, 758–762. https://doi.org/10.1136/jcp.55.10.758

Levett, D., Flecknell, P.A., Rudland, P.S., Barraclough, R., Neal, D.E., Mellon, J.K., Davies, B.R., 2002. Transfection of S100A4 produces metastatic variants of an orthotopic model of bladder cancer. Am. J. Pathol. 160, 693–700. https://doi.org/10.1016/S0002-9440(10)64889-4

Li, A.C.Y., 2003. Basement membrane components. J. Clin. Pathol. 56, 885–887. https://doi.org/10.1136/jcp.56.12.885

Li, H., Qiu, Z., Li, F., Wang, C., 2017. The relationship between MMP-2 and MMP-9 expression levels with breast cancer incidence and prognosis. Oncol. Lett. 14, 5865–5870. https://doi.org/10.3892/ol.2017.6924

Li, N., Song, M.M., Chen, X.H., Liu, L.H., Li, F.S., 2012. S100A4 siRNA inhibits human pancreatic cancer cell invasion in vitro. Biomed. Environ. Sci. 25, 465–70. https://doi.org/10.3967/0895-3988.2012.04.012

Li, Z.-H., Bresnick, A.R., 2006. The S100A4 metastasis factor regulates cellular motility via a direct interaction with myosin-IIA. Cancer Res. 66, 5173–80. https://doi.org/10.1158/0008-5472.CAN-05-3087

Lin, H. Bin, Cadete, V.J.J., Sra, B., Sawicka, J., Chen, Z., Bekar, L.K., Cayabyab, F., Sawicki, G., 2014. Inhibition of MMP-2 Expression with siRNA Increases Baseline Cardiomyocyte Contractility and Protects against Simulated Ischemic Reperfusion Injury. Biomed Res. Int. 2014, 1–11. https://doi.org/10.1155/2014/810371

Liotta, L.A., Tryggvason, K., Garbisa, S., Hart, I., Foltz, C.M., Shafie, S., 1980. Metastatic potential correlates with enzymatic degradation of basement membrane collagen. Nature 284, 67–68. https://doi.org/10.1038/284067a0

Liu, D., Rudland, P.S., Sibson, D.R., Platt-Higgins, A., Barraclough, R., 2005. Human homologue of cement gland protein, a novel metastasis inducer associated with

breast carcinomas. Cancer Res. 65, 3796–805. https://doi.org/10.1158/0008-5472.CAN-04-3823

Liu, D., Rudland, P.S., Sibson, D.R., Platt-Higgins, A., Barraclough, R., 2000. Expression of calcium-binding protein S100A2 in breast lesions. Br. J. Cancer 83, 1473–9. https://doi.org/10.1054/bjoc.2000.1488

Liu, Y., Myrvang, H.K., Dekker, L. V., 2015. Annexin A2 complexes with S100 proteins: Structure, function and pharmacological manipulation. Br. J. Pharmacol. 172, 1664–1676. https://doi.org/10.1111/bph.12978

Liu, Y., Wang, C., Shan, X., Wu, J., Liu, H., Liu, H., Zhang, J., Xu, W., Sha, Z., He, J., Fan, J., 2017. S100P is associated with proliferation and migration in nasopharyngeal carcinoma. Oncol. Lett. 14, 525–532. https://doi.org/10.3892/ol.2017.6198

Lloyd, B.H., Platt-Higgins, A., Rudland, P.S., Barraclough, R., 1998. Human S100A4 (p9Ka) induces the metastatic phenotype upon benign tumour cells. Oncogene 17, 465–73. https://doi.org/10.1038/sj.onc.1201948

Lombard, C., Saulnier, J., Wallach, J., 2005. Assays of matrix metalloproteinases (MMPs) activities: a review. Biochimie 87, 265–72. https://doi.org/10.1016/j.biochi.2005.01.007

Mackay, A., Jones, C., Dexter, T., Silva, R.L. a, Bulmer, K., Jones, A., Simpson, P., Harris, R. a, Jat, P.S., Neville, a M., Reis, L.F.L., Lakhani, S.R., O'Hare, M.J., 2003. cDNA microarray analysis of genes associated with ERBB2 (HER2/neu) overexpression in human mammary luminal epithelial cells. Oncogene 22, 2680–2688. https://doi.org/10.1038/sj.onc.1206349

Maelandsmo, G.M., Flørenes, V.A., Mellingsaeter, T., Hovig, E., Kerbel, R.S., Fodstad, O., 1997. Differential expression patterns of S100A2, S100A4 and S100A6 during progression of human malignant melanoma. Int. J. Cancer 74, 464–9.

Mahmood, T., Yang, P.C., 2012. Western blot: Technique, theory, and trouble shooting. N. Am. J. Med. Sci. 4, 429–434. https://doi.org/10.4103/1947-2714.100998

Makoukji, J., Makhoul, N.J., Khalil, M., El-Sitt, S., Aldin, E.S., Jabbour, M., Boulos, F., Gadaleta, E., Sangaralingam, A., Chelala, C., Boustany, R.M., Tfayli, A., 2016. Gene expression profiling of breast cancer in Lebanese women. Sci. Rep. 6, 1–13. https://doi.org/10.1038/srep36639

Maletzki, C., Bodammer, P., Breitruck, A., Kerkhoff, C., 2012. S100 proteins as diagnostic and prognostic markers in colorectal and hepatocellular carcinoma. Hepat. Mon. 12, e7240. https://doi.org/10.5812/hepatmon.7240

Mason, S.D., Joyce, J.A., 2011. Proteolytic networks in cancer. Trends Cell Biol. 21, 228–237. https://doi.org/10.1016/j.tcb.2010.12.002

Mcandrew, J., Fernig, D.G., Rudland, P.S., Smith, J.A., 1994. Secretion of transforming growth factor alpha and expression of its receptor in human mammary cell lines. Growth Factors 10, 281–287. https://doi.org/10.3109/08977199409010994

McCuaig, R., Wu, F., Dunn, J., Rao, S., Dahlstrom, J.E., 2017. The biological and clinical significance of stromal-epithelial interactions in breast cancer. Pathology 49, 133–140. https://doi.org/10.1016/j.pathol.2016.10.009

Mehner, C., Hockla, A., Miller, E., Ran, S., Radisky, D.C., Radisky, E.S., 2014. Tumor cell-produced matrix metalloproteinase 9 (MMP-9) drives malignant progression and metastasis of basal-like triple negative breast cancer. Oncotarget 5, 2736–2749. https://doi.org/10.18632/oncotarget.1932

Mercado-Pimentel, M.E., Onyeagucha, B.C., Li, Q., Pimentel, A.C., Jandova, J., Nelson, M.A., 2015. The S100P/RAGE signaling pathway regulates expression of microRNA-21 in colon cancer cells. FEBS Lett. 589, 2388–2393. https://doi.org/10.1016/j.febslet.2015.07.010

Mishra, S.K., Siddique, H.R., Saleem, M., 2012. S100A4 calcium-binding protein is key player in tumor progression and metastasis: Preclinical and clinical evidence. Cancer Metastasis Rev. 31, 163–172. https://doi.org/10.1007/s10555-011-9338-4

Moll, R., Franke, W.W., Schiller, D.L., 1982. The Catalog of Human Cytokeratins : Patterns of Expression in Normal Epithelia , Tumors and Cultured Cells. Cell 31, 11–24.

Moore, B.W., 1965. A soluble protein characteristic of the nervous system. Biochem. Biophys. Res. Commun. 19, 739–744. https://doi.org/10.1016/0006-291X(65)90320-7

Moravkova, P., Kohoutova, D., Rejchrt, S., Cyrany, J., Bures, J., 2016. Role of S100 Proteins in Colorectal Carcinogenesis. Gastroenterol. Res. Pract. 2016, 1–7. https://doi.org/10.1155/2016/2632703

Moutasim, K.A., Nystrom, M.L., Thomas, G.J., 2011. Cell migration and invasion assays., in: Methods in Molecular Biology (Clifton, N.J.). pp. 333–343. https://doi.org/10.1007/978-1-61779-080-5_27

Munesue, S., Yoshitomi, Y., Kusano, Y., Koyama, Y., Nishiyama, A., Nakanishi, H., Miyazaki, K., Ishimaru, T., Miyaura, S., Okayama, M., Oguri, K., 2007. A novel function of syndecan-2, suppression of matrix metalloproteinase-2 activation, which causes suppression of metastasis. J. Biol. Chem. 282, 28164–28174. https://doi.org/10.1074/jbc.M609812200

Nair, R.R., Solway, J., Boyd, D.D., 2006. Expression cloning identifies transgelin (SM22) as a novel repressor of 92-kDa type IV collagenase (MMP-9) expression. J. Biol. Chem. 281, 26424–26436. https://doi.org/10.1074/jbc.M602703200

Namba, T., Homan, T., Nishimura, T., Mima, S., Hoshino, T., Mizushima, T., 2009. Up-regulation of S100P Expression by Non-steroidal Anti-inflammatory Drugs and Its Role in Anti-tumorigenic Effects. J. Biol. Chem. 284, 4158–4167. https://doi.org/10.1074/jbc.M806051200

Nandakumar, M.P., Shen, J., Raman, B., Marten, M.R., 2003. Solubilization of Trichloroacetic Acid (TCA) Precipitated Microbial Proteins via NaOH for Two-Dimensional Electrophoresis. J. Proteome Res. 2, 89–93. https://doi.org/10.1021/pr025541x

Nasser, M.W., Wani, N.A., Ahirwar, D.K., Powell, C.A., Ravi, J., Elbaz, M., Zhao, H., Padilla, L., Zhang, X., Shilo, K., Ostrowski, M., Shapiro, C., Carson, W.E., Ganju, R.K., 2015. RAGE mediates S100A7-induced breast cancer growth and metastasis by modulating the tumor microenvironment. Cancer Res. 75, 974–985. https://doi.org/10.1158/0008-5472.CAN-14-2161

Nguyen, T.H., 2004. Mechanisms of metastasis. Clin. Dermatol. 22, 209–216. https://doi.org/10.1016/j.clindermatol.2003.12.007

Nielsen, B.S., Rank, F., López, J.M., Balbin, M., Vizoso, F., Lund, L.R., Danø, K., López-Otín, C., 2001. Collagenase-3 expression in breast myofibroblasts as a molecular marker of transition of ductal carcinoma in situ lesions to invasive ductal carcinomas. Cancer Res. 61, 7091–100.

Noda, M., Takahashi, C., 2007. Recklessness as a hallmark of aggressive cancer. Cancer Sci. 98, 1659–1665. https://doi.org/10.1111/j.1349-7006.2007.00588.x

Oates, A.J., Barraclough, R., Rudland, P.S., 1996. The identification of osteopontin as a metastasis-related gene product in a rodent mammary tumour model. Oncogene 13, 97–104.

Ogata, Y., Enghild, J.J., Nagase, H., 1992. Matrix metalloproteinase 3 (stromelysin) activates the precursor for the human matrix metalloproteinase 9. J. Biol. Chem. 267, 3581–4.

Okada, H., Danoff, T.M., Kalluri, R., Neilson, E.G., 1997. Early role of Fsp1 in epithelial-mesenchymal transformation. Am. J. Physiol. 273, F563–F574. https://doi.org/10.1016/0955-0674(93)90091-4

Okada, M., Tokumitsu, H., Kubota, Y., Kobayashi, R., 2002. Interaction of S100 proteins with the antiallergic drugs, olopatadine, amlexanox, and cromolyn: Identification of putative drug binding sites on S100A1 protein. Biochem. Biophys. Res. Commun. 292, 1023–1030. https://doi.org/10.1006/bbrc.2002.6761

Okada, Y., Gonoji, Y., Naka, K., Tomita, K., Nakanishi, I., Iwata, K., Yamashita, K., Hayakawa, T., 1992. Matrix metalloproteinase 9 (92-kDa gelatinase/type IV collagenase) from HT 1080 human fibrosarcoma cells. Purification and activation of the precursor and enzymic properties. J. Biol. Chem. 267, 21712–9.

Orgaz, J.L., Pandya, P., Dalmeida, R., Karagiannis, P., Sanchez-Laorden, B., Viros, A., Albrengues, J., Nestle, F.O., Ridley, A.J., Gaggioli, C., Marais, R., Karagiannis, S.N., Sanz-Moreno, V., 2014. Diverse matrix metalloproteinase functions regulate cancer amoeboid migration. Nat. Commun. 5, 4255. https://doi.org/10.1038/ncomms5255

Oyama, Y., Shishibori, T., Yamashita, K., Naya, T., Nakagiri, S., Maeta, H., Kobayashi, R., 1997. Two distinct anti-allergic drugs, amlexanox and cromolyn, bind to the same kinds of calcium binding proteins, except calmodulin, in bovine lung extract. Biochem. Biophys. Res. Commun. 240, 341–347. https://doi.org/10.1006/bbrc.1997.7476

Ozeki, N., Kawai, R., Yamaguchi, H., Hiyama, T., Kinoshita, K., Hase, N., Nakata, K., Kondo, A., Mogi, M., Nakamura, H., 2014. IL-1β-induced matrix metalloproteinase-13 is activated by a disintegrin and metalloprotease-28-regulated proliferation of human osteoblast-like cells. Exp. Cell Res. 323, 165–

177. https://doi.org/10.1016/j.yexcr.2014.02.018

Park, A.J., Matrisian, L.M., Kells, A.F., Pearson, R., Yuan, Z., Navre, M., 1991. Mutational analysis of the transin (rat stromelysin) autoinhibitor region demonstrates a role for residues surrounding the “cysteine switch.” J. Biol. Chem. 266, 1584–1590.

Peeters-Joris, C., Hammani, K., Singer, C.F., 1998. Differential regulation of MMP-13 (collagenase-3) and MMP-3 (stromelysin-1) in mouse calvariae. Biochim. Biophys. Acta - Mol. Cell Res. 1405, 14–28. https://doi.org/10.1016/S0167-4889(98)00094-9

Penumutchu, S.R., Chou, R.H., Yu, C., 2014. Structural insights into calcium-bound S100P and the V domain of the RAGE complex. PLoS One 9, e103947. https://doi.org/10.1371/journal.pone.0103947

Perrone, L., Peluso, G., Melone, M.A.B., 2008. RAGE recycles at the plasma membrane in S100B secretory vesicles and promotes Schwann cells morphological changes. J. Cell. Physiol. 217, 60–71. https://doi.org/10.1002/jcp.21474

Radia, A.-M., Yaser, A.-M., Ma, X., Zhang, J., Yang, C., Dong, Q., Rong, P., Ye, B., Liu, S., Wang, W., 2013. Specific siRNA Targeting Receptor for Advanced Glycation End Products (RAGE) Decreases Proliferation in Human Breast Cancer Cell Lines. Int. J. Mol. Sci. 14, 7959–7978. https://doi.org/10.3390/ijms14047959

Rai, V., Thomas, D.G., Beach, J.R., Egelhoff, T.T., 2017. Myosin IIA Heavy Chain Phosphorylation Mediates Adhesion Maturation and Protrusion in Three Dimensions. J. Biol. Chem. 292, 3099–3111. https://doi.org/10.1074/jbc.M116.733402

Ravanti, L., Heino, J., López-Otín, C., Kähäri, V.M., 1999. Induction of collagenase-3 (MMP-13) expression in human skin fibroblasts by three-dimensional collagen is mediated by p38 mitogen-activated protein kinase. J. Biol. Chem. 274, 2446–2455. https://doi.org/10.1074/jbc.274.4.2446

Rehbein, G., Simm, A., Hofmann, H.-S., Silber, R.-E., Bartling, B., 2008. Molecular regulation of S100P in human lung adenocarcinomas. Int. J. Mol. Med. 22, 69–77.

Ribatti, D., 2016. The chick embryo chorioallantoic membrane (CAM). A multifaceted experimental model. Mech. Dev. 141, 70–77.

https://doi.org/10.1016/j.mod.2016.05.003

Rizwan, A., Cheng, M., Bhujwalla, Z.M., Krishnamachary, B., Jiang, L., Glunde, K., 2015. Breast cancer cell adhesome and degradome interact to drive metastasis. npj Breast Cancer 1, 15017. https://doi.org/10.1038/npjbcancer.2015.17

Roomi, M.W., Monterrey, J.C., Kalinovsky, T., Rath, M., Niedzwiecki, A., 2010. In vitro modulation of MMP-2 and MMP-9 in human cervical and ovarian cancer cell lines by cytokines, inducers and inhibitors. Oncol. Rep. 23, 605–14.

Rudland, P.S., Leinster, S.J., Winstanley, J., Green, B., Atkinson, M., Zakhour, H.D., 1993. Immunocytochemical identification of cell types in benign and malignant breast diseases: Variations in cell markers accompany the malignant state. J. Histochem. Cytochem. 41, 543–553.

Rudland, P.S., Platt-Higgins, A., El-Tanani, M., De Silva Rudland, S., Barraclough, R., Winstanley, J.H.R., Howitt, R., West, C.R., 2002. Prognostic significance of the metastasis-associated protein osteopontin in human breast cancer. Cancer Res. 62, 3417–3427.

Rudland, P.S., Platt-Higgins, A., Renshaw, C., West, C.R., Winstanley, J.H.R., Robertson, L., Barraclough, R., 2000. Prognostic significance of the metastasis-inducing protein S100A4 (p9Ka) in human breast cancer. Cancer Res. 60, 1595–1603.

Sabattini, E., Bisgaard, K., Ascani, S., Poggi, S., Piccioli, M., Ceccarelli, C., Pieri, F., Fraternali-Orcioni, G., Pileri, S.A., 1998. The EnVision++ system: a new immunohistochemical method for diagnostics and research. Critical comparison with the APAAP, ChemMate, CSA, LABC, and SABC techniques. J. Clin. Pathol. 51, 506–11.

Sack, U., Walther, W., Scudiero, D., Selby, M., Aumann, J., Lemos, C., Fichtner, I., Schlag, P.M., Shoemaker, R.H., Stein, U., 2011. S100A4-induced cell motility and metastasis is restricted by the Wnt/ -catenin pathway inhibitor calcimycin in colon cancer cells. Mol. Biol. Cell 22, 3344–3354. https://doi.org/10.1091/mbc.E10-09-0739

Salama, I., Malone, P.S., Mihaimeed, F., Jones, J.L., 2008. A review of the S100 proteins in cancer. Eur. J. Surg. Oncol. 34, 357–364. https://doi.org/10.1016/j.ejso.2007.04.009

Salamonsen, L.A., 1996. Matrix metalloproteinases and their tissue inhibitors in endocrinology. Trends Endocrinol. Metab. 7, 28–34. https://doi.org/10.1016/1043-2760(95)00189-1

Saleem, M., Kweon, M.-H., Johnson, J.J., Adhami, V.M., Elcheva, I., Khan, N., Bin Hafeez, B., Bhat, K.M.R., Sarfaraz, S., Reagan-Shaw, S., Spiegelman, V.S., Setaluri, V., Mukhtar, H., 2006. S100A4 accelerates tumorigenesis and invasion of human prostate cancer through the transcriptional regulation of matrix metalloproteinase 9. Proc. Natl. Acad. Sci. U. S. A. 103, 14825–30. https://doi.org/10.1073/pnas.0606747103

Salo, T., Liotta, L.A., Keski-Oja, J., Turpeenniemi-Hujanen, T., Tryggvason, K., 1982. Secretion of basement membrane collagen degrading enzyme and plasminogen activator by transformed cells--role in metastasis. Int. J. Cancer 30, 669–73.

Sato, N., Fukushima, N., Matsubayashi, H., Goggins, M., 2004. Identification of maspin and S100P as novel hypomethylation targets in pancreatic cancer using global gene expression profiling. Oncogene 23, 1531–1538. https://doi.org/10.1038/sj.onc.1207269

Schäfer, B.W., Wicki, R., Engelkamp, D., Mattei, M. geneviève, Heizmann, C.W., 1995. Isolation of a YAC clone covering a cluster of nine S100 genes on human chromosome 1q21: rationale for a new nomenclature of the S100 calcium-binding protein family. Genomics 25, 638–643. https://doi.org/10.1016/0888-7543(95)80005-7

Scherer, W.F., 1953. Studies on the Propagation in Vitro of Poliomyelitis Viruses: Iv. Viral Multiplication in a Stable Strain of Human Malignant Epithelial Cells (Strain Hela) Derived From an Epidermoid Carcinoma of the Cervix. J. Exp. Med. 97, 695–710. https://doi.org/10.1084/jem.97.5.695

Schmidt-Hansen, B., Ornås, D., Grigorian, M., Klingelhöfer, J., Tulchinsky, E., Lukanidin, E., Ambartsumian, N., 2004. Extracellular S100A4(mts1) stimulates invasive growth of mouse endothelial cells and modulates MMP-13 matrix metalloproteinase activity. Oncogene 23, 5487–95. https://doi.org/10.1038/sj.onc.1207720

Schmidt-Kittler, O., Ragg, T., Daskalakis, A., Granzow, M., Ahr, A., Blankenstein, T.J.F., Kaufmann, M., Diebold, J., Arnholdt, H., Muller, P., Bischoff, J., Harich, D.,

Schlimok, G., Riethmuller, G., Eils, R., Klein, C. a, 2003. From latent disseminated cells to overt metastasis: genetic analysis of systemic breast cancer progression. Proc. Natl. Acad. Sci. U. S. A. 100, 7737–7742. https://doi.org/10.1073/pnas.1331931100

Schmidt, A., Yan, S., Yan, S., Stern, D., 2000. The biology of the receptor for advanced glycation end products and its ligands. Biochim Biophys Acta. 1498, 99–111. https://doi.org/10.1016/S0167-4889(00)00087-2

Schmidt, A.M., Vianna, M., Gerlach, M., Brett, J., Ryan, J., Kao, J., Esposito, C., Hegarty, H., Hurley, W., Clauss, M., Wang, F., Pan, Y.C.E., Tsang, T.C., Stern, D., 1992. Isolation and characterization of two binding proteins for advanced glycosylation end products from bovine lung which are present on the endothelial cell surface. J. Biol. Chem. 267, 14987–14997.

Schmidt, A.M., Yan, S. Du, Yan, S.F., Stern, D.M., 2001. The multiligand receptor RAGE as a progression factor amplifying immune and inflammatory responses. J. Clin. Invest. https://doi.org/10.1172/JCI200114002

Schröpfer, A., Kammerer, U., Kapp, M., Dietl, J., Feix, S., Anacker, J., 2010. Expression pattern of matrix metalloproteinases in human gynecological cancer cell lines. BMC Cancer 10, 553. https://doi.org/10.1186/1471-2407-10-553

Sela-Passwell, N., Rosenblum, G., Shoham, T., Sagi, I., 2010. Structural and functional bases for allosteric control of MMP activities: Can it pave the path for selective inhibition? Biochim. Biophys. Acta - Mol. Cell Res. 1803, 29–38. https://doi.org/10.1016/j.bbamcr.2009.04.010

Semov, A., Moreno, M.J., Onichtchenko, A., Abulrob, A., Ball, M., Ekiel, I., Pietrzynski, G., Stanimirovic, D., Alakhov, V., 2005. Metastasis-associated protein S100A4 induces angiogenesis through interaction with Annexin II and accelerated plasmin formation. J. Biol. Chem. 280, 20833–41. https://doi.org/10.1074/jbc.M412653200

Sen, T., Dutta, A., Maity, G., Chatterjee, A., 2010. Fibronectin induces matrix metalloproteinase-9 (MMP-9) in human laryngeal carcinoma cells by involving multiple signaling pathways. Biochimie 92, 1422–1434. https://doi.org/10.1016/j.biochi.2010.07.005

Shimokawa Ki, K., Katayama, M., Matsuda, Y., Takahashi, H., Hara, I., Sato, H., Kaneko,

S., 2002. Matrix metalloproteinase (MMP)-2 and MMP-9 activities in human seminal plasma. Mol. Hum. Reprod. 8, 32–6. https://doi.org/10.1093/MOLEHR/8.1.32

Shin, J.A., Kim, H.S., Vargas, A., Yu, W.Q., Eom, Y.S., Craft, C.M., Lee, E.J., 2016. Inhibition of matrix metalloproteinase 9 enhances rod survival in the s334ter-Line3 retinitis pigmentosa model. PLoS One 11, e0167102. https://doi.org/10.1371/journal.pone.0167102

SHISHIBORI, T., OYAMA, Y., MATSUSHITA, O., YAMASHITA, K., FURUICHI, H., OKABE, A., MAETA, H., HATA, Y., KOBAYASHI, R., 1999. Three distinct anti-allergic drugs, amlexanox, cromolyn and tranilast, bind to S100A12 and S100A13 of the S100 protein family. Biochem. J. 338, 583. https://doi.org/10.1042/0264-6021:3380583

Siddique, H.R., Adhami, V.M., Parray, A., Johnson, J.J., Siddiqui, I.A., Shekhani, M.T., Murtaza, I., Ambartsumian, N., Konety, B.R., Mukhtar, H., Saleem, M., 2013. The S100A4 Oncoprotein Promotes Prostate Tumorigenesis in a Transgenic Mouse Model: Regulating NFκB through the RAGE Receptor. Genes and Cancer 4, 224–234. https://doi.org/10.1177/1947601913492420

Siegel, R.L., Miller, K.D., Jemal, A., 2018. Cancer statistics, 2018. CA. Cancer J. Clin. 68, 7–30. https://doi.org/10.3322/caac.21442

Singer, C.F., Kronsteiner, N., Marton, E., Kubista, M., Cullen, K.J., Hirtenlehner, K., Seifert, M., Kubista, E., 2002. MMP-2 and MMP-9 expression in breast cancer-derived human fibroblasts is differentially regulated by stromal-epithelial interactions. Breast Cancer Res. Treat. 72, 69–77. https://doi.org/10.1023/A:1014918512569

Singletary, S.E., Connolly, J.L., 2006. Breast cancer staging: working with the sixth edition of the AJCC Cancer Staging Manual. CA. Cancer J. Clin. 56, 37-47; quiz 50-51. https://doi.org/10.3322/canjclin.56.1.37

Skiles, J.W., Monovich, L.G., Jeng, A.Y., 2000. Chapter 15. Matrix metalloproteinase inhibitors for treatment of cancer. Annu. Rep. Med. Chem. 35, 167–176. https://doi.org/10.1016/S0065-7743(00)35016-3

Snoek-van Beurden, P., Von den Hoff, J., 2005. Zymographic techniques for the analysis of matrix metalloproteinases and their inhibitors. Biotechniques 38, 73–

83. https://doi.org/10.2144/05381RV01

Snoek-van Beurden, P.A.M., Von den Hoff, J.W., 2005. Zymographic techniques for the analysis of matrix metalloproteinases and their inhibitors. Biotechniques 38, 73–83. https://doi.org/10.2144/05381RV01

Song, J., Wu, C., Zhang, X., Sorokin, L.M., 2013. In Vivo Processing of CXCL5 (LIX) by Matrix Metalloproteinase (MMP)-2 and MMP-9 Promotes Early Neutrophil Recruitment in IL-1 -Induced Peritonitis. J. Immunol. 190, 401–410. https://doi.org/10.4049/jimmunol.1202286

Sorlie, T., Tibshirani, R., Parker, J., Hastie, T., Marron, J.S., Nobel, A., Deng, S., Johnsen, H., Pesich, R., Geisler, S., Demeter, J., Perou, C.M., Lønning, P.E., Brown, P.O., Børresen-Dale, A.-L., Botstein, D., 2003. Repeated observation of breast tumor subtypes in independent gene expression data sets. Proc. Natl. Acad. Sci. U. S. A. 100, 8418–23. https://doi.org/10.1073/pnas.0932692100

Springman, E.B., Angleton, E.L., Birkedal-Hansen, H., Van Wart, H.E., 1990. Multiple modes of activation of latent human fibroblast collagenase: evidence for the role of a Cys73 active-site zinc complex in latency and a “cysteine switch” mechanism for activation. Proc. Natl. Acad. Sci. U. S. A. 87, 364–368. https://doi.org/10.1073/pnas.87.1.364

Stechmiller, J., Cowan, L., Schultz, G., 2010. The role of doxycycline as a matrix metalloproteinase inhibitor for the treatment of chronic wounds. Biol. Res. Nurs. 11, 336–344. https://doi.org/10.1177/1099800409346333

Stetler-Stevenson, W.G., 2001. The role of matrix metalloproteinases in tumor invasion, metastasis, and angiogenesis. Surg. Oncol. Clin. N. Am. 10, 383–92, x.

Stetler-Stevenson, W.G., 1990. Type IV collagenases in tumor invasion and metastasis. Cancer Metastasis Rev. 9, 289–303.

Stetler-Stevenson, W.G., Aznavoorian, S., Liotta, L.A., 1993. Tumor cell interactions with the extracellular matrix during invasion and metastasis. Annu. Rev. Cell Biol. 9, 541–73. https://doi.org/10.1146/annurev.cb.09.110193.002545

Streefkerk, J.G., 1972. Inhibition of erythrocyte pseudoperoxidase activity by treatment with hydrogen peroxide following methanol. J. Histochem. Cytochem. 20, 829–31.

Strutz, F., Okada, H., Lo, C.W., Danoff, T., Carone, R.L., Tomaszewski, J.E., Neilson,

E.G., 1995. Identification and characterization of a fibroblast marker: FSP1. J. Cell Biol. 130, 393–405. https://doi.org/10.1083/jcb.130.2.393

Su, P., Miao, Z., Hu, L., Li, R., Yin, C., Li, D., Chen, Z., Zhao, F., Qian, A., 2017. Methods of studying mammalian cell migration and invasion in vitro, in: 2017 14th International Bhurban Conference on Applied Sciences and Technology (IBCAST). IEEE, pp. 148–159. https://doi.org/10.1109/IBCAST.2017.7868048

Suzuki, K., Lees, M., Newlands, G.F.J., Nagaset, H., Woolley, D.E., 1995. Activation of precursors for matrix metalloproteinases 1 (interstitial collagenase) and 3 (stromelysin) by rat mast-cell proteinases I and 11. Biochem. J 305, 301–306.

Taguchi, A., Blood, D.C., Del Toro, G., Canet, A., Lee, D.C., Qu, W., Tanjl, N., Lu, Y., Lalla, E., Fu, C., Hofmann, M.A., Kislinger, T., Ingram, M., Lu, A., Tanaka, H., Hori, O., Ogawa, S., Stern, D.M., Schmidt, A.M., 2000. Blockade of RAGE-amphoterin signalling suppresses tumour growth and metastases. Nature 405, 354–360. https://doi.org/10.1038/35012626

Takada, M., Hirata, K., Ajiki, T., Suzuki, Y., Kuroda, Y., 2004. Expression of Receptor for Advanced Glycation End products (RAGE) and MMP-9 in human pancreatic cancer cells. Hepatogastroenterology. 51, 928–930.

Takenaga, K., Kozlova, E.N., 2006. Role of intracellular S100A4 for migration of rat astrocytes. Glia 53, 313–321. https://doi.org/10.1002/glia.20284

Takenaga, K., Nakamura, Y., Sakiyama, S., 1997. Expression of antisense RNA to S100A4 gene encoding an S100-related calcium-binding protein suppresses metastatic potential of high-metastatic Lewis lung carcinoma cells. Oncogene 14, 331–7. https://doi.org/10.1038/sj.onc.1200820

Takino, T., Koshikawa, N., Miyamori, H., Tanaka, M., Sasaki, T., Okada, Y., Seiki, M., Sato, H., 2003. Cleavage of metastasis suppressor gene product KiSS-1 protein/metastin by matrix metalloproteinases. Oncogene 22, 4617–4626. https://doi.org/10.1038/sj.onc.1206542

Takino, T., Sato, H., Shinagawa, A., Seiki, M., 1995. Identification of the second membrane-type matrix metalloproteinase (MT-MMP-2) gene from a human placenta cDNA library: MT-MMPs form a unique membrane-type subclass in the MMP family. J. Biol. Chem. 270, 23013–23020. https://doi.org/10.1074/jbc.270.39.23013

Tanjore, H., Kalluri, R., 2006. The role of type IV collagen and basement membranes in cancer progression and metastasis. Am. J. Pathol. 168, 715–717. https://doi.org/10.2353/ajpath.2006.051321

Toth, M., Fridman, R., 2001. Assessment of Gelatinases (MMP-2 and MMP-9 by Gelatin Zymography. Methods Mol. Med. 57, 163–74. https://doi.org/10.1385/1-59259-136-1:163

Toth, M., Sohail, A., Fridman, R., 2012a. Assessment of gelatinases (MMP-2 and MMP-9) by gelatin zymography., in: Methods in Molecular Biology (Clifton, N.J.). Humana Press, New Jersey, pp. 121–135. https://doi.org/10.1007/978-1-61779-854-2_8

Toth, M., Sohail, A., Fridman, R., 2012b. Assessment of gelatinases (MMP-2 and MMP-9) by gelatin zymography. Methods Mol. Biol. 878, 121–35. https://doi.org/10.1007/978-1-61779-854-2_8

Uría, J.A., Ståhle-Bäckdahl, M., Seiki, M., Fueyo, A., López-Otín, C., 1997. Regulation of collagenase-3 expression in human breast carcinomas is mediated by stromal-epithelial cell interactions. Cancer Res. 57, 4882–8.

Van Doren, S.R., 2015. Matrix metalloproteinase interactions with collagen and elastin. Matrix Biol. 44–46, 224–231. https://doi.org/10.1016/j.matbio.2015.01.005

Van Wart, H.E., Birkedal-Hansent, H., 1990. The cysteine switch: A principle of regulation of metalloproteinase activity with potential applicability to the entire matrix metalloproteinase gene family (collagenase/gelatinase/stromelysin/zinc enzyme). Biochemistry 87, 5578–5582. https://doi.org/10.1073/pnas.87.14.5578

Verma, R.P., Hansch, C., 2007. Matrix metalloproteinases (MMPs): Chemical-biological functions and (Q)SARs. Bioorganic Med. Chem. 15, 2223–2268. https://doi.org/10.1016/j.bmc.2007.01.011

Vicente-Manzanares, M., Zareno, J., Whitmore, L., Choi, C.K., Horwitz, A.F., 2007. Regulation of protrusion, adhesion dynamics, and polarity by myosins IIA and IIB in migrating cells. J. Cell Biol. 176, 573–80. https://doi.org/10.1083/jcb.200612043

Wang, G., Platt-Higgins, A., Carroll, J., De Silva Rudland, S., Winstanley, J.,

Barraclough, R., Rudland, P.S., 2006. Induction of metastasis by S100P in a rat mammary model and its association with poor survival of breast cancer patients. Cancer Res. 66, 1199–1207. https://doi.org/10.1158/0008-5472.CAN-05-2605

Wang, J.R., Li, X.H., Gao, X.J., An, S.C., Liu, H., Liang, J., Zhang, K., Liu, Z., Wang, J., Chen, Z., Sun, W., 2013. Expression of MMP-13 is associated with invasion and metastasis of papillary thyroid carcinoma. Eur. Rev. Med. Pharmacol. Sci. 17, 427–435.

Wang, L., Wang, X., Liang, Y., Diao, X., Chen, Q., 2012. S100A4 promotes invasion and angiogenesis in breast cancer MDA-MB-231 cells by upregulating matrix metalloproteinase-13. Acta Biochim. Pol. 59, 593–8.

Warburton, M.J., Ferns, S.A., Hughes, C.M., Sear, C.H., Rudland, P.S., 1987a. Generation of cell types with myoepithelial and mesenchymal phenotypes during the conversion of rat mammary tumor epithelial stem cells into elongated cells. J Natl Cancer Inst 78, 1191–1201.

Warburton, M.J., Ferns, S.A., Kimbell, R., Rudland, P.S., Monaghan, P., Gusterson, B.A., 1987b. Loss of basement membrane deposits and development of invasive potential by virally-transformed rat mammary cells are independent of collagenase production. Int. J. cancer 40, 270–7.

Warburton, M.J., Mitchell, D., Ormerod, E.J., Rudland, P., 1982. Distribution of myoepithelial cells and basement membrane proteins in the resting, pregnant, lactating, and involuting rat mammary gland. J. Histochem. Cytochem. 30, 667–676. https://doi.org/10.1177/30.7.6179984

Wellings, S.R., Jensen, H.M., Marcum, R.G., 1975. An atlas of subgross pathology of the human breast with special reference to possible precancerous lesions. J. Natl. Cancer Inst. 55, 231–73.

Weng, Z., Zhang, B., Asadi, S., Sismanopoulos, N., Butcher, A., Fu, X., Katsarou-Katsari, A., Antoniou, C., Theoharides, T.C., 2012. Quercetin is more effective than cromolyn in blocking human mast cell cytokine release and inhibits contact dermatitis and photosensitivity in humans. PLoS One 7, e33805. https://doi.org/10.1371/journal.pone.0033805

Wu, M.-H., Tsai, Y.-T., Hua, K.-T., Chang, K.-C., Kuo, M.-L., Lin, M.-T., 2012. Eicosapentaenoic acid and docosahexaenoic acid inhibit macrophage-induced

gastric cancer cell migration by attenuating the expression of matrix metalloproteinase 10. J. Nutr. Biochem. 23, 1434–1439. https://doi.org/10.1016/j.jnutbio.2011.09.004

Xie, J., Méndez, J.D., Méndez-Valenzuela, V., Aguilar-Hernández, M.M., 2013. Cellular signalling of the receptor for advanced glycation end products (RAGE). Cell. Signal. 25, 2185–2197. https://doi.org/10.1016/j.cellsig.2013.06.013

Xu, H., Li, M., Zhou, Y., Wang, F., Li, X., Wang, L., Fan, Q., 2016. S100A4 participates in epithelial-mesenchymal transition in breast cancer via targeting MMP2. Tumor Biol. 37, 2925–2932. https://doi.org/10.1007/s13277-015-3709-3

Xu, R., Rudd, T.R., Hughes, A.J., Siligardi, G., Fernig, D.G., Yates, E.A., 2013. Analysis of the fibroblast growth factor receptor (FGFR) signalling network with heparin as coreceptor: Evidence for the expansion of the core FGFR signalling network. FEBS J. 280, 2260–2270. https://doi.org/10.1111/febs.12201

Yammani, R.R., Carlson, C.S., Bresnick, A.R., Loeser, R.F., 2006. Increase in production of matrix metalloproteinase 13 by human articular chondrocytes due to stimulation with S100A4: Role of the receptor for advanced glycation end products. Arthritis Rheum. 54, 2901–2911. https://doi.org/10.1002/art.22042

Yang, M., Kurkinen, M., 1998. Cloning and characterization of a novel matrix metalloproteinase (MMP), CMMP, from chicken embryo fibroblasts. CMMP, xenopus XMMP, and human MMP19 have a conserved unique cysteine in the catalytic domain. J. Biol. Chem. 273, 17893–17900. https://doi.org/10.1074/jbc.273.28.17893

Yu, W., Woessner, J.F., 2001. Heparin-Enhanced Zymographic Detection of Matrilysin and Collagenases. Anal. Biochem. 293, 38–42. https://doi.org/10.1006/abio.2001.5099

Yue, B., 2014. Biology of the extracellular matrix: An overview. J. Glaucoma 23, S20–S23. https://doi.org/10.1097/IJG.0000000000000108

Zeng, Z.-S., Cohen, A.M., Guillem, J.G., 1999. Loss of basement membrane type IV collagen is associated with increased expression of metalloproteinases 2 and 9 (MMP-2 and MMP-9) during human colorectal tumorigenesis. Carcinogenesis 20, 749–755. https://doi.org/10.1093/carcin/20.5.749

Zhang, B., Cao, X., Liu, Y., Cao, W., Zhang, F., Zhang, S., Li, H., Ning, L., Fu, L., Niu, Y.,

Niu, R., Sun, B., Hao, X., 2008. Tumor-derived matrix metalloproteinase-13 (MMP-13) correlates with poor prognoses of invasive breast cancer. BMC Cancer 8, 83. https://doi.org/10.1186/1471-2407-8-83

Zhang, G., Li, M., Jin, J., Bai, Y., Yang, C., 2011. Knockdown of S100A4 decreases tumorigenesis and metastasis in osteosarcoma cells by repression of matrix metalloproteinase-9. Asian Pac. J. Cancer Prev. 12, 2075–80.

Zhang, K., Liu, X., Hao, F., Dong, A., Chen, D., 2016. Targeting TGF-β1 inhibits invasion of anaplastic thyroid carcinoma cell through. Am J Transl Res 8, 2196–2209.

Zhang, K., Zhang, M., Zhao, H., Yan, B., Zhang, D., Liang, J., 2012. S100A4 regulates motility and invasiveness of human esophageal squamous cell carcinoma through modulating the AKT/Slug signal pathway. Dis. Esophagus 25, 731–739. https://doi.org/10.1111/j.1442-2050.2012.01323.x

Zhang, S., Wang, Z., Liu, W., Lei, R., Shan, J., Li, L., Wang, X., 2017. Distinct prognostic values of S100 mRNA expression in breast cancer. Sci. Rep. 7, 39786. https://doi.org/10.1038/srep39786

Zhao, L., Yang, X., Khan, A., Kandil, D., 2014. Diagnostic role of immunohistochemistry in the evaluation of breast pathology specimens. Arch. Pathol. Lab. Med. 138, 16–24. https://doi.org/10.5858/arpa.2012-0440-RA

Zhou, C., Zhong, Q., Rhodes, L., 2012. Proteomic analysis of acquired tamoxifen resistance in MCF-7 cells reveals expression signatures associated with enhanced migration. Breast Cancer ….

Zhou, L.L., Cao, W., Xie, C., Tian, J., Zhou, Z., Zhou, Q., Zhu, P., Li, A., Liu, Y., Miyata, T., Hou, F.F., Nie, J., 2012. The receptor of advanced glycation end products plays a central role in advanced oxidation protein products-induced podocyte apoptosis. Kidney Int. 82, 759–770. https://doi.org/10.1038/ki.2012.184

Zhu, L., Ito, T., Nakahara, T., Nagae, K., Fuyuno, Y., Nakao, M., Akahoshi, M., Nakagawa, R., Tu, Y., Uchi, H., Furue, M., 2013. Upregulation of S100P, receptor for advanced glycation end products and ezrin in malignant melanoma. J. Dermatol. 40, 973–979. https://doi.org/10.1111/1346-8138.12323

Zhuang, X., Lv, M., Zhong, Z., Zhang, L., Jiang, R., Chen, J., 2016. Interplay between intergrin-linked kinase and ribonuclease inhibitor affects growth and metastasis of bladder cancer through signaling ILK pathways. J. Exp. Clin. Cancer Res. 35,

130. https://doi.org/10.1186/s13046-016-0408-x

Zitka, O., Kukacka, J., Krizkova, S., Huska, D., Adam, V., Masarik, M., Prusa, R., Kizek, R., 2010. Matrix metalloproteinases. Curr. Med. Chem. 17, 3751–68.

List of Publications

- **Journals**
  - Ismail, T.M., Bennett, D., Platt-Higgins, A.M., Al-Medhtiy, M., Barraclough, R., Rudland, P.S., 2017. S100A4 elevation empowers expression of metastasis effector molecules in human breast cancer. Cancer Res. 77, 780–789. https://doi.org/10.1158/0008-5472.CAN-16-1802. **(Awarded as a Best Paper)**

- **International Conferences and Workshops**
  - AL-Medhtiy, M., Wilkinson, M., Barraclough, R., Rudland, P.S., 2016. The role of Collagenase-3 in S100P and S100A4 overexpression metastatic breast cancer cells. NCRI Cancer Conference. 6-9/11/2016, Liverpool, UK.

Appendices

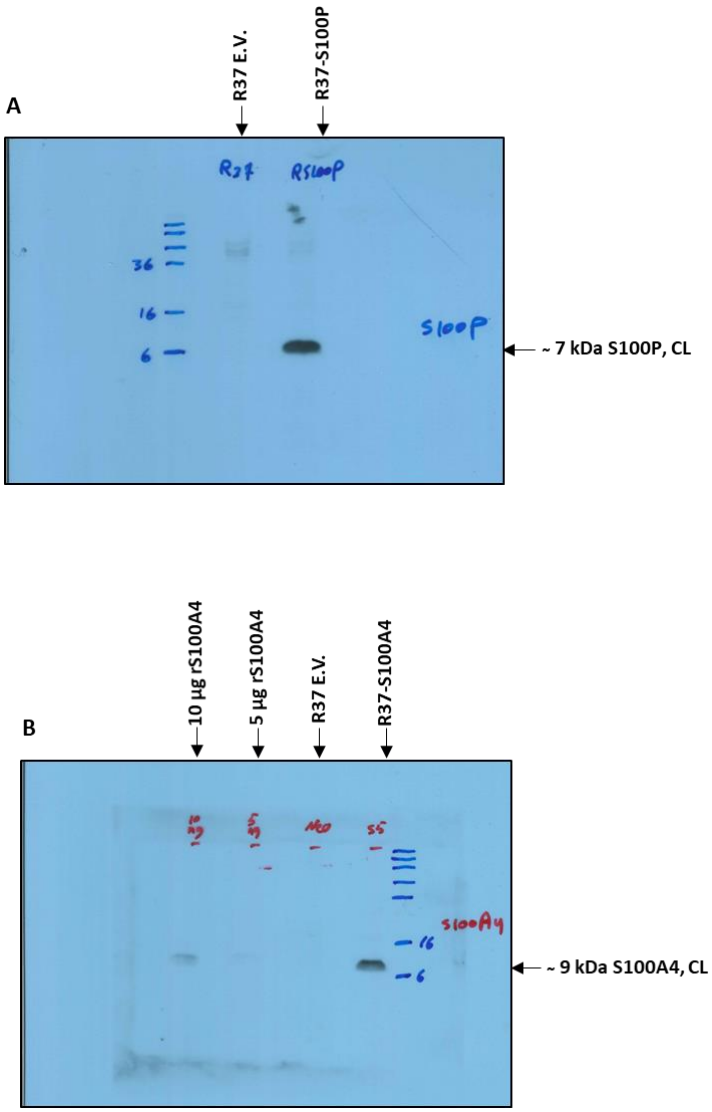

Appendix 1. Full length gel for overexpression of S100P and S100A4 proteins in transfected rat mammary cell lines.

(**A**) Cell lysate (CL) from stably transfected Rama 37 with empty vector (R37 E.V.) or from Rama 37 with S100P (R37-S100P) cell lines. (**B**) Cell lysates (CL) from R37 E.V. or from R37-S100A4 cell lines were run on similar SDS-PAGE gels. In controls, recombinant 5 or 10 ng purified S100A4 (rS100A4) was also run in parallel. (See **Figure 3.1**).

Appendix 2. MMP array for the rest of the MMPs: MMP-1, MMP-3, MMP-8 and MMP-10 in CM from S100P-induced HeLa-A3, Rama 37-S100P and Rama 37-S100A4 cell lines.

MMP [a]	Fold increase±SE [b]		
	HeLa-A3 [c]	R37-S100P [d]	R37-S100A4 [e]
MMP-1	1.25±0.18, *P*=0.18	1.09±0.05, *P*=0.60	1.23±0.03, *P*=0.26
MMP-3	1.22±0.26, *P*=0.55	1.21±0.11, *P*=0.21	1.23±0.14, *P*=0.26
MMP-8	1.57±0.41, *P*=0.83	1.29±0.47, *P*=0.88	1.07±0.56, *P*=0.50
MMP-10	1.29±0.47, *P*=0.23	2.63±0.50, *P*=0.008	3.63±0.57, *P*=0.003

[a] Matrix metalloproteinase.

[b] Fold increase over control cells (mean±SE, n=3) with corresponding *P* value (Student's t-test, 2-tailed).

[c] S100P-Induced human cervical cancer cell line.

[d] S100P cDNA stably transfected rat mammary cell line.

[e] S100A4 cDNA stably transfected rat mammary cell line.

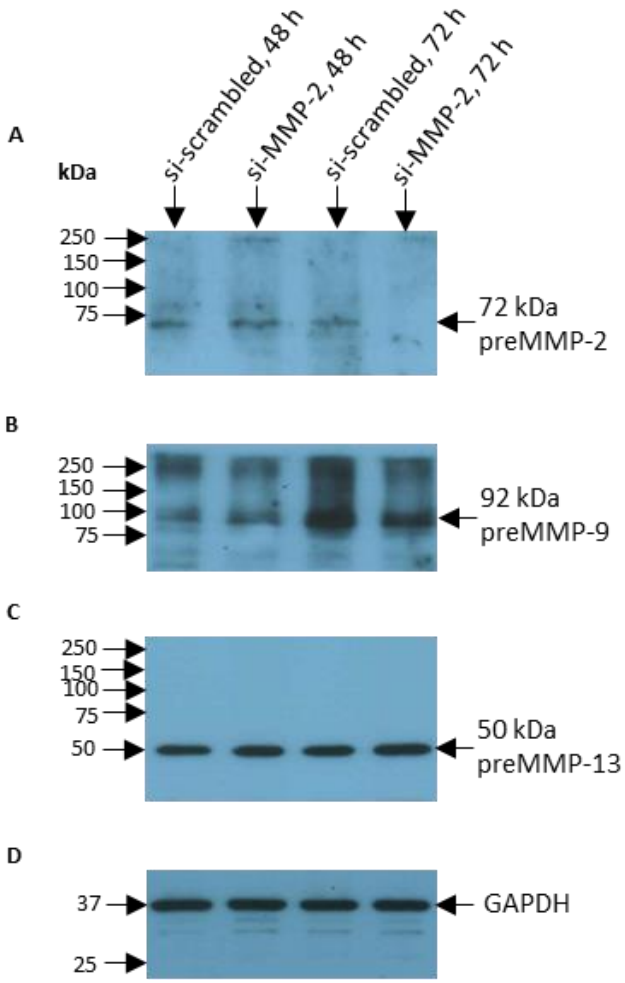

Appendix 3. Knockdown of MMP-2 with siRNA for MMP-2 (si-MMP-2) or scrambled (si-scrambled) for 48 and 72 hours (h).

Western blots for MMP-2, MMP-9 and MMP-13 from the same intracellular sample of the R37-S100P cell line are shown. Results show that preMMP-2 (72 kDa) was knocked down almost completely by 72 h ($P \leq 0.02$) (**Section 4.2.1.1** and **Figure 4.1**). In contrast, preMMP-9 (92 kDa) and preMMP-13 (50 kDa) were not significantly ($P \geq 0.380$) affected for the mean of 3 samples on separate gels.

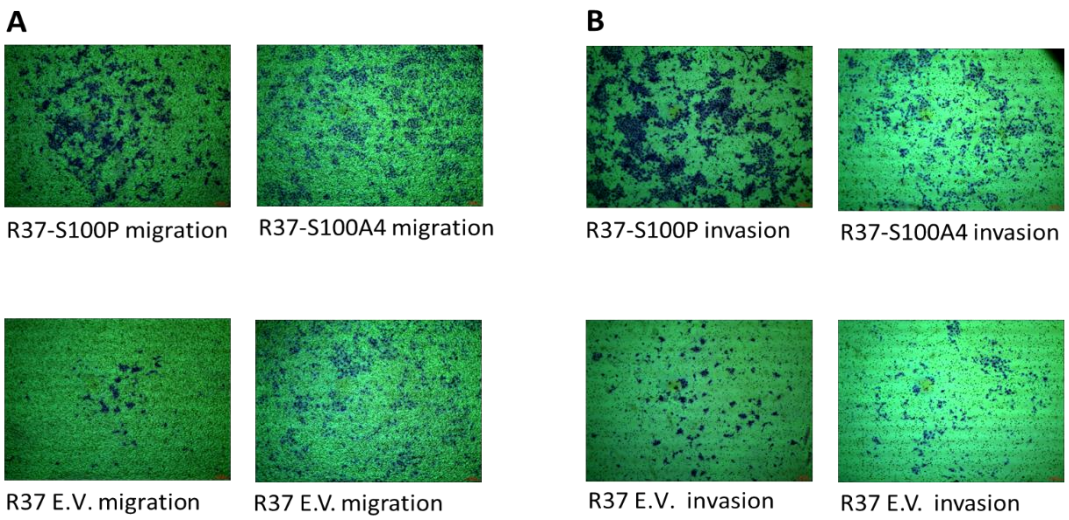

Appendix 4. Micrographs of migration and invasion assays for the Rama 37-S100P (R37-S100P), Rama 37-S100A4 (R37-S100A4) and Rama 37 empty vector (R37 E.V.) control cell lines.

(**A & B**) Representative images showing (**A**) Boyden chambers for cell migration and (**B**) Matrigel chambers for cell invasion assays, after culturing for 24 hours. Underside of membranes were photographed with a light microscope using a 4 x objective. Red bar = 100 µm. Three chambers for each group were used for migration or invasion assays and each experiment was performed three times (**Sections 2.13** and **2.14**). Quantitative details are shown in **Figure. 4.4**.

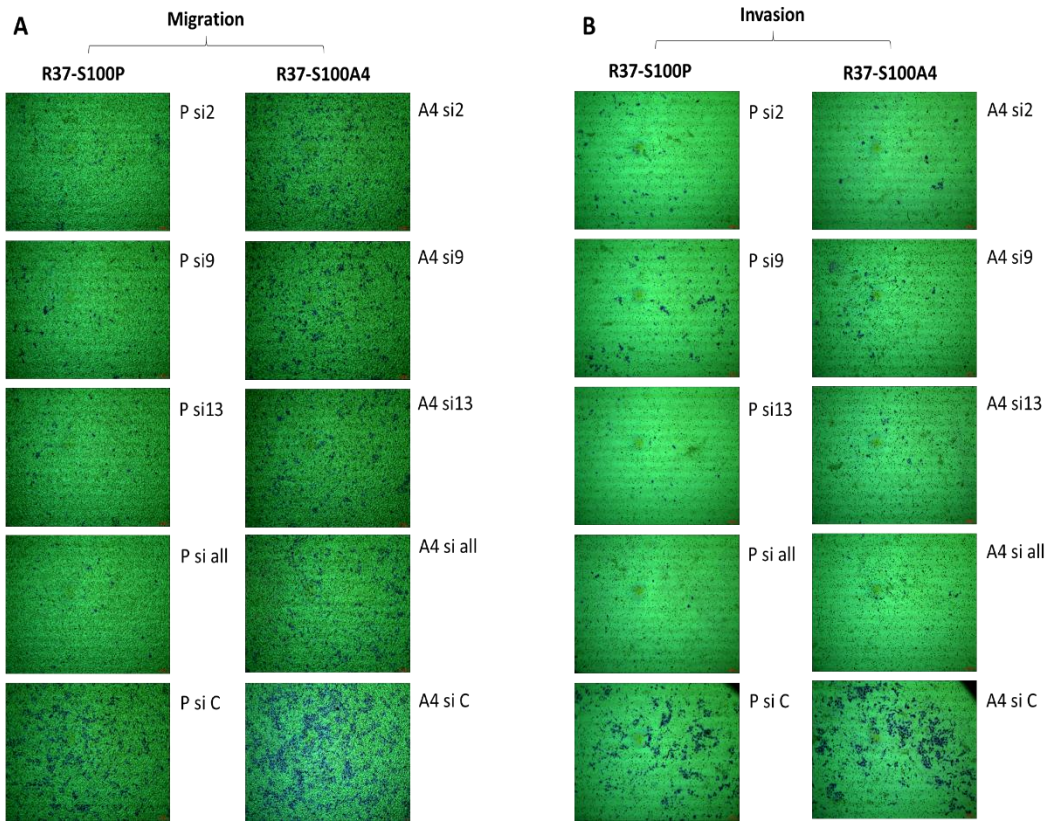

Appendix 5. Micrographs of migration and invasion assays of S100P/S100A4 overexpressing rat mammary cell lines after siRNA knock-down of different MMPs. (**A & B**) Representative images showing (**A**) Boyden chambers for cell migration and (**B**) Matrigel chambers for cell invasion assays, after culturing for 24 hours. Undersides of membranes were photographed with a light microscope using a 4 x objective. Red bar = 100 µm. Three chambers for each group were used for migration or invasion assays and each experiment was performed three times (**Sections 2.13** and **2.14**). Quantitative details are shown in **Figure 4.5**.

Abbreviations of cell lines and procedures used: P (R37-S100P cells), A4 (R37-S100A4 cells), si (siRNA), 2 (against MMP-2), 9 (against MMP-9), 13 (against MMP-13), all (against MMP-2, -9 & -13), and C (against scrambled control).

Appendix 6. Data for IHC staining of S100 proteins and MMPs in patients' specimens.

AnonNos[a]	MMP2[b]	MMP2at5%[c]	MMP9[d]	MMP9at5%[e]	MMP13[f]	MMP13at5%[g]	S100A4[h]	S100A4at5%[i]	S100P[j]	S100Pat5%[k]	SurvMonths[l]
286	1	0	1	0	1	0	1	0			231.37
4	2	0	1	0	1	0	5	1			166.62
6	1	0	2	0	4	1	3	1	2	0	226.22
289	4	1	3	1	2	0	2	0	5	1	224.54
290	2	0	1	0	1	0	2	0	2	0	72.08
291	1	0	1	0	1	0	3	1	4	1	91.59
9	3	1	2	0	3	1	3	1	2	0	36.37
11	2	0	1	0	1	0	5	1	1	0	219.97
12	1	0	2	0	1	0	1	0	1	0	219.74
294	1	0	1	0	1	0	3	1	4	1	76.77
295	3	1	1	0	3	1	3	1			43.73
297	1	0	1	0	1	0	1	0	1	0	218.3
13	1	0	2	0	2	0	1	0			217.87
298	1	0	1	0	1	0	1	0	2	0	167.94
15	2	0	2	0	1	0	1	0	3	1	104.47
16	3	1	2	0	3	1	5	1	5	1	99.9
18	4	1	3	1	4	1	3	1	3	1	19.12
19	2	0	1	0	1	0	4	1	3	1	85.61
20	2	0	1	0	1	0	1	0	2	0	106.83
301	1	0	1	0	1	0	1	0	2	0	214.82
302	3	1	1	0	1	0	2	0	3	1	166.92
24	2	0	1	0	4	1	1	0	1	0	212.39
303	4	1	1	0	4	1	4	1	3	1	191.06
25	2	0	1	0	2	0	1	0	1	0	212.06

26	2	0	2	0	3	1	1	0	3	1	41.62
304	1	0	1	0	1	0	1	0	1	0	211.89
27	3	1	2	0	2	0	3	1			78.02
305	5	1	1	0	3	1	3	1	3	1	53.25
307	3	1	4	1	3	1	2	0	2	0	96.68
308	2	0	2	0	1	0	1	0	1	0	143.82
310	1	0	1	0	1	0	3	1	2	0	79.7
311	1	0	1	0	1	0	1	0	1	0	207.52
32	1	0	2	0	4	1	1	0	3	1	207.33
99	4	1	3	1	4	1	3	1	5	1	46.71
34	3	1	1	0	4	1	4	1			48.82
71	1	0	1	0	1	0	1	0	1	0	206.64
72	1	0	1	0	1	0	1	0			206.6
100	2	0	3	1	5	1	3	1	4	1	46.06
73	1	0	1	0	1	0	1	0	1	0	206.41
312	4	1	1	0	2	0	3	1	1	0	48.59
35	5	1	2	0	4	1	4	1	4	1	76.31
36	2	0	1	0	1	0	1	0	3	1	206.34
74	1	0	2	0	1	0	1	0	1	0	206.11
38	2	0	3	1	3	1	3	1	3	1	33.9
313	3	1	1	0	1	0	2	0	4	1	74.31
314	1	0	1	0	1	0	1	0	1	0	204.99
75	1	0	1	0	2	0	1	0	2	0	204.96
40	5	1	5	1	5	1	3	1	3	1	50.95
317	5	1	1	0	3	1	2	0	5	1	106.44
41	2	0	1	0	1	0	1	0	2	0	203.42
76	4	1	1	0	4	1	3	1	3	1	64.45

43	1	0	1	0	1	0	1	0	1	0	202.96
321	1	0	1	0	2	0	2	0	2	0	1.97
45	1	0	2	0	1	0	3	1			89.49
46	3	1	2	0	4	1	1	0	5	1	91.03
103	5	1	3	1	5	1	4	1	4	1	21.65
104	4	1	3	1	5	1	3	1	5	1	91.72
107	5	1	1	0	5	1	1	0			51.31
77	5	1	1	0	2	0	3	1			53.32
322	1	0	1	0	1	0	1	0	1	0	55.32
78	2	0	1	0	1	0	3	1	3	1	54.5
79	2	0	1	0	1	0	1	0	3	1	43.43
80	2	0	2	0	2	0	1	0	3	1	44.91
108	4	1	2	0	3	1	3	1	3	1	4.24
109	5	1	3	1	5	1	2	0	5	1	10.15
110	2	0	1	0	3	1	1	0			52.37
113	2	0	1	0	3	1	2	0	5	1	104.57
114	2	0	1	0	5	1	2	0	5	1	44.58
325	5	1	1	0	3	1	2	0	3	1	151.77
326	5	1	5	1	5	1	3	1	5	1	25.49
115	1	0	2	0	3	1	4	1			3.25
81	4	1	1	0	1	0	2	0	2	0	21.71
48	3	1	1	0	2	0	3	1	5	1	21.25
330	1	0	1	0	1	0	1	0	1	0	43.63
82	1	0	1	0	1	0	1	0	1	0	198.75
117	3	1	4	1	5	1	3	1	5	1	7.33
122	5	1	3	1	5	1	3	1	5	1	51.38
331	1	0	1	0	1	0	1	0	1	0	209.79

123	1	0	1	0	3	1	1	0	3	1	51.71
125	2	0	1	0	3	1	1	0	4	1	42.12
126	3	1	1	0	3	1	1	0	2	0	197.21
128	5	1	2	0	4	1	2	0	5	1	139.95
129	4	1	2	0	4	1	2	0	4	1	28.42
130	2	0	1	0	4	1	1	0	5	1	63.63
52	1	0	1	0	1	0	3	1	2	0	197.54
131	3	1	4	1	3	1	3	1	4	1	36.07
133	5	1	3	1	4	1	3	1	5	1	16.26
83	1	0	1	0	1	0	1	0			196.22
334	1	0	1	0	1	0	1	0	1	0	117.97
335	1	0	1	0	1	0	1	0	2	0	146.19
84	4	1	4	1	4	1	2	0	5	1	162.32
337	1	0	1	0	1	0	1	0	2	0	193.99
339	3	1	1	0	4	1	2	0	4	1	26.54
340	1	0	1	0	2	0	1	0	1	0	193.76
56	1	0	1	0	1	0	1	0	1	0	12.98
57	1	0	1	0	1	0	1	0	1	0	83.25
58	2	0	2	0	1	0	3	1	3	1	57.65
59	1	0	1	0	1	0	2	0	3	1	40.11
85	4	1	1	0	3	1	3	1	2	0	36.79
86	3	1	3	1	4	1	3	1	3	1	9.49
342	1	0	1	0	1	0	2	0	3	1	33.28
140	2	0	1	0	2	0	1	0	2	0	191.92
141	5	1	1	0	4	1	3	1	5	1	35.81
60	3	1	1	0	2	0	1	0	4	1	41.39
343	2	0	1	0	1	0	1	0	2	0	55.16

146	2	0	2	0	3	1	1	0	2	0	190.08
147	3	1	2	0	2	0	3	1	4	1	50.85
149	1	0	1	0	3	1	1	0	2	0	189.85
152	2	0	1	0	1	0	1	0	2	0	189.82
61	5	1	2	0	1	0	4	1	3	1	32.42
92	4	1	1	0	2	0	3	1	4	1	22.83
154	5	1	3	1	4	1	4	1	3	1	43.4
156	4	1	1	0	4	1	3	1	4	1	64.22
93	1	0	1	0	1	0	1	0			100.33
157	1	0	1	0	3	1	3	1	2	0	109.82
94	2	0	1	0	1	0	1	0	1	0	188.7
158	3	1	2	0	4	1	4	1	5	1	5.72
161	2	0	1	0	4	1	3	1	4	1	27.5
162	1	0	1	0	2	0	1	0	2	0	188.4
163	5	1	4	1	5	1	3	1	4	1	12.58
346	1	0	1	0	1	0	1	0	1	0	188.01
96	5	1	4	1	5	1	2	0	2	0	6.18
347	3	1	1	0	4	1	3	1	4	1	34.86
348	2	0	2	0	1	0	1	0	2	0	187.48
97	2	0	1	0	1	0	1	0	2	0	187.09
175	1	0	1	0	1	0	1	0	1	0	186.86
350	2	0	1	0	2	0	1	0			186.83
64	2	0	2	0	2	0	3	1			23.69
65	1	0	1	0	1	0	1	0	2	0	186.4
98	4	1	2	0	3	1	3	1	3	1	3.94
182	2	0	1	0	4	1	1	0	4	1	30.12
183	2	0	1	0	2	0	1	0	3	1	107.88

351	2	0	3	1	4	1	3	1			25.49
184	3	1	1	0	2	0	2	0	3	1	185.28
185	4	1	2	0	4	1	3	1	4	1	170.07
186	1	0	1	0	2	0	1	0	2	0	185.25
188	1	0	1	0	2	0	1	0	2	0	185.18
189	2	0	1	0	2	0	1	0	4	1	29.63
352	4	1	1	0	1	0	3	1	4	1	32.23
353	3	1	1	0	3	1	3	1	3	1	37.22
354	1	0	1	0	2	0	1	0	1	0	184.56
69	2	0	1	0	3	1	3	1	5	1	28.84
202	3	1	1	0	3	1	1	0	4	1	87.65
355	1	0	1	0	1	0	4	1			56.67
205	5	1	1	0	4	1	3	1	4	1	105.49
206	4	1	2	0	5	1	5	1	5	1	82.85
207	2	0	1	0	2	0	1	0	1	0	182.65
210	4	1	3	1	4	1	2	0	2	0	182.26
211	2	0	1	0	2	0	1	0	2	0	182.16
212	1	0	1	0	1	0	1	0	2	0	182.06
218	2	0	1	0	2	0	3	1	3	1	181.04
222	2	0	1	0	2	0	1	0	2	0	180.19
223	1	0	1	0	3	1	2	0	4	1	180.19
224	1	0	1	0	2	0	1	0	1	0	179.4
227	1	0	2	0	3	1	1	0	1	0	179.04
235	3	1	2	0	2	0	1	0	1	0	176.02
236	1	0	1	0	2	0	1	0	2	0	175.99
237	2	0	1	0	3	1	1	0	3	1	175.82
239	1	0	1	0	3	1	1	0	2	0	174.41

240	2	0	1	0	3	1	1	0	1	0	173.75
241	2	0	1	0	2	0	1	0			173.55
242	1	0	1	0	2	0	1	0	2	0	172.5
243	3	1	3	1	5	1	3	1	5	1	53.48
244	2	0	1	0	2	0	1	0	1	0	172.14
245	1	0	1	0	1	0	1	0	1	0	185.71
247	3	1	3	1	4	1	3	1	3	1	12.84
248	4	1	1	0	5	1	4	1	5	1	41.03
252	3	1	3	1	4	1	3	1	3	1	32.33
255	3	1	2	0	4	1	3	1	4	1	29.43
357	4	1	1	0	4	1	1	0	1	0	179.63
259	3	1	2	0	4	1	3	1	2	0	16.06
262	4	1	1	0	4	1	2	0	2	0	18.82
264	2	0	1	0	5	1	3	1	5	1	80.72
267	1	0	2	0	2	0	1	0	2	0	176.31
268	5	1	1	0	5	1	2	0	2	0	1.48
269	3	1	1	0	5	1	3	1	3	1	48.06
270	5	1	3	1	3	1	3	1	4	1	7.03
272	5	1	1	0	2	0	2	0	2	0	15.34
275	5	1	4	1	4	1	3	1	2	0	27.53
276	1	0	1	0	2	0	1	0	2	0	173.52
279	3	1	1	0	3	1	1	0	1	0	221.78
281	3	1	1	0	4	1	3	1			21.68
282	5	1	1	0	4	1	3	1	2	0	53.35

[a] Anonymised case number.

[b] Staining for MMP2 (1-5 staining categories: 1= -, 2= +/-, 3= +, 4= ++, 5= +++).

[c] Two staining categories: 0= - or <5% positive staining, 1= + or >5% positive staining.

[d] MMP9 = MMP9 (1-5 staining categories).

[e] Two staining categories: 0= - or <5% positive staining, 1= + or >5% positive staining.

[f] Staining for MMP13 (1-5 staining categories).

[g] Two staining categories: 0= - or <5% positive staining, 1= + or >5% positive staining.

[h] Staining for S100A4 (1-5 staining categories).

[i] Two staining categories: 0= - or <5% positive staining, 1= + or >5% positive staining.

[j] Staining for S100P (1-5 staining categories).

[k] Two staining categories: 0= - or <5% positive staining, 1= + or >5% positive staining.

[l] Patient survival time in months.